Salish Sea Ambient Noise Evaluation 2016–2017

ECHO Program Study Summary

This study was undertaken for Vancouver Fraser Port Authority's Enhancing Cetacean Habitat and Observation (ECHO) Program to analyze regional acoustic data collected over two years (2016–2017) at three sites in the Salish Sea: Haro Strait, Boundary Pass and the Strait of Georgia. These sites were selected by the ECHO Program to be representative of three sub-areas of interest in the region in important habitat for marine mammals, including southern resident killer whales (SRKW).

This summary document describes how and why the project was conducted, its key findings and conclusions.

What questions was the study trying to answer?

The ambient noise evaluation study investigated the following questions:

- What were the variabilities and/or trends in ambient noise over time and for each site, and did these hold true for all three sites?
- What key factors affected ambient noise differences and variability at each site?
- What are the key requirements for future monitoring of ambient noise to better understand the contribution of commercial vessel traffic to ambient noise levels, and how ambient noise may be monitored in the future?

Who conducted the project?

JASCO Applied Sciences (Canada) Ltd., SMRU Consulting North America, and the Coastal & Ocean Resource Analysis Laboratory (CORAL) of University of Victoria were collaboratively retained by the port authority to conduct the study. All three organizations were involved in data collection and analysis at one or more of the three study sites over the two-year time frame of acoustic data collection.

What methods were used?

Ambient noise data were analyzed from cabled, seabed-mounted underwater recording systems in Haro Strait, Boundary Pass and the Strait of Georgia. Five categories of potentially influential factors were studied to determine how they contributed to underwater ambient noise levels at each site.

The presence of vessel traffic, whether large commercial ships or smaller recreational boats, is an important factor when evaluating ambient noise. At each site, the presence of large vessels was assessed using the Automatic Identification System (commonly referred to as AIS). Where possible, the presence of smaller boats not equipped with AIS was evaluated through acoustic detection methods or through photographs taken from land.

System noise (including sensitivity range and calibration of the hydrophone system) relates to the ways in which a recording system itself affects measurements of underwater ambient noise. System noise for each station was assessed aurally and/or visually through sound level plots.

Weather and tidal conditions consider the ways that meteorological sources such as wind, rain and water currents affect measurements of underwater ambient noise. Sound levels were analyzed and correlated with wind and rain data collected at the nearest available weather station, and with water currents from a tidal prediction model and/or measurements from an acoustic Doppler current profiler.

Sound speed profile variability and acoustic propagation relate to the ways that oceanographic conditions like temperature, salinity, and sea-surface roughness, as well as water depth and seabed composition (e.g., sand, silt and clay) affect the propagation of underwater noise. Sound speed profile measurements in the Salish Sea were used along with wind speed measurements and seabed properties to model acoustic propagation at each site.

Biological presence relates to the way that underwater sounds generated by marine animals, such as vocalizations and echolocation clicks, affect ambient noise. The effect of biological presence was analyzed by comparing sound levels at times with and without acoustic detections of marine mammals.

What were the key findings?

The conditions at each study site varied by recording system and hydrophone specifications, propagation environments, deployment depths, distances from the shipping lane, vessel traffic density levels and system noise contamination. These differences made comparisons between sites very challenging; however, some key findings of the study include:

- Vessel presence was found to be the most important factor influencing ambient noise at all sites. Large vessel traffic was a fairly consistent contributor, whereas small vessel traffic appears to increase sound levels mainly during summer daylight hours. Proximity of the vessel traffic to the hydrophone strongly influences the noise contribution.
- System noise influenced ambient noise in a manner unique to each recording system. System noise effects could be observed in the data at different frequencies and different intensities, dependent on the site. Recommendations on hydrophone calibrations and how to check for system noise are provided in the technical report.
- The extent to which ambient noise is influenced by variable environmental factors such as water currents, wind and rain is specific to each site. Effects of wind, and intensity of the currents were influential at lower frequencies for some sites.
- The distance of weather and current measurement equipment to the hydrophone plays in important role in understanding how these factors affect ambient noise. The report recommends locating weather stations and current meters proximate to the hydrophone, while limiting the potential contribution of oceanographic monitoring equipment to the received noise levels.
- Sound speed profile variability and acoustic propagation effects should be considered when evaluating ambient noise. Measuring and modelling of these effects under three different seasonal sound speed profiles—summer (downward refracting), winter (upward refracting), and spring or fall (transition)—is recommended.
- The ability to measure a change in ambient noise due to marine animal vocalizations was challenging, and may have been hindered by the relatively high and consistent ambient noise levels at some sites.

Conclusions

This analysis considered the influence of vessel traffic, system noise, weather and currents, sound speed profiles and sound propagation, and biological presence on ambient noise levels recorded on three hydrophone systems in Haro Strait, Boundary Pass and the Strait of Georgia from 2016 to 2017. The study found all factors affect the soundscape in ways that varied significantly between sites, with both large and small vessel traffic being the most influential contributors to ambient noise for the sites analyzed. When monitoring changes in underwater ambient noise over time, or when evaluating potential noise mitigation strategies, the influence of these factors on ambient noise should be considered.

Salish Sea Ambient Noise Evaluation 2016–2017

Enhancing Cetacean Habitat and Observation Program

Submitted to:

Krista Trounce
Vancouver Fraser Port Authority
Project: 18-0258

Authors:

Graham Warner[1]
Jason Wood[2]
Sandra Frey[3]
Alexander MacGillivray[1]
Dominic Tollit[2]
Zizheng Li[1]
Lauren McWhinnie[3]

12 December 2019

P001455-001
Document 01756
Version 2.0

[1]**JASCO Applied Sciences (Canada) Ltd**
Suite 2305, 4464 Markham St.
Victoria, BC V8Z 7X8 Canada
Tel: +1-250-483-3300
www.jasco.com

[2]**SMRU Consulting**
Suite 604, 55 Water St.
Vancouver, BC V6B 1A1 Canada
Tel: +1-604-737-7678
www.smruconsulting.com

[3]**Coastal and Ocean Resource Analysis Laboratory**
Department of Geography, University of Victoria
PO Box 3060 STN CSC
Victoria, BC V8W 3R4 Canada
Tel: +1-250-472-4624
coral.geog.uvic.ca

Suggested citation:

Warner, G.A., J.D. Wood, S. Frey, A.O. MacGillivray, D.J. Tollit, Z. Li, and L. McWhinnie, 2019. *Salish Sea Ambient Noise Evaluation 2016–2017: Enhancing Cetacean Habitat and Observation Program*. Document 01756, Version 2.0. Technical report by JASCO Applied Sciences, SMRU Consulting, and Coastal and Ocean Resource Analysis Laboratory for Vancouver Fraser Port Authority.

Affiliations:

JASCO Applied Sciences	*SMRU Consulting*	*Coastal and Ocean Resource Analysis Laboratory*
Graham Warner	Jason Wood	Sandra Frey
Alex MacGillivray	Dominic Tollit	Lauren McWhinnie
Zizheng Li		

Disclaimer:

The results presented herein are relevant within the specific context described in this report. They could be misinterpreted if not considered in the light of all the information contained in this report. Accordingly, if information from this report is used in documents released to the public or to regulatory bodies, such documents must clearly cite the original report, which shall be made readily available to the recipients in integral and unedited form.

Contents

Figures

Tables

Executive Summary

Introduction and Methods

This study was undertaken for Vancouver Fraser Port Authority's (VFPA's) Enhancing Cetacean Habitat and Observation (ECHO) Program to analyze acoustic data collected over two years (2016–2017) at three sites in the Salish Sea: Haro Strait, Boundary Pass, and Strait of Georgia (Figure 1). These sites were selected by the ECHO Program to be representative of three sub-areas of interest in the region, and they are in important habitat for marine mammals, including Southern Resident Killer Whales (SRKW).

The project goals were to seek answers to the following questions:

1. What were the temporal variabilities and/or trends in ambient noise (across both broadband and finer-scale frequency bands) for each site, and did these hold true for all three sites?
2. What key factors affected ambient noise differences and variability at each site, and what trends (if any) relating to these factors were observed?
3. What are the key requirements for future monitoring of ambient noise (i.e., including system performance resolution and analytical approaches) to best understand the contribution of commercial vessel traffic to ambient noise levels, and for how ambient noise may be monitored in the future?

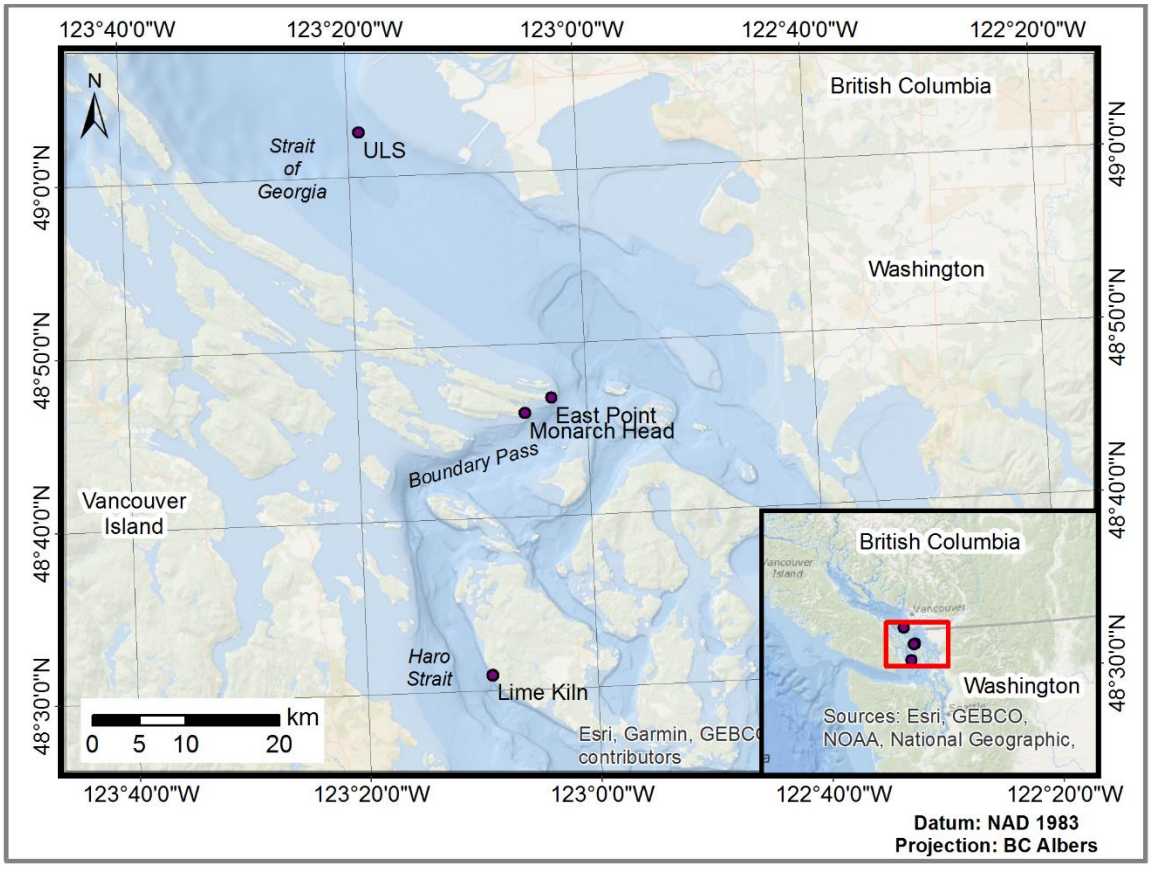

Figure 1. Map of the study area with the locations of the hydrophone recorders (circles) in Strait of Georgia, Boundary Pass, and Haro Strait.

For this study, the following five categories of key influential factors were studied to determine how they contributed to underwater ambient noise levels at each site:

1. System noise, sensitivity range, and calibration—These factors relate to the ways in which a recording system itself affects measurements of underwater ambient noise. System noise was assessed aurally, and sound level plots were assessed visually.
2. Weather and tidal conditions—These factors relate to the ways that meteorological sources (e.g., wind and rain) and water currents affect measurements of underwater ambient noise. Sound levels were analyzed with wind and rain data collected at the nearest available weather station and water currents from the WebTide Tidal Prediction Model (v0.7.1) (Foreman et al. 2000, Institute of Ocean Sciences 2015) or acoustic doppler current profiler (ADCP) measurements.
3. Sound speed profile (SSP) variability and acoustic propagation effects—These factors relate to the ways that oceanographic conditions (e.g., temperature, salinity, and sea-surface roughness), bathymetry, and seabed composition (e.g., sand, silt, and clay) affect the propagation of underwater noise measured at each site. SSP measurements in the Salish Sea were obtained from the Water Properties Group at the Institute of Ocean Sciences (Water Properties Group 2019) and were used, with wind speed measurements and seabed properties to model acoustic propagation at each site.
4. Vessel traffic—This factor is generally the dominant source of underwater noise in the Salish Sea (Bassett et al. 2012). Movements of large vessels can be reliably monitored using the Automated Identification System (AIS), but the movements of smaller vessels (including many recreational craft) cannot. To assess the influence of vessel traffic on sound levels, AIS data were used at all sites, photographic data were used in Boundary Pass, and acoustic detector data were used at Lime Kiln.
5. Biological presence—This factor relates to the way that underwater sounds generated by marine animals affect ambient noise (e.g., mammal vocalizations[1] and echolocation clicks). The effect of biological presence was analyzed by comparing sound levels at times with and without acoustic detections of marine mammals.

In general, it was difficult to identify consistent temporal variabilities and trends between all three sites because the influence of these factors had frequency- and temporally dependent effects on ambient noise levels. Median sound levels were highest at Lime Kiln (~108 dB re 1µPa). Corresponding sound levels at the ULS were slightly lower (~107 dB re 1µPa), and were lowest in Boundary Pass (~95–99 dB re 1µPa). Standard deviations of monthly median SPL (which represent variability in sound levels) were 0.8 dB for ULS, 1.2 dB for Lime Kiln, 1.4 dB for Monarch Head, and 2.3 dB for East Point. The L_{eq} and L_5 levels showed similar between-site trends. L_{eq} SPL were below L_5 values, but well above (>10 dB) the L_{50} (median) at all sites. This indicates short-term, but high-amplitude, noise sources were present. In contrast to L_{50}, the lowest temporal variability in both L_{eq} and L_5 metrics was observed at Lime Kiln and East Point. The observed variability and SPL ranges across key lunar month metrics (2–6 dB) highlight the analytical challenges in determining appropriate baselines, detecting future trends, and assessing efficacy of short-term mitigation measures.

Since the influence of the five categories of key influential factors varied between sites, this study focussed on each site separately. The following sections describe the important factors at each location.

[1] Although many sounds marine mammals make do not originate from vocal cords, this report uses the generic term “vocalization” to mean all sounds marine mammals produce.

Lime Kiln Results

The recording location in Haro Strait was located near Lime Kiln, off the western shoreline of San Juan Island. The Lime Kiln hydrophone was deployed at 23 m water depth, approximately 2.5 and 5 km east of the inbound and outbound international shipping lanes, respectively.

The most important factors contributing to ambient noise at Lime Kiln were vessel noise, tidal currents, SRKW presence, and system noise. The seasonal pattern of vessel traffic volume increased in summer and decreased in winter, largely due to increased recreational and sailing vessel traffic during midday in summer. Large-vessel traffic was relatively consistent with time of day and season.

Both large- and small-vessel traffic increased measured sound levels in all decade bands when compared to periods with no vessels. Large vessels increased sound levels the most in the 10–100 Hz band, while small vessels increased sound levels in the 0.1–1, 1–10, and 10–100 kHz bands. Small-vessel effects were concentrated in summer.

Low-frequency flow noise caused by tidal currents appeared to increase sound levels in the 10–100 Hz band for currents speeds greater than 0.4 m/s, but the relationship was difficult to quantify. It is suspected that the modelled current speeds may be inaccurate at Lime Kiln. Measuring currents at the site is recommended in future.

Biological presence was found to increase sound levels at Lime Kiln during summer and fall due to SRKW vocalizations. SRKW vocalizations increased sound levels in the 1–10 kHz (vocalization) and 10–100 kHz (click) decade bands when compared to periods when they were not vocalizing. This was likely driven by how often SRKW were near the hydrophone (, i.e., within one km) when they transited past Lime Kiln.

System noise also contributed to measured sound levels during quiet periods at Lime Kiln. This occurred intermittently in the 10–100 Hz band and consistently in the 10–100 kHz band.

High winds were associated with increased sound levels at Lime Kiln during quiet periods in January but not July, even though the wind speed distributions were similar between months. It is suspected that wind speed measured on the closest metocean buoy, which was 20 km south of the hydrophone, may not have always been representative of the winds at Lime Kiln.

The effects of SSP variability on transmission loss were predicted to be small at Lime Kiln, but this may have been due to the poor temporal coverage of SSP measurements. Only a few SSP measurements were available in Haro Strait, primarily in April, June, and September.

East Point and Monarch Head Results

There were two recording locations in Boundary Pass, at East Point and Monarch Head, off the southeastern shore of Saturna Island. The East Point hydrophone was operational from January 2016 until March 2017. The Monarch Head hydrophone was operational during all of 2017. Both hydrophones were deployed in waters shallower than 30 m, approximately 1 and 2 km northwest of the outbound and inbound international shipping lanes, respectively.

The most important factors identified for the Boundary Pass East Point and Monarch Head recorders were vessel noise, wind-driven ambient noise, and system noise. AIS vessel traffic volume increased in summer, largely due to an increase in recreational and other seasonal traffic. Recreational and sailing vessel traffic increased substantially during midday in summer. Container ship traffic was relatively consistent seasonally but had higher volume early in the day (peaking around 2:00 am).

Analysis of Boundary Pass camera data showed few non-AIS broadcasting vessels in winter but a marked increase in this traffic during summer. The total number of vessel transits during daytime increased by almost 500% in August compared to February, and the proportion of non-AIS vessels to total traffic volumes increased from 15 to 72%. Most of these non-broadcasting vessels were sailboats and motorboats, which suggests that summer daytime vessel activity in Boundary Pass largely consisted of recreational vessels.

AIS-broadcasting vessel traffic increased measured sound levels in all decade bands, and non-AIS-broadcasting vessel traffic increased levels in the 0.1–1, 1–10, and 10–32 kHz bands when within 3 km of the hydrophone. Vessels identified on camera (both AIS and non-AIS) were associated with higher ambient noise levels on the East Point hydrophone (in winter) than on the Monarch Head hydrophone (in summer). It is unknown whether this represents a seasonal trend because these two hydrophones were situated 3 km apart and the camera was located near the East Point hydrophone. The differences in location likely affected how the hydrophones received vessel noise (e.g., due to differences in the local bathymetry or shoreline features). The overall contribution of smaller vessels to ambient noise, in terms of sound exposure, is expected to be greater during summer than in winter because of the substantial increase in small-vessel traffic in summer.

During quiet periods in January, wind-driven ambient noise at East Point increased sound levels in the 0.1–1, 1–10, and 10–32 kHz bands when wind speeds were greater than ~5 m/s. This noise likely included sounds from waves crashing on shore, as the hydrophone was located near shore. This effect was not seen in July, likely because of the lower wind speeds in summer.

System noise was substantial for both East Point and Monarch Head recorders and was frequently present in all decade bands, therefore these data may not be entirely representative of baseline conditions. At East Point, a 60 Hz tone and higher-frequency harmonics from the recorder's power supply limited the ability to measure accurate ambient noise levels and determine effects of other factors most of the time. Broadband sound levels were higher in winter than in summer at East Point because of this noise, which dominated broadband sound levels. It is unknown why noise from the power supply decreased in summer. Low-frequency sound levels at East Point did not appear correlated with current speed, likely because the 60 Hz power supply tone masked flow noise.

There was less system noise at Monarch Head, which may have contributed to quieter sound levels there (2017) than at East Point (2016). Monarch Head recordings, however, contained persistent Global Positioning System (GPS) timing signals that limited the recorder's ability to measure low-frequency sound levels. A high-frequency calibration error introduced an upward bias to the 10-64 kHz decade band levels.

The effects of SSP variability on transmission loss were predicted to be small at East Point, but this may be due to the poor temporal coverage of SSP measurements. Only a few SSP measurements were available in Boundary Pass, primarily in April, June, and September.

Biological presence (killer whales) did not appear to substantially contribute to the ambient noise at East Point. The large difference in the contribution of SRKW vocalizations between East Point and Lime Kiln may be related to their proximity at each site and the duration of their transits.

ULS Results

The recording location in the Strait of Georgia was the ECHO Underwater Listening Station (ULS), which was located approximately 10 km west of Roberts Bank on the Victoria Experimental Network Under the Sea (VENUS) East Node. The ECHO ULS was located between the northbound and southbound traffic lanes in the Strait of Georgia, at 173 m water depth.

The most important factors identified for the ULS in the Strait of Georgia were vessel noise, tidal currents, SSP variability, and system noise. The Strait of Georgia had the highest AIS traffic volume (vessel hours), exceeding that of Haro Strait and Lime Kiln by 2–3 times. Tug and ferry traffic was particularly high in the Strait of Georgia compared to the other sites.

Traffic volume in the Strait of Georgia exhibited seasonal, weekly, and hourly trends. Traffic volume increased in summer and decreased in winter. Vessel traffic was highest on Thursdays and lowest on Sundays. Early morning tug traffic was particularly high, and the daily pattern of ferry traffic contributed to higher vessel traffic during most hours except between 1:00 and 4:00 am (PST).

The ULS location was in the middle of the shipping lanes, so vessels frequently passed near the recorder and elevated sound levels more than at other sites. Higher large commercial vessel traffic volume increased median sound levels in most frequency bands.

Tidal currents produced substantial flow noise on the ULS recorder and increased 10–100 Hz levels during high-current periods. High-quality ADCP current measurements allowed quantification of the effect, with sound levels in the 10–100 Hz band increasing by approximately 55 dB for every metre-per-second increase in current speed between 0.4 and 0.8 m/s. High-frequency sounds from the ADCP and other nearby sonars and electrical equipment limited the ability to accurately characterize ambient noise levels at high frequencies (greater than ~10 kHz).

The SSP in the Strait of Georgia varied more than at the other sites; however, this may have been due to greater temporal coverage of the SSP measurements. Sound propagation modelling showed that transmission loss was higher during summer (downwards-refracting) SSP conditions. Nonetheless, measured sound levels were generally higher in summer than in winter. This indicates that traffic volume was more influential than seasonal changes in the SSP on ambient sound levels at this site.

Lower sound levels at the ULS in 2016 during February were due to extended periods of military redactions (the Saturna Island Marine Research & Education Society (SIMRES) and Lime Kiln hydrophones were not subject to redactions). These redactions filtered out sound levels below 4 kHz, and sound level statistics were calculated over durations including the redaction periods. This artificially reduced the monthly average sound levels calculated in the 10–100, 100–1000, and 1000–10000 Hz bands.

Wind speed and biological presence did not appear to be important factors in the Strait of Georgia, likely because vessel noise masked their effects.

Limitations of Available Datasets

At times, limitations in the available datasets hindered the ability to draw strong conclusions in the following areas:

1. System noise was particularly difficult to assess because persistent sources are hard to identify after the fact and can change over time. Differences between recording systems at the different sites also hindered comparisons of sound levels.
2. Weather and tidal conditions had much clearer effects when there were high-quality and local covariate data with a fine temporal resolution (e.g., current speed as measured at the ULS with an ADCP).
3. In Haro Strait and Boundary Pass, sound speed profile data were good quality, but spatial and temporal coverage were poor.
4. AIS recording systems stored the data differently making it difficult to classify vessel type consistently between locations. This did not, however, affect the fraction of unclassifiable vessels that were present at each site.
5. At East Point, photographic data of vessel traffic was limited to daylight hours during periods of good visibility. Vessels, especially when travelling quickly and near the camera, could transit past the camera’s field of view without being photographed.
6. At Lime Kiln, acoustic detections of small vessels during the day were correct 75% of the time. Night detections can be excluded, but the detector needs improvement.
7. Biological data quality was good with effective acoustic detectors, but the ability to measure a change in ambient noise due to the presence of whales may have been hindered by consistently high ambient noise levels at some sites.

Recommendations for Future Ambient Monitoring

Table 1 lists recommendations for future ambient noise monitoring efforts that intend to monitor the effectiveness of noise mitigation methods.

Table 1. Summary of recommendations for future ambient noise monitoring.

Covariate	Recommendation	Schedule
Acoustic data analysis	1-minute SPL in 1/3-octave and decade bands, weekly and (lunar) monthly spectrograms and PSD exceedances	Continuous at 1-minute resolution
Temporal and spatial sampling	Duty cycling not recommended	Continuous
	Keep consistent hydrophone location and depth year-over-year	Annual
Calibration	Characterize system response over the full frequency range of interest, calibration with pistonphone	Annual
System noise	Measure system noise floor	Before, after deployment
	Plot minimum 1/3-octave and PSD levels to monitor noise floor	Monthly
Water currents, wind, and rain	Measure in proximity of hydrophone	Continuous at 1-minute resolution
Sound speed profile	Measure in deep water near hydrophone	Seasonally
	Model effect on sound propagation	
Vessel traffic	Use combination of AIS, photographs, acoustic detectors, and potentially radar	Continuous
Biological presence	Use automatic detectors and manually validate a portion of detections	Continuous

Conclusions

The analyses considered the influence of system noise, environmental conditions, vessel traffic, and biological presence on ambient sound levels recorded by four hydroacoustic recording systems: one in Haro Strait, two in Boundary Pass, and one in the Strait of Georgia. The most important factor at all sites was vessel noise. System noise was unique to each recording system, but data from all recorders was contaminated with narrow-band tones from electrical power supplies and other equipment. In the future, system noise could be characterized by co-locating different recorders for brief periods and comparing ambient noise levels. These results could be used to correct or filter the affected recordings. Environmental conditions, such as tidal currents, wind, rain, and sound speed profile variability, affected sound levels and propagation; however, it was not always possible to determine the contribution of each factor with the data available for this study. Characterizing the effects of these factors requires local and frequently sampled covariate data. More SSP measurements are needed in Haro Strait and Boundary Pass to verify the relatively small variability in transmission loss. Biological presence from SRKW was found to increase sound levels at Lime Kiln in the 1–100 kHz frequency range, but biological presence from killer and humpback whales had little to no influence on sound levels at the other sites.

The influence of all these factors on ambient noise must be considered when assessing the effectiveness of a noise mitigation strategy. Selecting a baseline or control period is crucial because some of these factors can change on monthly timescales (e.g., SSP) and can be unpredictable (e.g., system noise and biological presence). Therefore, it is advised that baseline noise levels, where possible, be selected appropriately (e.g., from periods just before or after a noise mitigation action is undertaken, or from the same time period during a previous year). Furthermore, fine-scale, local covariate data (e.g., SSP, meteorological, and currents) should be collected to further control for their effects. Temporarily positioning additional hydrophones nearer the targeted noise source could make it easier to determine the effect of noise mitigation strategies, as such recordings would be less susceptible to influence by other factors.

1. Introduction

The Vancouver Fraser Port Authority's (VFPA's) Enhancing Cetacean Habitat and Observation (ECHO) Program is a VFPA-led initiative aimed at better understanding and managing the impact of shipping activities on at-risk whales throughout the southern coast of British Columbia. One of the priorities of the ECHO program is to develop mitigation measures that will lead to quantifiable reductions in regional underwater noise caused by marine shipping, which the Fisheries and Oceans Canada (DFO) Recovery Strategy identifies as one of the key threats impacting Southern Resident Killer Whales (SRKW) in British Columbia. To this end, the ECHO Program initiated a monitoring program in 2016 to measure baseline regional ambient underwater noise conditions at three sites in the Salish Sea: Haro Strait, Boundary Pass, and Strait of Georgia. Acoustic data were collected for approximately two years at these three sites (2016–2017). Subsequently, in 2018, the ECHO Acoustic Technical Committee (ATC) met to review the collected data from the monitoring program and to plan a project to identify key factors that must be understood for evaluating the effectiveness of applied mitigation efforts.

After the ATC meeting, the VFPA initiated the Ambient Noise Evaluation Project to seek answers to the following questions:

1. What were the temporal variabilities and/or trends in ambient noise (across both broadband and finer-scale frequency bands) for each site, and did these hold true for all three sites?
2. What key factors affected ambient noise differences and variability at each site, and what trends (if any) relating to these factors were observed?
3. What are the key requirements for future monitoring of ambient noise (i.e., including system performance resolution and analytical approaches) to best understand the contribution of commercial vessel traffic to ambient noise levels, and how ambient noise may be monitored in the future?

The Ambient Noise Evaluation Project was undertaken for VFPA as a collaborative study by JASCO Applied Sciences, SMRU Consulting, and the Coastal and Ocean Resource Analysis Laboratory (CORAL) at the University of Victoria. To answer the research questions identified by ECHO, the collected ambient noise data were analyzed from four cabled seabed-mounted underwater recording systems in Haro Strait, Boundary Pass, and the Strait of Georgia (Figure 2) in relation to several key influential factors identified by the ATC (Vancouver Fraser Port Authority 2018).

For this study, the following five categories of key influential factors were examined to determine how they contributed to underwater ambient noise levels at each site:

1. System noise, sensitivity range, and calibration—These factors relate to the ways in which a recording system itself affects measurements of underwater ambient noise. This includes the frequency-dependent sensitivity of the hydrophone, induced (non-acoustic) electrical noise on the recording system, interfering (acoustic) noise from nearby equipment, and the overall calibration of the system itself. These factors determine the minimum level of ambient noise that can be measured at each site and may vary gradually over days or months, depending on the characteristics of the recording system.
2. Weather and tidal conditions—These factors relate to the ways that meteorological sources and water currents affect measurements of underwater ambient noise. This includes acoustic noise generated at the sea surface by wind and rain. It also includes acoustic and non-acoustic noise (i.e., pseudo-noise) generated by water turbulence associated with ocean currents (currents in the study area are predominantly driven by tidal forcing). These factors typically vary on temporal scales of minutes or hours.
3. Sound speed profile (SSP) variability and acoustic propagation effects—These factors relate to the ways that oceanographic conditions (e.g., temperature, salinity, and sea-surface roughness), bathymetry, and seabed composition (e.g., sand, silt, and clay) affect the propagation of underwater noise measured at each site. The SSP is determined by the depth-dependent temperature and salinity in seawater. The shape of the sound speed profile influences how sounds propagate from sources at longer distances to the hydrophone (beyond ~1–2 km). The sound speed profile varies diurnally, especially in the upper water column, and these variations follow seasonal patterns. Site-

specific bathymetry and seabed composition also strongly influence noise propagation, with shallow water and soft seabed materials blocking and absorbing more incident sound, respectively, than deeper water and harder seabed materials.

4. Vessel traffic—This factor is generally the dominant source of underwater noise in the Salish Sea (Bassett et al. 2012) and is comprised of a diverse range of vessel sizes and types, ranging from large container ships, tankers, and bulk carriers to small recreational craft, fishing, and ecotourism vessels. Movements of large vessels can be reliably monitored using the Automated Identification System (AIS), but the movements of smaller vessels (including many recreational craft) cannot. Noise from vessel traffic typically varies on many different timescales (e.g., minutes, hours, and seasonally) in the study area, as different vessels transit near a receiver location. Proximity of vessel traffic to the hydrophone is influential and was assessed using AIS and visual data.
5. Biological presence—This factor relates to the way that underwater sounds generated by marine animals affect ambient noise and includes mammal echolocation clicks, mammal vocalizations, and fish choruses. Biological sounds are generally associated with the presence of a different species of animals at each site (e.g., killer whales and humpback whales), although animals do not always vocalization when they are present. Sounds from biological sources may be manually identified by a human analyst or automatically detected by software (although the latter are usually subjected to manual review). Biological noise is highly variable in the study area, with some days having many vocalizations and other days having none. Marine mammal proximity to the hydrophone may be influential, but localization data were not available for this study.

This technical report presents the results of the Ambient Noise Evaluation Project. Section 2 describes the analysis methods used to evaluate each influential factor, and Section 3 provides the detailed results of the analysis. Section 4 presents a discussion of the findings, including a ranking of the influential factors at each site and recommendations for future monitoring. The conclusions of this study are presented in Section 5.

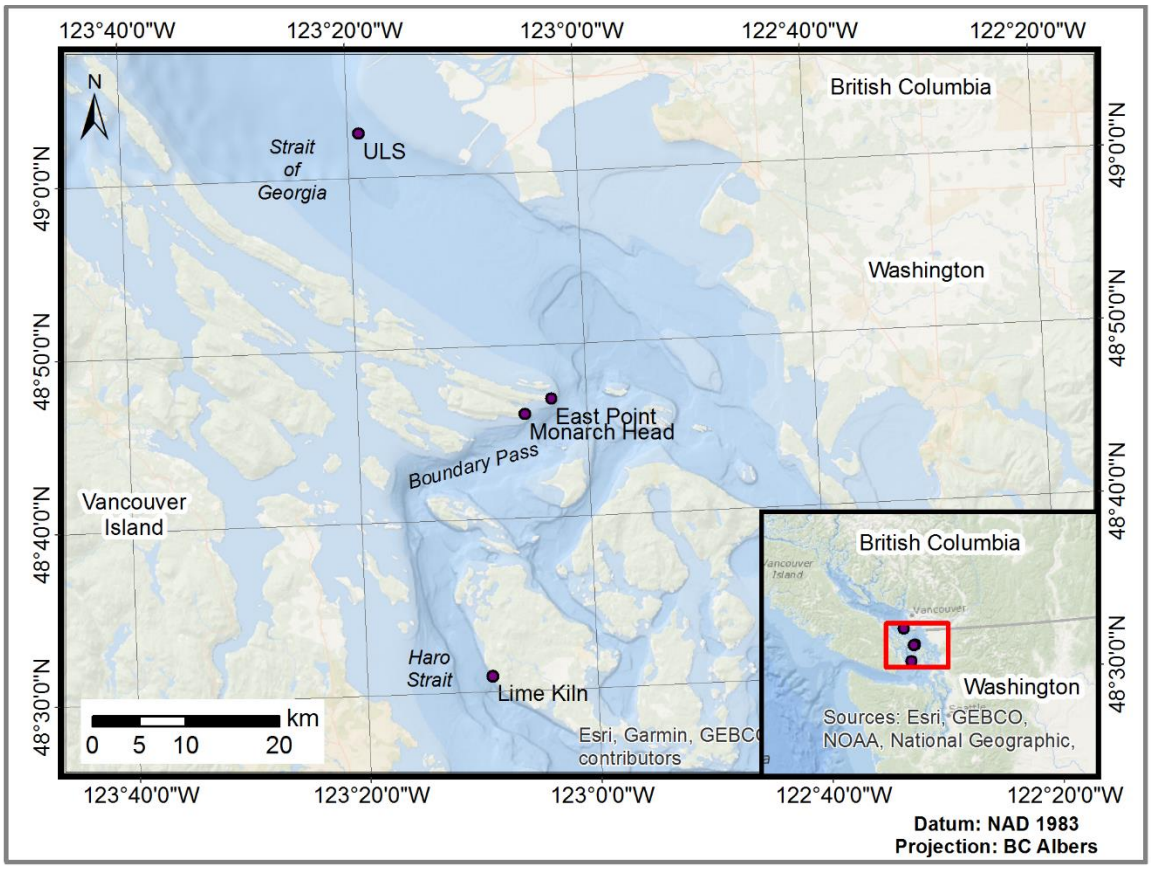

Figure 2. Map of the study area with the locations of the hydrophone recorders (circles) in Strait of Georgia, Boundary Pass, and Haro Strait.

1.1. Measurement Sites

1.1.1. Haro Strait

The recording location in Haro Strait was located near Lime Kiln, off the western shoreline of San Juan Island. The hydrophone system at this location was operated by SMRU Consulting, in collaboration with the Whale Museum at Like Kiln Point State Park, WA. The Lime Kiln hydrophone was deployed at 23 m water depth, approximately 2.5–5 km, respectively, to the east of the inbound and outbound international shipping lanes in Haro Strait. This location is an important feeding area for southern resident killer whales (SRKW), particularly in summer.

1.1.2. Boundary Pass

There were two recording locations in Boundary Pass, at East Point and Monarch Head, off the southeastern shore of Saturna Island. Hydrophone systems at both locations were operated by the Saturna Island Marine Research & Education Society (SIMRES). The East Point hydrophone was operational from January 2016 until March 2017. The Monarch Head hydrophone was operational during all of 2017. Both hydrophones were deployed in waters shallower than 30 m, ~1–2 km northwest of the international shipping lanes. Boundary Pass is an important area where SRKW travel and forage before entering Haro Strait.

1.1.3. Strait of Georgia

The recording location in the Strait of Georgia was the ECHO Underwater Listening Station (ULS), located approximately 10 km west of Roberts Bank on the Victoria Experimental Network Under the Sea (VENUS) East Node. This recording system was operated jointly by Ocean Networks Canada (ONC) and JASCO. The ECHO ULS was situated between the northbound and southbound traffic lanes in the Strait of Georgia, at 173 m water depth. This is an area of high vessel traffic concentration and is also located next to the Tsawwassen-Nanaimo ferry route. The ULS is located near the northernmost extent of the critical habitat for SRKW as designated under the Species at Risk Act (SARA).

2. Methods

2.1. System Noise, Sensitivity Range, and Calibration

System noise, sensitivity range, and calibration values are affected by the recording hardware used and how it is integrated and maintained. These factors were analyzed for the Lime Kiln, East Point, Monarch Head, and the ULS recorders (Section 3.1). Recordings were analyzed aurally, and sound level plots (spectrograms and power spectral density percentiles) were analyzed visually to determine the effect of system-noise sources. Results include hardware specifications, recorder sensitivity, noise floor plots, minimum 1/3-octave-band levels (1 minute average) during selected months throughout the study period, details of system-noise sources, and the effects on measured sound levels. Minimum 1/3-octave-band levels were analyzed to see if the noise floor changed with time. Appendix B contains supplementary spectrograms and waveform plots of several noise sources.

2.2. Influence of Weather and Tidal Conditions

2.2.1. Water currents

Water currents can affect ambient noise measurements because they create water turbulence, which can induce acoustic and non-acoustic flow noise around a hydrophone. Tidal forcing is the dominant factor determining water currents at all three sites considered in this study. Flow noise is typically strongest at low frequencies (e.g., in the 10–100 Hz band). It can mask real acoustic signals and limit the ability of recording systems to measure ambient sound levels during quiet periods. The effect of flow noise on sound levels was analyzed by calculating 2-D histograms of 1-minute sound pressure level (SPL) in the 10–100 Hz band as a function of current speed for two months at Lime Kiln, East Point, and the ULS.

At the Lime Kiln and East Point locations, current speeds were obtained from the WebTide Tidal Prediction Model (v0.7.1) (Foreman et al. 2000, Institute of Ocean Sciences 2015) with 1-minute resolution (interpolated from 1-hour resolution). The WebTide current model predicts currents at specified geographic coordinates but does not provide depth-dependent currents, so the modelled currents may not be representative of the currents at the hydrophone depth. At the ULS in the Strait of Georgia, current speeds were obtained from Acoustic Doppler Current Profiler (ADCP) data collected within 120 m of the ULS. ADCP data were processed to calculate the average water current magnitude at the seafloor with 1-minute resolution.

2.2.2. Wind

The effect of wind on underwater noise is due to wave-entrapped bubble collapse and surface spray. This noise increases with wind speed and generally occurs at frequencies between 300 Hz and 100 kHz (Jensen et al. 1994). For this study, the effect of wind speed on ambient noise levels at Lime Kiln, East Point, and the ULS was investigated. Historical wind speed data were obtained from the nearest available weather stations (Table 2). For all locations, 2-D histograms of hourly SPL were created in decade bands as a function of hourly wind speed (this was the finest time resolution found for historical wind speed). The trend of the 90th percentile exceedance level (L_{90}) versus wind speed was also examined to show how sound levels during quieter periods may be limited by wind-driven ambient noise. The hourly SPLs were compared to expected sound levels for open-ocean wind-driven ambient noise, as predicted by the well-known Knudsen curves (Knudsen et al. 1948).

Table 2. Sources of wind speed data used in the present study.

Site	Wind speed data source		
	Name	Geographic coordinates	Distance from site (km)
Lime Kiln	NOAA* Environmental Buoy 46088	48° 20.04000' N, 123° 9.90000' W	20
East Point	Saturna Island	49° 6.35375' N, 123° 18.20205' W	0.63
ULS	Sand Heads Lighthouse	49° 6.35375' N, 123° 18.20205' W	7

* National Oceanic and Atmospheric Administration

2.2.3. Rain

Rain falling on the sea surface creates underwater sound between ~2 and 20 kHz (Medwin et al. 1992). For this study, the effect of rain on sound levels at Lime Kiln, East Point, and the ULS was analyzed. Historical rainfall data were obtained from weather station records at the Vancouver and Victoria International Airports (Table 3). These stations reported qualitative weather conditions each hour. The nearest weather station to each location was used for analysis. No rainfall data could be acquired nearer to the hydrophones that had a time resolution finer than 1 hour. For all sites, box-and-whisker plots were used to compare the distributions of hourly SPL in the 1–10 kHz band during periods with and without rain in January and July (Section 3.2.3), to determine if any effect of rain could be observed in the ambient noise data.

Table 3. Rain data source parameters.

Site	Rain data source		
	Weather station	Geographic coordinates	Distance from weather station to site (km)
Lime Kiln	Victoria International Airport	48° 38.88600' N, 123° 25.72200' W	25
East Point			31
ULS	Vancouver International Airport	49° 11.80200' N, 123° 10.89000' W	20

2.3. Sound Speed Profile Variability and Effects of Modelled Acoustic Propagation

2.3.1. Modelling approach

Transmission loss modelling was conducted using JASCO's Marine Operations Noise Model (MONM) at Lime Kiln, East Point, and the ULS for propagation of sound at four frequencies: 30, 300, 3000, and 30000 Hz. Appendix A describes MONM in more detail, including the bathymetry and seabed properties that were used to model sound propagation at each site.

MONM was used to calculate maps of transmission loss contours at each site for a range of sound speed profiles (Section 2.3.2) and surface roughness (as determined by wind speed) conditions (Section 2.3.3). These were used to quantify the effect of sound speed profile and wind speed variability on modelled

acoustic propagation. For each scenario, transmission loss was averaged for sources at 2, 4, and 6 m depth, to simulate the transmission loss from near-surface sources (e.g., wind driven waves or ships) to the hydrophones. Transmission loss was analyzed along single radials toward the international shipping lanes (along headings of 234, 180, and 219° for Lime Kiln, East Point, and the ULS, respectively). Transmission loss was averaged along the chosen radials between 2 and 4 km range, which was selected as a representative range of distances from the hydrophones for vessels transiting in the shipping lanes at all sites.

2.3.2. Sound speed profile

Historical sound speed profile (SSP) measurements in the Salish Sea were obtained from the Water Properties Group at the Institute of Ocean Sciences (Water Properties Group 2019). A total of 3687 SSP measurements were obtained during 2008–2018 near the hydrophone locations. Figure 3 shows a map of the SSP measurement locations, and Figure 4 shows a histogram of the month and year of the SSP data. There were more SSP measurements in the Strait of Georgia compared to Boundary Pass and Haro Strait. For the Strait of Georgia, most seasons were well sampled, but measurements were infrequent for some months (e.g., January and August). For Haro Strait and Boundary Pass, the sound speed profile was well sampled in April, June, and September, but there were few data for other months.

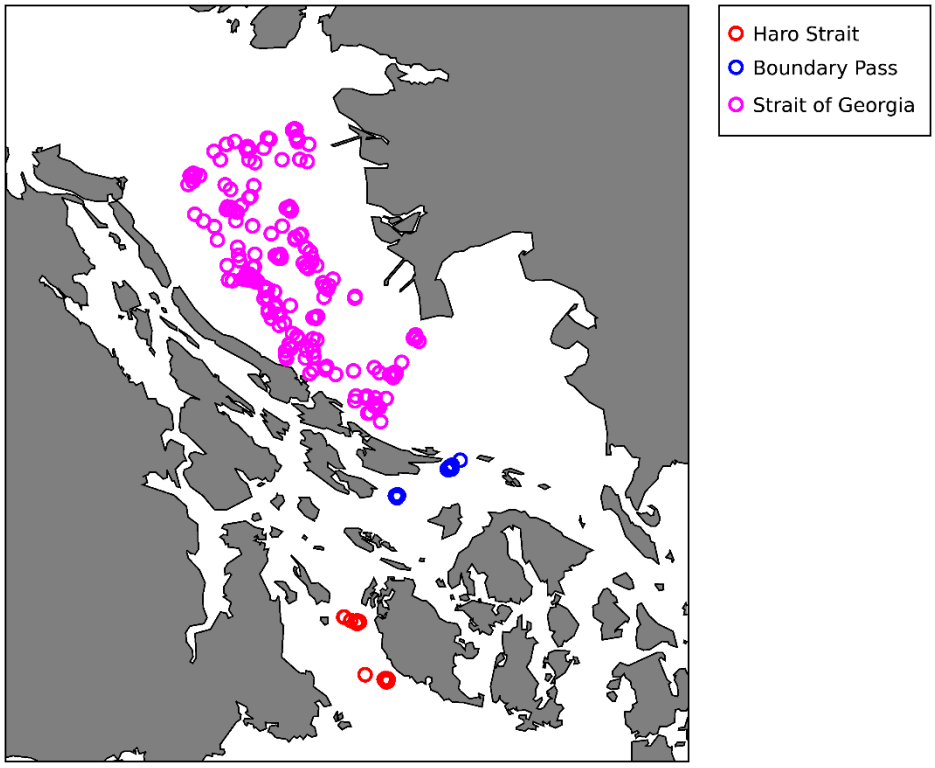

Figure 3. Map showing sound speed profile (SSP) measurement locations (circles) from the Water Properties Group database that were analyzed for this study (Water Properties Group 2019).

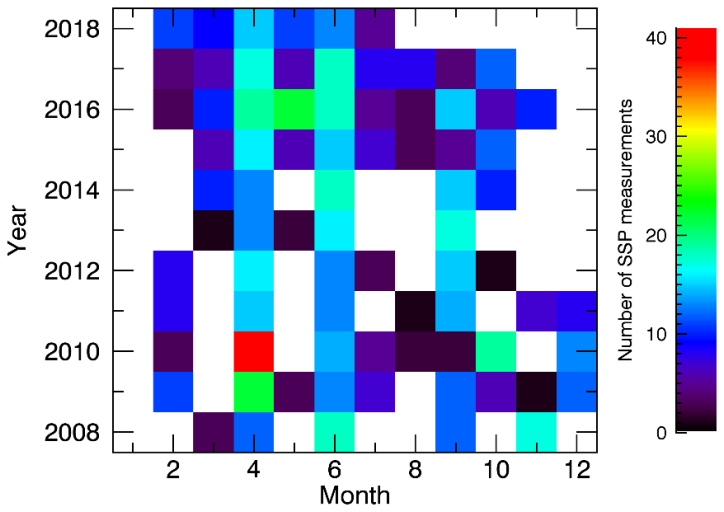

Figure 4. Histogram of the months and years of the analyzed sound speed profile (SSP) measurements from all sites. White boxes indicate periods with no measurements.

Sound propagation is mainly influenced by the shape of the SSP rather than by the absolute value of sound speed, so the first step in assessing SSP variability was to subtract the mean sound speed from each profile. This ensured that two SSP measurements that differed only by a depth-independent sound speed factor were treated the same in subsequent analysis. For each site, the variability of the adjusted site-specific SSP measurements was then assessed by performing a Principle Component Analysis (PCA) on the SSP measurements over the upper 100 m of the water column (where there was the most sound speed variation). This analysis is sensitive to the variance, or differences, between measurements. Three profiles were choosen from each PCA that represented the range of variation among SSP measurements that approximately corresponded to the 5th, 50th, and 95th percentile of the most significant principle component. Figures 5, 6, and 7 show the SSP measurements and the selected profiles for modelling for Haro Strait, Boundary Pass, and the Strait of Georgia, respectively. Profile 1 is generally downwards refracting and represents summmer conditions. Profile 3 is generally upwards refracting and represents winter conditions. Profile 2 is inbetween and represents fall or spring conditions.

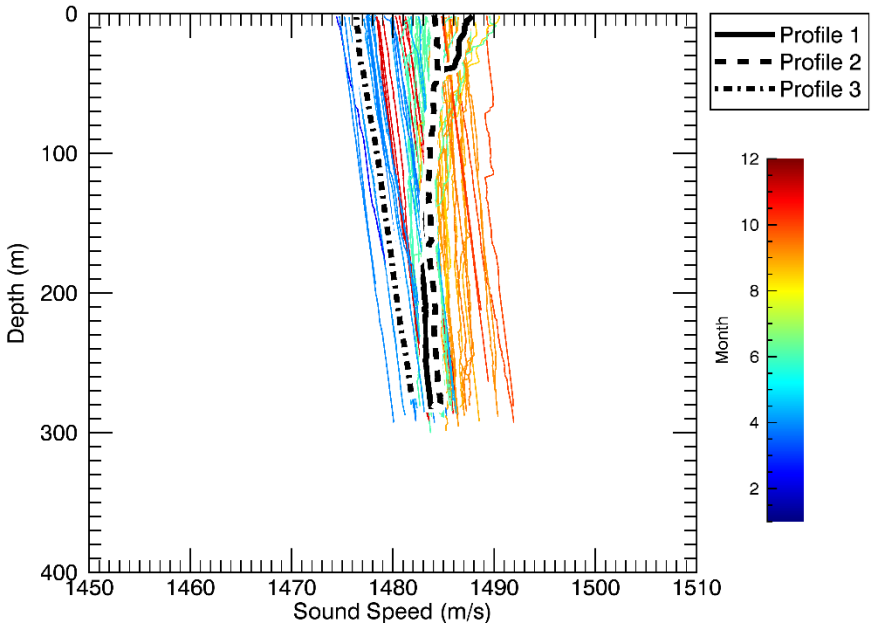

Figure 5. Haro Strait: Sound speed profile (SSP) measurements. Profiles 1, 2, and 3 were selected to represent the observed range of SSP variability at this site.

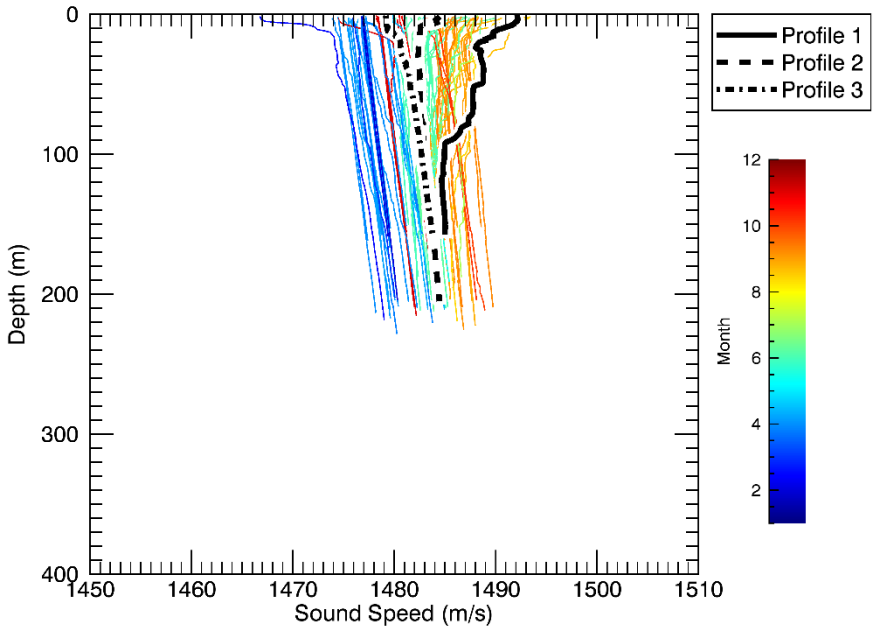

Figure 6. Boundary Pass: Sound speed profile (SSP) measurements. Profiles 1, 2, and 3 were selected to represent the observed range of SSP variability at this site.

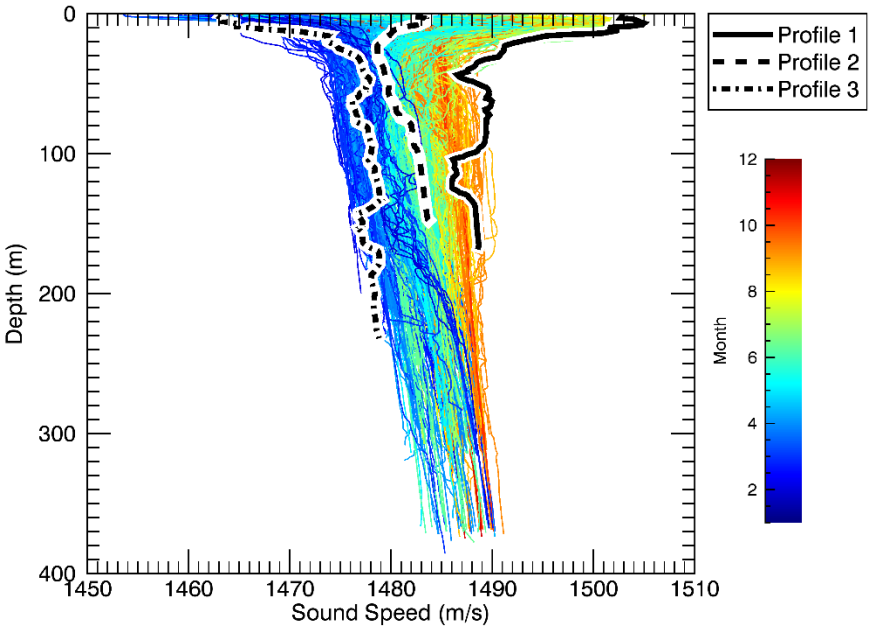

Figure 7. Strait of Georgia: Sound speed profile (SSP) measurements in the. Profiles 1, 2, and 3 were selected to represent the observed range of SSP variability at this site. The sound channels at ~50 and 120 m will not have a large effect on transmission loss between shallow noise sources (e.g., ships and waves) and the hydrophone at 170 m depth.

2.3.3. Wind speed

Rough seas, which are typically caused by high winds, increase transmission loss by scattering sound near the sea surface. The effect of surface roughness is greater for higher frequencies (smaller wavelengths). The effect of wind speed on transmission loss was assessed at each location at sound frequencies of 3 and 30 kHz (the effect is negligible for 30 and 300 Hz). Wind speed measurements at the Sand Heads Lighthouse in the Strait of Georgia showed little seasonal variation in wind speed although some months had more high-wind events (Figure 8 shows a box-and-whisker plot of hourly wind speed measurements; the plot format is explained in detail in the Glossary). The 5th, 50th, and 95th percentile wind speeds for all measurements, which were 0.83, 4.72, and 10.28 m/s, respectively, were used in the acoustic propagation model to assess the variability of transmission loss from observed variability in wind speed at each site.

The wind speed distributions at Hein Bank (near Haro Strait) and East Point were very similar to those at Sand Heads, although the wind speed was generally lower at East Point in summer. The selected wind speeds for modelling were all within the observed measurements at each site. Wind speeds were converted to wave height using data from Schulkin and Shaffer (1964), and scattering loss at the sea surface was calculated from root-mean-square wave height using the Eckhart scattering model (Jensen et al. 1994).

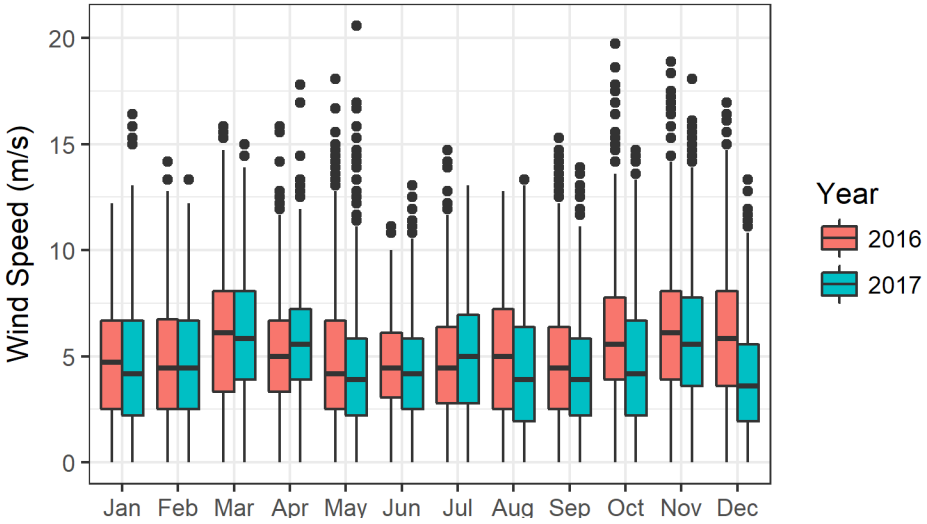

Figure 8. Box-and-whisker plot of hourly wind speed for measurements at the Sand Heads Lighthouse in the Strait of Georgia. The box edges represent the 25th and 75th percentiles, the horizontal line within the box represents the median (50th percentile), and the whiskers show the highest and lowest observations. Points are shown for observations that exceed the 75th percentile by 1.5 times the interquartile range (the box height). The mean and standard deviation of the number of observations for each year/month combination were 720 and 51, respectively.

2.4. Influence of Vessel Traffic on Sound Levels

In this study, three different data sources were used for assessing the effect of vessel traffic on sound levels:

- Automatic Identification System (AIS),
- Photographs, and
- Hydroacoustic recordings.

Each data source has its advantages and disadvantages. Only vessels over 300 tons (excluding fishing vessels) and passenger vessels over 150 tons carrying over 12 passengers are required to broadcast AIS information at regular intervals for traffic safety reasons. Other vessels are not required to transmit AIS data but can voluntarily choose to do so. AIS data therefore captures a portion of the overall vessel traffic, and the proportion of the types of vessels transmitting AIS information can change over time. Currently, there seems to be an increasing trend in small vessels voluntarily broadcasting AIS information due to the added safety benefits. AIS data quality can be affected by source errors (i.e., a source vessel transmitting incorrect data such as the type of vessel it is) or by transmission errors (i.e., transmission drops because of interference with the marine VHF signal). Nonetheless, these errors typically only affect a small proportion of AIS transmissions. Thus, AIS is generally a reliable source for monitoring the movements of vessels that carry AIS transceivers. However, vessels that do not carry AIS transceivers cannot be accounted for using this method.

Photographs can capture traffic of all sizes of vessels whether or not they broadcast AIS messages. Manual analysis of photographs allows for finer vessel category distinctions than is typically possible from the “ShipType” code in raw AIS messages (e.g., bulk carriers and container ships broadcast the same code). Combining photographs with AIS data allows for a comparison between AIS and non-AIS broadcasting vessel traffic, which can be used to assess their relative contributions to sound levels. Furthermore, vessel locations can be determined from photographs if the field of view has been calibrated with measurements. Photographs are limited by available daylight and to some extent weather (e.g., fog).

Acoustic recordings and acoustic detectors can continuously monitor for vessel traffic over long periods of time, day or night and during inclement weather. Depending on the local bathymetry and sound transmission properties, large vessels may be detected up to ranges of 6 to 10 km at the sites considered in this study. Smaller vessels will typically be detected at much shorter ranges, because of their lower overall source levels. The ability to differentiate between large and small vessels (here loosely defined as those required to transmit AIS and those that are not required to transmit AIS) will depend on the quality of the acoustic detectors used. In addition, the range, speed, direction, and other information will not be available from acoustic detectors run on single hydrophones. Changing oceanographic and ambient noise conditions will also affect the performance of acoustic detectors.

These traffic data sources were not necessarily available at all sites, which limited a consistent analysis approach. However, AIS data for all sites was purchased from MarineTraffic.com, which allowed a consistent analysis of AIS vessel traffic and the effects on sound levels (described further in Sections 2.4.1 and 2.4.2). In addition, digital photos were available for the East Point location and were analyzed with AIS data collected at the shore-based recording station to assess the effect of AIS and non-AIS vessel traffic on Boundary Pass sound levels (Section 2.4.3). Acoustic vessel detection results were available at Lime Kiln and were used to assess the effect of large- and small-vessel traffic on sound levels (Section 2.4.4).

2.4.1. MarineTraffic AIS vessel traffic analysis

Historical AIS data from MarineTraffic.com were used to determine temporal and spatial vessel-traffic patterns for all sites over the full study period (2016–2017). AIS data were limited to distances within 10 km of the Lime Kiln, East Point, and the ULS hydrophones. Approximately 3.2 million time-stamped AIS vessel position records were obtained. For each site, only AIS records for vessel traffic that would be expected to have an effect on measured sound levels were included. This was done by discarding AIS records at locations beyond 10 km range or at locations that would be undetectable at the hydrophone, whichever threshold was closer. The maximum detection range in any direction was taken to be the distance to the 120 dB transmission loss contour (at 300 Hz for sound speed Profile 2; see Section 2.3). Approximately 1.6 million AIS records were retained in the traffic analysis.

Vessel tracks were created by grouping time-stamped AIS position records for a given vessel (maritime mobile service identity (MMSI)) where consecutive AIS record times differed by less than 6 minutes. The number of vessel hours for each record was determined from the accumulated time differences between consecutive records within tracks. These data were analyzed to quantify the vessel traffic within different vessel categories, speeds, distances from the hydrophones, and temporal trends in the AIS vessel traffic.

2.4.2. Traffic volume at Lime Kiln, East Point, and ULS

Traffic volume was assessed using the MarineTraffic AIS data according to the number of large commercial vessel hours at each site. Large commercial vessel categories include Bulker/General Cargo, Container, Passenger (over 100 m), Tanker, Ferry, and Vehicle Carrier. At each site, the quartiles for the number of large commercial vessel hours per day were calculated; local time was used to assess daily traffic volume. Low, medium, and high traffic volume days were defined based on the percentiles of daily large commercial vessel hours (Table 4) at each site, because vessel traffic volume differed substantially between sites. Section 3.4.1 contains the site-specific daily traffic volume percentiles. Then the distributions of hourly decade-band sound levels were analyzed as a function of vessel traffic volume category for two months. Sound levels are presented in box-and-whisker plots, and percentiles are shown in tables.

Table 4. Relationship between low, medium, and high traffic volume days and the percentiles of daily large commercial vessel hours.

Traffic volume	Daily large commercial vessel hour interval
Low	0 to 25th percentile
Medium	25th to 75th percentile
High	75th to 100th percentile

2.4.3. AIS versus non-AIS traffic in Boundary Pass

Boundary Pass is a spatially restricted marine area used as a major shipping route into the Port of Vancouver, connecting Haro Strait and the Strait of Georgia. Since December 2016, the University of Victoria has been monitoring AIS and non-AIS vessel traffic in Boundary Pass using a land-based camera at East Point, Saturna Island, BC.

This remote camera unit points across the northern end of Boundary Pass, collecting imagery data on vessel traffic moving through Boundary Pass. The field of view captures Skipjack Island at the centre of Boundary Pass and is bounded by Waldron Island in the background (Figure 9). The camera is set to capture a burst of three images separated by a 5-second interval at the beginning of every minute during daylight hours, as based on civil twilight. During fair weather conditions, these images provided sufficient

resolution to detect even small vessels (i.e., 5–10 m vessel length) across the width of Boundary Pass against Waldron Island, a distance of ~7.5 km (Figure 10).

To assess vessel traffic in Boundary Pass throughout the year, vessel traffic was quantified and characterized using imagery data from a sample winter month (February) and a sample summer month (August) in 2017. Collected images were manually processed using a specially developed tool that highlighted AIS-broadcasting vessels present in each image and detailed the AIS class (A versus B) and MMSI number. AIS Class A transponders receive higher priority on the AIS channel and are generally used by commercial vessels, whereas Class B transponders are less expensive and often used by recreational vessels. AIS information was collected via a land-based Digital Yacht AISnet base station receiver at the camera location. For each detected vessel, it was noted whether the vessel was broadcasting ("AIS") or non-broadcasting ("non-AIS"), distance from shore to Saturna Island, and vessel type (see Appendix E, Tables 27–28 for details on AIS and non-AIS vessel type categorization). Small non-AIS vessels were classified as "motorboat" when the vessel type was not identifiable but clearly not a sailboat. Vessel distance was determined by calibrating against known distance points on Skipjack Island.

To establish a valid comparison between the representative summer and winter month, a 21-day sampling period was selected in each month during which the camera was fully operational (see Appendix E, Table 29 for details on selected sampling period).

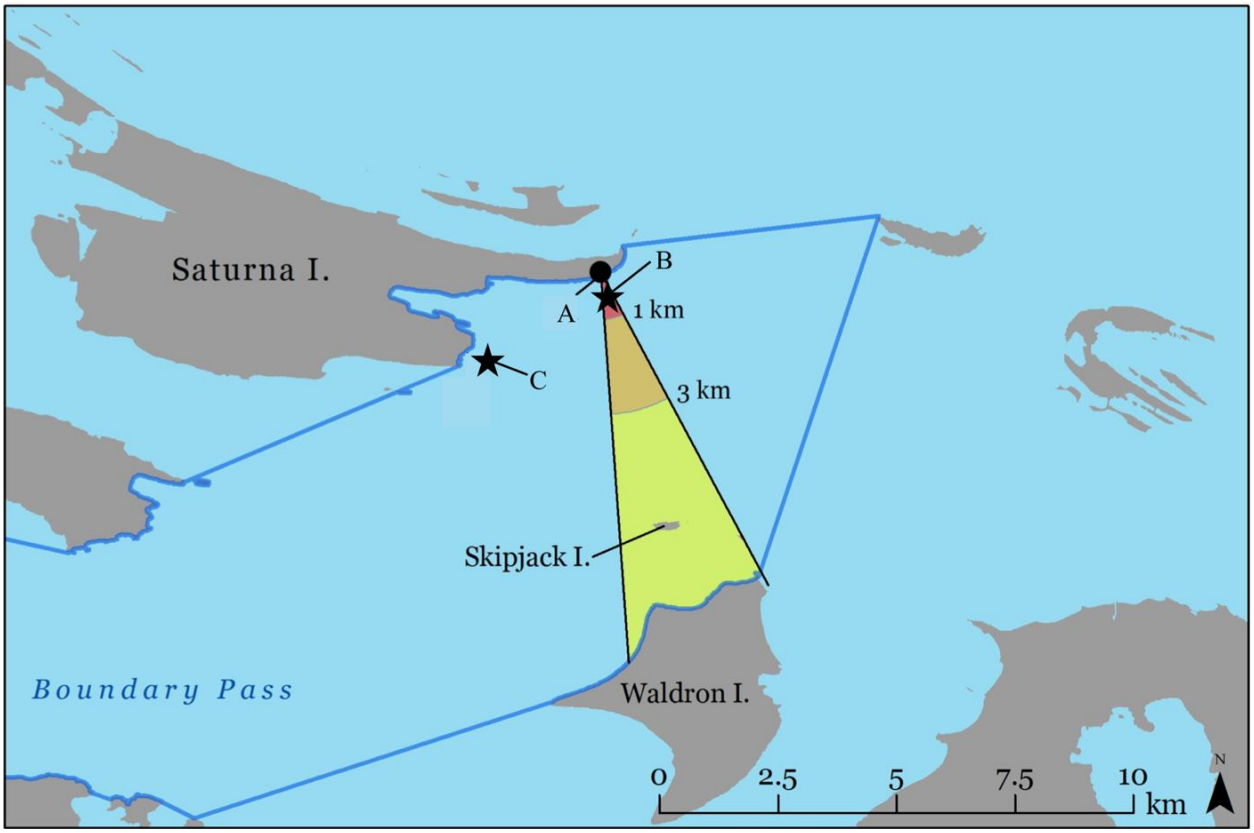

Figure 9. A land-based camera unit (A) on East Point, Saturna Island captured images of vessels moving through Boundary Pass, BC (outlined in dark blue). Two hydrophones collected data on ambient noise levels within Boundary Pass: East Point hydrophone (B) is located in line with the camera at A, while Monarch Head hydrophone (C) is located ~3 km southeast of the camera. The triangular area outlines the camera's field of view with different colours representing three distance bands: the red area is within 1 km ("Near"), orange is between 1 and 3 km ("Mid"), and yellow is greater than 3 km from the camera ("Far").

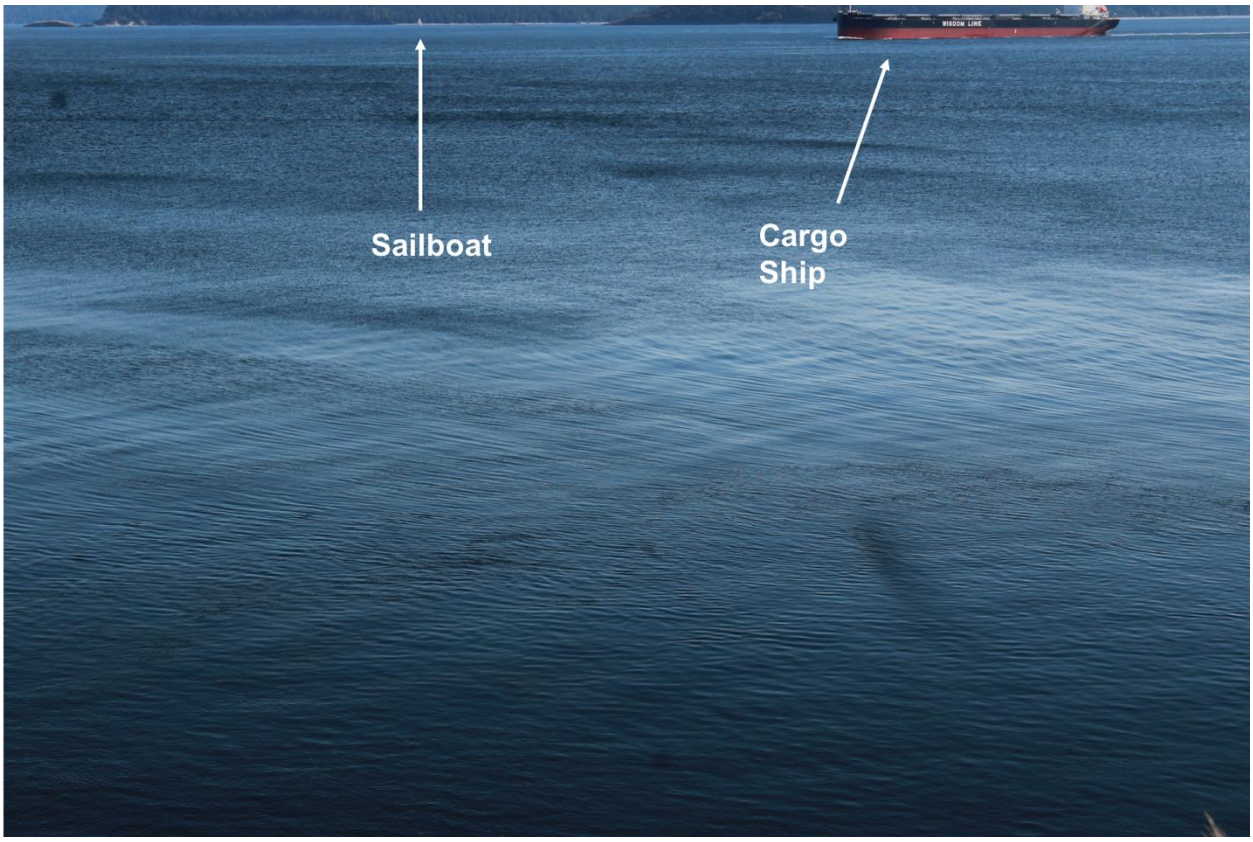

Figure 10. Cargo ship and sailboat moving through Boundary Pass, 28 Aug 2017. Imagery collected by the land-based camera provided sufficient resolution to detect vessels at a distance of over 7 km.

To evaluate noise contributions of AIS and non-AIS vessels in Boundary Pass, ambient noise levels detected by near-shore hydrophones on Saturna Island, BC, were compared to vessel presence, type, and distance-to-shoreline data. Vessel traffic was assessed on a minute-by-minute basis for comparison with detected ambient noise levels across four decade bands during a concurrent 1-minute window. These "vessel-minutes" were the basis of the comparisons between vessel traffic and ambient noise levels: each vessel-minute detailed the number of vessels, the broadcasting status (AIS versus non-AIS), vessel type, distance to the Saturna Island shoreline, and noise levels across four frequency ranges. Vessel-minutes during which acoustic or camera data were unavailable were excluded, and the combined data were truncated to include only daylight hours based on civil twilight hours (see Appendix E Tables 30 and 31 for details on the truncated daytime sampling periods). For vessel distance, vessels within 1 km of the camera position on the Saturna shoreline were categorized as "Near", vessels moving through the middle of Boundary Pass between 1–3 km as "Mid", and those exceeding a 3 km distance as "Far" (Figure 9). During high traffic-volume periods, camera images often captured multiple vessels across different distance zones. Noise contributions from vessels nearer the shoreline and hydrophone were expected to have a more substantial contribution to recorded ambient noise levels. Therefore, vessels detected over different distance zones (but of the same broadcasting status; i.e., AIS versus non-AIS) were grouped into the distance zone of the vessel closest to the hydrophone. Minutes when both AIS and non-AIS vessels were detected were excluded from analysis.

Compared to the high levels of non-AIS vessel traffic observed in Boundary Pass during summer, very little non-AIS traffic was present during winter. To provide sufficient data on non-AIS vessel presence for comparison to detected ambient noise levels across distance zones, an expanded study period from December 2016 to March 2017 was selected as the winter sample (see Appendix E, Table 30). Imagery data on vessel traffic was compared to ambient noise levels recorded by the East Point hydrophone deployed in-line with the camera. Any sampling days when the hydrophone was nonoperational were

excluded, as were days when the camera collected an incomplete imagery dataset. This rendered a total of 60 sampling days for the winter study period.

For summer, a representative week from 28 Jun to 4 Jul encompassing a period of high vessel traffic (see Appendix E, Table 31) was selected for analysis. This 7-day period provided sufficient data on both AIS and non-AIS vessel detections during summer. As ambient noise data from the East Point hydrophone were unavailable during summer, acoustic data collected by the Monarch Head hydrophone located 3 km southwest of the camera unit (see Figure 9) were relied on. Given the position of Monarch Head hydrophone relative to the camera, all "Near" AIS and non-AIS vessel detections were grouped with "Mid"-zone detections in Boundary Pass.

2.4.4. Large- and small-vessel traffic at Lime Kiln

The effect of large- and small-vessel traffic on ambient noise levels at Lime Kiln was assessed using acoustic detectors and AIS data during January and July 2017 as representative months for winter and summer. Ambient noise metrics were parsed into 1-minute time periods. An energy band detector that compared SPL in the 100–1000 Hz decade band with SPL in the 10–100 kHz decade band determined if large-, small- or no-vessels were present in each minute of data. If the SPL in the 100–1000 Hz decade band is above 105 dB re 1µPa but below 105 dB re 1µPa in the 10–100 kHz decade band, then a ship is considered to be present. If the SPL exceeds 105 dB re 1µPa in both of these decade bands, a boat is considered to be present. A total of 120 minutes of audio data were checked manually to validate the acoustic detector. These 120 minutes were randomly subsampled by month, day/night, and detection type (i.e., large-, small-, or no-vessel) such that each combination had ten minutes (e.g., January daytime with large-vessels had ten randomly chosen minutes for validation.). These detections were also compared to AIS data within 6 km of Lime Kiln. Cumulative probability plots were used to compare ambient noise levels when large-, small- and no-vessels were present at Lime Kiln.

2.5. Influence of Biological Presence

The effect of biological presence on ambient noise levels was analyzed by comparing sound levels during periods with and without marine mammal vocalization detections. For the Lime Kiln data, periods with validated SRKW vocalization and echolocation click detections were focused on. For the East Point and the ULS data, the contribution of killer whale vocalizations during the days with the highest number of detections per species was analyzed. Analysis of humpback whale vocalizations was also performed using ULS data. Time periods without detections were selected from periods before or after detections to minimize the effect of time-varying ambient noise conditions. The time period before and after detections was chosen based on the site-specific vocalization detection time resolution. Times with other noise-contributing factors (e.g., vessel presence) were not excluded from the analysis because they were assumed to have a consistent effect around the vocalization detection time periods.

3. Results

3.1. System Noise, Sensitivity Range, and Calibration

3.1.1. Lime Kiln

The hydrophone at Lime Kiln was calibrated before deployment, from 10 Hz to 2 kHz, by the U.S. Naval Undersea Warfare Center. From 5 to 100 kHz, the manufacturer (Reson) provided their own calibration response for this specific hydrophone. These two sensitivity curves were combined and adjusted based on pistonphone calibrations in the field at 250 Hz using a GRAS 42AC pistonphone with the acoustic system assembled at Lime Kiln, but with the hydrophone cable looped back to shore so that the hydrophone was temporarily on land. These calibrations occurred on 12 Aug 2016 and 26 Jun 2017.

Hardware specifications at Lime Kiln are provided in Table 5. The sensitivity of the hydrophone by frequency is plotted in Figure 11. The pistonphone calibrations on 12 Aug 2016 and 26 Jun 2017 found the same sensitivity at 250 Hz. This suggests that the hydrophone sensitivity did not change during this period, and therefore only a single curve is depicted in Figure 11.

To estimate the noise floor of the combined acoustic system, the following three methods were applied:

1. Calculating power spectral density (PSD) with the hydrophone in air during calibrations,
2. Comparing the minimum 1/3-octave-band levels across months, and
3. Identifying frequency regions in month-long PSD plots where the lower percentile levels approached a constant value.

The PSD method (method 1 above) involved using the two pistonphone calibration periods. Twenty seconds of quiet audio data were extracted when the pistonphone coupler was attached to the hydrophone but no piston tone was being produced. The 95% exceedance percentile PSD were extracted and plotted for these two periods in comparison to each other and with the manufacturer reported noise floor for the hydrophone.

The in-air PSD measurements are provided in Figure 12. If the manufacturer reported noise floor is taken as a level that indicates a system performing within specifications, then any deviations in estimates of the system noise that are above the manufacturer noise floor may indicate a raised noise floor. In the 2016 noise floor estimate, most PSD levels were below the manufacturer's noise floor, with a few exceptions (e.g., the spike at 240 Hz) that were probably driven by electrical noise in the Lime Kiln lighthouse. In 2017, the noise floor estimate below ~300 Hz increased consistently above the manufacturer’s noise floor, suggesting an elevated noise floor at these frequencies. This was also true in the 2017 data above ~20 kHz. These high-frequency spikes may have been related to changes in electrical noise in the lighthouse, as different equipment by other users was swapped out. This elevated noise floor during the 2017 calibration may have been short-term noise and not indicative of typical noise floor conditions.

The 1/3-octave-band level noise floor estimate (Figure 13) did not show any consistent deviation between the selected months at frequencies <300 Hz, until December 2017 when a spike from a 60 Hz hum was evident. Likewise, at other frequencies there was no consistent temporal trend in levels, suggesting that the system had a similar noise floor during 2016 and 2017.

The month-long PSD plot in Figure 14 shows percentile levels dropping sharply below ~20 Hz (annotation 1) due to a 10 Hz high-pass filter implemented on the digitizer. Percentile levels approach each other above ~10 kHz (annotation 2), which suggests that the system noise floor was reached above these frequencies. This means that the system was unable to record PSD below this noise floor, but it was still be able to measure above the noise floor.

Table 5. Lime Kiln: Hardware specifications.

Hardware	February 2016 to December 2017
Hydrophone model	Reson TC4032-1
Number of hydrophones	1
Nominal hydrophone sensitivity	−164 dB re 1 V/µPa
Sample rate	250 ksps
Bits per sample	16
Digitizer	SAIL DAQ
Recorder	PAMGuard installed on computer
Power supply	DC from battery in Lighthouse
Calibration method	GRAS pistonphone (250 Hz)

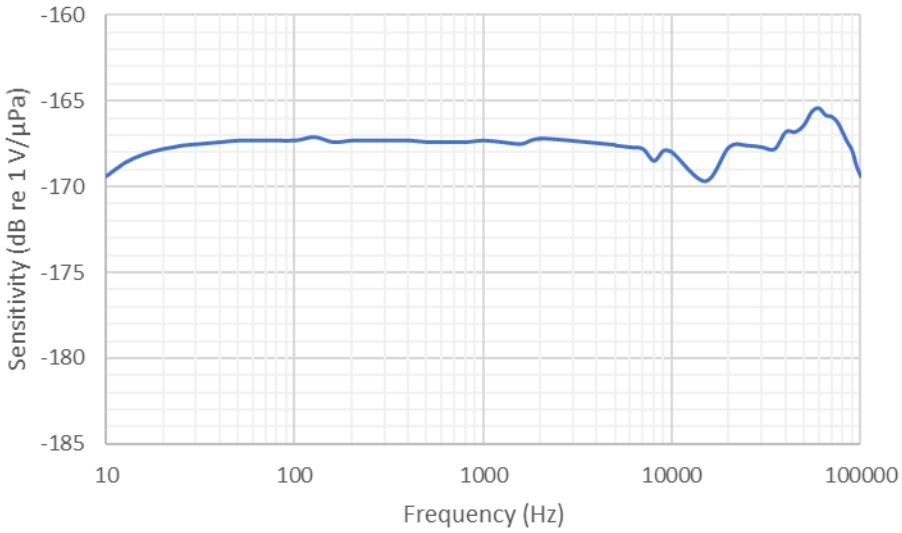

Figure 11. Lime Kiln: Recorder sensitivity as a function of frequency.

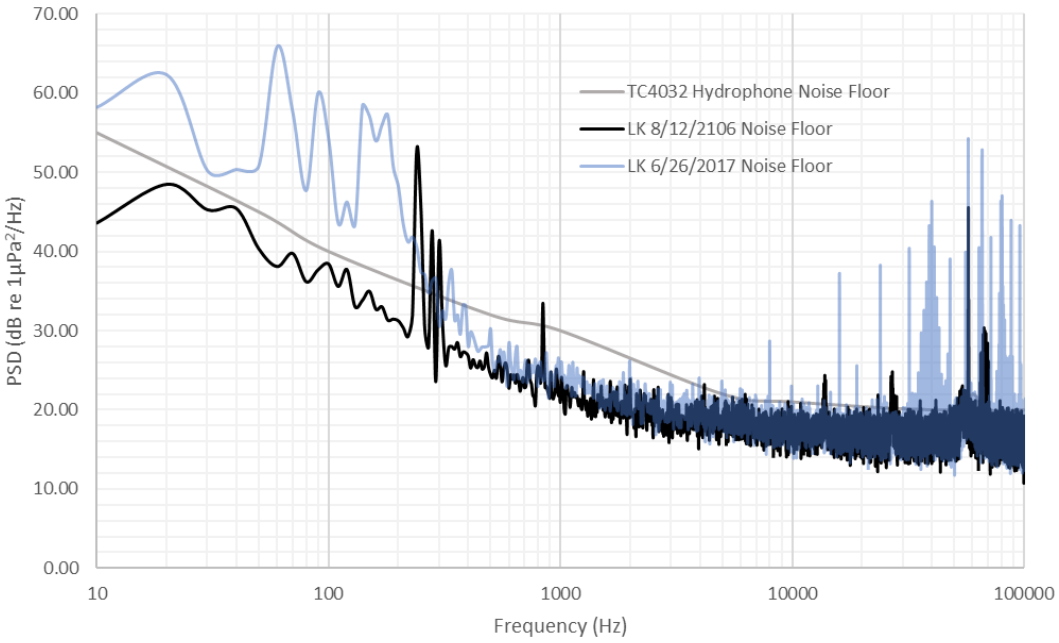

Figure 12. Lime Kiln: Noise floor for Reson TC4032 hydrophone and the recording system during pistonphone calibration in August 2016 and June 2017. Units are Power Spectral Density (PSD) levels.

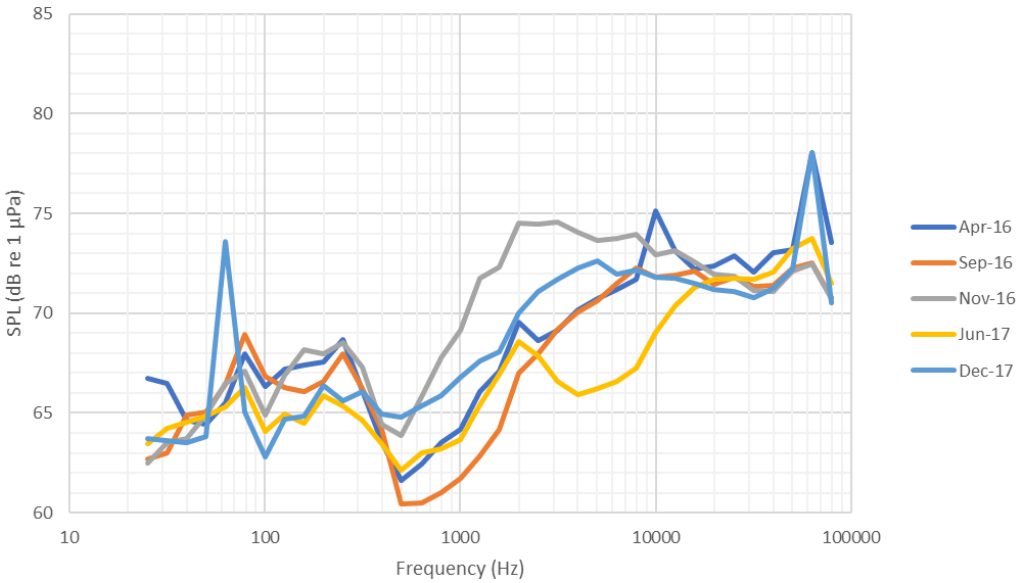

Figure 13. Lime Kiln: Minimum 1/3-octave-band sound pressure levels (SPL; 1 minute average) during different months of the study period.

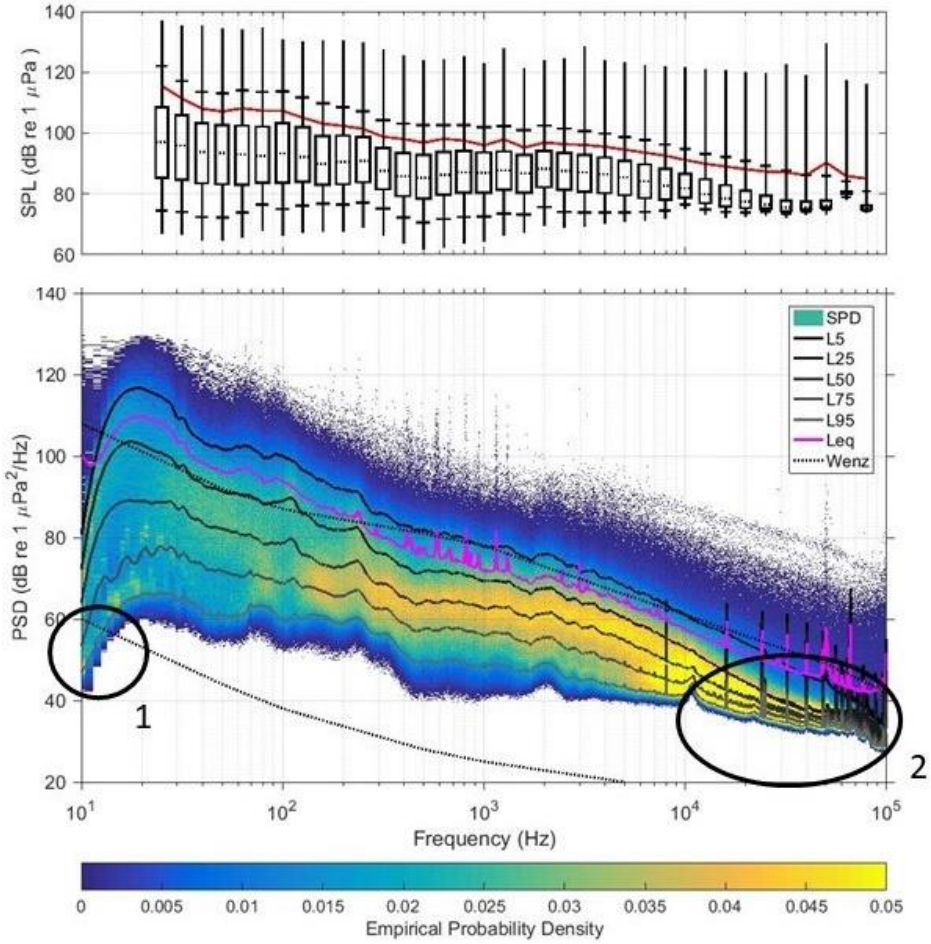

Figure 14. Lime Kiln: One-third-octave-band and power spectral density (PSD) levels recorded from 21 Apr 2016 to 21 May 2016 with annotated system noise features. Annotation 1 indicates the effect of a 10 Hz high-pass filter. Annotation 2 indicates the reaching of the system noise floor.

3.1.2. East Point

Hardware specifications at East Point are provided in Table 6, and Figure 15 shows the sensitivity of the recording system as a function of frequency. ONC records indicate the hydrophones were calibrated by ONC and/or the equipment manufacturer (Ocean Sonics), but the calibration methods are unknown.

Figure 16 shows minimum 1/3-octave-band SPL (1-minute average) during selected months of the study period. The spike in the 60 Hz band was due to induced noise from the power supply. The level of this tone fluctuated over time and is discussed further in this section. Band levels were consistent between months, except during August 2016 for frequencies above ~150 Hz. Sound levels in the 32 kHz band were much lower than those in the adjacent 25 kHz band because of a low-pass anti-aliasing filter.

System-noise sources and their characteristics are listed in Table 7, and their effects on PSD levels are shown in Figure 17. There were many tones in the 100–3000 Hz range that were harmonics of the 60 Hz power supply noise. There was also system noise around 16.6 kHz, which was due to a BC Hydro solar panel that feeds into the power grid.

Table 6. East Point: Hardware specifications.

Hardware	January 2016 to March 2017
Hydrophone model	icListen HF
Number of hydrophones	1
Nominal hydrophone sensitivity	−171 dB re 1 V/µPa
Sample rate	64 ksps
Bits per sample	24
Digitizer	icListen HF
Recorder	Computer
Power supply	BC Hydro AC

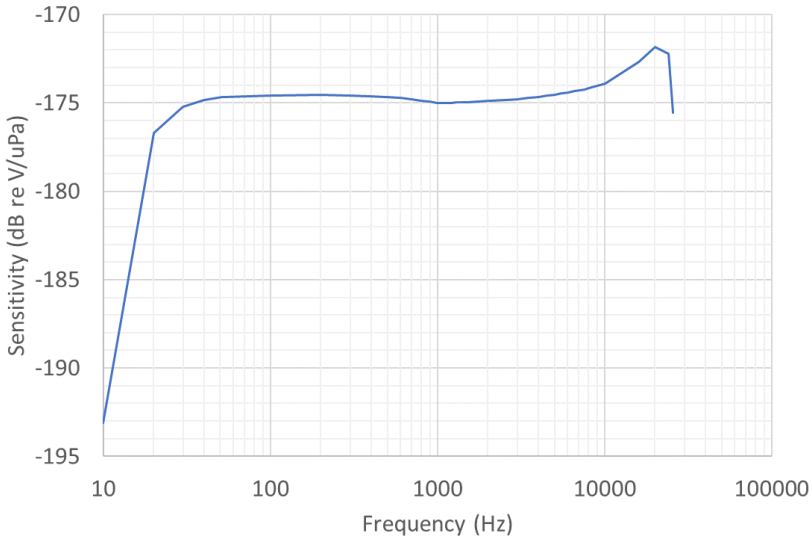

Figure 15. East Point: Recorder sensitivity as a function of frequency. Recorder sensitivity above 25.6 kHz was unavailable.

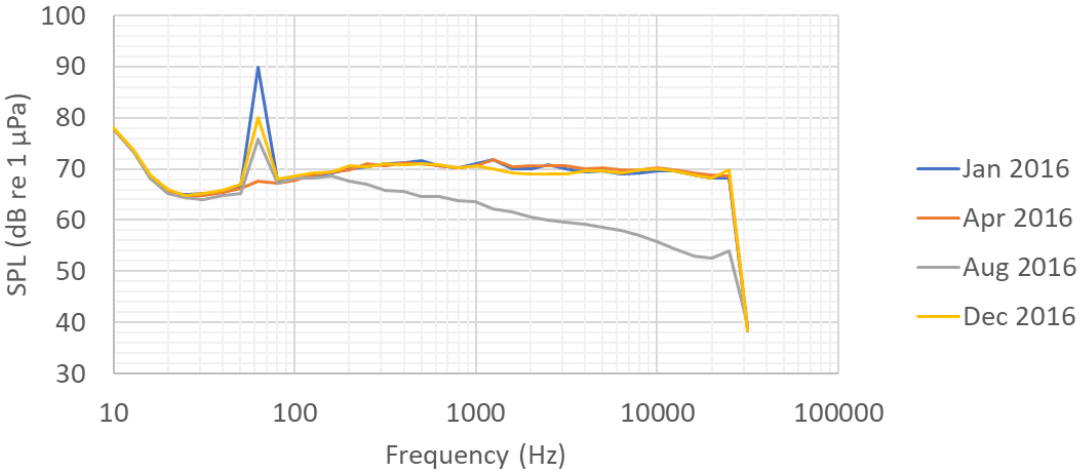

Figure 16. East Point: Minimum 1/3-octave-band sound pressure levels (SPL; 1 minute average) during different months of the study period. The spike at 60 Hz was due to a power supply issue.

Table 7. East Point: System noise sources observed from January to December 2016.

Source	Description	Frequencies	Percentile affected	Sound level	Annotation and figure reference
Anti-aliasing filter	Low levels of high-frequency sound	25–32 kHz	All	Sound levels in this frequency range are higher than reported	Annotation 1 in Figure 66
Power supply	Tone	60 Hz	All	89.8–117.6 dB re 1 µPa	Annotation 1 in Figure 17 Annotation 1 in Figure 67
Power supply harmonics	Tone	180, 300, 420, 480, 540, 660, 780, 900, 1020, 1140, 1260, 1380, 1500, 1620, 1740, 1860, 1980, 2100, 2220, 2460, 2580, 2700, 2820, 2940, 3060, 3180, 3300, and 3780 Hz	L_{95}, L_{75}, L_{50}, L_{25}	75.7–91.0 dB re 1 µPa	Annotation 2 in Figures 17, 68, 69, and 70
BC Hydro solar panel feeding BC Hydro power grid	Tone	16666, 16544, and 16785 Hz	All	57.0–64.1 dB re 1 µPa	Annotation 3 in Figure 17
Noise floor	Lower-level percentiles converge	Up to ~40 Hz for the listed percentiles affected and at higher frequencies (up to ~500 Hz) for lower sound levels	L_{95}, L_{75}, L_{50}, L_{25}	Sound levels are lower than reported	Annotation 4 in Figure 17

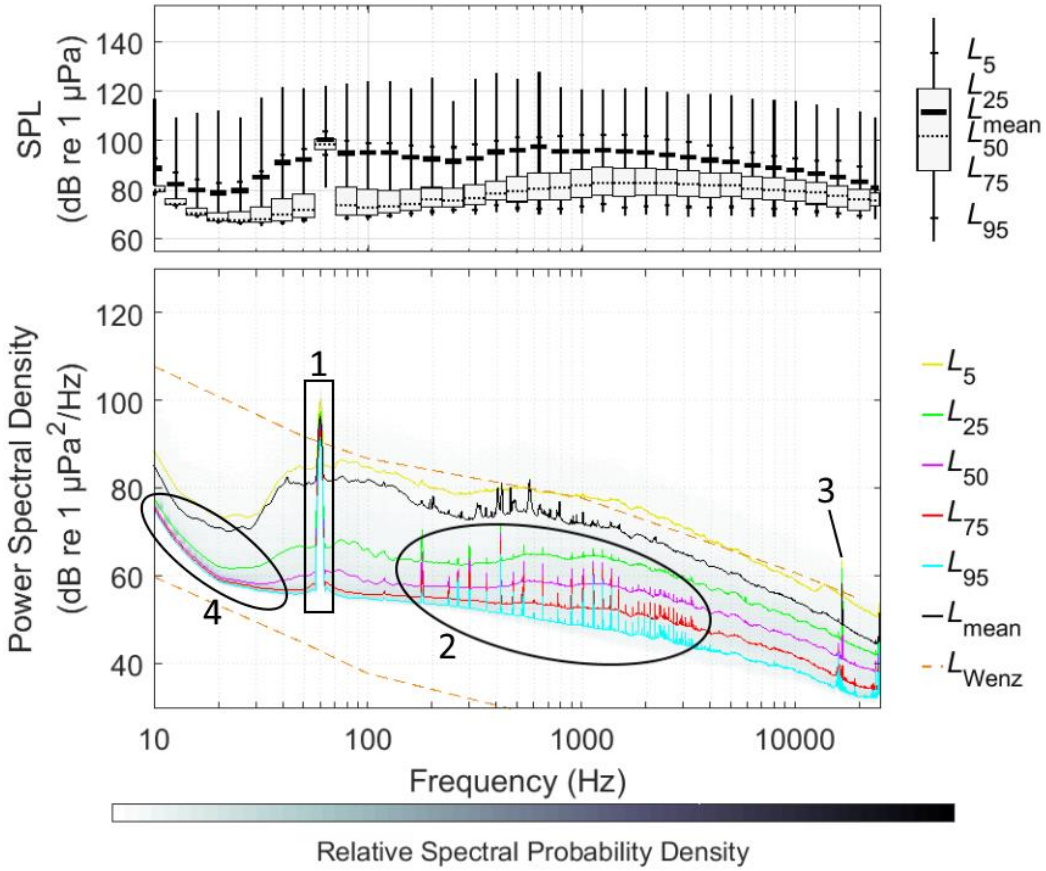

Figure 17. East Point: One-third-octave-band and power spectral density (PSD) levels recorded from 22 Jan 2016 to 21 Feb 2016 with annotated system noise features. Annotation 1 shows the 60 Hz power supply tone. Annotation 2 shows harmonics from the power supply tone. Annotation 3 shows tones from a BC Hydro solar panel feeding the power grid. Annotation 4 shows the low-frequency noise floor. See Table 7 for more details.

3.1.3. Monarch Head

Hardware specifications at Monarch Head are provided in Table 8, and Figure 18 shows the sensitivity of the recording system as a function of frequency. ONC records indicate the hydrophones were calibrated by ONC and/or the equipment manufacturer (Ocean Sonics), but the calibration methods are unknown.

Figure 19 shows minimum 1/3-octave-band SPL (1-minute average) during selected months of the study period. Minimum band levels were consistent between months, except during December 2017 when minimum levels were lower than other months. The sample rate of this hydrophone was increased in August 2017, which is why the plotted bandwidth is larger in August and December 2017. Sound levels in the highest frequency band were much lower than those in the second-highest frequency band because of the low-pass anti-aliasing filters (which had different cut-off frequencies depending on the sample rate).

System-noise sources and their characteristics are listed in Table 9, and their effects on PSD levels are shown in Figures 20 and 21. This system did not have the strong 60 Hz power supply tone and the related harmonics like at East Point, but noise from the Global Positioning System (GPS) signal contaminated low-frequency measurements during quieter periods. There were also several tones in the 300–10000 Hz range that only appear at the L_{50}, L_{25}, and L_5 percentiles, which indicates these tones were not present in all recordings but were substantially above background noise when present (Annotation 4 in Figure 20). These tones were caused by the recorder's solar power supply and were present during daylight hours. A calibration error was present in the August to December 2017 data, which affected measured sound levels above 25 kHz (Annotation 1 in Figure 21).

Table 8. Monarch Head: Hardware specifications.

Hardware	Jan to Jul 2017	Aug to Dec 2017
Hydrophone model	icListen HF	
Number of hydrophones	1	
Nominal hydrophone sensitivity	−171 dB re 1 V/µPa	
Sample rate	64 ksps	128 ksps
Bits per sample	24	
Digitizer	icListen HF	
Recorder	Computer	
Power supply	Solar panel and battery	

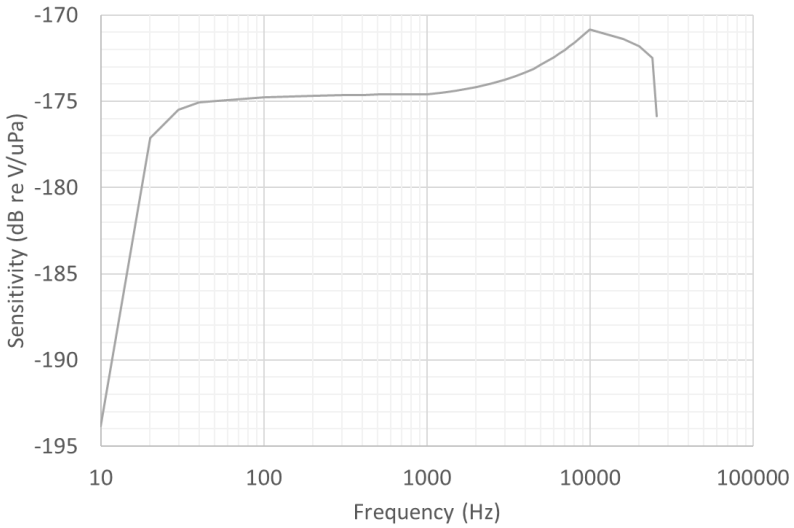

Figure 18. Monarch Head: Recorder sensitivity as a function of frequency. Recorder sensitivity above 25.6 kHz was unavailable.

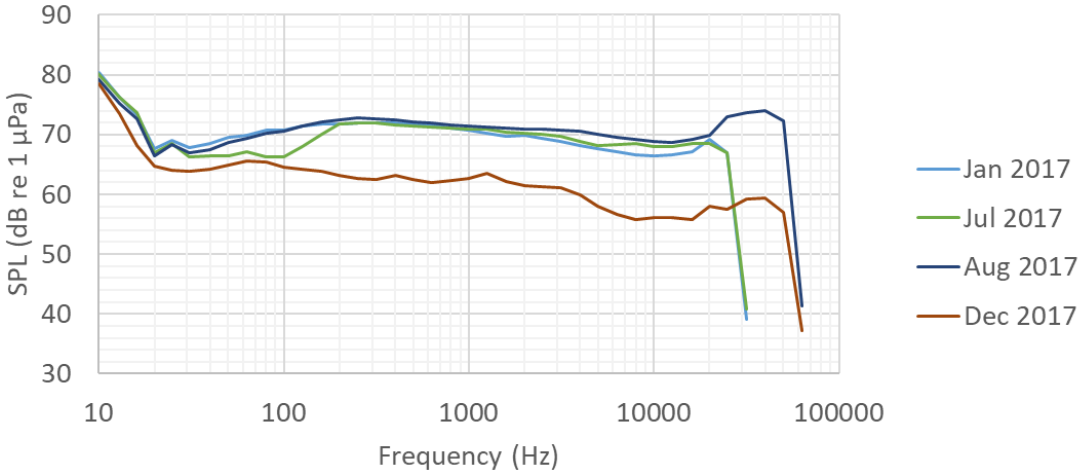

Figure 19. Monarch Head: Minimum 1/3-octave-band sound pressure levels (SPL; 1 minute average) during different months of the study period. Levels from August and December 2017 are shown up to 64 kHz because the recorder sampled at 128 kHz during this period. Levels in the highest frequency band were substantially lower than those in the second-highest frequency band because of the anti-aliasing filter, and were therefore artificially low.

Table 9. Monarch Head: System noise sources observed during different months of the study period.

Source	Description	Frequencies	Time period	Percentile affected	Sound level	Annotation and figure reference
Anti-aliasing filter	Low levels of high-frequency sound	25–32 kHz	Jan to Jul 2017	All	Sound levels in this frequency range are higher than reported	Annotation 1 in Figure 71
Pulse per second GPS chip	Double pulse	10 Hz to 5 kHz	Jan to Dec 2017	L_{95}, L_{75}, L_{50}	100.5–101.5 SPL, 113.7–115.9 peak (dB re 1 µPa)	Annotation 3 in Figure 71 Annotation 1 in Figures 72, 73 Annotation 1 in Figure 20
Switching power supply	Tone	20.6 kHz (900 Hz bandwidth)	Jan 2017	All	101.1 dB re 1 µPa	Annotation 2 in Figure 71, and Annotation 2 in Figure 20
Unknown	Tone	16 kHz	Jan, Jul, Aug 2017	L_{95}, L_{75}, L_{50}	40–45.8 dB re 1 µPa^2/Hz	Annotation 3 in Figure 20
			Dec 2017	L_{95}, L_{75}, L_{50}, L_{25}	68.7 dB re 1 µPa^2/Hz	-
Switching power supply	Tone	20 kHz	Jan, Jul, Aug 2017	All	44.9–45.3 dB re 1 µPa^2/Hz	-
			Dec 2017	L_{95}, L_{75}, L_{50}, L_{25}	67 dB re 1 µPa^2/Hz	-
Unknown	Tone	25 kHz (600 Hz bandwidth)	Aug 2017	Unknown	87.9 dB re 1 µPa	Annotation 1 in Figure 75
Unknown	Tone	37.5 kHz (300 Hz bandwidth)	Aug 2017	Unknown	82.2 dB re 1 µPa	Annotation 2 in Figure 75
Unknown	Tone	50 kHz	Aug 2017	Unknown	Too low relative to background levels to determine sound level	Annotation 3 in Figure 75

Source	Description	Frequencies	Time period	Percentile affected	Sound level	Annotation and figure reference
Anti-aliasing filter	Low levels of high-frequency sound	50–64 kHz	Aug to Dec 2017	All	Sound levels in this frequency range are higher than reported	Annotation 4 in Figure 75
Calibration error	High-frequency sound levels reported too high	25–50 kHz	Aug to Dec 2017	All	Unknown	Annotation 1 in Figure 21
Unknown	Near-constant pressure time series (no acoustic signals recorded)	0–64 kHz	Sporadic in Dec 2017	All	N/A	Annotation 1 in Figure 77
Unknown	Tone	10.6 kHz (150 Hz bandwidth)	Dec 2017	L_{95}, L_{75}	86.8 dB re 1 µPa	Annotation 1 in Figure 76
Unknown	Tone	21.1 kHz (500 Hz bandwidth)	Dec 2017	All	93.6 dB re 1 µPa	Annotation 2 in Figure 76
Unknown	Tone	31.7 and 42.2 kHz	Dec 2017	All	Too low relative to background levels to determine sound level	Annotations 3 and 4 in Figure 76
Noise floor	Lower-level percentiles converge	Up to ~40 Hz for the listed percentiles affected and at higher frequencies (up to ~300 Hz) for lower sound levels	Jan to Dec 2017	L_{95}, L_{75}, L_{50}, L_{25}	Sound levels are lower than reported	Annotation 5 in Figure 20
Solar power supply noise	Tones	300 Hz and higher-frequency harmonics	Jan to Dec 2017 during daylight hours	L_{50}, L_{25}, L_{5}	Sound levels are lower than reported	Annotation 4 in Figure 20

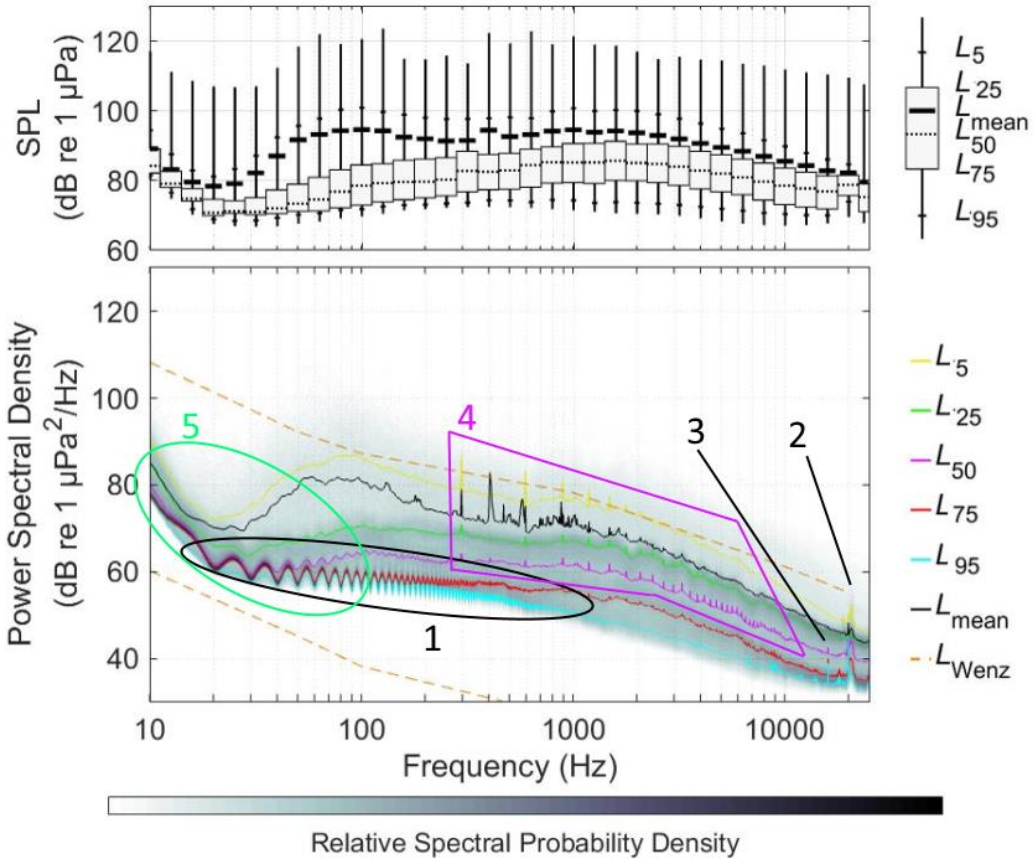

Figure 20. Monarch Head: Band and power spectral density (PSD) levels recorded from 26 Jan 2017 to 9 Feb 2017. Annotation 1 shows the effect from the Global Positioning System (GPS)-induced double pulse. Annotation 2 shows the 20.6 kHz switching power supply tone. Annotation 3 shows a 16 kHz tone from an unknown source. Annotation 4 shows solar power supply noise. Annotation 5 shows the low-frequency noise floor. See Table 9 for more details.

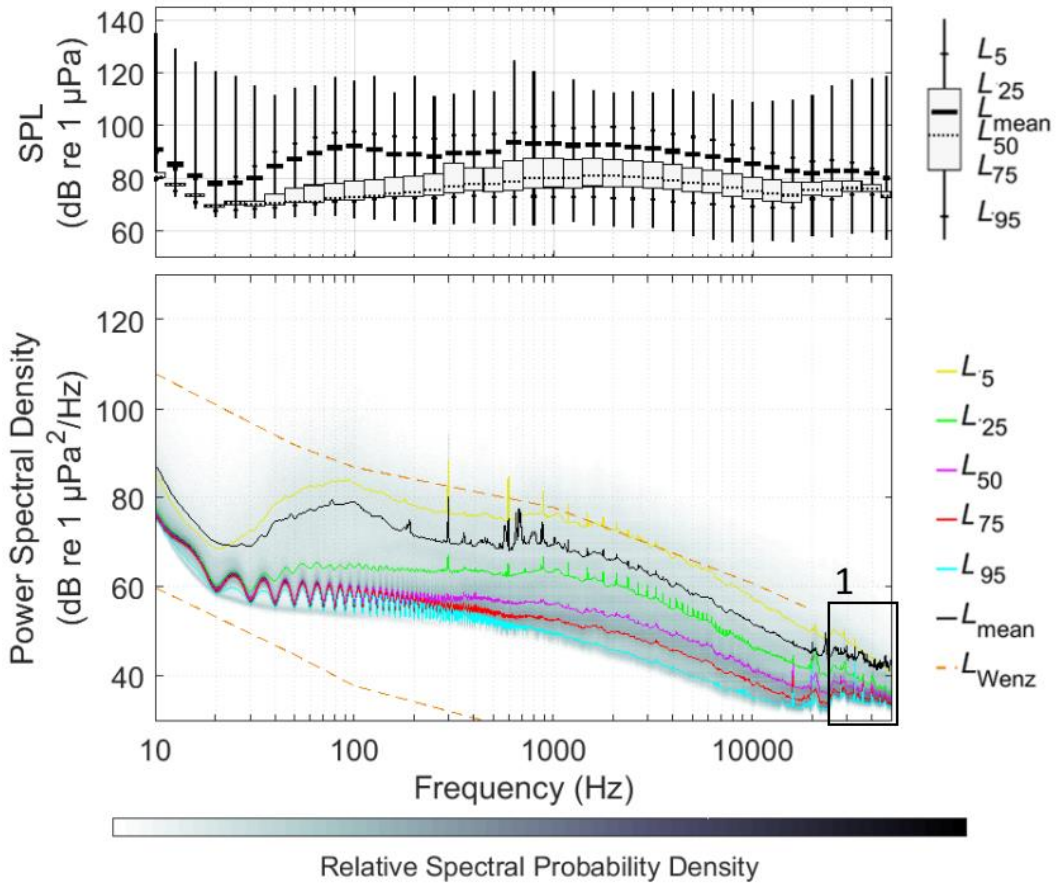

Figure 21. Monarch Head: One-third-octave-band and power spectral density (PSD) levels recorded from 2 Dec 2017 to 31 Dec 2017. Annotation 1 shows the effect of the calibration error (described in Table 9).

3.1.4. Strait of Georgia ULS

Strait of Georgia ULS used four hydrophones that were calibrated before deployment and after retrieval at 250 Hz using a GRAS 42AC pistonphone. An acoustic speaker was also used to play sounds in 1/3-octave-bands daily to check for drifting hydrophone sensitivity over time. One hydrophone was designated as the primary hydrophone for calculating and reporting sound levels.

Hardware specifications for the Strait of Georgia ULS are provided in Table 10. Figure 22 shows the sensitivity of the recording system as a function of frequency, and Figure 23 shows the noise floor of the system.

Figure 24 shows minimum 1/3-octave-band SPL (1-minute average) during selected months of the study period. Minimum band levels were generally consistent within a few decibels between months, except during November 2016 when minimum levels were higher than during other periods. This is attributed to an unknown noise source that was particularly loud during November 2016 (see Figures 80 and 81). The larger bandwidth in December 2017 was due to the increased sample rate during that period. Sound levels in the highest frequency band were lower than those in the second-highest frequency band because of the low-pass anti-aliasing filters (which had different cut-off frequencies depending on the sample rate). This effect was not as strong as at East Point and Monarch Head because the anti-aliasing filter was not as strong for the ULS.

System-noise sources and their characteristics are listed in Table 11, and their effects on PSD levels are annotated in Figure 25.

Table 10. Underwater Listening Station (ULS): Hardware specifications.

Hardware	January 2016 to October 2016 (Deployment 1)	November 2016 to October 2017 (Deployment 2)	November 2017 to December 2017 (Deployment 3)
Hydrophone model	GeoSpectrum M36-V35-100		
Number of hydrophones	4		
Nominal hydrophone sensitivity	−165 dB re 1 V/µPa		
Sample rate	64 ksps	64 ksps	128 ksps
Bits per sample	24	24	24
Digitizer	AMAR	AMAR	Observer
Recorder	JASCO drivers installed on ONC computer		
Power supply	Direct current from VENUS Strait of Georgia East node		
Calibration method	GRAS pistonphone (250 Hz) and acoustic speaker		

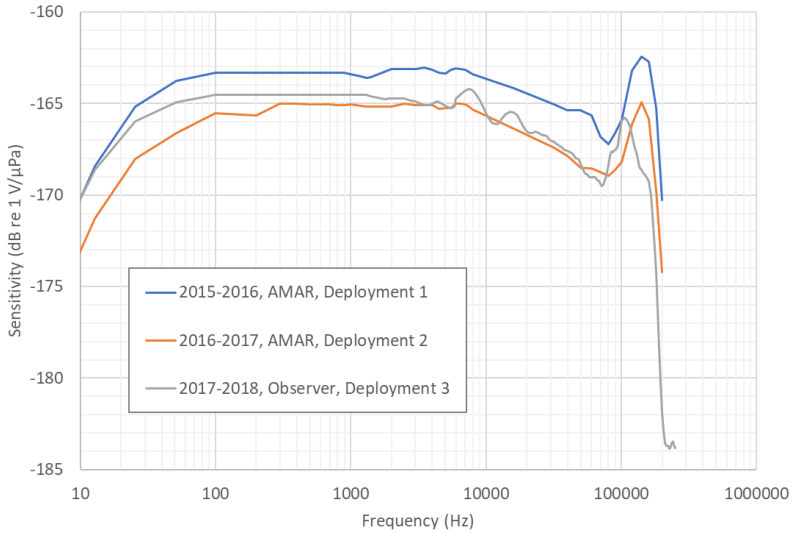

Figure 22. Underwater Listening Station (ULS): Recorder sensitivity as a function of frequency.

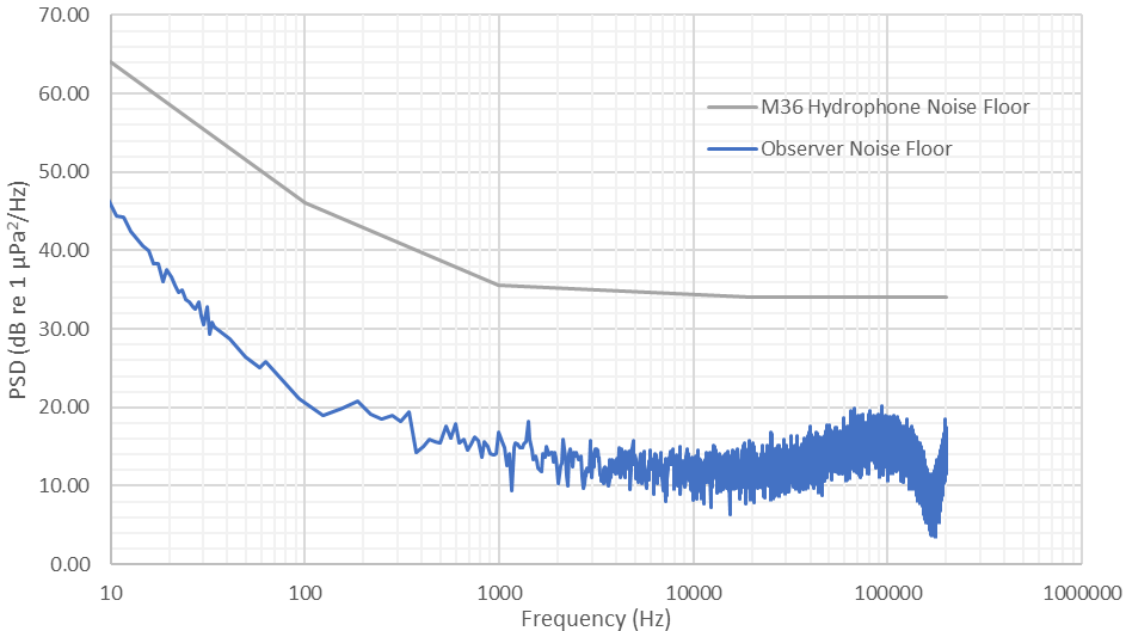

Figure 23. Underwater Listening Station (ULS): Noise floor for the GeoSpectrum M36 hydrophone and Observer. The Autonomous Multichannel Acoustic Recorder (AMAR) noise floor (not shown) was 3–6 dB lower than the M36 hydrophone noise floor. Units are Power Spectral Density (PSD) levels.

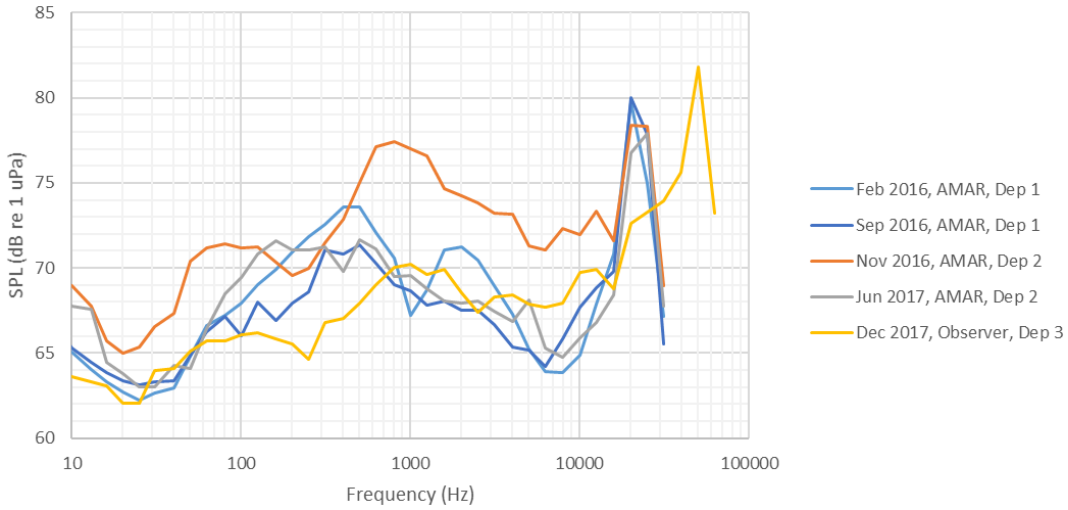

Figure 24. Underwater Listening Station (ULS): Minimum 1/3-octave-band sound pressure levels (SPL; 1 minute average) during different months of the study period. Higher levels for November 2016 were due to a particularly persistent unknown noise source during that month (also see Figure 80). The legend specifies the month and year, digitizer, and ULS deployment (“Dep”).

Table 11. Underwater Listening Station (ULS): System noise sources observed during different months of the study period.

Source	Description	Frequencies	Time period	Percentile affected	Sound level	Annotation and figure reference
ADCP	Brief pulse every 2 seconds	7–64+ kHz (15.0 kHz centre frequency)	2016–2017	L_{95}, L_{75}, L_{50}, L_{25}	70–85 dB re 1 µPa for bands >= 12 kHz	Annotation 1 in Figure 78 Annotation 2 in Figure 25,
Acoustic Zooplankton Fish Profiler (AZFP)	Brief pulse every 2 seconds	22–45 kHz (38 kHz centre frequency)	2016–2017	L_{95}, L_{75}, L_{50}, L_{25}	75–85 dB re 1 µPa for 20 and 25 kHz bands	Annotation 2 in Figure 78 Annotation 2 in Figure 25 Annotation 5 in Figure 83
Unknown	Tones	9, 10, 11.3, 20.1, 22.6, 30.2 kHz	2016–2017	All	77.5–108.7 dB re 1 µPa	Annotation 3 in Figure 78 Annotation 1 in Figure 79
Unknown	Tones	40.3, 45.2, 50.4, 56.5, 60.4 kHz	Nov to Dec 2017	All	83.1–101.2 dB re 1 µPa	Annotation 5 in Figure 83
Hydrophone noise floor	Low-frequency limit	10–30 Hz	2016–2017	L_{95}	65–70 dB re 1 µPa	Annotation 1 in Figure 25
Anti-aliasing filter	Low levels of high-frequency sound	60.5–64.0 kHz	Nov to Dec 2017	All	Sound levels in this frequency range may be higher than reported	Annotation 3 in Figure 83
Unknown[1]	Brief pulse every 2 seconds	0–32 kHz	Nov 2016	L_{95}, L_{75}, L_{50}, L_{25}	70–85 dB re 1 µPa for bands >= 12 kHz	Annotation 1 in Figures 80 and 81
Unknown	Infrequent mid-frequency sound	10–20 kHz	Jun 2017	None (less frequent than ADCP noise)	-	Annotation 1 in Figure 82
Unknown	Infrequent sound	52.8–54.0 kHz	Dec 2017	None (very infrequent)	-	Annotation 1 in Figure 83
Unknown	Infrequent sound	10–64 kHz	Dec 2017	None (very infrequent)	-	Annotation 2 in Figure 83

[1] This noise could have been caused by the ADCP as described with in this table.

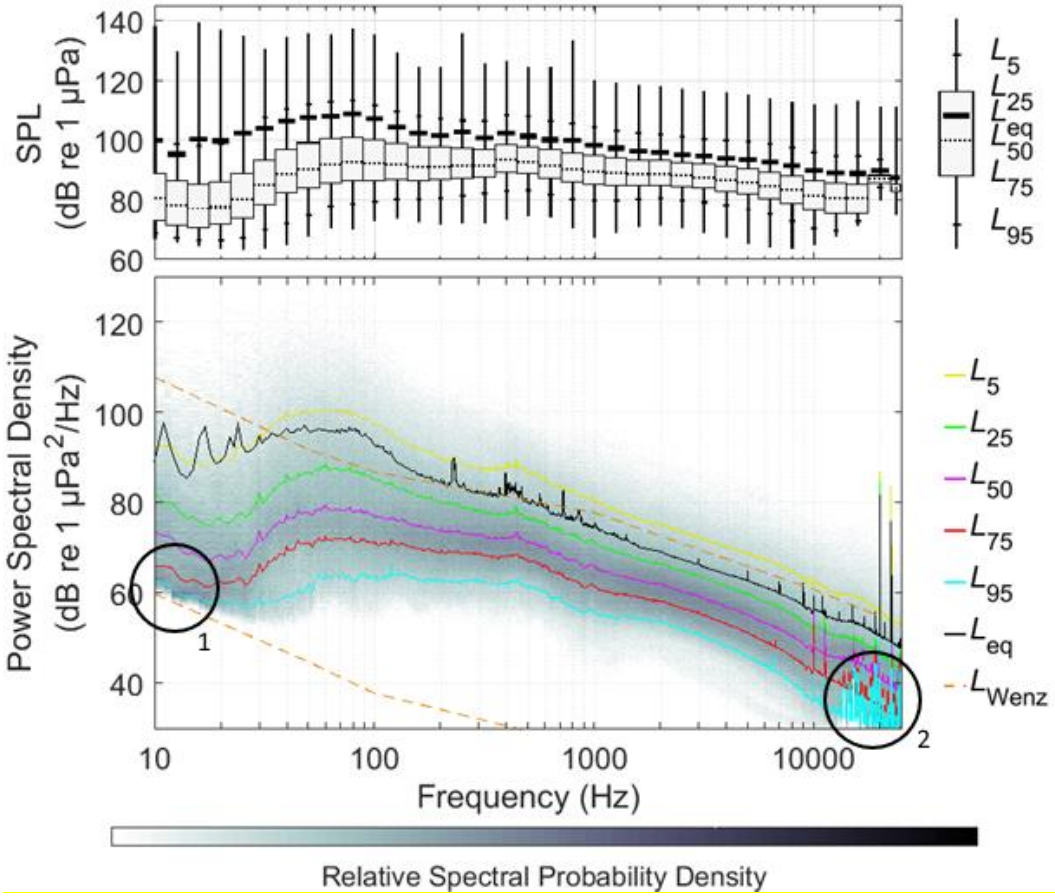

Figure 25. Underwater Listening Station (ULS): One-third-octave-band and power spectral density (PSD) levels recorded from 14 Feb 2016 to 12 Mar 2016 with annotated system noise features. Annotations are described in Appendix B.3.

3.2. Influence of Weather and Tidal Conditions

3.2.1. Water currents

The observed variations of sound levels with water currents are shown with 2-dimensional (2-D) histograms of SPL (1-minute average) in the 10–100 Hz decade band versus current speed magnitude (no substantial effect of water currents on sound levels above 100 Hz were observed). Figure 26 shows Lime Kiln results in January and July 2017, Figure 27 shows East Point results in January and July 2016, and Figure 28 shows the ULS results in January and July 2017. Water current speeds at the Lime Kiln and East Point hydrophone locations were obtained from the WebTide Tidal Prediction Model (v0.7.1) (Foreman et al. 2000, Institute of Ocean Sciences 2015) with 1-minute resolution (linearly interpolated from 1 hour resolution). For the ULS, water current speeds at the seabed were calculated from ADCP data recorded ~120 m from the station with a 1-minute resolution.

At Lime Kiln, there appears to be a weak trend of increasing SPL with increasing current velocity, particularly in the July dataset. The lack of a strong correlation is likely due to the poor ability of the WebTide model to predict currents at the Lime Kiln hydrophone. This is possibly because the WebTide model is less reliable at near-shore locations than at mid-channel locations (WebTide predictions generally showed good agreement with ADCP data at the ULS, as reported in MacGillivray et al. (2019)). At East Point, SPL appears uncorrelated with current speed. It is suspected this was because system noise from the 60 Hz power supply masked flow noise at East Point (see Section 3.1.2). At the ULS, there

was no SPL-current speed correlation at speeds less than ~0.3 m/s; however, at higher speeds, there was a strong correlation. A linear regression was fit to high-current, low-SPL data (i.e., data within the dashed lines in Figure 28) to quantify the effect of current speed on sound levels. Sound levels increased by ~55 dB per m/s between 0.4 m/s and 0.75 m/s current speed during January and July.

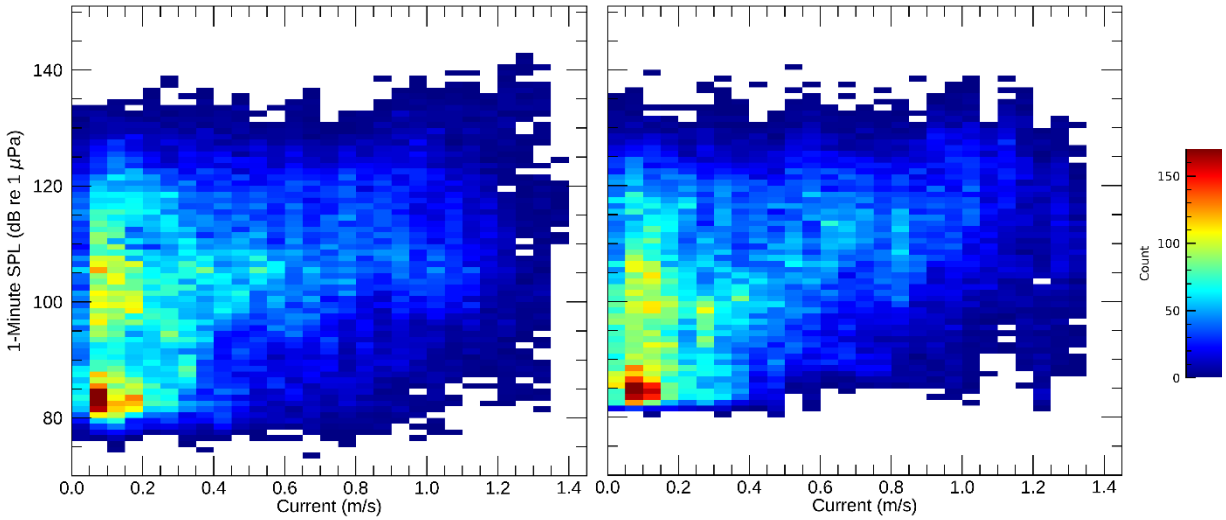

Figure 26. Lime Kiln: Sound pressure levels (SPL; 1-minute average) in the 10–100 Hz decade band as a function of water current speed for (left) January and (right) July 2017.

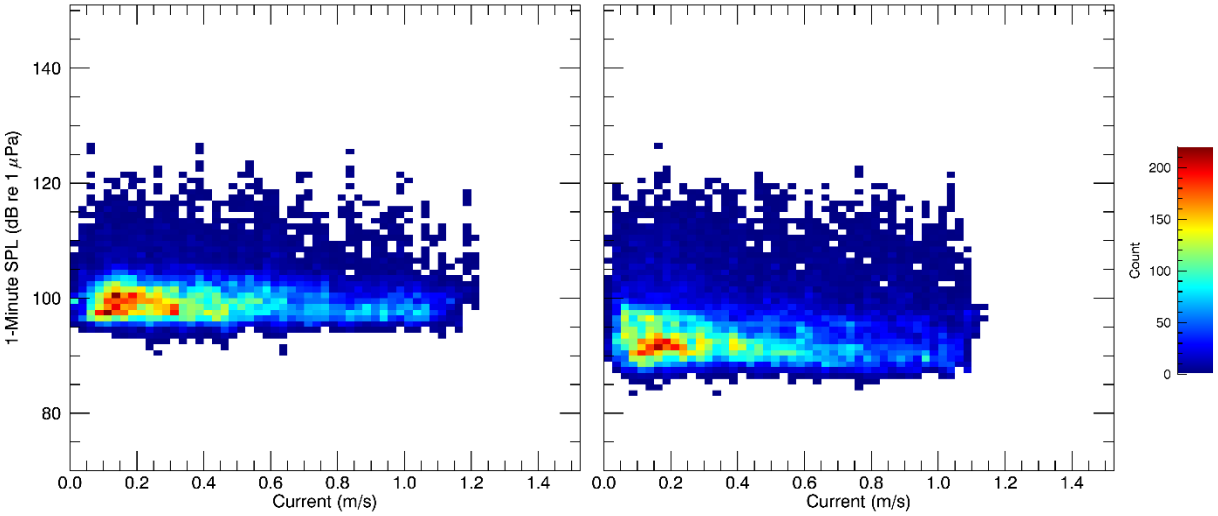

Figure 27. East Point in Boundary Pass: Sound pressure levels (SPL; 1-minute average) in the 10–100 Hz decade band as a function of water current speed for (left) January and (right) July 2016.

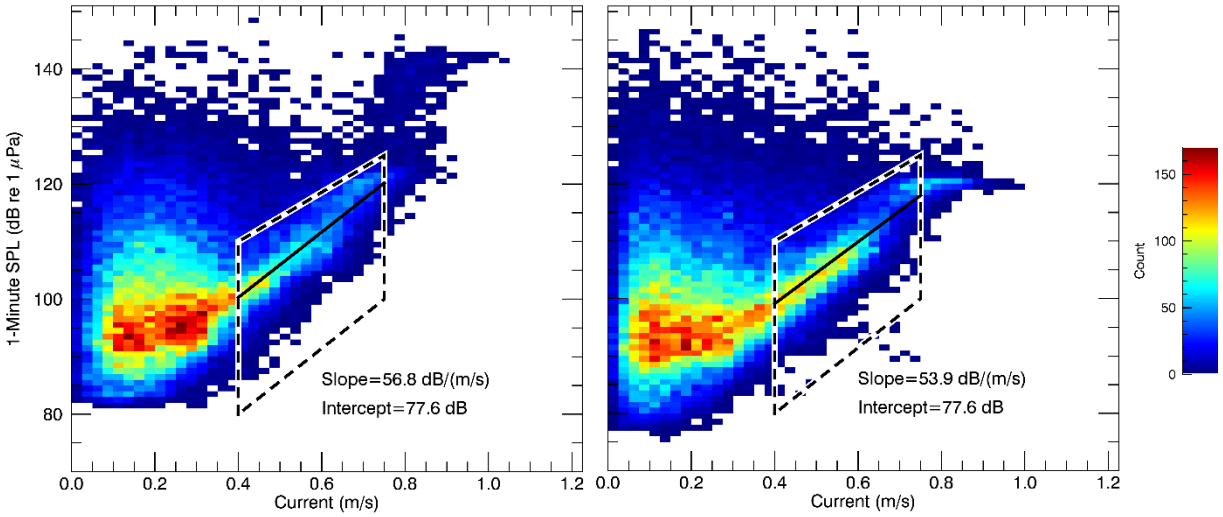

Figure 28. Underwater Listening Station (ULS) in the Strait of Georgia: Sound pressure levels (SPL; 1-minute average) in the 10–100 Hz decade band as a function of water current speed for (left) January and (right) July 2017. Linear regressions (solid black lines) were fit to the data within the dashed line.

3.2.2. Wind

The observed variations of sound levels with wind speed are shown with 2-D histograms of hourly SPL versus hourly wind speed magnitude, for the three decade frequency bands above 100 Hz. Figure 29 shows Lime Kiln results in January and July 2017, Figure 30 shows East Point results for January and July 2016, and Figure 31 shows the ULS results in January and July 2017. Hourly wind speed for Lime Kiln was obtained from the National Oceanic and Atmospheric Administration (NOAA) Environmental Buoy 46088 (~20 km from the Lime Kiln hydrophone; NOAA 2017). Hourly wind speed for East Point was obtained from the Saturna Island CS weather station (~630 m from the East Point hydrophone). Hourly wind speed for the ULS was obtained from the Sand Heads Lighthouse (~7 km from the ULS). The 2-D histogram plots also show the 10th percentile levels in each wind speed bin, and expected wind-driven ambient noise levels based on the Knudsen curves (Knudsen et al. 1948).

At Lime Kiln, there appears to be no correlation between SPL and wind speed in July; however, there did appear to be a strong correlation in January for wind speeds above ~5 m/s for the 100–1000 and 1000–10000 Hz bands. For these wind speeds, the January L_{10} followed the same trend but was systematically lower than the Knudsen curves by 8, and 5 dB for the 100–1000 and 1000–10000 Hz, bands, respectively. There was no correlation in the 10–100 kHz band.

At East Point, there also appeared to be no correlation between SPL and wind speed in July; however, there did appear to be a strong correlation in January for wind speeds above ~5 m/s. For these wind speeds, the January L_{10} followed the same trend but was systematically lower than the Knudsen curves by 8.7, 4.5, and 4.5 dB for the 100–1000 Hz, 1000–10000 Hz, and 10–32 kHz bands, respectively. It is suspected that this trend was not seen in the July data for Lime Kiln and East Point because of the lower wind speeds during that month.

At the ULS, there appeared to be no correlation between SPL and wind speed. It is believed this was because the hourly sound levels were primarily influenced by noise from the nearly constant presence of vessels in the area surrounding the ULS, which masked the wind-induced ambient noise. The deeper hydrophone depth is unlikely to be a factor in the weaker correlation between SPL and wind speed at the ULS.

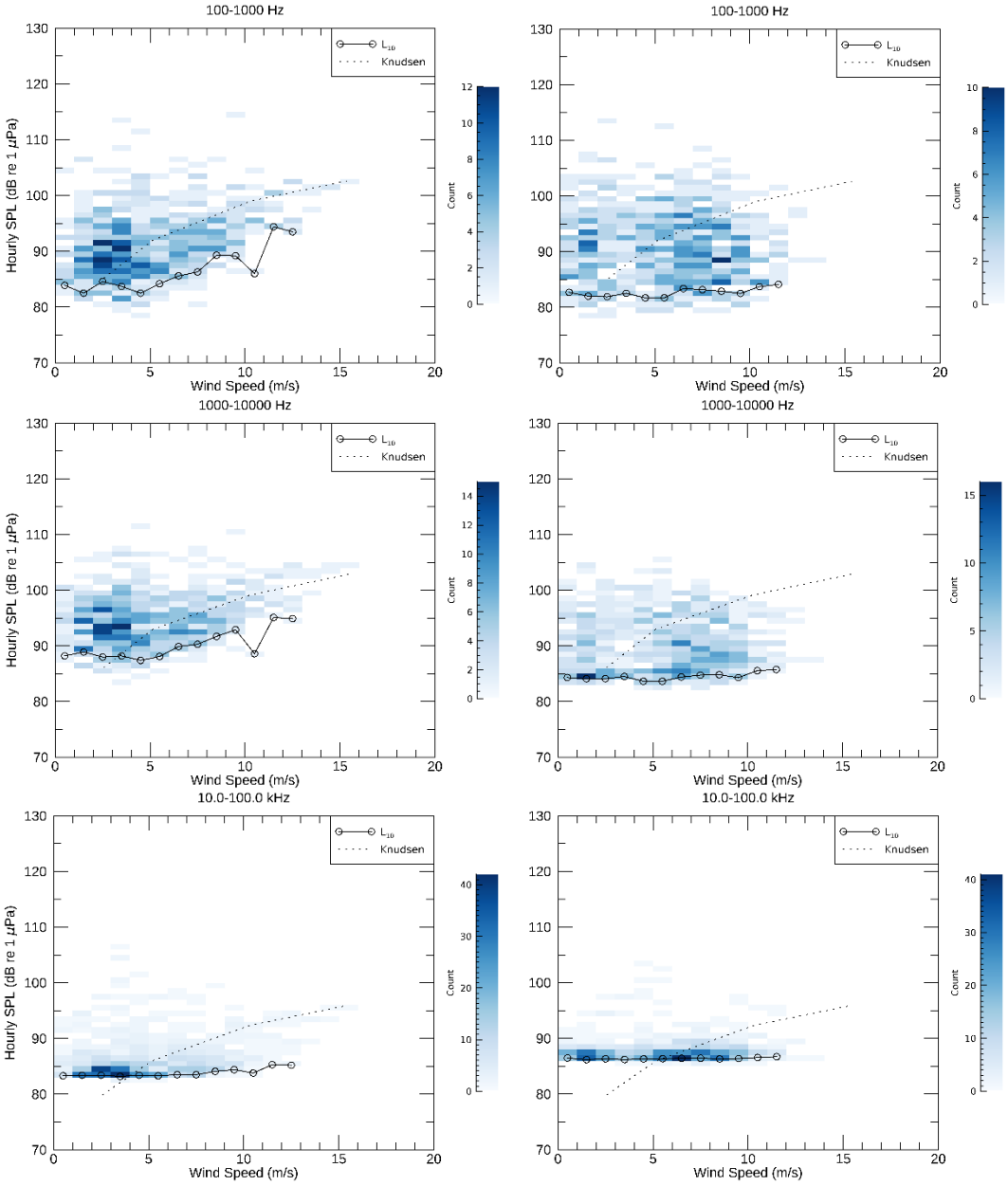

Figure 29. Lime Kiln: Hourly sound pressure levels (SPL) as a function of wind speed. Left and right panels show data from January and July 2017. The lower 10th percentile of hourly SPL (L_{10}) within each wind speed bin is shown with a solid black and circled line (where there are at least 10 SPL measurements in the wind speed bin). The predicted sound level from (Knudsen et al. 1948) are shown with a dotted line.

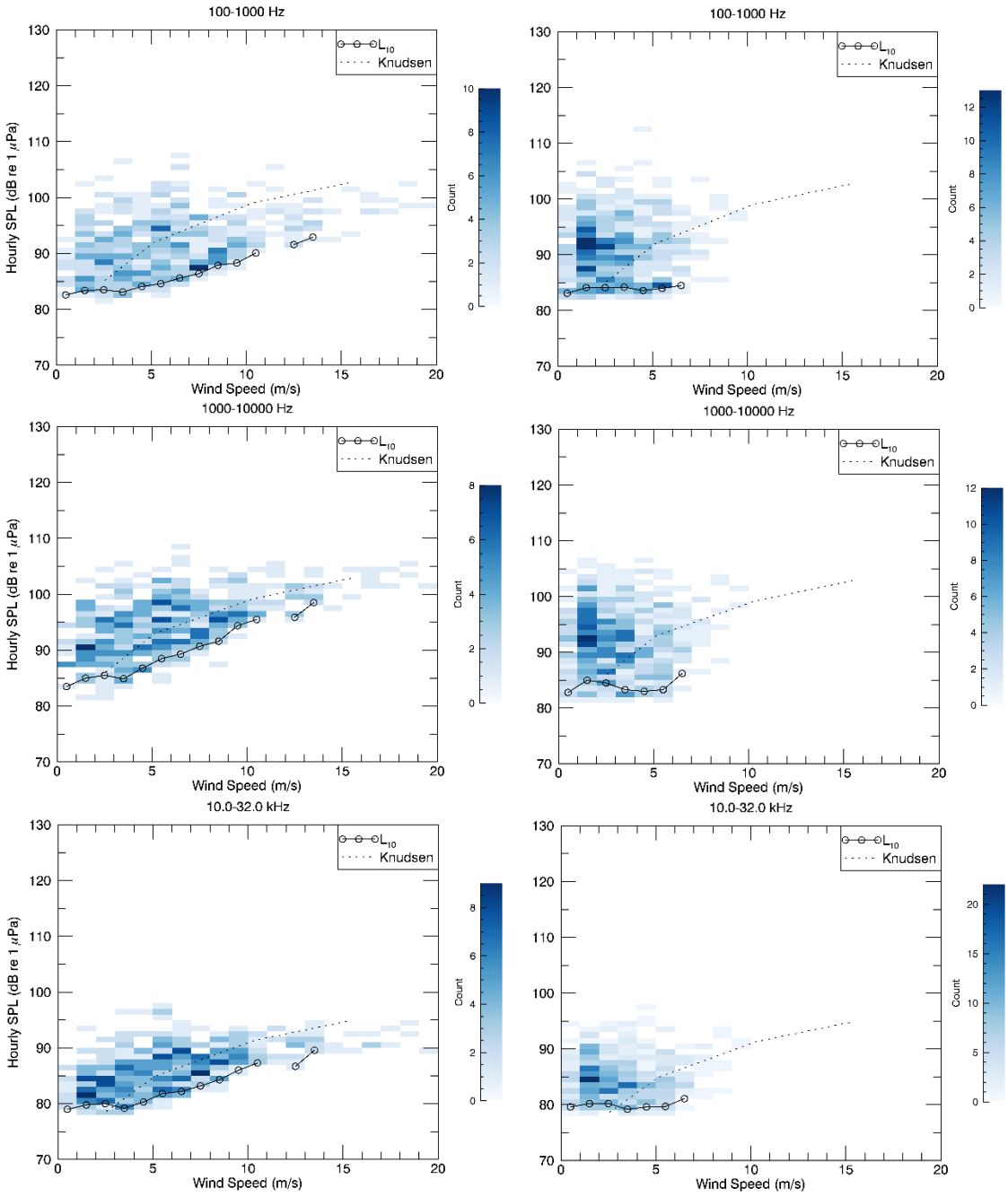

Figure 30. East Point: Hourly sound pressure levels (SPL) as a function of wind speed. Left and right panels show data from January and July 2016. The lower 10th percentile of hourly SPL (L_{10}) within each wind speed bin is shown with a solid black and circled line (where there are at least 10 SPL measurements in the wind speed bin). The predicted sound level from (Knudsen et al. 1948) are shown with a dotted line.

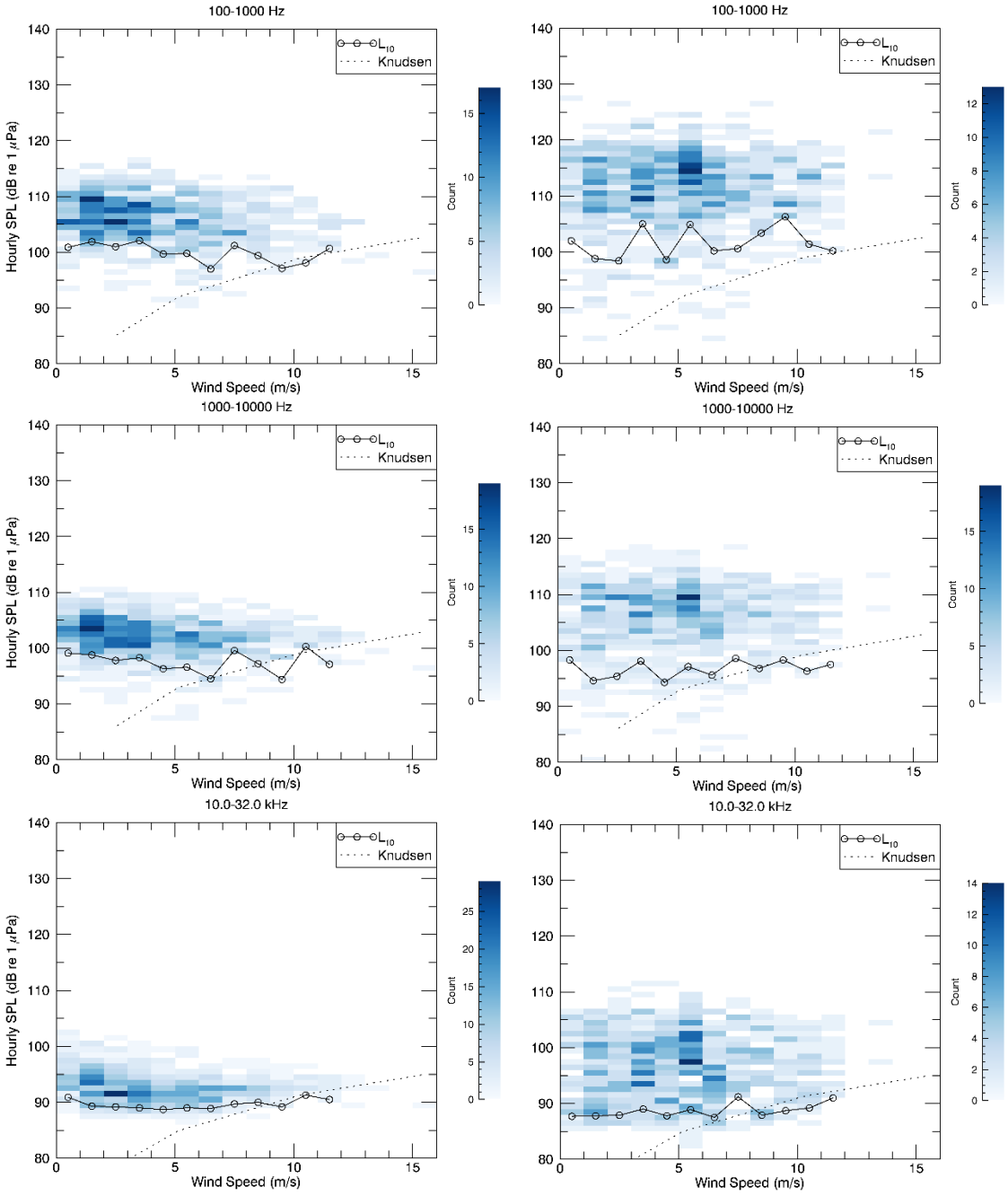

Figure 31. Underwater Listening Station (ULS): Hourly sound pressure levels (SPL) as a function of wind speed. Left and right panels show January and July 2017 data, respectively. The lower 10th percentile of hourly SPL (L_{10}) within each wind speed bin is shown with a solid black and circled line (where there are at least 10 SPL measurements in the wind speed bin). The predicted sound level from (Knudsen et al. 1948) are shown with a dotted line.

3.2.3. Rain

The effect of rain on sound levels was investigated by plotting sound level distributions during periods with and without rain. Figure 32 shows Lime Kiln results in January and July 2017, Figure 34 shows East Point results in January and July 2016, and Figure 35 shows the ULS results in January and July 2017. The plots include periods with and without rain, as determined from hourly records from the Victoria International Airport (Lime Kiln and East Point) or the Vancouver International Airport (ULS). The distribution of SPL did not appear to increase due to rain at any site. It is suspected that the effect of rain on hourly SPL may not be detectable because rain is often ephemeral (within an hour) and localized. Figure 33 shows the ephemeral nature of rain sounds recorded at the relatively shallow Lime Kiln hydrophone (in this case at 23 m depth). The signature of a rain squall is evident between 300 to 400 seconds in the long-term spectrogram average and at ~15.6 kHz (faint blue area). An even fainter squall is seen between 600 and 700 seconds. These brief periods of rain noise are unlikely to increase in the hourly average sound levels by a measurable amount.

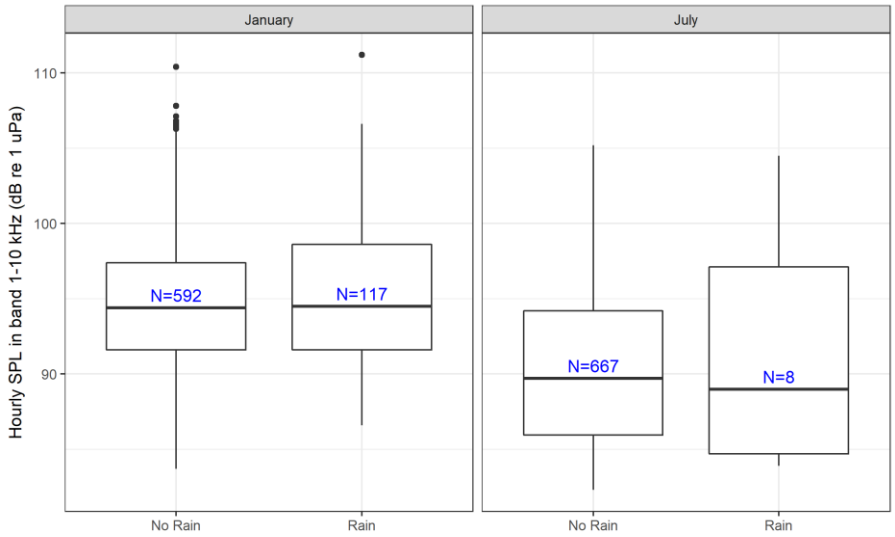

Figure 32. Lime Kiln: Box-and-whisker plots of hourly sound pressure levels (SPL) in the 1–10 kHz band in January and July 2017, during periods with and without rain.

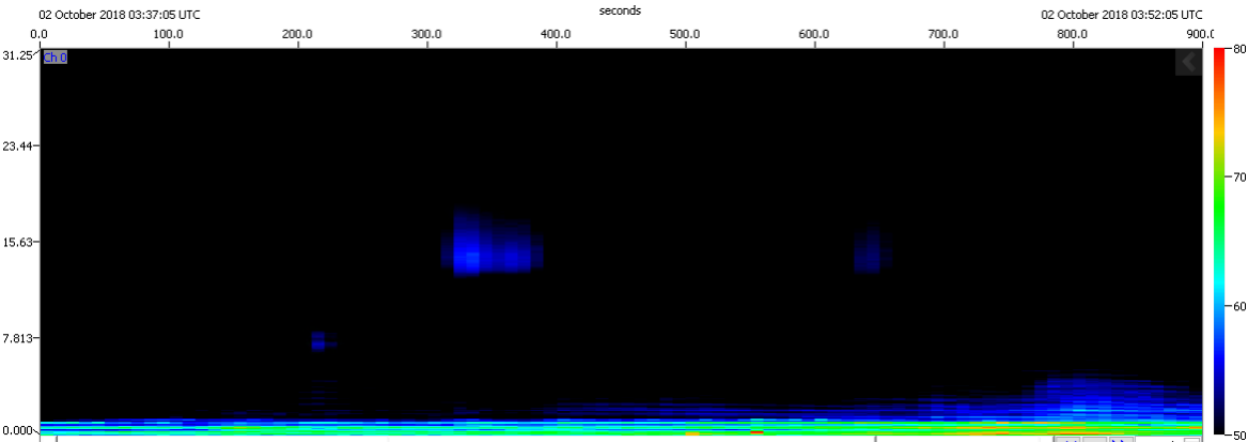

Figure 33. Long-term spectrogram average at Lime Kiln during a short rain squall. The X-axis is in seconds (15 minutes of data shown here) and the Y-axis is in kilohertz. The color bar indicates sound pressure level (SPL; in dB re 1µPa). The rain signature is evident between seconds 300 and 400 and around 15.6 kHz.

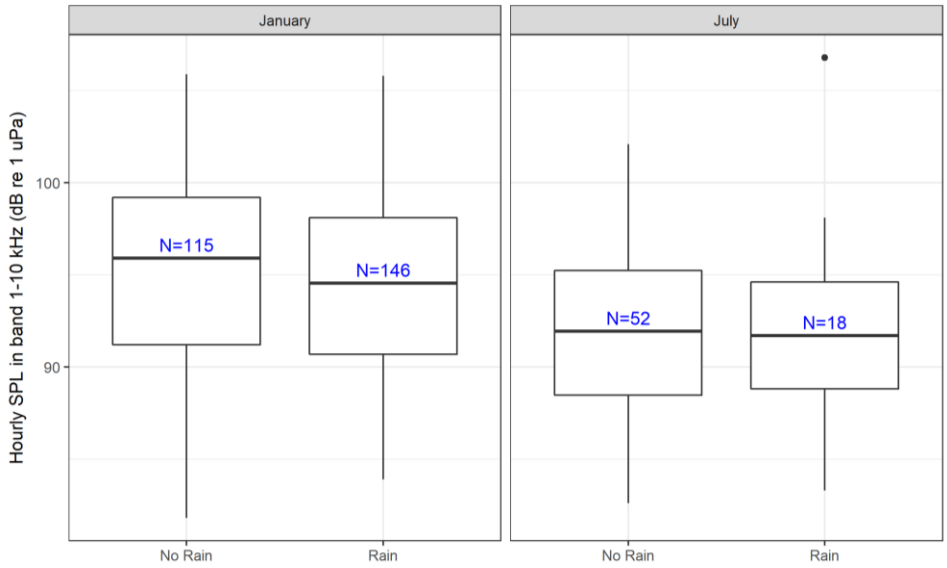

Figure 34. East Point: Box-and-whisker plots of hourly sound pressure levels (SPL) in the 1–10 kHz band in January and July 2016, during periods with and without rain.

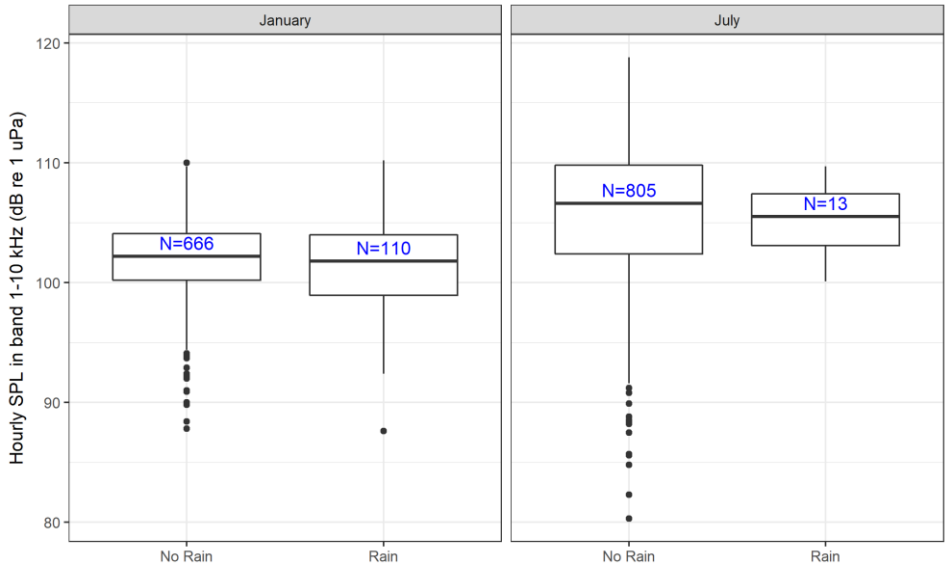

Figure 35. Underwater Listening Station (ULS): Box-and-whisker plots of hourly sound pressure levels (SPL) in the 1–10 kHz band in January and July 2017, during periods with and without rain.

3.3. Sound Speed Profile Variability and Effects of Acoustic Propagation

3.3.1. Sound speed profile variability

At each site, transmission loss (TL) from a near-surface source to the hydrophone was modelled using three site-specific sound speed profiles (see Section 2.3.2). Appendix C contains maps of TL contours and plots of TL versus range for each modelled frequency and sound speed profile at each site. Figure 36 shows the average TL between 2 and 4 km range along a transect from the hydrophone to the international shipping lanes for different sound speed profiles. This distance interval was chosen because it was far enough that the sound speed profile would noticeably influence sound propagation, a large fraction of the vessel traffic would transit within the interval, and it did not reach so far that land or complex bathymetry features would strongly increase TL. The differences in TL as a result of different sound speed profiles are expected to be larger at longer ranges and smaller at closer ranges.

At all sites, transmission loss was lowest for the mid-frequencies (300 and 3000 Hz). TL was similar at East Point and Lime Kiln because of their similar bathymetry and hydrophone depths. At these sites, the hydrophones were located near shore in relatively shallow water (less than 30 m deep), and the bathymetry to the shipping lanes slopes downwards to a couple hundred metres depth. There was little effect of sound speed profile variability on modelled TL.

At the ULS, the TL variability due to sound speed profile effects was much greater than at the other two sites. The hydrophone depth and bathymetry were also quite different than at the other sites, with the hydrophone at ~175 m depth and a relatively flat bathymetry toward the shipping lanes. The larger TL variability is attributed to the larger variability in observed sound speed profiles in the Strait of Georgia (see Section 2.3.2). Profile 1 was downwards refracting, Profile 3 was upwards refracting, and Profile 2 did not have a strong gradient with depth. The highest TL was found for Profile 1, where downward refraction increased loss due to (potentially multiple) seabed reflections before reaching the hydrophone at distances longer than 1 km. Profile 3 had the second highest TL (for 3 and 30 kHz) where upwards refraction limited sound from reaching the near-seabed hydrophone. Increased mid-frequency transmission loss in Strait of Georgia, associated with warming of surface waters during summer, is expected to reduce received levels of underwater noise from marine vessels transiting in the shipping lanes.

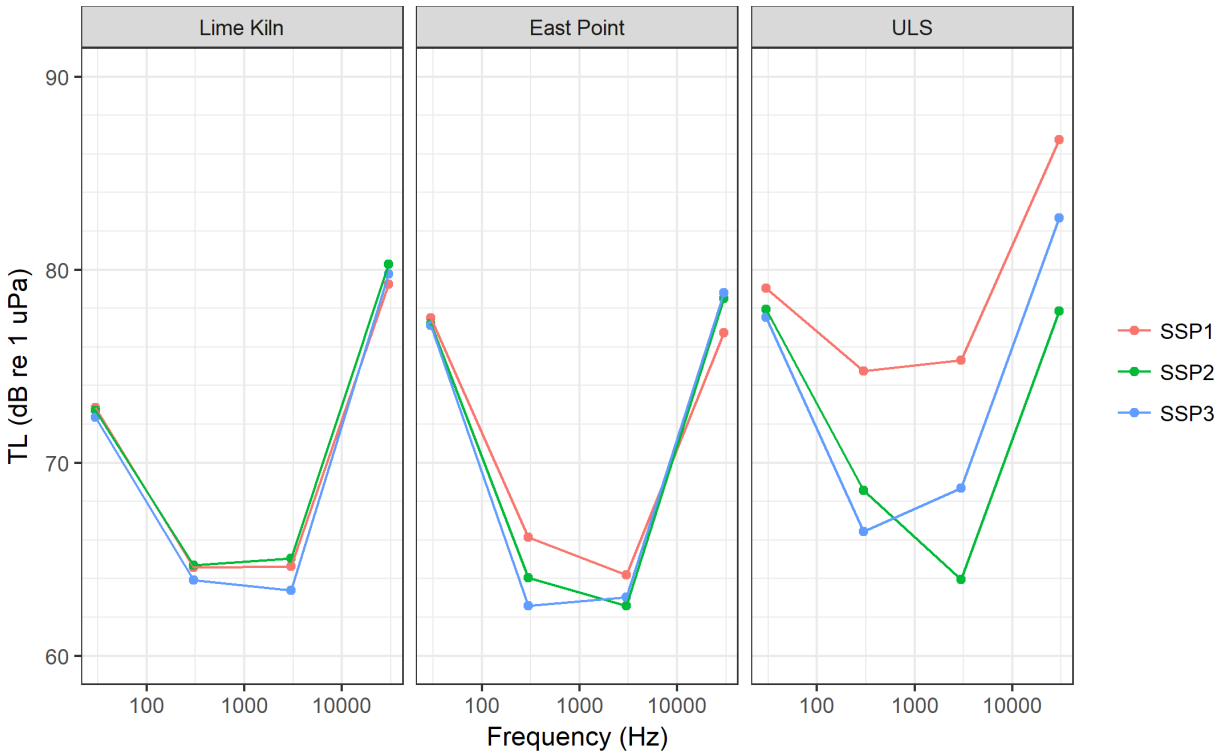

Figure 36. Average transmission loss (TL) for a near-surface source between 2 and 4 km range along a radial between the international shipping lanes and the hydrophone. Line colours represent the sound speed profiles (SSPs) used for modelling (which differed between sites–see Section 2.3.2).

3.3.2. Wind speed

At each site, transmission loss was modelled at 3,000 and 30,000 Hz from a near-surface source to the hydrophone using low, medium, and high wind speeds (1, 9, and 20 kn, respectively) with each of the three site-specific sound speed profiles (see Sections 2.3.2 and 2.3.3). Appendix D contains maps of transmission loss contours and plots of TL versus range for each modelled frequency, wind speed, and sound speed profile at each site. Figure 37 shows the increase in average TL between 2 and 4 km range along a transect from the hydrophone to the international shipping lanes, relative to the baseline (1 kn) wind speed scenario. In general, TL increases with wind speed and the effect is greater at higher frequencies. For 3,000 Hz, the increase in TL for moderate winds was less than 0.33 dB, but for high wind speeds the increase was much greater (between 2.2 and 9.1 dB). For 30,000 Hz, the increase in TL was similar for moderate and high wind speeds. The greatest variability in TL was near the ULS, due to the interaction between surface roughness and variations in the sound speed profile near the sea surface. The highest TL occurred for downwards-refracting and high wind speed conditions, where sound interacted multiple times with the seafloor and surface before reaching the hydrophone. This result shows that the influence of wind speed on sound propagation depends strongly on the shape of the sound speed profile.

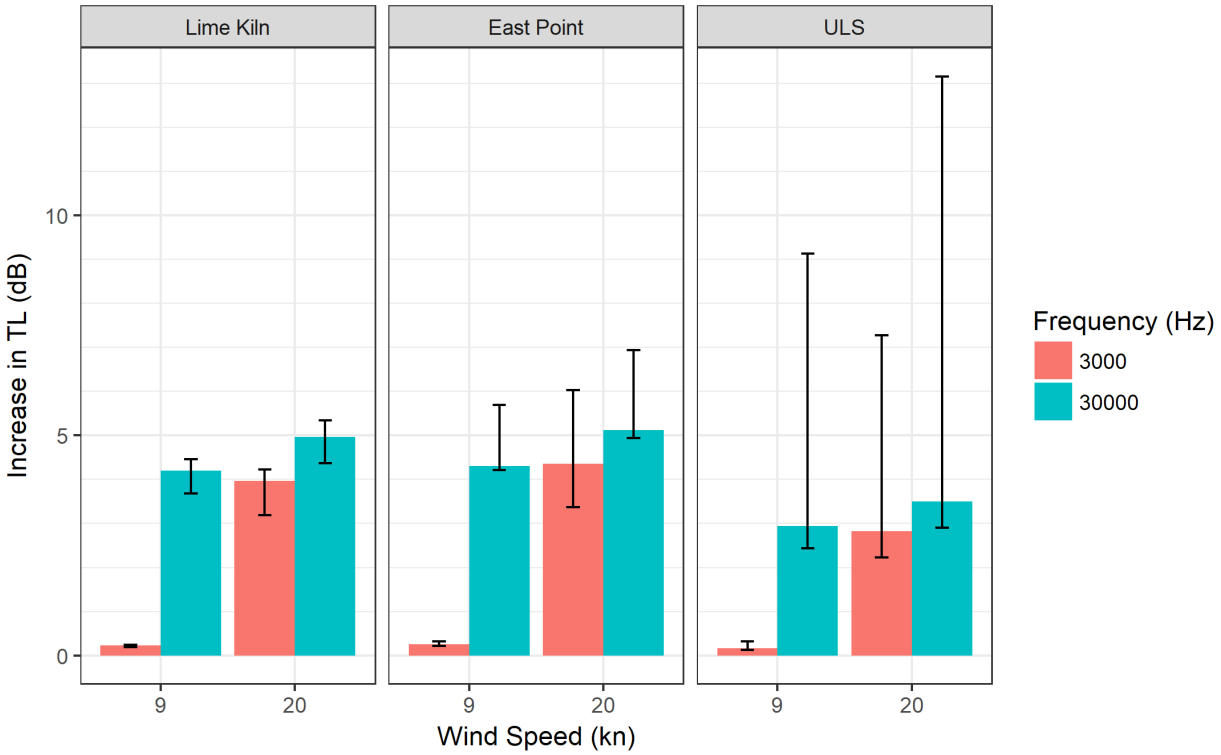

Figure 37. Increase in transmission loss (TL) from moderate and high wind speeds (9 and 20 kn, respectively) relative to the reference case (1 kn wind speed). Transmission loss was calculated for a near-surface source between 2 and 4 km range along a radial between the international shipping lanes and the hydrophone. The bars indicate the median increase and the whiskers indicate the minimum and maximum increases, using the three sound speed profiles (SSPs) for each site.

3.4. Influence of Vessel Traffic

3.4.1. MarineTraffic AIS vessel traffic analysis

This section describes results from the MarineTraffic AIS data analysis where AIS data were restricted to be within 10 km of the hydrophone (the East Point hydrophone location was used for Boundary Pass) and the 120 dB transmission loss contour. The relatively high 120 dB transmission loss contour was selected to filter out AIS data for vessels whose sounds would likely not be recorded at the hydrophone (e.g., for vessels where the acoustic path to the hydrophone was blocked by land). Figure 38 shows the total vessel hours during the study period (2016–2017) at each site and by vessel category. The Strait of Georgia had the most overall AIS vessel traffic, with the largest differences appearing in the Tug and Ferry categories.

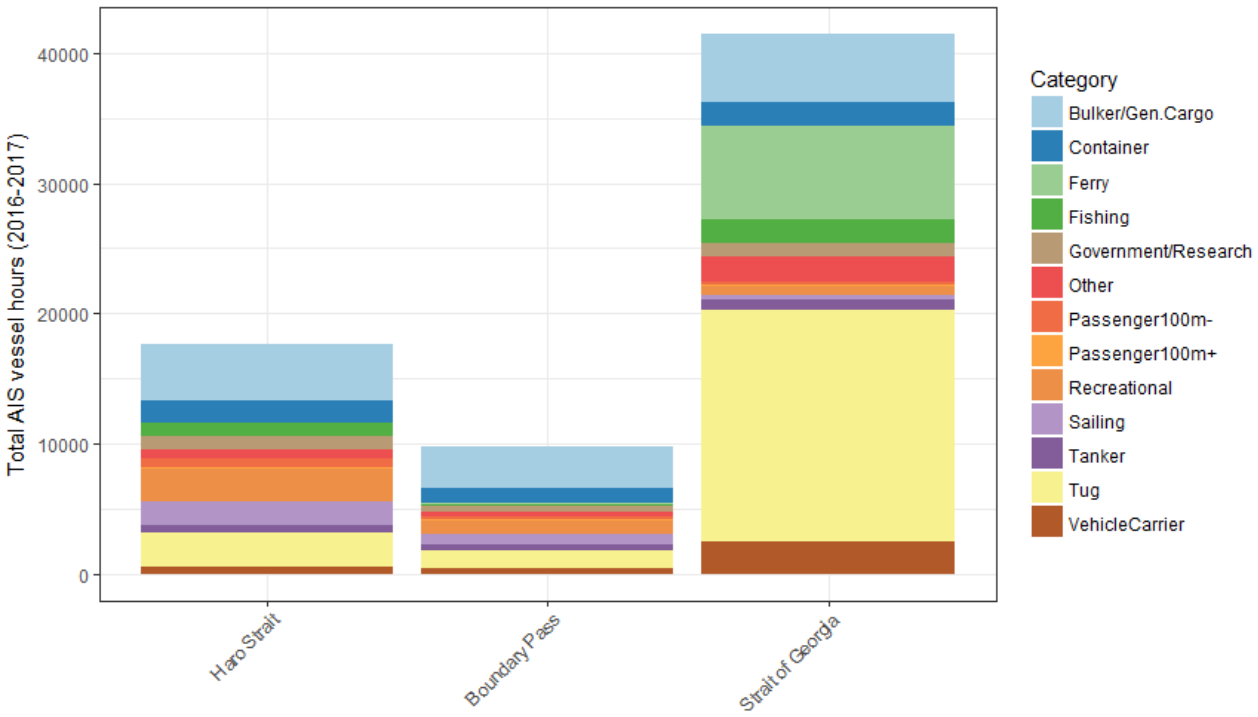

Figure 38. Total Automated Identification System (AIS) vessel hours during the study period by site and vessel category.

Figure 39 shows a density plot of vessel traffic hours versus distance from the hydrophone at each site. The spike in the density plot around 6.25 km in the Strait of Georgia was primarily due to tug traffic entering and exiting the Fraser River. In Haro Strait, the peaks at 2.5 and 4.5 km ranges correspond to the inbound and outbound international shipping lanes, respectively. Although the amount of traffic in the inbound and outbound shipping lanes was approximately equal in Haro Strait, the density plot was higher for the more distant lane because as distance increases, the corresponding area increases. The peak in the Boundary Pass density plot at 2 km range was due to vessel traffic in both the inbound and outbound shipping lanes. The lane separation is smaller in Boundary Pass than in Haro Strait, and the contribution from the different lanes appears combined in the figure. The increases in Boundary Pass and Haro Strait densities beyond 8 km were due to the inclusion of distant tangential traffic routes (NW–SE in the Strait of Georgia and N–S traffic in western Haro Strait, respectively).

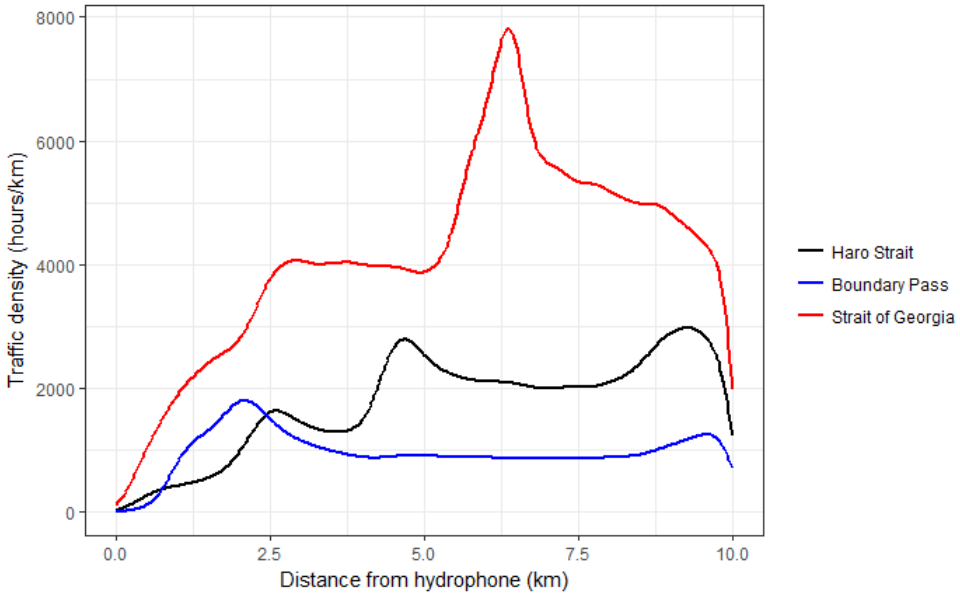

Figure 39. Density plot of vessel traffic hours versus distance from the hydrophone at each site.

For all subsequent analysis in this section, the AIS data were further restricted to within 6 km of the hydrophones, for consistency with previous AIS analysis performed at Lime Kiln (Wood et al. 2018). This is the approximate range of consistent acoustic detections of large vessels at Lime Kiln. Figure 40 shows the daily vessel hours at each site during the study period, for the two year study period. AIS vessel traffic followed a seasonal pattern at all sites, with vessel traffic highest in summer and lowest in winter. The variability in daily vessel hours was large compared to the seasonal trends, particularly for Haro Strait in summer.

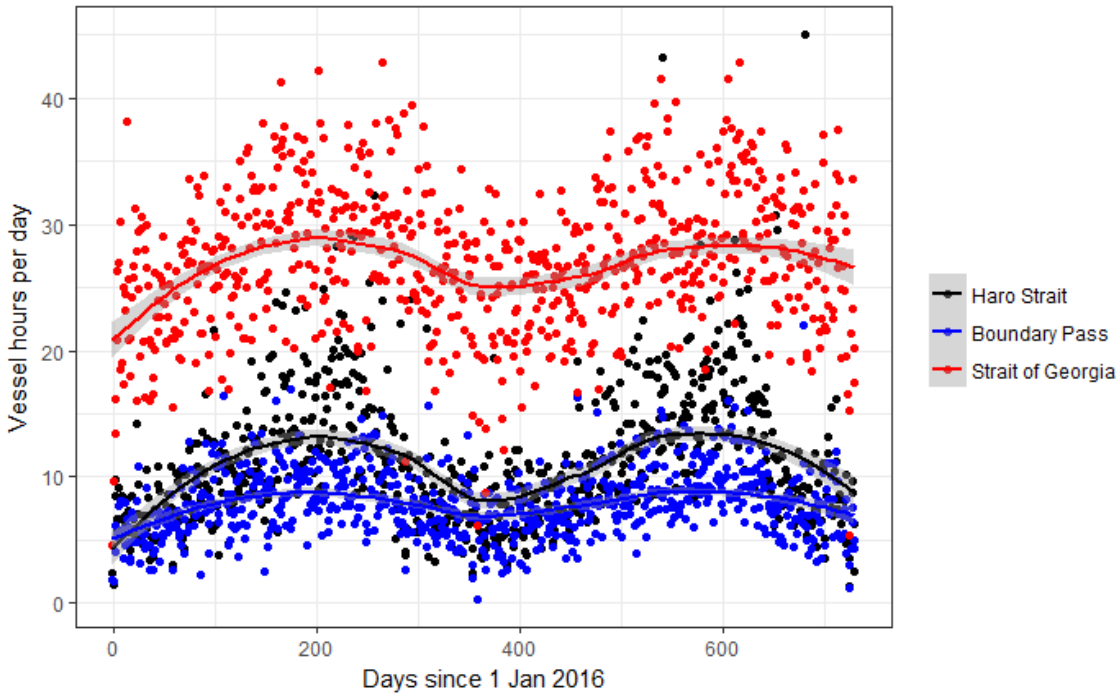

Figure 40. Daily Automated Identification System (AIS) vessel hours at each site during the study period (2016–2017). Dots show vessel hours on each day and lines show the moving average [Local Regression (LOESS) method].

Figure 41 shows the vessel hours at each site versus of days of the week. There did not appear to be a trend for Boundary Pass and Haro Strait. In the Strait of Georgia, mean vessel hours peaked on Thursdays and were lowest on Sundays. The error bars, showing one standard deviation, indicate there was relatively large variation in daily vessel hours compared to the trend of the mean hours.

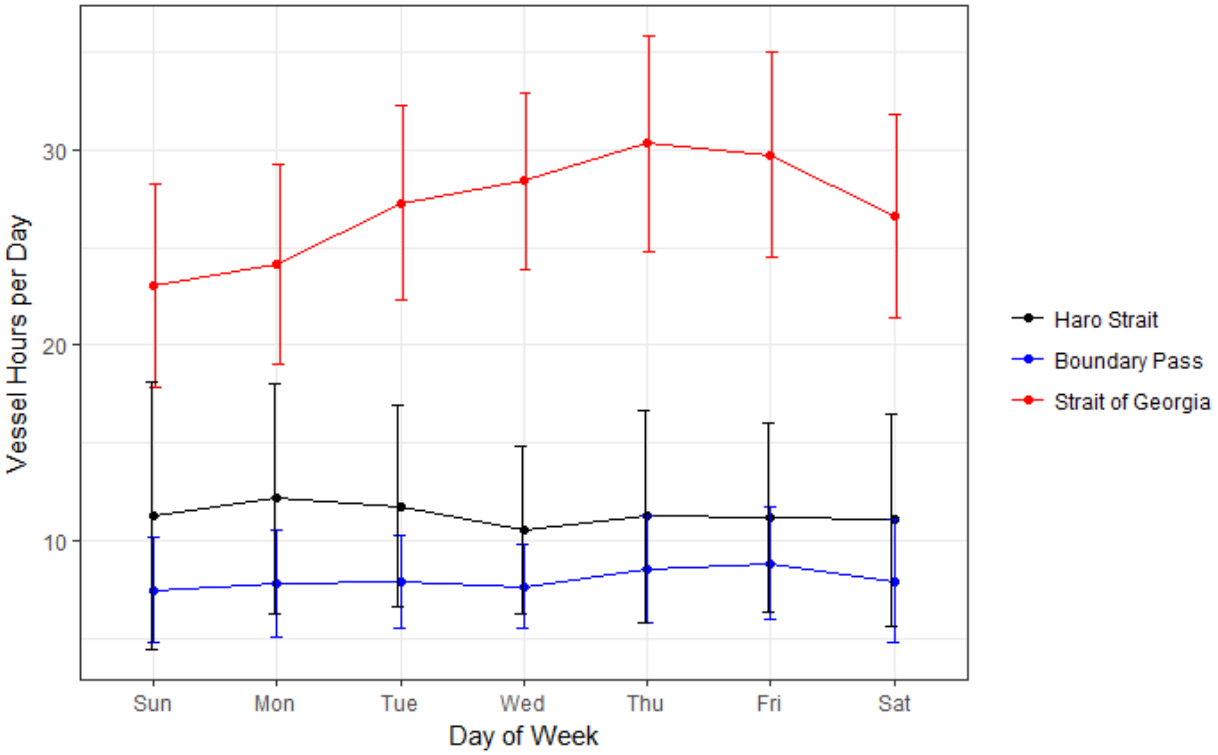

Figure 41. Automated Identification System (AIS) vessel hours per day as a function of day of the week. Points indicate mean values and error bars represent one standard deviation.

Figure 42 shows the mean AIS vessel hours versus time of day, vessel category, and site. In Boundary Pass and Haro Strait, vessel traffic peaked around noon primarily due to Recreational and Sailing vessels. In Boundary Pass, there was a secondary peak around 2:00 am, which was primarily due to increased Container ship, Tug, and Vehicle Carrier traffic. Mean hourly AIS vessel traffic in the Strait of Georgia did not show the same diurnal trend as at the other sites and varied more between hours of the day. Tug traffic was particularly high in the early mornings in the Strait of Georgia.

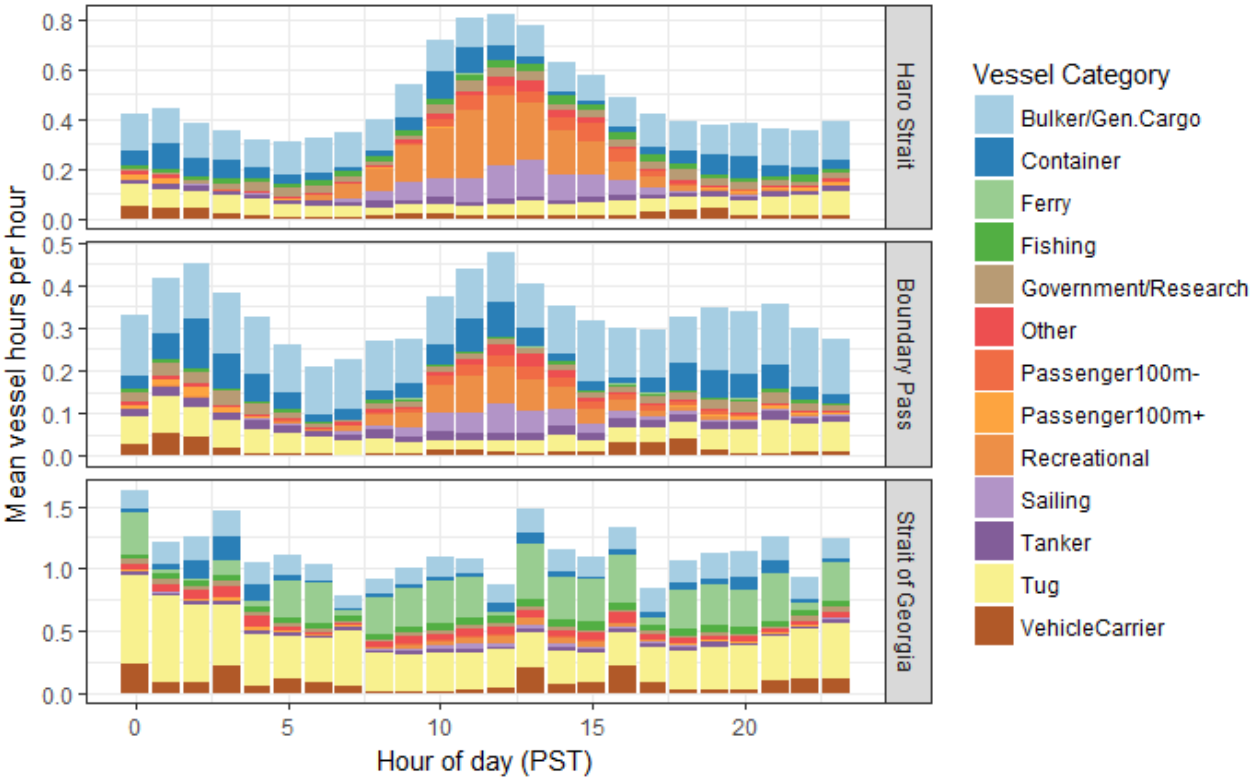

Figure 42. Mean hourly Automated Identification System (AIS) vessel hours as a function of time of day, vessel category, and site. Note the y-axis scale change.

Figures 43 and 44 show histograms of AIS vessel hours and tracks, respectively, for large commercial vessels at each site. These vessel categories include Bulker/General Cargo, Container, Passenger (over 100 m), Tanker, Ferry, and Vehicle Carrier. Although tug traffic makes up a large portion of the overall vessel traffic in the Strait of Georgia, it was excluded from this and subsequent analysis in Section 3.4.2 because the majority of tug traffic does not pass near the ULS and would therefore not contribute as much to ambient sound levels as closer vessels. Tug traffic was excluded from the other sites for consistency. Table 12 lists the quartiles of these distributions. Combined daily large commercial vessel traffic was similar between Boundary Pass and Haro Strait; traffic was higher in the Strait of Georgia. The number of AIS vessel hours was strongly correlated with the number of vessel tracks, which indicates that either metric is suitable for assessing traffic volume. No seasonal trends of the combined traffic from all large commercial vessels were observed at any of the three sites.

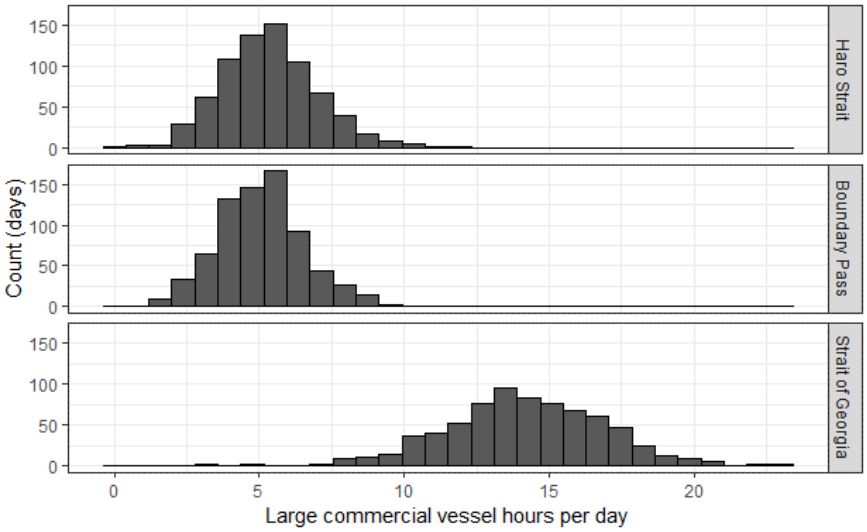

Figure 43. Histograms of hours per day for large commercial vessels. Vessel categories include Bulker/General Cargo, Container, Passenger (over 100 m), Tanker, Ferry, and Vehicle Carrier.

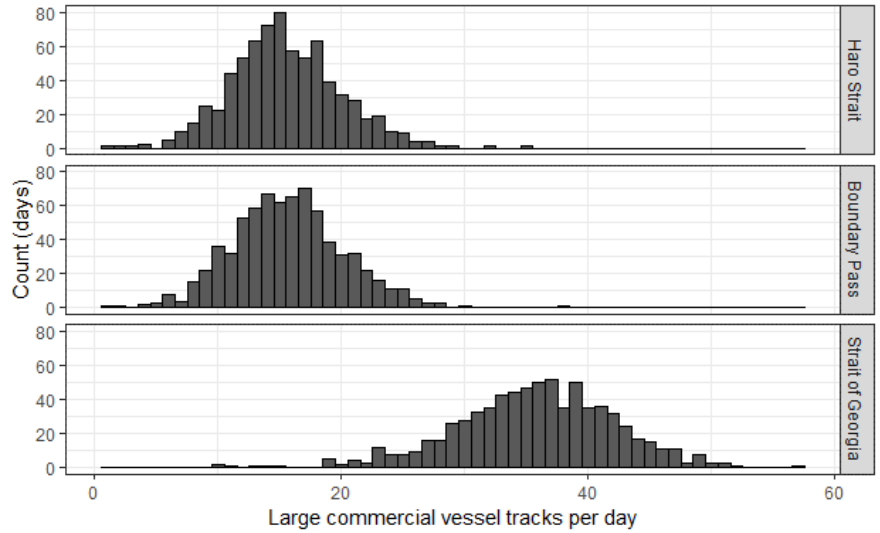

Figure 44. Histograms tracks per day for large commercial vessels. Vessel categories include Bulker/General Cargo, Container, Passenger (over 100 m), Tanker, Ferry, and Vehicle Carrier.

Table 12. Quartiles of vessel hours and tracks per day for large commercial vessels at each site.

Site	Hours per day			Tracks per day		
	25th percentile	50th percentile	75th percentile	25th percentile	50th percentile	75th percentile
Boundary Pass	4.1	5.1	5.9	13	16	18
Haro Strait	4.2	5.3	6.3	13	15	18
Strait of Georgia	12.4	14.1	15.9	32	36	40

3.4.2. Influence of traffic volume from large commercial vessels at Lime Kiln, East Point, and ULS

In this section, hourly decade-band sound levels versus vessel traffic volume are presented for large commercial vessels (see Section 3.4.1). Low, medium, and high traffic volume days were determined from daily large commercial vessel traffic hours in the 0–25th, 25th–75th, and 75th–100th percentiles, respectively, for each site (see Table 12 for site-specific vessel traffic hours).

Figure 45 shows Lime Kiln results in January and July 2017, Figure 46 shows East Point results in January and July 2016, and Figure 47 shows the ULS results in January and July 2017. Sound level statistics are listed in Tables 13–15 for Lime Kiln, East Point, and the ULS, respectively. Note that some of the tabulated sound level statistics (i.e., L_{95}, L_5, L_{eq}) are not shown in the corresponding figures but are included here for consistency with related studies. At Lime Kiln, sound levels increased with vessel traffic volume in the first three decade bands, especially in January. At East Point, no consistent trend between sound levels and vessel traffic volume was apparent. At the ULS, hourly sound levels generally increased with vessel traffic volume, but the trend was less clear as at Lime Kiln.

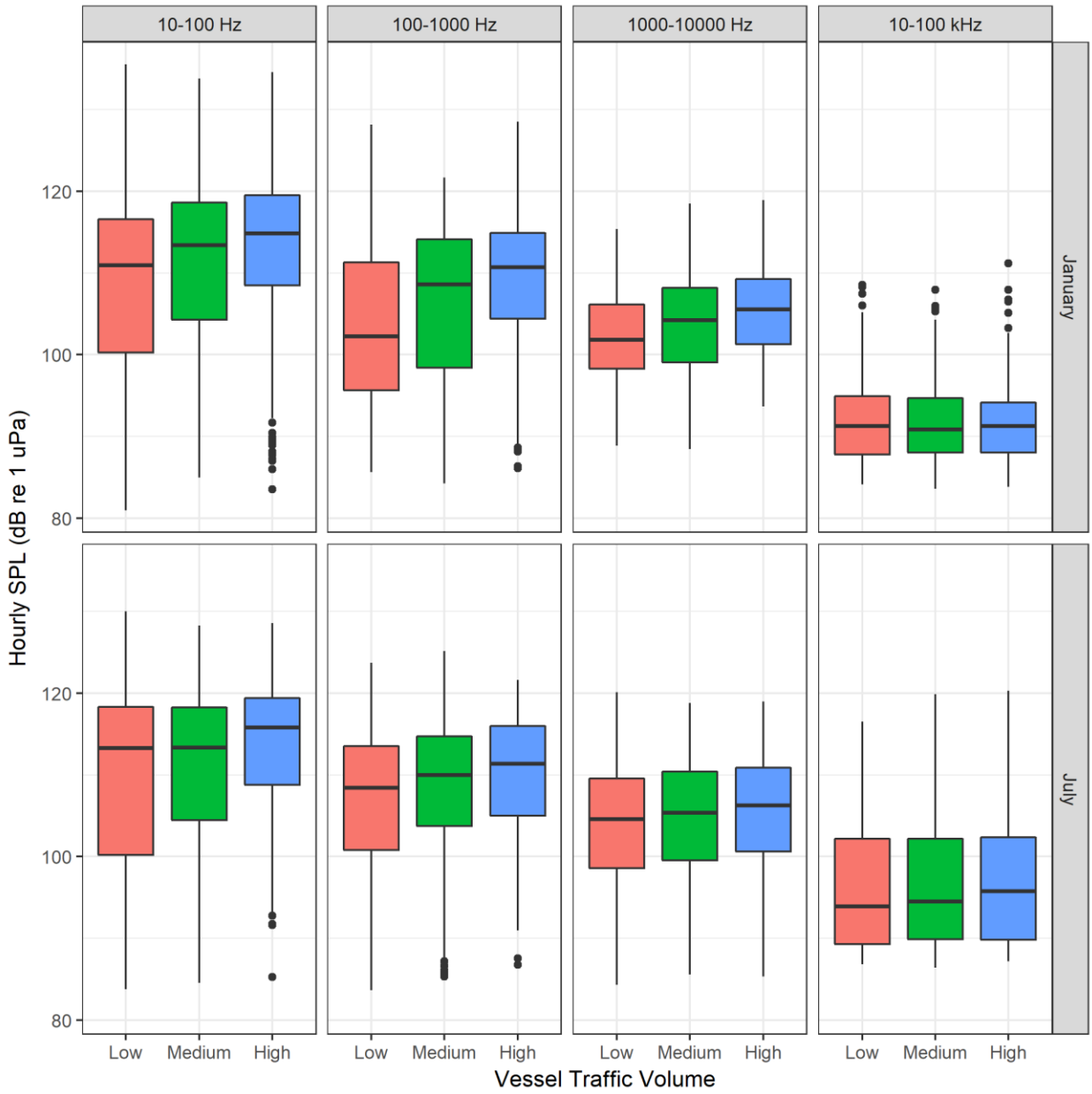

Figure 45. Lime Kiln: Box-and-whisker plots of hourly decade-band sound levels versus large commercial vessel traffic volume in January and July 2017.

Table 13. Lime Kiln: Hourly SPL (dB re 1 µPa) exceedance statistics for different vessel traffic volumes, frequency bands, and months (2017). L_n is the sound level exceeded n% of the time. L_{eq} is the power-average sound level (i.e., the decibel level of the average hourly mean-square pressure).

Frequency band	**10–100 Hz**			**100–1000 Hz**			**1000–10000 Hz**			**10–100 kHz**		
Traffic volume	Low	Medium	High	Low	Medium	High	Low	Medium	High	Low	Medium	High
January												
L_{95}	86.4	90.3	89.5	89.7	91.3	91.3	94.3	93.0	94.9	85.2	84.6	84.6
L_{50}	110.9	113.4	114.8	102.3	108.6	110.7	101.8	104.2	105.4	91.3	90.8	91.3
L_5	124.5	124.1	125.0	117.4	119.0	119.9	112.4	112.9	113.7	99.6	101.9	101.1
L_{eq}	118.5	119.0	119.8	111.7	112.6	114.4	105.9	107.4	108.4	95.3	95.5	96.3
July												
L_{95}	86.6	90.5	93.4	86.5	89.2	93.8	85.7	88.6	89.8	87.4	87.7	88.0
L_{50}	113.2	113.3	115.7	108.4	110.0	111.2	104.6	105.3	106.2	93.9	94.5	95.8
L_5	124.4	124.2	124.0	118.1	119.2	119.0	115.6	114.7	115.5	110.3	109.2	109.3
L_{eq}	117.9	117.7	118.5	112.7	113.6	114.3	109.2	109.1	109.8	103.6	103.1	104.3

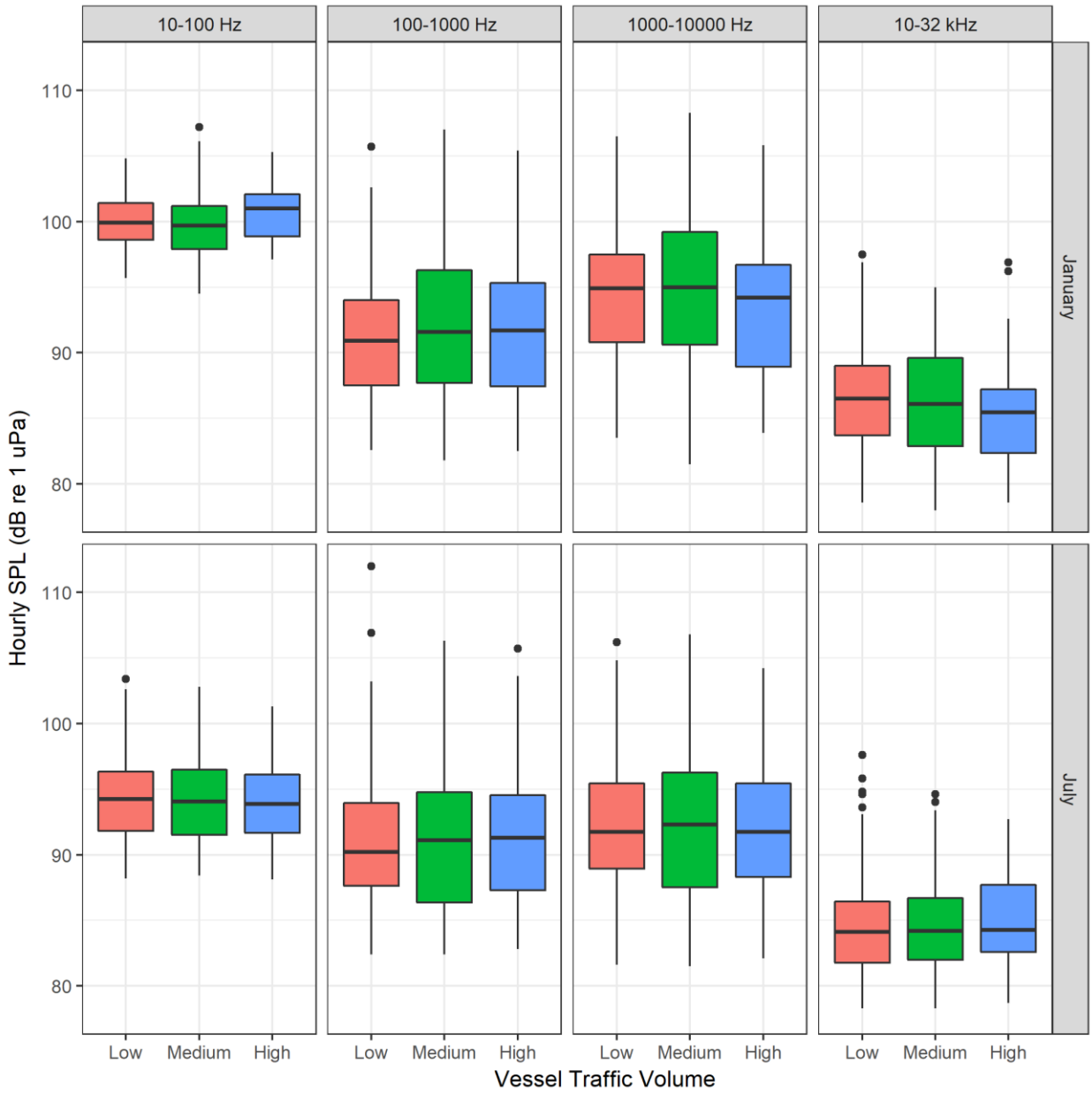

Figure 46. East Point: Box-and-whisker plots of hourly decade-band sound levels versus large commercial vessel traffic volume in January and July 2016.

Table 14. East Point: Hourly SPL (dB re 1 µPa) exceedance statistics for different vessel traffic volumes, frequency bands, and months (2016). L_n is the sound level exceeded n% of the time. L_{eq} is the power-average sound level (i.e., the decibel level of the average hourly mean-square pressure).

Frequency band	**10–100 Hz**			**100–1000 Hz**			**1000–10000 Hz**			**10–32 kHz**		
Traffic volume	Low	Medium	High	Low	Medium	High	Low	Medium	High	Low	Medium	High
January												
L_{95}	96.9	96.5	97.4	83.8	84.1	83.4	86.1	87.0	84.9	80.0	79.9	80.4
L_{50}	99.9	99.7	101.0	90.9	91.6	91.7	94.9	95.0	94.2	86.5	86.1	85.5
L_5	103.1	103.5	104.1	98.8	101.4	101.6	101.6	103.4	100.2	92.6	92.8	92.6
L_{eq}	100.4	100.3	101.2	93.4	95.6	95.3	96.6	98.1	96.3	88.2	88.0	87.9
July												
L_{95}	89.3	89.5	89.8	83.3	83.3	83.7	82.8	82.6	83.6	79.2	79.3	79.8
L_{50}	94.3	94.1	93.9	90.2	91.1	91.3	91.8	92.3	91.8	84.1	84.2	84.3
L_5	99.8	99.6	98.8	100.3	99.9	100.4	101.4	102.0	100.7	93.2	90.6	90.4
L_{eq}	95.5	95.4	94.9	96.4	94.4	94.9	95.4	95.8	95.0	87.3	86.2	86.2

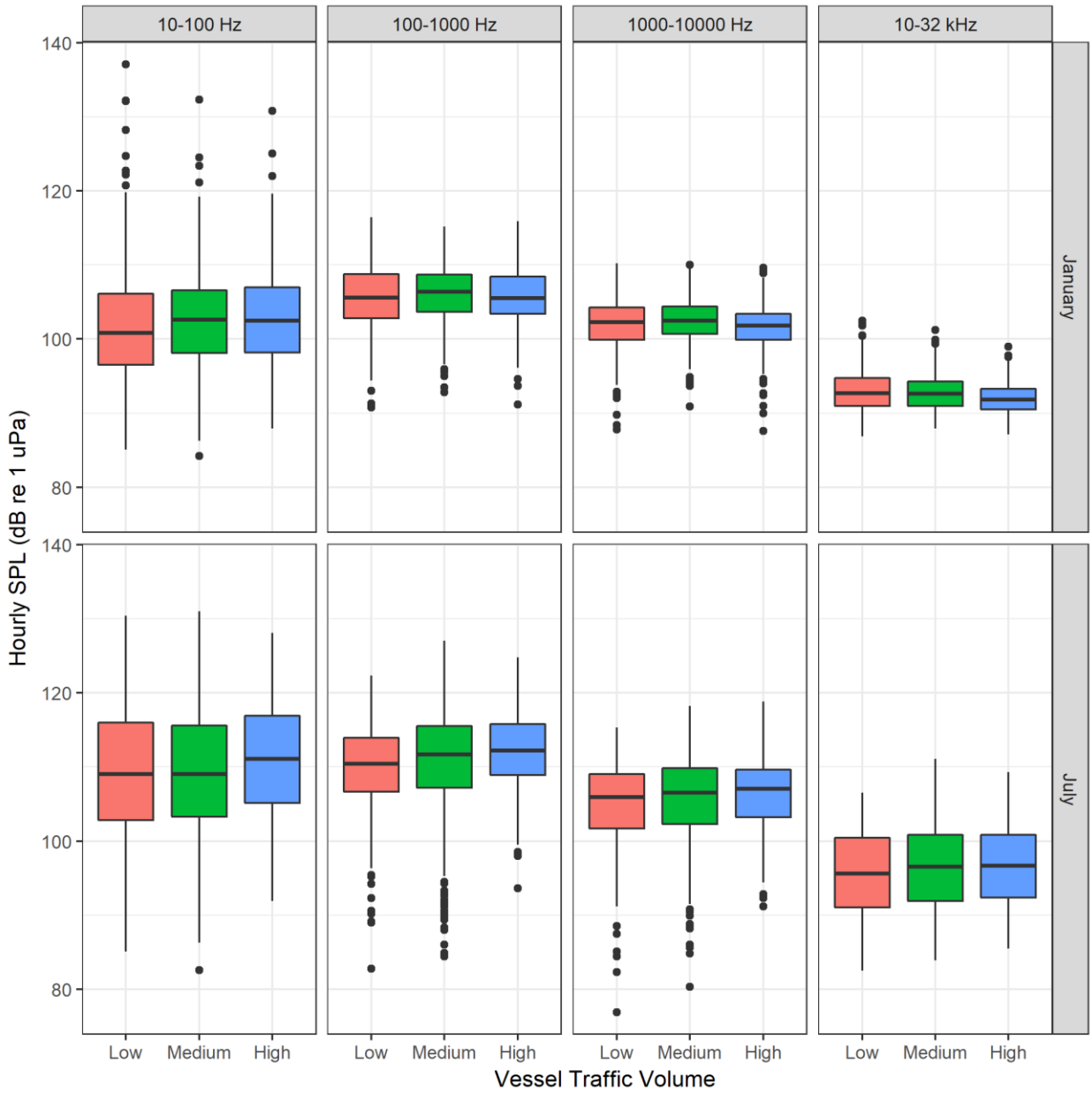

Figure 47. Underwater Listening Station (ULS): Box-and-whisker plots of hourly decade-band sound levels versus large commercial vessel traffic volume in January and July 2017.

Table 15. Underwater Listening Station (ULS): Hourly SPL (dB re 1 µPa) exceedance statistics for different vessel traffic volumes, frequency bands, and months (2017). L_n is the sound level exceeded n% of the time. L_{eq} is the power-average sound level (i.e., the decibel level of the average hourly mean-square pressure).

Frequency band	10–100 Hz			100–1000 Hz			1000–10000 Hz			10–32 kHz		
Traffic volume	Low	Medium	High	Low	Medium	High	Low	Medium	High	Low	Medium	High
January												
L_{95}	90.2	91.7	93.2	98.1	99.2	99.6	95.1	96.2	96.3	88.5	89.1	88.7
L_{50}	100.8	102.6	102.5	105.6	106.4	105.5	102.3	102.5	101.8	92.7	92.6	91.8
L_5	115.3	114.9	114.5	112.4	111.8	111.8	107.4	107.0	106.4	99.1	97.1	96.0
L_{eq}	115.7	112.0	110.8	107.5	107.8	107.4	103.2	103.4	102.6	94.3	93.6	92.6
July												
L_{95}	94.5	94.0	99.6	96.8	98.2	102.4	94.5	94.1	96.3	86.8	86.9	87.4
L_{50}	109.0	109.0	111.1	110.4	111.7	112.2	105.9	106.5	107.1	95.6	96.5	96.7
L_5	122.5	124.4	122.3	118.7	119.4	119.9	112.8	113.6	113.4	104.7	105.7	105.3
L_{eq}	116.8	117.5	116.3	113.1	114.5	114.8	107.8	108.6	108.8	99.2	100.0	99.9

3.4.3. AIS versus non-AIS traffic in Boundary Pass

Analysis of camera imagery data from Boundary Pass showed daytime vessel traffic in the 21-day winter month was largely comprised of AIS-broadcasting vessels (Figure 48a), including bulker/general cargo and container ships (Figure 49a). Of the 190 vessel detections observed for the winter sample month of February, 162 were AIS Class A vessels (Table 16). No Class B AIS-broadcasting vessels were observed during the winter sample month. Most vessels were cargo and container ships, with tankers, naval vessels, tugboats, and government/research vessels also present in Boundary Pass (Figure 49a). Non-AIS vessels were less active in Boundary Pass (Figure 48a), with only 28 non-AIS vessel detections comprised of motorboats, sailboats, ecotourism, and non-commercial fishing vessels (Figure 49b).

A marked increase in the proportion of non-AIS vessels in Boundary Pass was observed during summer (Figure 48b), due to increased presence of smaller vessels (Figure 49b). Of the 789 non-AIS detections, the most included motorboats and sailboats, with ecotourism and fishing vessels also present to a lesser extent (Figure 49b). In addition to a large influx of small non-AIS vessels, AIS Class A and Class B vessel detections also increased for a combined total of 312 AIS detections (Table 16). While the number of cargo and container ships observed during daylight hours decreased compared to February, tanker, naval vessel, and tugboat traffic increased (Figure 49a). Furthermore, a considerable influx of Class B AIS traffic (n = 141) was also observed during the summer sample month. Class B AIS traffic was largely characterized by smaller vessels for tourism and recreational use, including pleasure crafts, sailboats, ecotourism vessels, and fishing boats (Figure 49a).

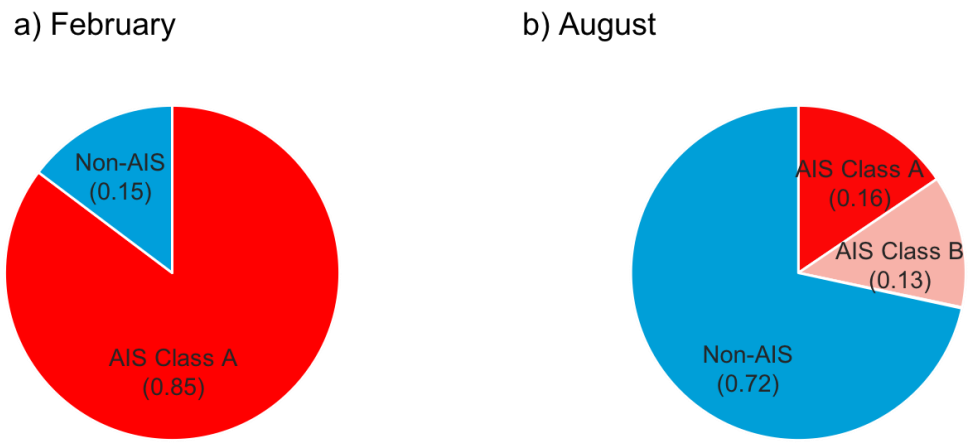

Figure 48. Proportions of Automated Identification System (AIS) versus non-AIS vessels to total observed vessel traffic in Boundary Pass for: a) February and b) August 2017. Proportions of AIS-broadcasting Class A and B vessels depicted in shades of red and non-broadcasting vessel proportions in blue. Listed proportions in August exceed 1 due to rounding.

Table 16. Number of observed broadcasting Automated Identification System (AIS) Class A, Class B, and non-AIS vessels detected on camera during a 21-day sampling period for February and August 2017.

Broadcasting status	February	August
AIS - Class A	162	171
AIS - Class B	0	141
Non-AIS	28	789
Total	**190**	**1,101**

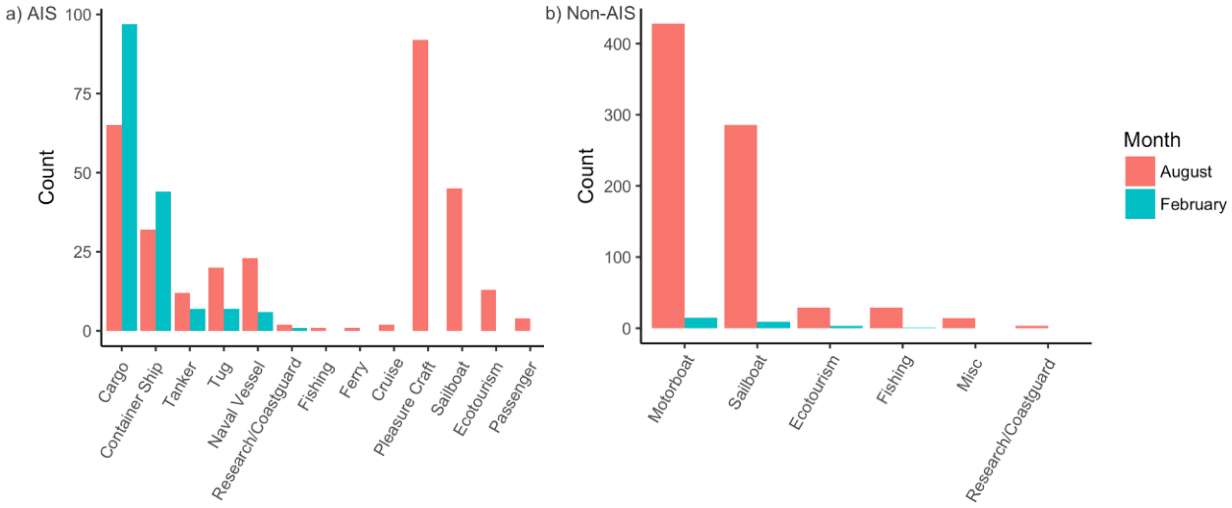

Figure 49. Total counts for: a) Automated Identification System (AIS) and b) non-AIS vessel types detected over a 21-day period in August (red) versus February (blue) 2017 in Boundary Pass, BC.

3.4.4. Noise contributions of AIS and non-AIS vessel traffic in Boundary Pass

3.4.4.1. Winter (East Point Hydrophone)

During the expanded winter period (see Appendix E, Table 30), highest ambient noise levels at the East Point hydrophone in Boundary Pass occurred when AIS vessels were present, a trend consistent across all four decade bands (Figure 50). Median 1-minute decade band SPL increased by up to 24.8 dB when AIS vessels were present, compared to when no vessels were detected on camera (Appendix E, Table 32). Median sound levels increased by up to 27.7 dB when both AIS and non-AIS vessels were present (Appendix E, Table 32), but the low number (n = 8) of observed vessel-minutes with both vessel types present may not be representative of the true contribution (Figure 50).

Most AIS traffic appeared to be travelling within the international shipping lanes, corresponding to the delineated “Mid” zone. Although few (n = 32) AIS vessels were detected in the “Near” zone of Boundary Pass, they appeared to have the most substantial contribution to ambient noise levels detected across the three higher frequency ranges (Figure 51b–d; Appendix E, Table 33). Only a select few of these “Near” zone AIS detections included commercial shipping vessels, and these were largely observed to be travelling at the farthest distance limit of the 1 km “Near” zone. Of the observed non-AIS vessel traffic, “Near” and “Mid” vessels contributed to increased ambient noise levels across the three higher decade bands (Figure 51b–d; Appendix E, Table 33). “Far” non-AIS vessels, which formed most non-AIS vessel traffic, did not appear to increase sound levels above those when no vessels were present (Figure 51).

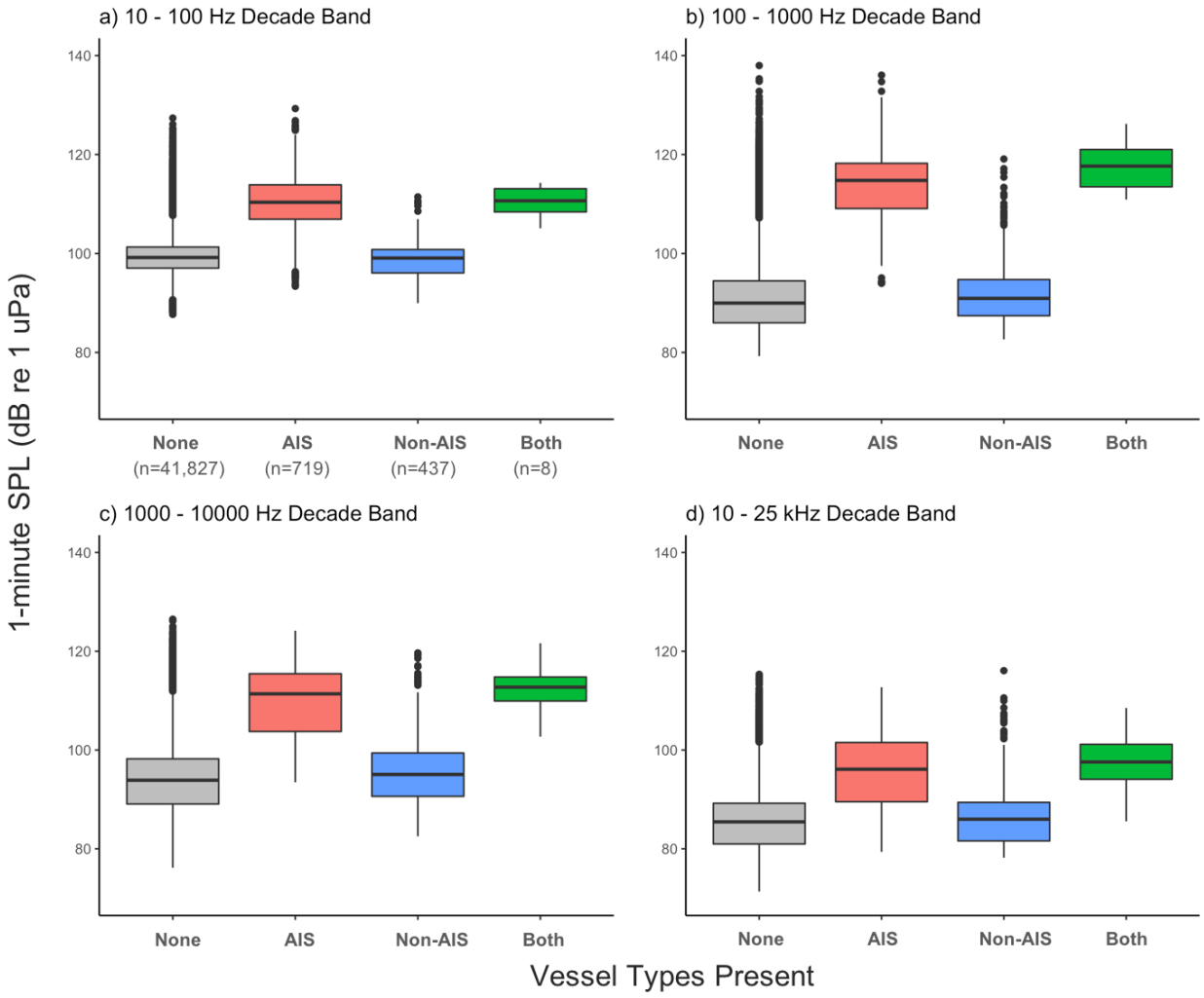

Figure 50. East Point hydrophone: Box-and-whisker plots of ambient noise levels (1-minute SPL) observed when no vessels, Automated Identification System (AIS) only, non-AIS only, and both AIS and non-AIS vessels were detected on camera during the 60-day winter sampling period from December 2016 to March 2017. Ambient noise levels measured across 4 decade bands: a) 10–100 Hz, b) 100–1000 Hz, c) 1000–10,000 Hz, and d) 10–25 kHz. The number of measurements in panel a) applies to all four panels.

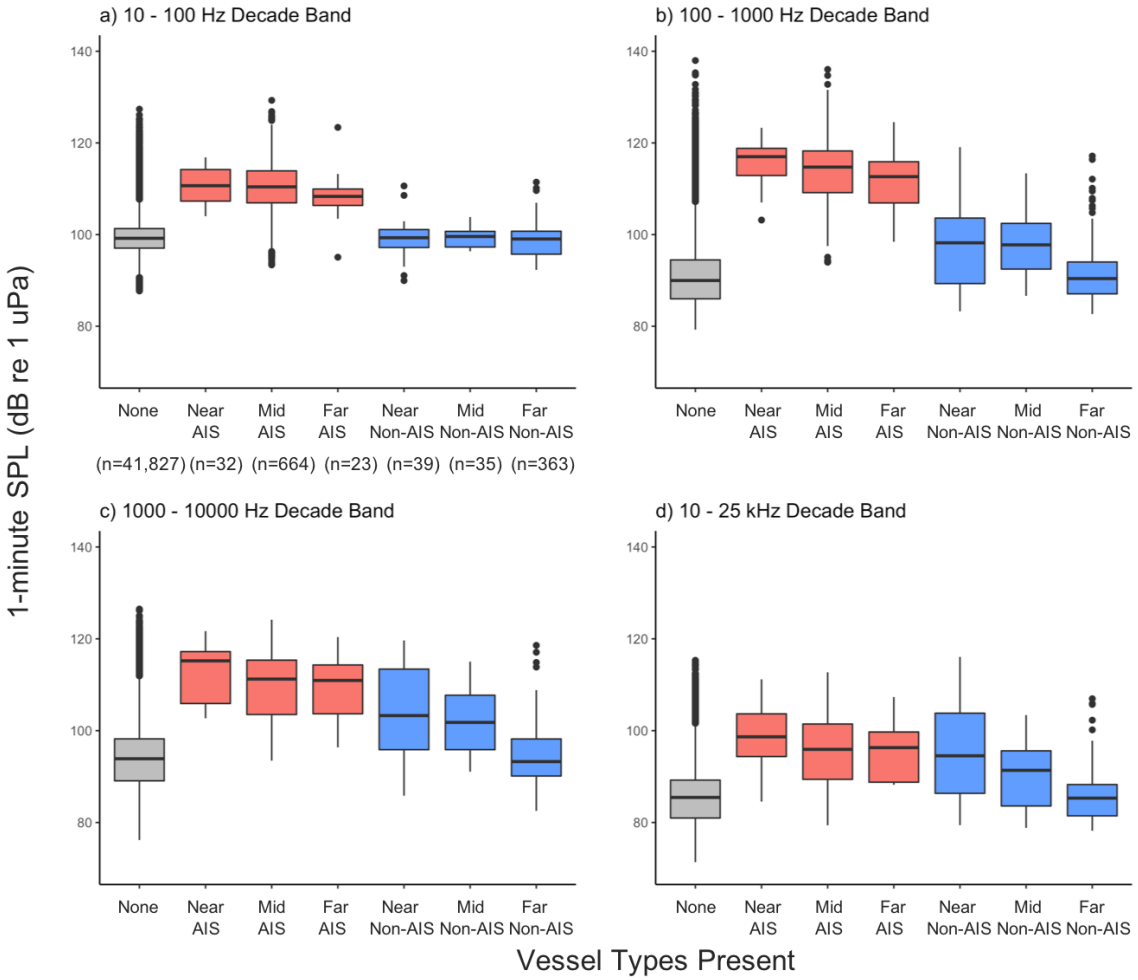

Figure 51. East Point hydrophone: Box-and-whisker plots of ambient noise levels (1-minute SPL) observed when no vessels (grey), Automated Identification System (AIS) (red), and non-AIS vessels (blue) were detected on camera in the near-shore (<1 km from East Point hydrophone), mid-shore (1–3 km), and far-shore (>3 km) distance zone of Boundary Pass during the 60-day winter sampling period from December 2016 to March 2017. Ambient noise levels measured across 4 decade bands: a) 10–100 Hz, b) 100–1000 Hz, c) 1000–10,000 Hz, and d) 10–25 kHz. The number of measurements in panel a) applies to all four panels.

3.4.4.2. Summer (Monarch Head hydrophone)

Similar to winter, highest ambient noise levels were detected at the Monarch Head hydrophone in Boundary Pass when AIS vessels were present (Figure 52) during the 7-day summer sampling period of 28 Jun to 4 Jul 2017. Ambient noise levels increased by up to 9.2 dB when only AIS vessels were detected, compared to when no vessels were detected on camera (Appendix E, Table 32). Highest median ambient noise levels consistently occurred when AIS-broadcasting vessels were present the "Mid" zone of Boundary Pass (Figure 53; Appendix E, Table 33). This distance category also included vessels detected in the "Near" zone, grouped into the "Mid" zone category due to the position of Monarch Head hydrophone relative to the camera. When both AIS and non-AIS vessels were detected on camera, median ambient noise levels increased by only up to 5.8 dB (Appendix E, Table 32). The smaller noise contribution in comparison to AIS-only detections may have been driven by incongruities between visual detection of vessels on camera at East Point and detected noise levels at Monarch Head, especially when vessels were moving in opposite directions through Boundary Pass.

Non-AIS vessels elevated sound levels in the three higher decade bands for mid-zone vessels (Figure 53b–d; Appendix E, Table 33). Far-zone non-AIS vessels contributed little to ambient noise, with a slight increase in sound levels observed at the mid-frequency ranges (Figure 53b and c; Appendix E, Table 33).

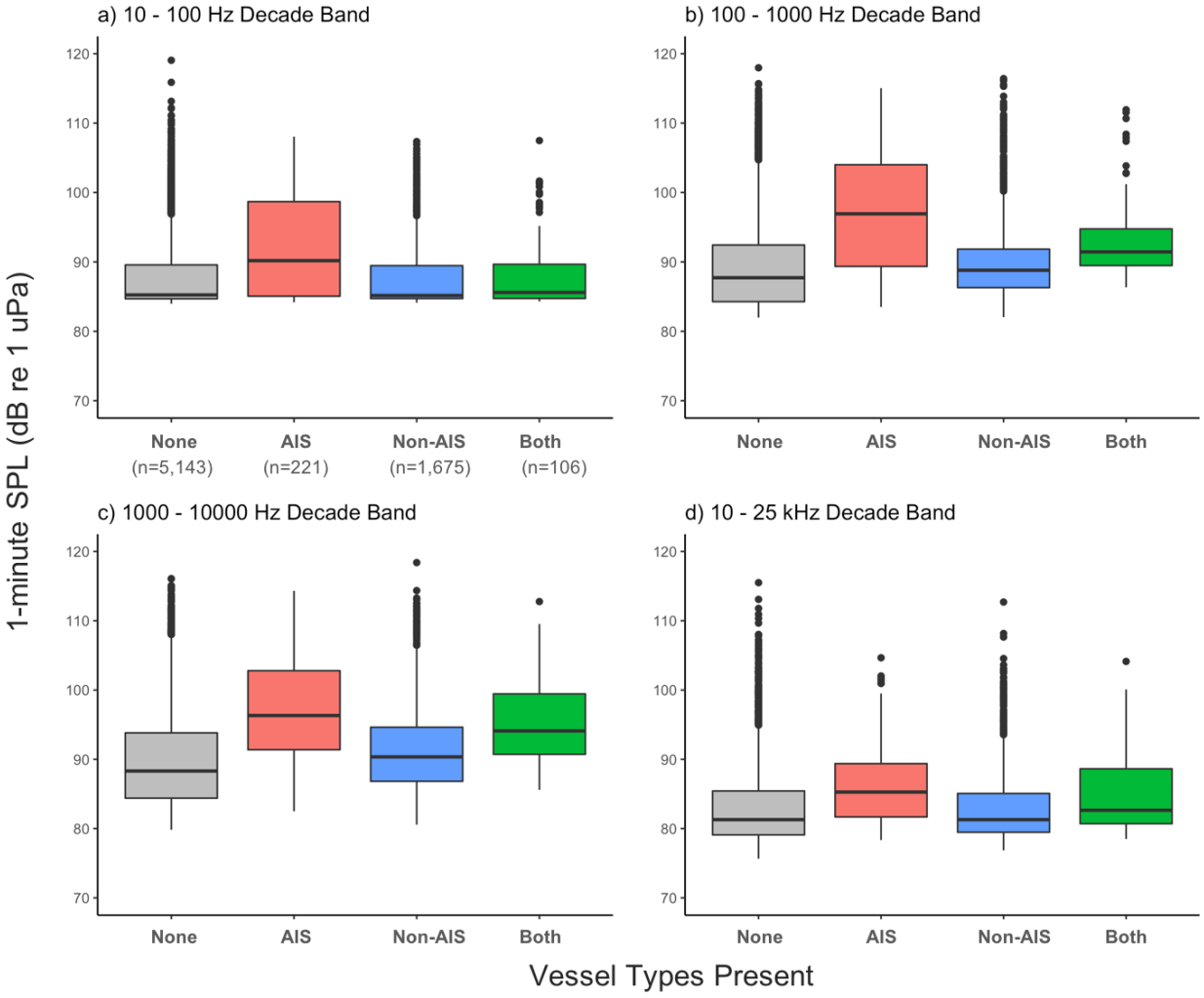

Figure 52. Monarch Head hydrophone: Box-and-whisker plots of ambient noise levels (1-minute SPL) observed when no vessels (grey), Automated Identification System (AIS) only (red), non-AIS only (blue), and both AIS and non-AIS vessels (green) were detected on camera for Boundary Pass during 28 Jun to 4 Jul 2017. Ambient noise levels measured across 4 decade bands: a) 10–100 Hz, b) 100–1000 Hz, c) 1000–10,000 Hz, and d) 10–25 kHz. The number of measurements in panel a) applies to all four panels.

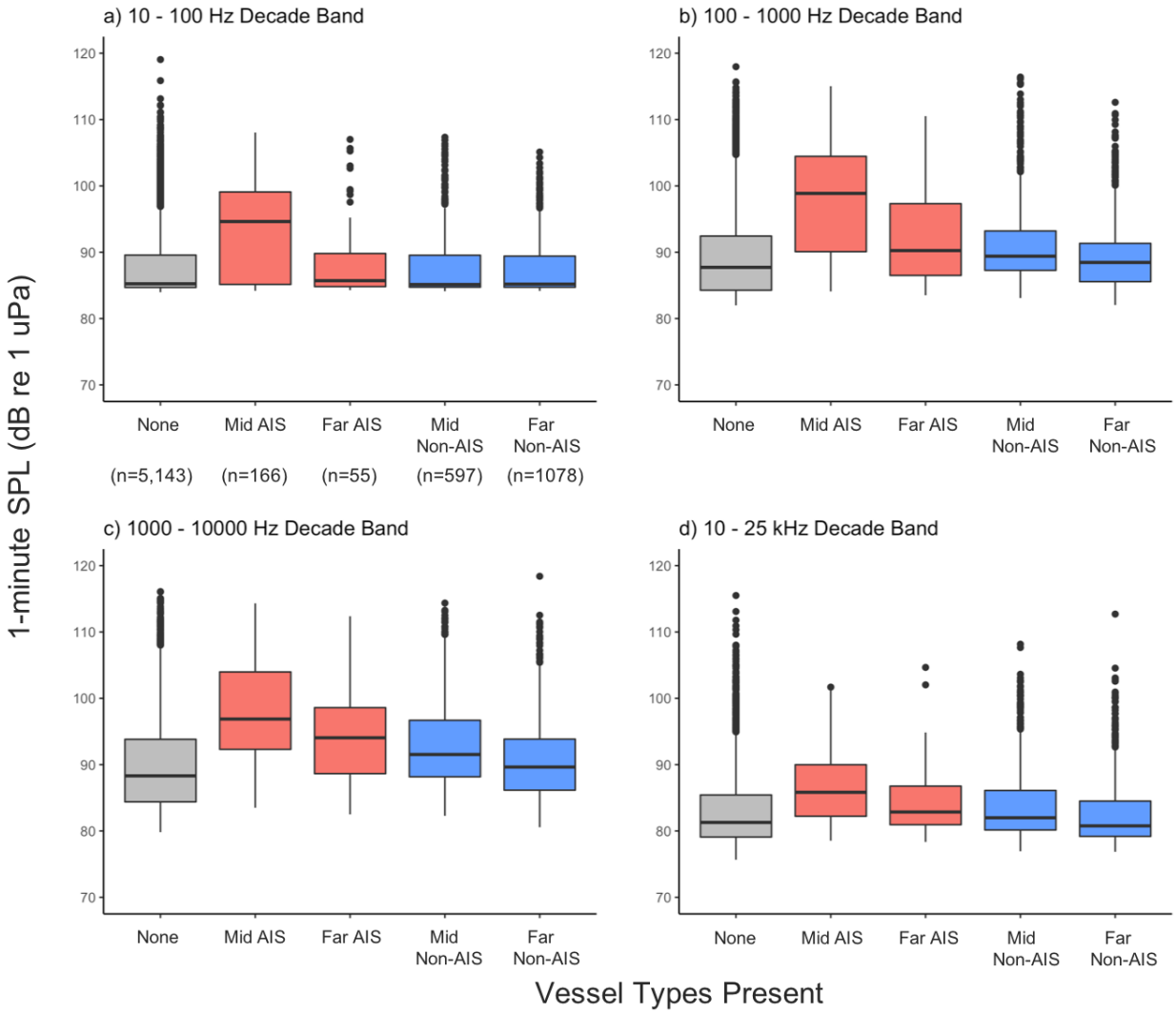

Figure 53. Monarch Head hydrophone: Box-and-whisker plots of ambient noise levels (1-minute SPL) observed when no vessels (grey), Automated Identification System (AIS) (red), and non-AIS vessels (blue) were detected on camera in mid-shore (0–3 km) and far-shore (>3 km) distance zone during 28 Jun to 4 Jul 2017. Ambient noise levels measured across 4 decade bands: a) 10–100 Hz, b) 100–1000 Hz, c) 1000–10,000 Hz, and d) 10–25 kHz. The number of measurements in panel a) applies to all four panels.

3.4.5. Influence of large- and small-vessel traffic at Lime Kiln

Table 17 shows the number of minutes included in the large-and-small vessel traffic analyses at Lime Kiln during January and July 2017 (including split by day/night), as well as the proportion of that time that the acoustic detector noted large-, small-, and no-vessels present. Large-vessels were present at Lime Kiln ~30% of the time, year-round, day and night. Small-vessels showed a large seasonal trend with acoustic detections <1% of the daytime in January and >6% of the daytime in July. Most nighttime small-vessel detections were false positives. Of the 120 minutes of detections that were validated, large-vessel detections were correct 95.0% of the time and no-vessel detections were correct 82.5% of the time. If all time periods are included, the small-vessel detector was only correct 40.0% of the time, but this increased to 75.0% correct during daytime. Therefore, the nighttime small-vessel detections should be ignored and assumed to be near zero, and efforts to improve the small-vessel detector should be made. Overall, false positives tended to be other vessel types, flow noise (and occasional associated strumming of debris such as kelp), and biologicals.

The large-vessel detector consistently detected more large vessels than there were broadcasting AIS <6 km from Lime Kiln. Given the high true positive rate for the large-vessel detector, this may indicate that the acoustic detector was at times operating at ranges >6 km. The discrepancy may also have been due to some faulty AIS transmissions or shadowing of the AIS receiver antenna. An analysis of the AIS data <6 km from Lime Kiln using the 'ShipType', two-digit code, indicated a consistent number of combined Bulker/General Cargo, Container, and Vehicle carrier, as well as tanker vessel traffic in January and July (Figure 54), which was consistent with the acoustic detector for large-vessels. The two-digit 'ShipType' code does not distinguish between container vessels, bulk carriers, car carriers, etc. and combines them all as 'cargo'. The biggest change between January and July was in the number of sailing vessels and pleasure craft, with a large increase in July; also consistent with the small-vessel detector. Of the AIS data transmitted in January, it is estimated that 34.9% were from small-vessels not required to transmit AIS signals. This number increased to 46.6% of AIS data in July.

Table 17. Number of minutes included in analyses of January and July 2017 acoustic data, as well as the proportion of those minutes when large-, small-, and no-vessels were present in the data, according to an acoustic detector. For comparison, the proportion of minutes with an Automated Identification System (AIS) transmitting vessel within 6 km of Lime Kiln is also provided.

Metric	*N* (minutes)	Large vessels	Small vessels	No vessels	AIS <6 km
January					
All	43,200	29.2%	1.0%	69.8%	20.3%
Day	15,990	27.5%	0.8%	71.7%	17.8%
Night	27,210	30.2%	1.1%	68.7%	21.8%
July					
All	41,003	33.0%	4.4%	62.6%	19.8%
Day	26,891	34.6%	6.6%	58.8%	20.1%
Night	14,112	30.0%	0.2%	69.8%	19.3%

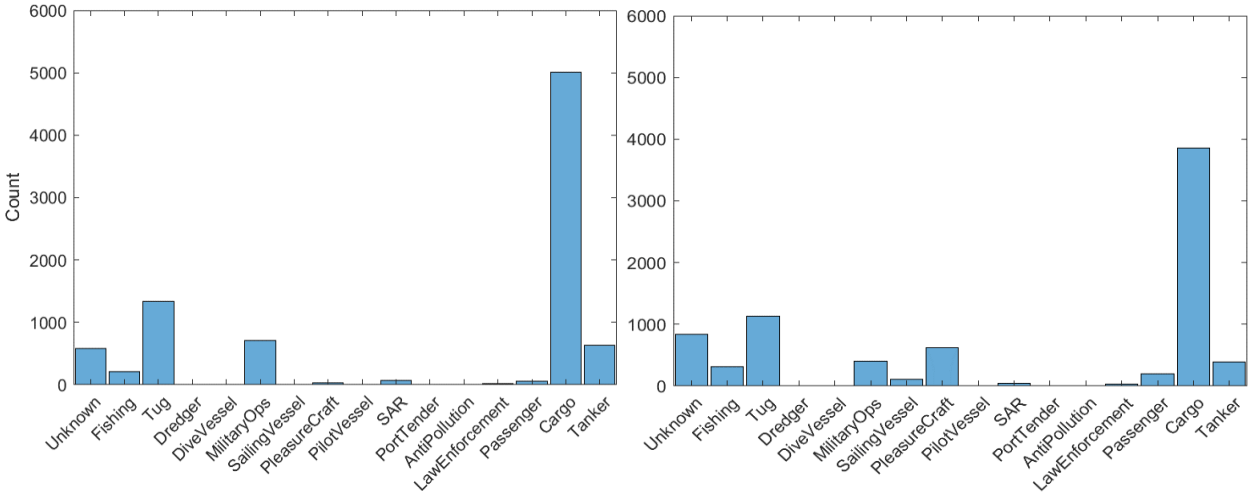

Figure 54. Histograms of Automated Identification System (AIS) data by vessel type in January (left) and July (right) 2017. These are based on vessel class information transmitted by these vessels (called 'ShipType'). The AIS ship type category of 'Cargo' shown in these figures includes Bulker/General Cargo, Container Ship and Vehicle Carrier.

Figure 55 shows the broadband (10 Hz to 100 kHz) cumulative exceedance probability plots for January and July 2017 during periods when large-, small-, and no-vessels were detected at Lime Kiln. Plots for periods when there were AIS transmissions <6 km from Lime Kiln are also provided for comparison with the large-vessel detection periods. Relevant statistics from these periods are provided in Table 18. On average (L_{50}), small-vessels at Lime Kiln produced broadband ambient noise levels 3.7 dB higher than large-vessels in July (e.g., 121.9 versus 118.2 dB re 1 µPa). The July estimates for small-vessel ambient noise levels are considered better than January estimates given the small sample size in January and concerns with the acoustic detector. Small-vessels pass closer to the Lime Kiln hydrophone than large-vessels and thus produced higher ambient noise levels, on average. Periods with no-vessel detections were on average (L_{50}) between 103 and 104 dB re 1 µPa. Cumulative exceedance curves for both the large-vessels and periods with AIS transmissions at <6 km from Lime Kiln agreed well, especially at lower exceedance probabilities (i.e., higher SPL levels). This is to be expected as the acoustic detector will perform less well at lower SPL. Appendix F provides tables with these results broken down to decade bands.

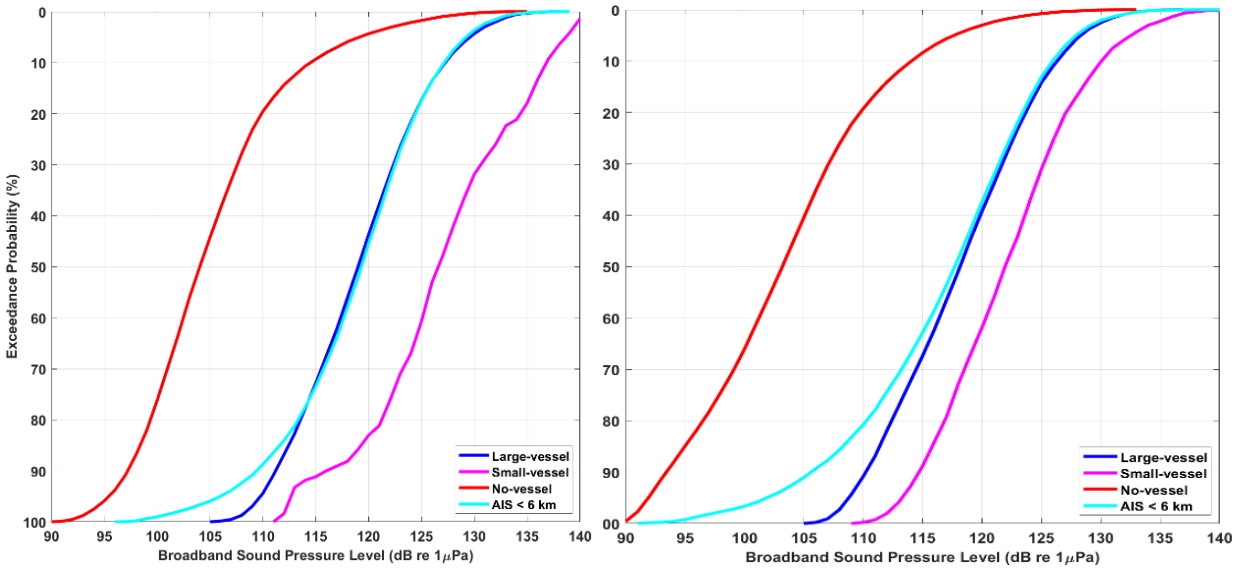

Figure 55. Broadband (10 Hz to 100 kHz) 1-minute cumulative exceedance probability plots for January (left) and July (right) 2017 during time periods with detections of large-, small-, and no-vessels as well as Automated Identification System (AIS) transmissions <6 km of Lime Kiln.

Table 18. One-minute broadband (10 Hz to 100 kHz) sound pressure level (SPL; dB re 1 µPa) statistics during time periods with different acoustic detections and times when there were Automated Identification System (AIS) transmissions <6 km from Lime Kiln during January and July 2017. L_n is the sound level exceeded n% of the time. L_{eq} is the power-average sound level (i.e., the decibel level of the average 1-minute mean-square pressure).

Detector	Large vessel	Small vessel	No vessel	AIS <6 km
January				
L_{95}	109.8	112.7	95.4	106.0
L_{50}	119.0	126.6	104.0	119.3
L_5	129.6	138.7	119.1	129.2
L_{eq}	119.6	127.3	105.6	119.2
July				
L_{95}	108.8	113.3	91.9	101.9
L_{50}	118.2	121.9	103.2	117.7
L_5	128.3	132.6	117.6	127.9
L_{eq}	118.7	122.7	104.1	117.2

3.5. Influence of Biological Presence

3.5.1. Lime Kiln

Acoustic detectors for SRKW were run on Lime Kiln acoustic data from 14 Aug to 14 Sep 2016 and 6 Jul to 6 Oct 2017 (122 days of data). The acoustic detections were validated by an experienced analyst to ensure these detections were true positives. SRKW were detected acoustically for 4,149 minutes and not detected for 171,088 minutes. Figure 56 shows the cumulative exceedance probability plots for broadband (10 Hz to 100 kHz), SRKW 'vocalization' decade band (1–10 kHz) and SRKW 'click' decade band (10–100 kHz) during periods with and without SRKW detections. Table 19 shows the relevant statistics for these periods and bands. On average (L_{50}), there was very little difference in the broadband SPL, but there was a 3.0 dB increase in the SRKW 'vocalization' decade band and a 7.4 dB increase in the SRKW 'click' decade band when SRKW were present, compared to when they were not.

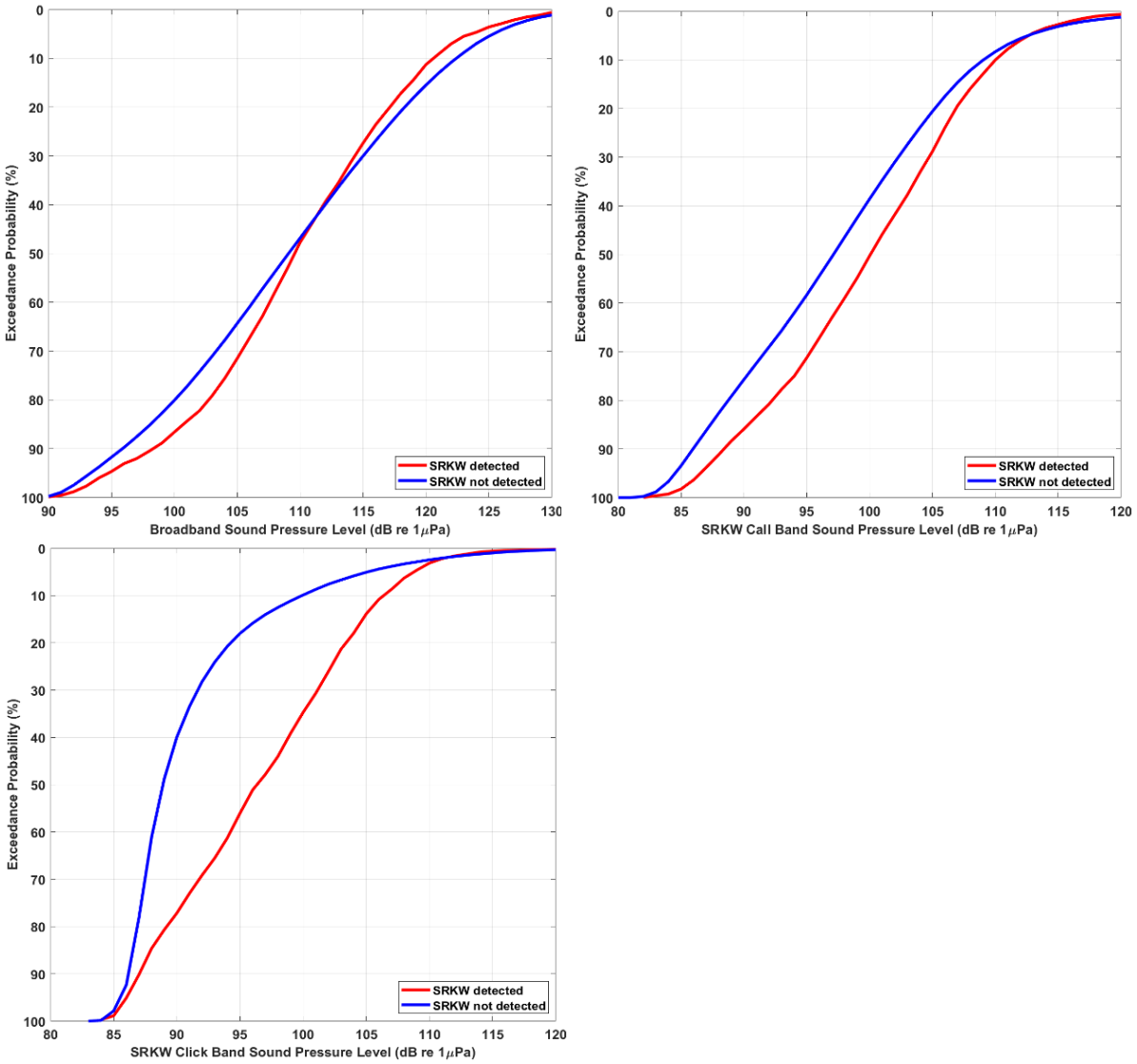

Figure 56. Lime Kiln: One-minute cumulative exceedance probability plots for periods with and without Southern Resident killer whale (SRKW) detections for broadband sound pressure level (SPL; 10 Hz to 100 kHz) (top left), SRKW 'vocalization' decade band SPL (1–10 kHz) (top right), and SRKW 'click' decade band SPL (10–100 kHz) (bottom).

Table 19. Lime Kiln: One-minute sound pressure level (SPL; dB re 1 µPa) statistics during time periods with and without Southern Resident killer whale (SRKW) acoustic detections in broad, SRKW 'vocalization' decade band and SRKW 'click' decade band. L_n is the sound level exceeded n% of the time. L_{eq} is the power-average sound level (i.e., the decibel level of the average 1-minute mean-square pressure).

Detector	SRKW present	SRKW not present
Broadband (10 Hz to 100 kHz)		
L_{95}	94.8	93.3
L_{50}	109.6	109.1
L_5	123.6	125.4
L_{eq}	110.2	98.0
SRKW vocalization *band (1–10 kHz)*		
L_{95}	86.5	84.5
L_{50}	100.1	97.1
L_5	112.7	112.6
L_{eq}	100.4	98.0
SRKW click band (10–100 kHz)		
L_{95}	86.0	85.5
L_{50}	96.3	88.9
L_5	108.8	105.1
L_{eq}	97.2	91.7

3.5.2. East Point

Figure 57 shows a box-and-whisker plot of 1-minute SPL from the East Point hydrophone during time periods with and without killer whale detections on 20 Apr 2016. The time resolution of the killer whale detections was 5 minutes so for each detection, all five 1-minute SPL were included in the "with detection" statistics. This date had the highest number of killer whale detections (605) during 2016 for East Point. Time periods without detections were limited to those within 30 minutes of killer whale detections in order to have a comparable number of minutes without detections. Sound levels were generally lower for time periods with detections, although the lower sound levels (e.g., L_{75}) and median levels were slightly higher for some frequency bands. The maximum increase in the median level due to killer whale vocalizations was 1 dB for the 2 kHz band. These results show there was very little acoustic contribution to ambient noise levels from killer whales on a 1-minute basis; therefore, a CDF and wider frequency band analysis similar to that done at Lime Kiln (Section 3.5.1) was not performed. The results may also indicate that whale vocalization detections were only possible during quieter periods and/or that whales were only vocalizing during quieter periods.

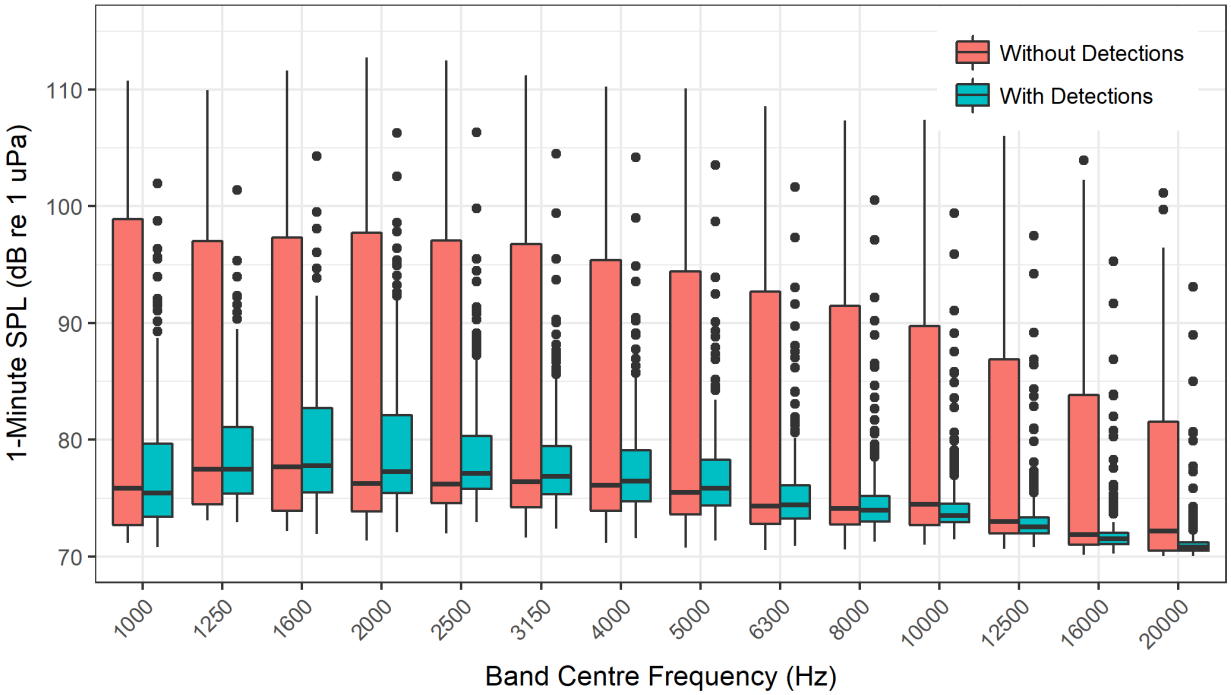

Figure 57. East Point: Box-and-whisker plot of 1-minute sound pressure levels (SPL) in 1/3-octave-bands during time periods with and without killer whale detections measured by the hydrophone on 20 Apr 2016. There were 220 and 195 minutes with and without detections, respectively.

3.5.3. ULS

Figure 58 shows a box-and-whisker plot of 1-minute SPL from the ULS during time periods with and without killer whale detections on 5 Sep 2017. The time resolution of the killer whale detections was 1 minute. This date had the highest number of killer whale detections (1355) during 2016–2017 for the ULS. Time periods without detections were limited to those within 5 minutes of killer whale detections in order to have a comparable number of minutes without detections. Sound levels appear to be lower for time periods with detections. Figure 59 shows results of a similar analysis applied to humpback whale detections from the ULS on 27 Nov 2017. This date had 512 humpback whale detections. Similar to the killer whale analysis, sound levels for minutes with humpback detections were lower than those without detections. A CDF and wider frequency band analysis similar to that done at Lime Kiln (Section 3.5.1) was therefore not performed. These findings may indicate that whale vocalization detections were only possible during quieter periods and/or that whales were vocalizing during quieter periods.

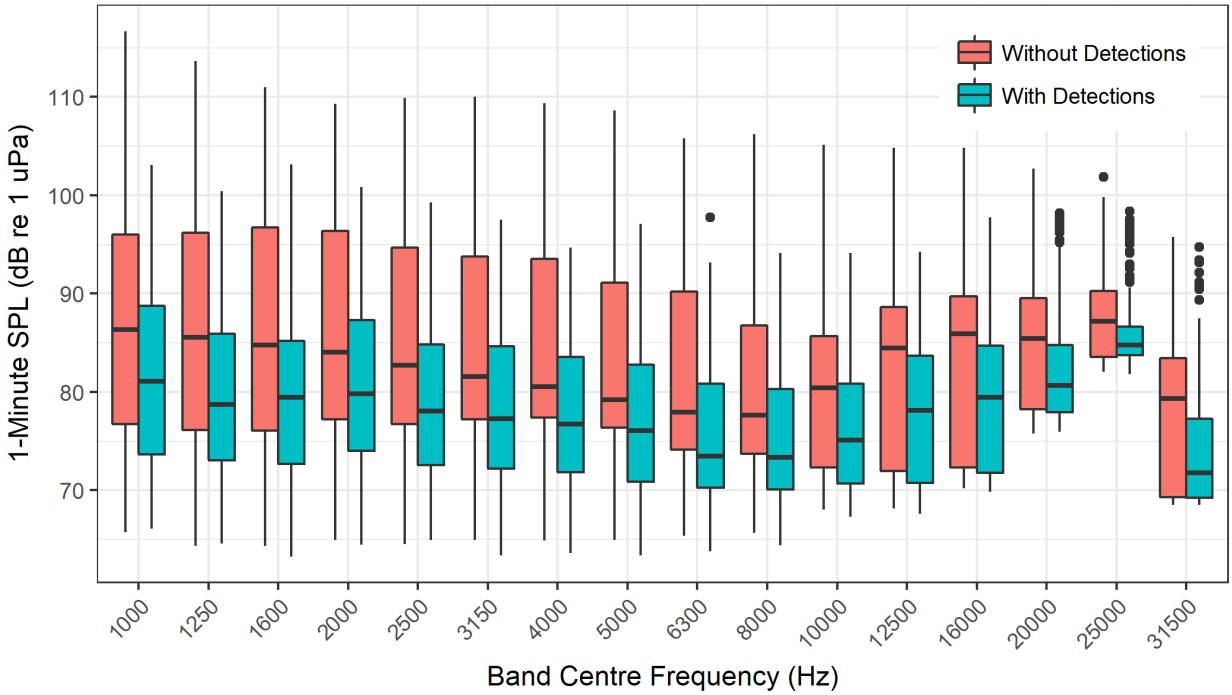

Figure 58. Underwater Listening Station (ULS): Box-and-whisker plot of 1-minute sound pressure levels (SPL) in 1/3-octave-bands during time periods with and without killer whale detections measured on 5 Sep 2017. There were 149 and 60 minutes with and without detections, respectively.

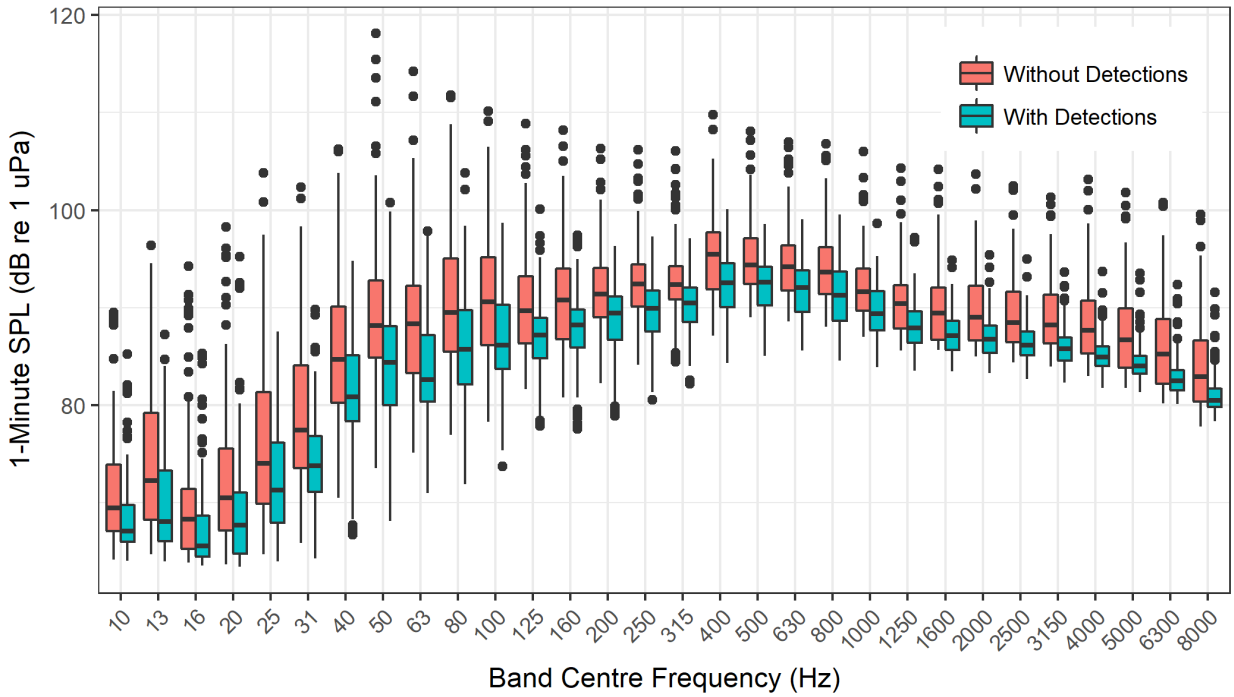

Figure 59. Underwater Listening Station (ULS): Box-and-whisker plot of 1-minute sound pressure levels (SPL) in 1/3-octave-bands during time periods with and without humpback whale detections measured on 27 Nov 2017. There were 105 minutes with detections and 105 minutes without detections.

4. Discussion

4.1. Temporal Variability and Trends

4.1.1. Monthly data

Temporal variability and trends for several of the key factors analyzed in this study help to explain features that were observed in the monthly measured sound levels at the four locations. As previously highlighted, conditions at each location are very different. These include recording systems and hydrophones, propagation environments, deployment depths, distances from the shipping lane, as well as vessel traffic levels and system noise contamination. This makes direct site-to-site comparison difficult, as highlighted by recommendations by the ECHO Program Acoustic Technical Committee to focus on within-site sound level assessments. Nevertheless, a high-level overview of potential causes of variability across the monitoring sites is possible. Figure 60 shows lunar monthly median (L_{50}) ambient noise levels (1-minute broadband SPL) at each location during the study period.

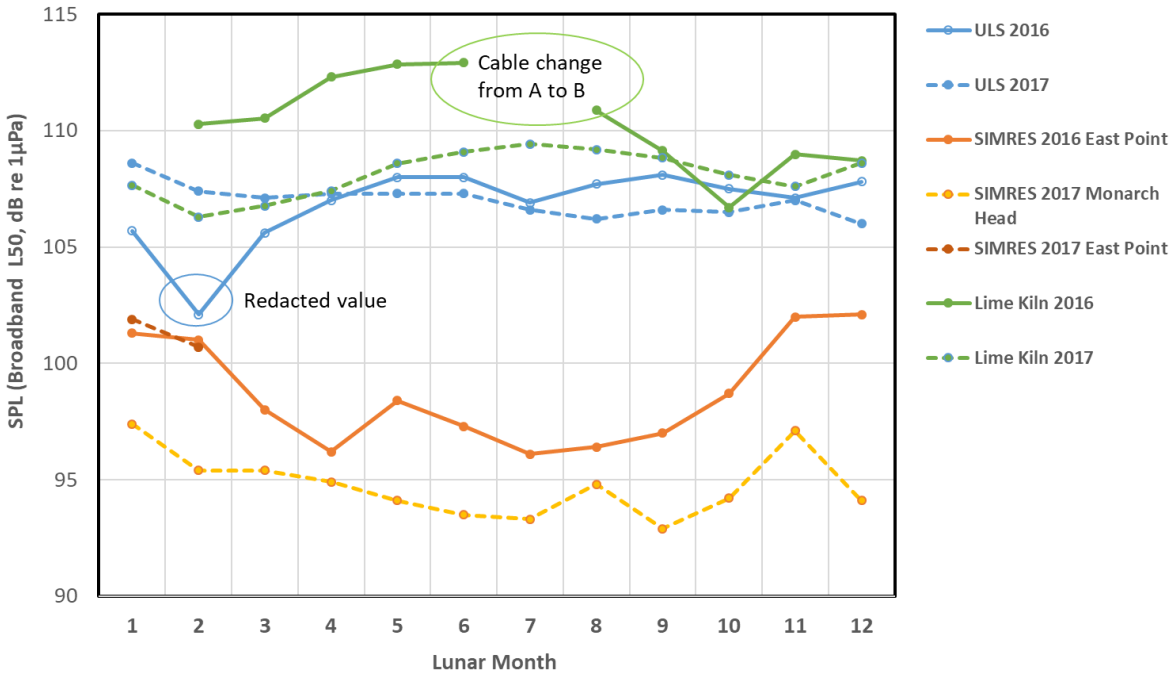

Figure 60. Median 1-minute sound pressure level (SPL; broadband by lunar month) during the study period. Two factors are immediately notable and are annotated in Figure 60. First, the lower sound level at the ULS in February 2016 (month 2) was due to extended periods of military redactions (the SIMRES and Lime Kiln hydrophones were not subject to redactions). These redactions filtered out sound levels below 4 kHz, which reduced the monthly average sound levels calculated in the 10–100, 100–1000, and 1000–10000 Hz bands. Sound level statistics should always be calculated after excluding redacted periods. Sound level statistics for July 2016 at the ULS were calculated after excluding substantial military redaction periods and resulted in a consistent median level with those measured during the preceding and following months.

Second, broadband sound levels at Lime Kiln from February to June were approximately 5 dB higher in 2016 than in 2017. These levels were dominated by the 10–100 Hz band. In July 2016, the Lime Kiln hydrophone was upgraded with a new cable (cable B) and the removal of the thicker (by 20 mm) cable A and an unnecessary junction box. This change in system set-up is believed to have resulted in subsequently lower recorded sound levels (as no other important factors were changed over the monitoring study period). This second factor highlights that major system changes can result in major

changes in recorded ambient sound levels and that such changes should always be noted but also minimized in any long-term monitoring program. As a result of these two factors, the February 2016 redacted SPL results (10–10000 Hz) at the ULS have been removed from subsequent analysis and Lime Kiln data have been partitioned into time periods associated with cables A and B.

The mean (and standard deviation) lunar month median (L_{50}) broadband SPLs at each hydrophone site are shown for each year and over the study period in Figure 61. The mean of the L_{50} SPL was highest at Lime Kiln (~108 dB re 1 µPa; cable B), followed closely by SPL at the ULS (~107 dB re 1 µPa). Corresponding sound levels at both sites in Boundary Pass were considerably lower (~95–99 dB re 1 µPa). Variability across years and months was clearly lowest at the ULS and slightly larger at Lime Kiln. Highest variability was observed at both locations in Boundary Pass. Standard deviations around monthly median SPL were 0.8 dB for ULS, 1.2 dB for Lime Kiln (Cable B), 1.4 dB for Monarch Head, and 2.3 dB for East Point.

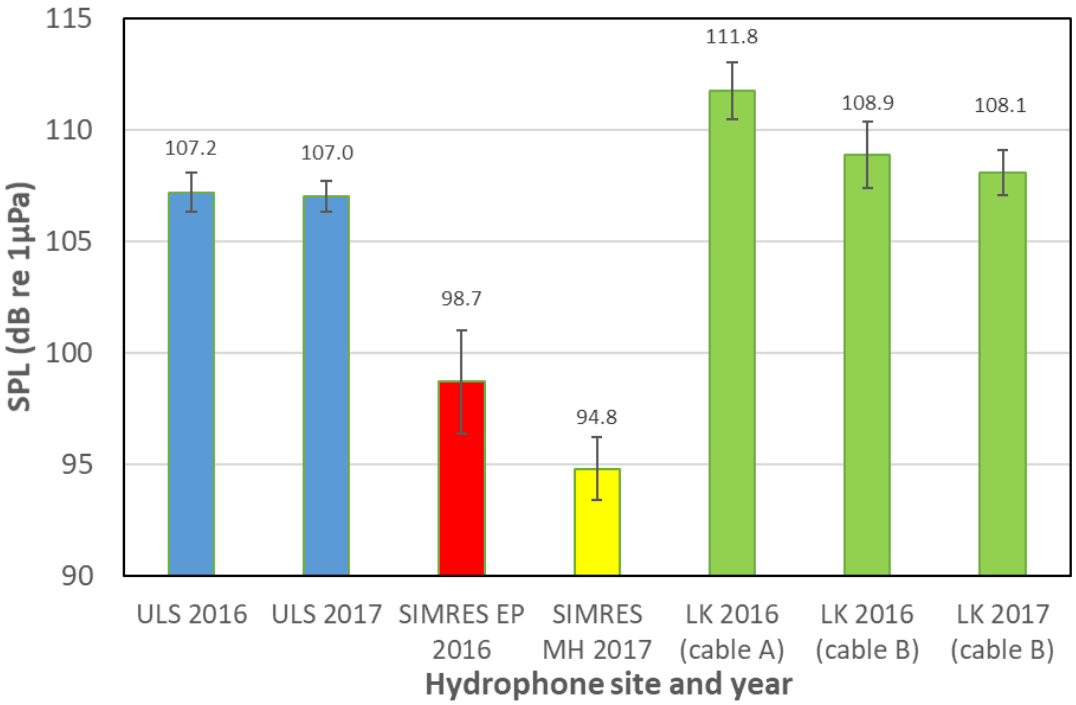

Figure 61. Median 1-minute sound pressure level (SPL; broadband lunar month L_{50} mean and standard deviation) during the study period for each hydrophone location. Sound levels at Lime Kiln in 2016 have been partitioned into periods corresponding to the different cables used, and one redacted month (February 2016) was removed from ULS data.

Temporal variability in the SPL data were further explored using L_{50} decade frequency band SPL and two additional metrics, the arithmetic mean (L_{eq}) and the 5% exceedance value (L_5). The arithmetic mean is the adopted acoustic metric for low-frequency (63 and 125 Hz) long-term ambient noise monitoring within the European Marine Strategy Framework Directive (e.g., Dekeling et al. 2014). The difference between the arithmetic mean and median is a measure of variability and skewness (i.e., lack of symmetry) of received levels. L_5 was proposed by Heise et al. (2017) as one of three acoustic metrics to better understand change in ambient noise levels resident killer whales may be exposed to. Figure 62 shows monthly levels and variability in these metrics for each measurement location. Summary data statistics by site are provided in Table 20 for reference, noting that Lime Kiln data are from cable B only.

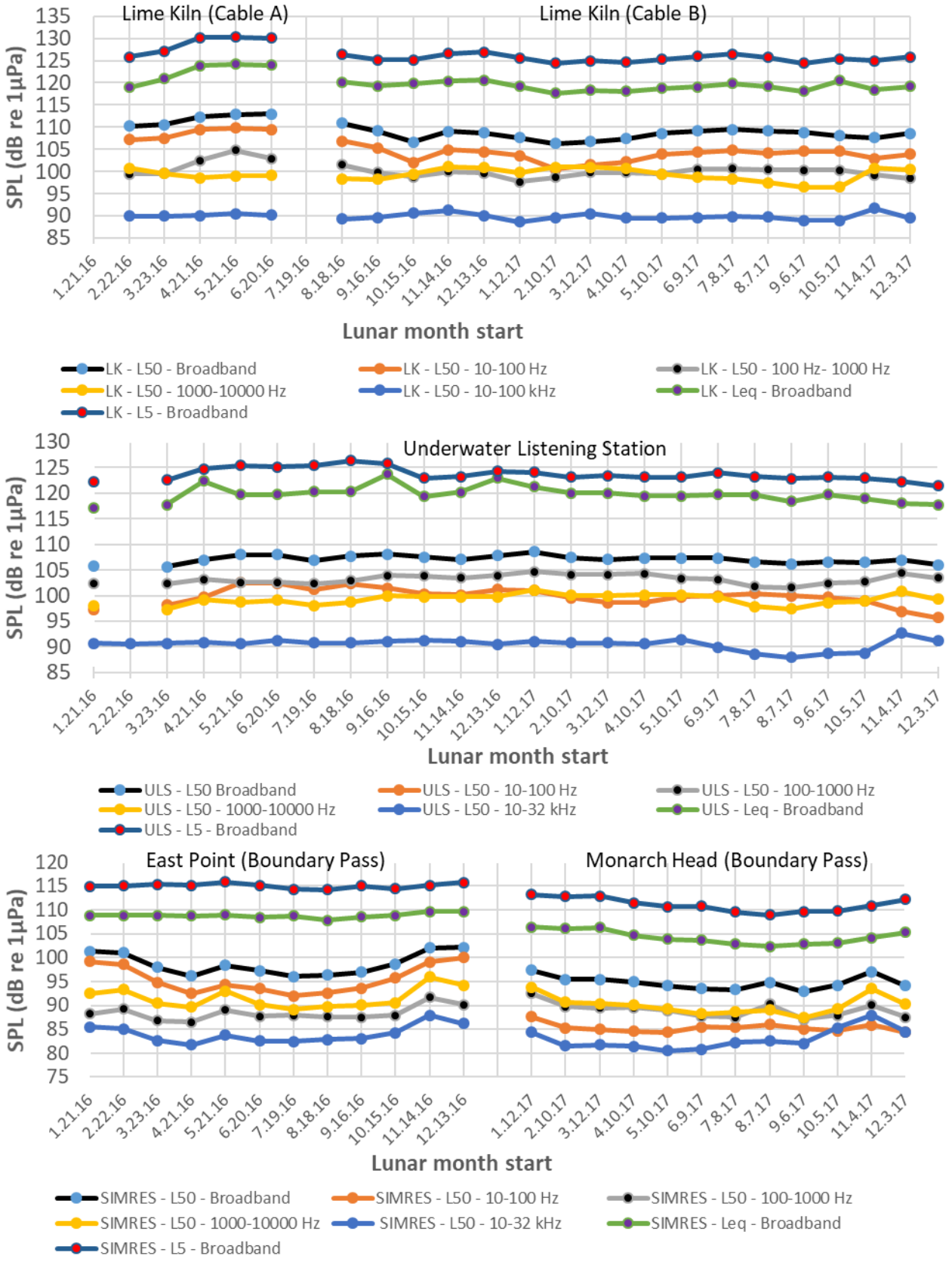

Figure 62. Sound pressure level (SPL, 1-minute average) metrics by lunar month during the study period for each hydrophone location.

Table 20. Summary sound pressure level (SPL; 1-minute average, dB re 1 µPa) metrics during the study period for each acoustic monitoring location.

Hydrophone Location	Year	Metric	Frequency band	Monthly mean SPL (dB)	Monthly std. dev. SPL (dB)	Monthly range SPL (dB)
Lime Kiln	2016/2017 (Cable B)	L_{50}	10 Hz to 100 kHz	108.4	1.2	106.3–110.9
		L_{50}	10–100 Hz	103.8	1.5	100.6–106.8
		L_{50}	100–1000 Hz	99.7	0.9	97.7–101.6
		L_{50}	1–10 kHz	99.3	1.6	96.5–101.1
		L_{50}	10–100 kHz	89.8	0.8	88.6–91.7
		L_{eq}	10 Hz to 100 kHz	119.2	0.9	117.6–120.6
		L_5	10 Hz to 100 kHz	125.5	0.8	124.4–126.9
East Point	2016	L_{50}	10 Hz to 32 kHz	98.7	2.3	96.1–102.1
		L_{50}	10–100 Hz	95.5	3.0	92.0–100.0
		L_{50}	100–1000 Hz	88.4	1.5	86.5–91.7
		L_{50}	1–10 kHz	91.6	2.2	89.1–96.0
		L_{50}	10–32 kHz	84.0	1.9	87.1–87.9
		L_{eq}	10 Hz to 32 kHz	108.8	0.5	107.8–109.7
		L_5	10 Hz to 32 kHz	115.0	0.5	114.2–115.9
Monarch Head	2017	L_{50}	10 Hz to 32 kHz	94.8	1.4	92.4–97.4
		L_{50}	10–100 Hz	85.3	0.9	84.4–87.6
		L_{50}	100–1000 Hz	89.0	1.6	87.1–92.5
		L_{50}	1–10 kHz	90.0	1.9	87.4–93.8
		L_{50}	10–32 kHz	82.9	2.2	80.5–87.9
		L_{eq}	10 Hz to 32 kHz	104.3	1.4	102.4–106.4
		L_5	10 Hz to 32 kHz	111.1	1.4	109.0–113.2
ULS	2016/2017	L_{50}	10 Hz to 32 kHz	107.1	0.8	105.6–108.6
		L_{50}	10–100 Hz	99.8	1.7	95.7–102.5
		L_{50}	100–1000 Hz	103.2	0.9	101.6–104.7
		L_{50}	1–10 kHz	99.3	1.0	97.3–101.1
		L_{50}	10–32 kHz	90.5	1.1	88.0–92.7
		L_{eq}	10 Hz to 32 kHz	119.8	1.6	117.2–123.7
		L_5	10 Hz to 32 kHz	123.7	1.3	121.4–126.3

The between-site differences in L_{eq} and L_5 are similar to those of the L_{50}. L_{eq} SPLs are below L_5 values, but well above (>10 dB) the L_{50} (median) at all sites. This indicates the presence of short term but high amplitude noise sources (Merchant et al. 2013). Most of these high amplitude noise sources are known to be transiting ships and boats. Acoustic shadowing of the shipping lanes from bathymetry features at both the Boundary Pass locations may help explain the lower SPLs noted at this site. This site also had the lowest number of vessel hours (Figure 40). In contrast to L_{50}, the lowest temporal variability in both L_{eq} and L_5 metrics was observed at Lime Kiln and East Point. The observed variability and SPL ranges across key lunar month metrics (2–6 dB) do highlight the analytical challenges in determining appropriate baselines, detecting future trends, and assessing efficacy of short-term mitigation measures. Across L_{50}

decade band sound levels, variability was highest in the first decade band (10–100 Hz) at all sites except Monarch Head, where variability was highest in the highest frequency band (10–32 kHz). At Lime Kiln and East Point, the first decade band had the highest recorded SPLs, whereas at the ULS, the highest SPLs were in the second band (100-1000 Hz) and at Monarch Head the highest SPLs were in the third decade band (1-10 kHz, Table 20). These decade band differences are explored within the following sections as influencing factors within each decade band are further quantified and discussed.

On average, broadband L_{50} SPLs in summer were higher than in winter at Lime Kiln. This is believed to reflect seasonal increases in vessel traffic (Figure 40), particularly for small boat traffic (shown to increase by four fold in summer at Lime Kiln; Table 17). Seasonal sound level trends at the ULS were not evident, potentially because lower transmission loss due to downward refracting propagation conditions in winter may have counteracted the effect of decreased vessel traffic(see Section 3.3.1). In contrast, both sites in Boundary Pass showed higher sound levels in winter than summer (Figure 60). At East Point, this effect was primarily due to the 60 Hz power supply tone dominating the broadband sound levels. It is unknown why noise from the power supply (shown in Figure 16) decreased in summer. Sound levels at Monarch Head in 2017 were lower than those at East Point in 2016, largely because the Monarch Head recorder had lower system noise at low frequencies. The Monarch Head recorder had low-frequency system noise from GPS-induced clicking (10–1000 Hz), but this noise was quieter and relatively stable with time. The long-term pattern of higher levels during winter months in the 0.1–1, 1–10, and 10–32 kHz bands (Figure 62) in Boundary Pass (East Point and Monarch Head hydrophones) may be attributable to higher wind speeds during winter in Boundary Pass (see Figure 63). Wind and wave direction may also influence sound levels, particularly for near-shore hydrophones, but these factors have not been investigated for this study.

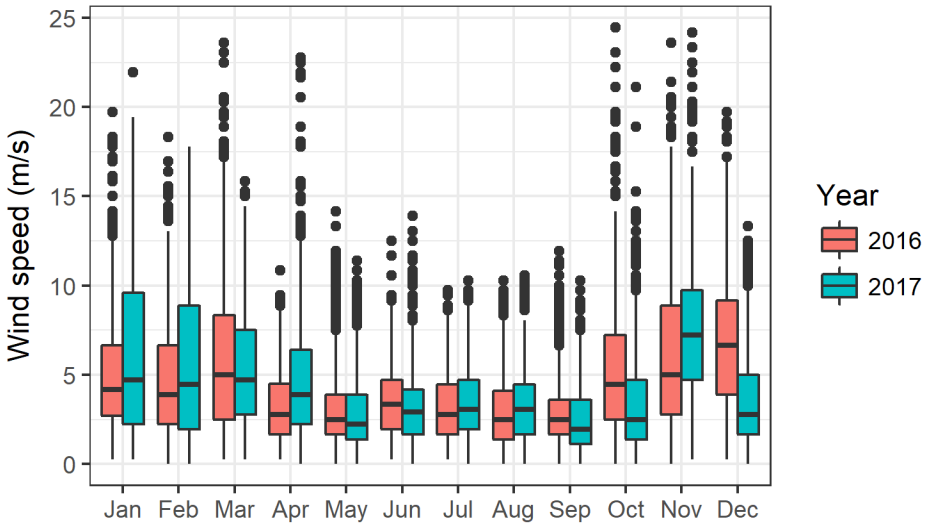

Figure 63. Box-and-whisker plot of hourly wind speed for measurements at the Saturna Island CS weather station, ~630 m from the Boundary Pass East Point hydrophone. The mean and standard deviation of the number of observations for each year/month combination were 726 and 21, respectively.

4.1.2. Influential Factors

Low-frequency flow noise caused by tidal currents was found to affect sound levels at Lime Kiln and the ULS (Section 3.2.1). This effect was demonstrated more clearly at the ULS, due to the high-quality ADCP current data available for that site. Tidal forcing in the Salish Sea is primarily mixed semidiurnal, i.e., there are two high and two low tides of different sizes per lunar day. Currents typically peak between high and low tides, during maximum ebbing and flowing. Sound levels at East Point did not appear correlated with current speed (Figure 27). We expect this was due to the 60 Hz power supply tone masking flow noise.

High winds were associated with increased sound levels at Lime Kiln in January but not July, even though the wind speed distributions were similar between months. We suspect the wind measurements made 20 km south of the Lime Kiln hydrophone may not always be representative of the winds at Lime Kiln. At East Point, sound levels increased with wind speed in January but not July. The effect was observed in January for wind speeds greater than 5 m/s. Wind speeds were lower in July (Figure 63), which may explain the lack of influence of wind speed on sound levels in summer at East Point. Wind effects were not observed at the ULS, likely because of persistent vessel traffic.

AIS vessel traffic exhibited several temporal trends. The seasonal pattern of traffic volume increased in summer and decreased in winter at all sites (Figure 40). In the Strait of Georgia, vessel traffic followed a weekly trend, with highest traffic on Thursdays and lowest traffic on Sundays (Figure 41). Vessel traffic varied with the time of day at each site (Figure 42). In Haro Strait and Boundary Pass, recreational and sailing vessel traffic increased substantially midday. Container ship and vehicle carrier traffic in Boundary Pass was higher early in the day (around 1–2 am). In the Strait of Georgia, early morning tug traffic was particularly high, and the daily pattern of ferry traffic contributed to higher vessel traffic during most hours except between ~1:00 and 4:00 am (PST) (Figure 42).

Analysis of Boundary Pass camera data showed few non-AIS broadcasting vessels in winter but a marked increase in this traffic during summer (Figure 48). Total daytime vessel traffic increased by almost 500% in August compared to February, and the proportion of non-AIS vessel traffic increased from 15 to 72%. Most of these non-broadcasting vessels were sailboats and motorboats, which suggests that summer daytime vessel activity in Boundary Pass largely consisted of recreational vessels.

In Boundary Pass, vessels identified on camera (both AIS and non-AIS) were associated with higher ambient noise levels on the East Point hydrophone (in winter) than on the Monarch Head hydrophone (in summer). It is unknown whether this represents a seasonal trend, however, because these two hydrophones were situated 3 km apart. The differences in location likely affected how the hydrophones received vessel noise (e.g., due to differences in the local bathymetry or shoreline features). Part of the difference may be explained by the fact that the Monarch Head hydrophone was farther from the camera. Certainly, such seasonal differences could have been caused by higher transmission loss in summer due to downwards refracting sound speed profile conditions (despite the paucity of SSP data, we suspect such conditions occur in Boundary Pass due to sea-surface heating in summer). There were, however, substantially more non-AIS vessels detected during summer than during winter. Thus, the overall contribution of smaller vessels to ambient noise, in terms of sound exposure, is expected to be greater during summer than in winter.

Acoustic detections of vessel traffic at Lime Kiln showed small-vessel traffic increased during daytime in summer, whereas large-vessel traffic was relatively consistent with time of day and season. These findings were consistent with AIS records. Although less prevalent in winter, small vessels increased sound levels (SPL) more than in summer. The increase in overall sound exposure due to small vessels in Haro Strait, however, is likely higher in summer due to increased vessel traffic.

Biological presence was found to increase sound levels at Lime Kiln but not the other sites. At Lime Kiln, SRKW vocalizations increased sound levels during summer and fall (Section 3.5.1). SRKW migrate south for winter, so their contribution to ambient sound levels is seasonal.

4.2. Relative Importance of Influential Factors

This section identifies the most important factors contributing to ambient noise measured at each site, based on the results of the analysis. For each site, the factors that could be reliably associated with changes in ambient noise levels are listed, using the available data and methods applied in this study. If a factor is not listed, it does not necessarily indicate that the factor did not influence ambient noise levels. It simply may be the case that unlisted factors affected ambient noise levels on a shorter timescale or a narrower frequency band than was analyzed here, or their effects were masked by more important factors. For example, the effects of rain occurred over too short of a duration for their contribution to the soundscape to be detected with the available covariate data.

4.2.1. Lime Kiln

The most important factors contributing to ambient noise at Lime Kiln were vessel noise, tidal currents, SRKW presence, and system noise (Table 21). Both large- and small-vessel traffic increased measured sound levels in all decade bands when compared to periods with no-vessels. Large-vessels increased sound levels the most in the 10–100 Hz band while small-vessels increased sound levels the most in the 0.1–1, 1–10, and 10–100 kHz bands. Increased AIS vessel traffic volume also increased measured noise levels in all frequency bands. In the 10–100 Hz band, tidal current also appeared to increase sound levels at currents speeds greater than 0.4 m/s. The relationship between current speed and ambient noise was weaker than was observed at the ULS, but this was likely due to unreliable current model predictions at Lime Kiln. It is expected that a relationship such as that found at the ULS would be present at Lime Kiln, had current speed been measured directly. SRKW vocalizations at Lime Kiln increased sound levels in the 1–10 (vocalization) and 10–100 kHz (click) decade bands when compared to periods when they were not vocalizing. This was likely driven by how often SRKW were near the hydrophone when they transited past Lime Kiln. While some of this increased sound level could be attributed to small-vessels engaged in whale watching (i.e., as reflected by small changes in the broadband level), this contribution was likely minimized by voluntary guidelines that ask small-vessels to maintain a 0.5 mile (805 m) buffer from Lime Kiln when whales are present. System noise also contributed to measured sound levels during quiet periods at Lime Kiln. This occurred intermittently in the 10–100 Hz band (at 60 Hz) and consistently in the 10–100 kHz band due to electronic noise interference. While wind driven noise appeared to increase measured sound levels in winter, it was excluded from the list of important factors (Table 21), as it had a minor effect compared to the other factors and was only evident during quiet periods.

Table 21. Lime Kiln: Important factors contributing to ambient noise in Haro Strait. Factors are sorted in order of descending importance within each frequency band. A reported change in median sound levels by a range of decibels indicates the variability depending on either the season or traffic volume.

Frequency	Factor	Effect
10–100 Hz	Large-vessel traffic	Median sound levels were ~17 dB higher than periods with no-vessels. There was <1 dB difference across season. Median sound levels were 3–4 dB higher for days with high large-vessel traffic volume than for days with low large-vessel traffic volume, and were 1 dB higher in summer than in winter.
	Small-vessel traffic	Median sound levels were ~15 dB higher than periods with no-vessels in summer. Winter periods had too small a sample size to measure difference
	Tidal currents	A positive relationship between current velocity and sound levels which is a similar relationship as at the ULS but weaker correlation due to lower quality current data
	System noise	Occasional influence at 60 Hz due to power supply
100–1000 Hz	Small-vessel traffic	Median sound levels were ~19 dB higher than periods with no-vessels in summer. Winter periods had too small a sample size to measure difference
	Large-vessel traffic	Median sound levels were 17–18 dB higher than periods with no vessels. Median sound levels were 3–8 dB higher for days with high large-vessel traffic volume than for days with low large-vessel traffic volume.
1–10 kHz	Small-vessel traffic	Median sound levels were ~22 dB higher than periods with no-vessels in summer. Winter periods had too small a sample size to measure difference
	Large-vessel traffic	Median sound levels were 10–11 dB higher than periods with no-vessels and were 3 dB lower in summer than in winter. Median sound levels were 2–4 dB higher for days with high AIS vessel traffic volume than for days with low AIS vessel traffic volume, and were 1 dB higher in summer than in winter.
	SRKW	SRKW vocalizations increased median levels by ~3 dB compared to periods without SRKW
10–100 kHz	Small-vessel traffic	Median sound levels were ~21 dB higher than periods with no-vessels in summer. Winter periods had too small a sample size to measure difference
	SRKW	SRKW vocalizations increased median levels by ~7 dB compared to periods without SRKW
	Large-vessel traffic	Median sound levels were 3–5 dB higher than periods with no-vessels and were 1 dB lower in summer than in winter. Median sound levels were 0–2 dB higher for days with high large-vessel traffic volume days than for day with low large-vessel traffic volume, and were 4 dB higher in summer than in winter.
	System noise	Various electronic noise caused interference in tonal bands

4.2.2. East Point and Monarch Head

The most important factors identified for the Boundary Pass East Point and Monarch Head recorders were vessel noise, wind-driven ambient noise, and system noise (Table 22). AIS vessel traffic increased measured sound levels in all measured decade bands, and non-AIS vessel traffic increased levels in the 0.1–1, 1–10, and 10–32 kHz bands in the near and mid-range zones (within 3 km of the hydrophone). During quiet periods in January, wind-driven ambient noise increased sound levels in the 0.1–1, 1–10, and 10–32 kHz bands when wind speeds were greater than ~5 m/s. This noise likely included sounds from waves crashing on shore, as both East Point and Monarch Head hydrophones were located less than 40 m from shore. This effect was not seen in July, likely because of the lower wind speeds in summer. System noise was substantial for both recorders and was frequently present in all decade bands, so using these data as baseline measurements is not recommended without careful consideration. At East Point, the 60 Hz tone and higher-frequency harmonics from the power supply limited the ability to measure accurate ambient noise levels most of the time. There was less system noise at Monarch Head, but the persistent GPS-induced clicks limited the recorder's ability to measure low-frequency sound levels. A high-frequency calibration error biased the 10–64 kHz decade band levels too high.

Although no correlation between current speed and low-frequency sound levels at East Point was found, it is expected that flow noise was an important factor in Boundary Pass because of the relatively strong currents. It is also believed that the lack of correlation was due to system noise masking flow noise at East Point. The effects of sound speed profile variability on transmission loss were predicted to be small, but this may have been due to the poor temporal coverage of sound speed profile measurements. Only a few sound speed profile measurements were available, primarily in April, June, and September. Biological presence (killer whales) did not appear to substantially contribute to the ambient noise at East Point. The large difference in the contribution of SRKW vocalizations between East Point and Lime Kiln may be related to their proximity at each site and the duration of their transits.

Table 22. East Point and Monarch Head: Important factors identified in Boundary Pass. Factors are sorted in order of descending importance within each frequency band. A reported change in median sound levels by a range of decibels indicates the variability depending on either the season or traffic volume.

Frequency	Factor	Effect
10–100 Hz	AIS vessel traffic	Median sound levels increased by 5–11 dB when AIS vessel traffic was present
	System noise at East Point	60 Hz power supply tone (89.8–117.6 dB re 1 µPa) and low-frequency noise floor limited ability to accurately measure ambient noise
	System noise at Monarch Head	GPS-induced clicking (101 dB re 1 µPa) and low-frequency noise floor limited ability to accurately measure ambient noise
100–1000 Hz	AIS vessel traffic	Median sound levels increased by 9–25 dB when AIS vessel traffic was present
	Non-AIS vessel traffic within ~3 km of hydrophone	Median sound levels increased by 2–8 dB
	Wind-induced ambient noise	Sound levels during quiet periods increased by ~1 dB/m/s for wind speeds greater than ~4 m/s*
	System noise at East Point	Power supply harmonics limited ability to accurately measure ambient noise except when levels exceeded the L_{25}
	System noise at Monarch Head	GPS-induced clicking (101 dB re 1 µPa) and diurnal power supply tones limited ability to accurately measure ambient noise except when levels exceeded the L_{75} during darkness.
1–10 kHz	AIS vessel traffic	Median sound levels increased by 8–18 dB when AIS vessel traffic was present
	Non-AIS vessel traffic within ~3 km of hydrophone	Median sound levels increased by 3–8 dB
	Wind-induced ambient noise	Sound levels during quiet periods increased by ~1.5 dB/m/s. This effect was only observed in January, likely because the wind speeds were higher in January than in July.
	System noise at East Point	Power supply harmonics limited ability to accurately measure ambient noise except when levels exceeded the L_{25}
	System noise at Monarch Head	Diurnal power supply tones limited ability to accurately measure ambient noise during daylight hours.
10–32/64 kHz	AIS vessel traffic	Median sound levels increased by 4–11 dB when AIS vessel traffic was present
	Non-AIS vessel traffic within ~3 km of hydrophone	Median sound levels increased by 1–6 dB
	Wind-induced ambient noise	Sound levels during quiet periods increased by ~1 dB/m/s for wind speeds greater than ~5 m/s. This effect was not observed in July.
	System noise at Monarch Head	Switching power supply high frequency tones and incorrect recorder sensitivity limited ability to accurately measure ambient noise.

4.2.3. ULS

The most important factors identified for the ULS in the Strait of Georgia were vessel noise, tidal currents, sound speed profile variability, and system noise (Table 23). The Strait of Georgia had the highest AIS traffic volume, exceeding that of Haro Strait and Lime Kiln by 2–3 times. Tug and ferry traffic was particularly high in the Strait of Georgia compared to the other sites. The ULS location was in the middle of the shipping lanes, so vessels frequently passed near to the recorder and elevated sound levels more than at other locations. Higher large commercial vessel traffic volume increased median sound levels in most frequency bands.

Tidal currents produced substantial flow noise on the ULS recorder and increased 10–100 Hz levels during high-current periods. At such times, this noise limited the recorder's ability to measure low levels of low-frequency sounds.

The sound speed profile in the Strait of Georgia varied more than at the other sites; however, this may have been due to greater temporal coverage of the sound speed profile measurements. The amount of variability in the three modelled profiles is expected to occur over month-long timescales. Although transmission loss was higher for downwards-refracting (summer) conditions, sound levels were generally higher in summer than in winter, so the sound speed profile effect was smaller than that due to the overall vessel traffic volume.

Sounds from nearby electrical equipment and sonars limited the ability to accurately characterize ambient noise levels at high frequencies (greater than ~10 kHz).

Wind speed did not appear to be an important factor in the Strait of Georgia, likely because vessel noise masked wind effects. Biological presence (killer and humpback whales) did not appear to contribute to the ambient noise levels at the ULS.

Table 23. Underwater Listening Station (ULS): Important factors identified in the Strait of Georgia. Factors are sorted in order of descending importance within each frequency band. A reported change in median sound levels by a range of decibels indicates the variability depending on either the season or traffic volume.

Frequency	Factor	Effect
10–100 Hz	Large-vessel traffic	Median sound levels were ~2 dB higher for high large commercial vessel traffic volume days than for low large commercial vessel traffic volume days, and were 6–8 dB higher in summer than in winter.
	Tidal currents	Sound levels varied between 100 and 120 dB and increased by ~55 dB/(m/s) for current speeds greater than 0.4 m/s. These currents occurred ~22% of the time.
100–1000 Hz	Large-vessel traffic	Median sound levels were 0–2 dB higher for high large commercial vessel traffic volume days than for low large commercial vessel traffic volume days, and were 5–7 dB higher in summer than in winter.
	Sound speed profile seasonal variability	Transmission loss was 6–8 dB greater during downwards-refracting conditions (e.g., summer) than during other sound speed profile conditions (iso-speed or upwards refracting).
1–10 kHz	Large-vessel traffic	Median sound levels were 0–2 dB higher for high large commercial vessel traffic volume days than for low large commercial vessel traffic volume days, and were 4–5 dB higher in summer than in winter.
	Sound speed profile seasonal variability	Transmission loss was 6–10 dB greater during downwards-refracting conditions (e.g., summer) than during other sound speed profile conditions (iso-speed or upwards refracting).
10–32 kHz	Large-vessel traffic	Median sound levels 3–5 dB higher in summer than in winter.
	Sound speed profile seasonal variability	Transmission loss was 2–4 dB greater during downwards-refracting conditions (e.g., summer) than during other sound speed profile conditions (iso-speed or upwards refracting).
	System noise	Nearby sonars and electrical equipment limited ability to accurately measure ambient noise.

4.3. Limitations of Available Datasets

At times, limitations in the available datasets hindered the ability to draw strong conclusions in the following areas:

1. System noise was particularly difficult to assess because persistent sources are difficult to identify, can change over time and are sometimes beyond control (e.g., quality of mains power or nearby equipment operated by others). Appropriate time periods to measure system noise and sensitivity were not always available and were not standard across sites. Differences between recording systems at the different sites also hindered comparisons of sound levels. Short periods of co-locating different hardware at a single site could provide information about system noise.
2. Weather and tidal conditions had much clearer effects when there were high-quality and local covariate data with a fine temporal resolution (e.g., measured at the ULS with an ADCP). At other sites, the covariate data were at too coarse a time resolution and/or too far away to draw firm conclusions.
3. Sound speed profile data quality were good, but spatial and temporal coverage were poor at times (e.g., coverage was good in the Strait of Georgia but poor in Boundary Pass and Haro Strait). This made the transmission loss-related conclusions for the ULS in the Strait of Georgia much firmer than those at other sites.

4. AIS recording systems stored the data differently making it difficult to classify vessel type consistently between sites.
5. At East Point, photographic data of vessel traffic was limited to daylight hours during periods of good visibility. Vessels, especially when travelling quickly and near the camera, could transit through the field of view between photographs. Furthermore, the acoustic signature of a vessel may exceed the 1-minute window that was delimited for the analysis, increasing ambient noise levels in minutes when no vessels were present on camera. Also, “false absences” (minutes during which a vessel passed in front of the camera but was not detected on camera) would likewise contribute to increased ambient noise levels during minutes classified as having no vessels present. Such false absences would be especially likely for small fast-moving vessels, which spend less time within the camera’s field of view, in the near and mid-zones. Therefore, the relative contributions by both AIS and non-AIS vessels to ambient noise levels in Boundary Pass were likely higher than reported here.
6. Acoustic detections of large-vessels at Lime Kiln were higher than counts of AIS-broadcasting vessels <6 km from Lime Kiln, probably because large-vessels were acoustically detected at distances >6 km. Daytime small-vessel detections were correct 75% of the time. Nighttime small-vessel detections should be disregarded. Small-vessel false positives tended to be large-vessels, flow noise, strumming noise from debris (such as kelp), and biological noise.
7. Biological data quality was good with effective acoustic detectors, but the ability to measure a change in ambient noise due to the presence of whales may have been hindered by consistently high ambient noise levels at some sites and by limited frequency bandwidth (i.e., higher bandwidths at the ULS and Boundary Pass might have captured more echolocation clicks).

4.4. Recommendations for Future Ambient Monitoring

Various mitigation methods are currently being considered, or implemented, to reduce the effects of vessel noise on marine mammals (particularly SRKW) in the Salish Sea. It is important from a management perspective to be able to demonstrate the effectiveness of these mitigation methods through long-term ambient noise monitoring. However, hydrophone data alone is insufficient for establishing the effectiveness of future mitigation actions for reducing vessel noise. Results from this study clearly demonstrate that other streams of data must be collected, in parallel with acoustic data, to properly account for changes in the various influential factors that can affect trends in ambient noise conditions over time. During the review of the 2016–2017 datasets, it was difficult to attribute changes in ambient noise to specific influential factors, without additional data to control for short- and long-term changes in these factors. Thus, a list of requirements was prepared for future ambient noise data monitoring that will be necessary to monitor the effectiveness of noise mitigation methods with a high degree of confidence (summarized in Table 24):

1. Acoustic data analysis:
    a. Sound levels (broadband, decade-band, and 1/3-octave-band) should continue to be calculated on a 1-minute basis and statistics reported by lunar month. Spectrum levels (1-minute PSD) should continue to be reported in monthly and weekly spectrograms and exceedance plots.
    b. Redactions and other outages should be excluded from reported sound level statistics. This was done for some, but not all redaction periods that affected the ULS recordings.
2. Temporal and spatial sampling:
    a. Data collection systems analyzed in this study did not employ duty cycling; therefore, a thorough evaluation of duty cycling could not be completed. Given the large storage and battery capacity of available recording devices, duty cycling should not be necessary and is not recommended.
    b. Hydrophone sampling must be conducted at the same location and depth, year-over-year, to confidently establish long term trends. This is particularly important for near-shore hydrophones, which can be substantially affected by bathymetry features and shorelines blocking sounds from noise sources in large areas from reaching the hydrophone.

3. Calibration:
    a. The response curve of the hydrophone and recording system must be characterized to within ±1 dB over the full frequency range of interest (e.g., 1 Hz to 100 kHz).
    b. The end-to-end system calibrations must be spot-checked, at minimum, annually (using, e.g., a pistonphone or other controlled sound source) to ensure that there are no long-term changes in sensitivity of recording systems. Trends in sensitivity changes should be investigated.
4. System noise:
    a. Before deployment, the noise floor (1-minute PSD spectrum) of the hydrophone and recording system should be measured in a quiet laboratory setting. Tonal noise sources should be identified.
    b. After deployment, the noise floor (1-minute PSD spectrum) of the hydrophone and recording system should be measured monthly during a quiet period (e.g., nighttime, no vessels present, slack tide, low wind). Interfering noise sources should be identified in situ, if possible.
    c. The minimum 1-minute 1/3-octave-band noise level should be reviewed monthly, to monitor changes in system noise characteristics. Any large changes in system noise characteristics should be investigated, as they may be indicative of impending system failure (e.g., increased low frequency noise may be associated with water ingress into hydrophone electronics).
    d. When possible, different recorders should be co-located and ambient noise levels should be compared to characterize system noise. This could be particularly useful if one recorder is autonomous, since they are often less susceptible to system noise.
5. Water currents, wind, and rain:
    a. A meteorological station should record wind and rain data as near as possible to the hydrophone location. Wind speed, wind direction, and precipitation should be recorded on a 1-minute basis. Wind data should be collected at a standard elevation (ideally, on a mast 10 m above sea level).
    b. A current meter (mechanical or acoustical) should be used to record direction and speed of water currents near the hydrophone. If an acoustical meter is used, it should be situated at sufficient distance from the hydrophone to minimize noise contamination on the hydrophone. The amount of noise contamination depends on the characteristics of the current meter (e.g., frequency, power, and beam pattern), recorder (e.g., sample rate and frequency response), and transmission loss. Determining an appropriate separation distance to minimize acoustic contamination may require acoustic modelling and/or test measurements. If a mechanical meter is used, periodic maintenance may be required (e.g., to clear biofouling).
6. Sound speed profile:
    a. Temperature and salinity profiles should be sampled, at minimum, seasonally in deep water near the hydrophone. Recent storm events and freshwater outflow (principally from the Fraser River) will affect measured profiles and so their influence should be considered when interpreting sampled profile data.
    b. Transmission loss modelling should be carried out on a seasonal basis (using method similar to those used in the present report) to quantify the effects of the measured SSPs on underwater sound propagation at the hydrophone.
7. Vessel traffic:
    a. Vessel traffic should continue to be monitored using a land-based AIS receiver near the hydrophone location. It is also recommended to store all raw AIS data and use consistent vessel classification methods. Periods with AIS receiver outages must be identified.
    b. Transits of non-AIS vessel traffic should be monitored at the hydrophone location, using a combination of acoustic and non-acoustic methods to increase the detection rate. Results from this study suggest that a combination of camera and hydrophone detections would be an effective

method. Alternative monitoring methods (e.g., radar) may also be effective for monitoring non-AIS vessels, though they have not been evaluated for this study.

8. Biological presence:
    a. Biological noise sources should continue to be monitored using automated vocalization detectors. A portion of all automatic detections should be manually validated.

Table 24. Summary of recommendations for future ambient noise monitoring.

Covariate	Recommendation	Schedule
Acoustic data analysis	1-minute SPL in 1/3-octave and decade bands, weekly and (lunar) monthly spectrograms and PSD exceedances	Continuous at 1-minute resolution
Temporal and spatial sampling	Duty cycling not recommended	Continuous
	Keep consistent hydrophone location and depth year-over-year	Annual
Calibration	Characterize system response over the full frequency range of interest, calibration with pistonphone	Annual
System noise	Measure system noise floor	Before, after deployment
	Plot minimum 1/3-octave and PSD levels to monitor noise floor	Monthly
Water currents, wind, and rain	Measure in proximity of hydrophone	Continuous at 1-minute resolution
Sound speed profile	Measure in deep water near hydrophone	Seasonally
	Model effect on sound propagation	
Vessel traffic	Use combination of AIS, photographs, acoustic detectors, and potentially radar	Continuous
Biological presence	Use automatic detectors and manually validate a portion of detections	Continuous

5. Conclusions

the influence of system noise, environmental conditions, vessel traffic, and biological presence on ambient sound levels recorded by four hydroacoustic recording systems in Haro Strait, Boundary Pass, and the Strait of Georgia was analyzed. The most important factor at all sites was vessel noise. The Strait of Georgia had the highest vessel traffic, particularly because of tug and ferry traffic. In Haro Strait and Boundary Pass, a substantial proportion of the vessel traffic was recreational and was higher in the daytime and in summer. Photographs of vessel traffic in Boundary Pass and acoustic detections of small vessels in Haro Strait showed that non-AIS vessels contributed to ambient sound levels in daytime summer periods, but the overall long-term contribution to sound exposure was lower than that from large vessels. Small vessels appeared to increase sound levels more at Lime Kiln than at East Point or Monarch Head. It is suspected that this is because small vessel traffic often transits near the Lime Kiln hydrophone but far from the Boundary Pass hydrophones, and sound levels when vessels were not detected in the photographs may have been influenced by vessels that were near the hydrophone but out of view of the camera. The former likely affected the Boundary Pass analysis in summer because the East Point camera was relatively far from the Monarch Head hydrophone.

System noise was unique to each recording system, but data from all recorders was contaminated with narrow-band tones from electrical power supplies and other equipment.. Some system noises varied with time (e.g., 60 Hz tone at East Point), but others were consistent (e.g., GPS clicking at Monarch Head). It was difficult to characterize the effect of system noise at times because it can mask the true acoustic signal.

Environmental conditions, such as tidal currents, wind, rain, and sound speed profile variability, affect sound levels and propagation; however, it was not always possible to determine the contribution of each factor with the data available for this study. The effect of tidal currents was well characterized at the ULS with ADCP measurements. The effect was less clear at Lime Kiln and not observed at East Point. It is suspected that the lack of observed influence at East Point was due to high system noise. High quality ADCP measurements also had disadvantages, however, as the high-frequency chirps contaminated the acoustic recordings at the ULS. Mechanical current meters may therefore be preferable for future ambient monitoring, although they provide only a point measurement.

Wind creates breaking waves and elevates ambient noise levels during quiet periods, and it also increases high-frequency transmission loss due to rough sea surface induced back scatter and weakened coherent reflections. These combined effects can mask quiet sources but typically not loud sources, such as vessels. Wind-induced changes in ambient noise were observed in Haro Strait and Boundary Pass in January but not July. It is suspected that the effect was not observed in July because wind speeds were lower (in Boundary Pass) and wind measurements were not always made at the same location as the hydrophone. No increases in ambient noise levels due to wind were observed in the Strait of Georgia, likely because persistent vessel traffic noise masked wind effects.

Sound speed profile coverage in Haro Strait and Boundary Pass was poor and may have limited the variability in modelled transmission loss in these areas. Sound from rain was observed in the acoustic data at Lime Kiln, but the contribution of rain to ambient sound levels was negligible. In future, rainfall data collected at the hydrophone location and on a finer (e.g., 1-minute) timescale might reveal the contribution of rain to ambient noise.

Biological presence from SRKW was found to increase sound levels at Lime Kiln in the 1–100 kHz frequency range, but biological presence from killer and humpback whales had little to no influence on sound levels in Boundary Pass or the Strait of Georgia, for the limited data analyzed. SRKW travel and vocalize near the Lime Kiln hydrophone relatively often compared to East Point and the ULS, which is why it is suspected that biological presence had more of an influence at Lime Kiln.

The influence of all these factors on ambient noise must be considered when assessing the effectiveness of a noise mitigation strategy (e.g., such as a vessel slowdown initiative). Selecting a baseline or control period is crucial because some of these factors can change on monthly timescales (e.g., SSP) and can be unpredictable (e.g., system noise and biological presence). Therefore, it is advised that baseline noise levels, where possible, be selected appropriately (e.g., from periods just before or after a noise mitigation

action is undertaken, or from the same time period during a previous year). Furthermore, fine-scale, local covariate data should be collected to further control for their effects. Temporarily positioning additional hydrophones nearer to the targeted noise source (e.g., as was done during the 2017 Haro Strait slowdown trial (MacGillivray and Li 2018)) can make it easier to determine the effect of noise mitigation strategies, as such recordings could be less susceptible to other factors.

6. Acknowledgements

The authors of this report would like to acknowledge the contribution of Karen Scanlon, who performed detailed copy-editing, proof-reading, formatting, and review of multiple revisions of this report. The authors would also like to thank Krista Trounce, Justin Eickmeier, and the members of the ECHO Acoustics Technical Committee for their detailed comments on a draft version of this report. This work was undoubtedly improved as a result of their feedback.

Glossary

1/3-octave
One third of an octave. Note: A one-third octave is approximately equal to one decidecade (1/3 oct ≈ 1.003 ddec) (ISO 2017).

1/3-octave-band
Frequency band whose bandwidth is one one-third octave. Note: The bandwidth of a one-third octave-band increases with increasing centre frequency.

absorption
The reduction of acoustic pressure amplitude due to acoustic particle motion energy converting to heat in the propagation medium.

acoustic impedance
The ratio of the sound pressure in a medium to the rate of alternating flow of the medium through a specified surface due to the sound wave.

ambient noise
All-encompassing sound at a given place, usually a composite of sound from many sources near and far (ANSI S1.1-1994 R2004), e.g., shipping vessels, seismic activity, precipitation, sea ice movement, wave action, and biological activity.

attenuation
The gradual loss of acoustic energy from absorption and scattering as sound propagates through a medium.

azimuth
A horizontal angle relative to a reference direction, which is often magnetic north or the direction of travel. In navigation it is also called bearing.

background noise
Total of all sources of interference in a system used for the production, detection, measurement, or recording of a signal, independent of the presence of the signal (ANSI S1.1-1994 R2004). Ambient noise detected, measured, or recorded with a signal is part of the background noise.

bandwidth
The range of frequencies over which a sound occurs. Broadband refers to a source that produces sound over a broad range of frequencies (e.g., seismic airguns, vessels) whereas narrowband sources produce sounds over a narrow frequency range (e.g., sonar) (ANSI/ASA S1.13-2005 R2010).

bar
Unit of pressure equal to 100 kPa, which is approximately equal to the atmospheric pressure on Earth at sea level. 1 bar is equal to 10^5 Pa or 10^{11} µPa.

box-and-whisker plot
A plot that illustrates the centre, spread, and overall range of data from a visual 5-number summary. The ends of the box are the upper and lower quartiles (25th and 75th percentiles). The horizontal line inside the box is the median (50th percentile). The whiskers and points extend outside the box to the highest and lowest observations, where the points correspond to outlier observations (i.e., observations that fall more than 1.5 × IQR beyond the upper and lower quartiles, where IQR is the interquartile range).

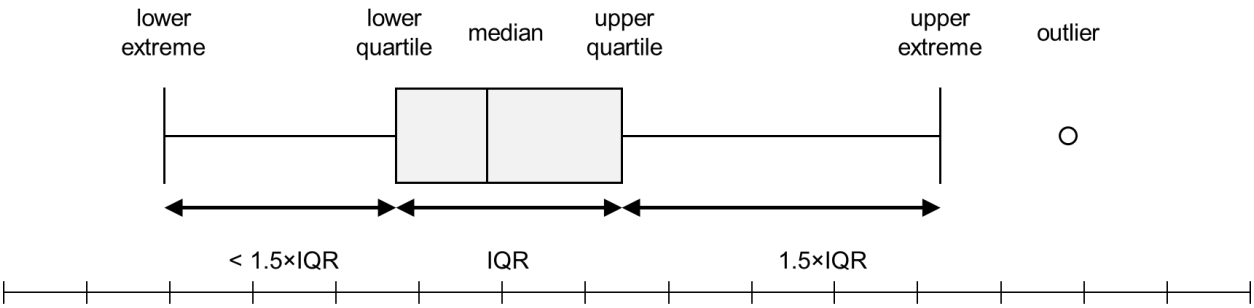

Figure 64. Diagram showing how quantiles are displayed on a box-and-whisker plot. IQR = interquartile range (i.e., the range between the 25th and 75th percentile). Box-and-whisker (box) plots are used throughout this report.

broadband sound level
The total sound pressure level measured over a specified frequency range. If the frequency range is unspecified, it refers to the entire measured frequency range.

cavitation
A rapid formation and collapse of vapor cavities (i.e., bubbles or voids) in water, most often caused by a rapid change in pressure. Fast-spinning vessel propellers typically cause cavitation, which creates a lot of noise.

cetacean
Any animal in the order Cetacea. These are aquatic, mostly marine mammals and include whales, dolphins, and porpoises.

compressional wave
A mechanical vibration wave in which the direction of particle motion is parallel to the direction of propagation. Also called primary wave or P-wave.

continuous sound
A sound whose sound pressure level remains above ambient sound during the observation period (ANSI/ASA S1.13-2005 R2010). A sound that gradually varies in intensity with time, for example, sound from a marine vessel.

CTD (conductivity-temperature-depth)
Measurement data of the ocean's conductivity, temperature, and depth; used to compute sound speed and salinity.

decade
Logarithmic frequency interval whose upper bound is ten times larger than its lower bound (ISO 2006).

decidecade
One tenth of a decade (ISO 2017). Note: An alternative name for decidecade (symbol ddec) is "one-tenth decade". A decidecade is approximately equal to one third of an octave (1 ddec ≈ 0.3322 oct) and for this reason is sometimes referred to as a "one-third octave".

decidecade band
Frequency band whose bandwidth is one decidecade. Note: The bandwidth of a decidecade band increases with increasing centre frequency.

decibel (dB)
One-tenth of a bel. Unit of level when the base of the logarithm is the tenth root of ten, and the quantities concerned are proportional to power (ANSI S1.1-1994 R2004).

frequency
The rate of oscillation of a periodic function measured in cycles-per-unit-time. The reciprocal of the period. Unit: hertz (Hz). Symbol: *f*. 1 Hz is equal to 1 cycle per second.

geoacoustic
Relating to the acoustic properties of the seabed.

Global Positioning System (GPS)
A satellite based navigation system providing accurate worldwide location and time information.

harmonic
A sinusoidal sound component that has a frequency that is an integer multiple of the frequency of a sound to which it is related. For example, the second harmonic of a sound has a frequency that is double the fundamental frequency of the sound.

hertz (Hz)
A unit of frequency defined as one cycle per second.

hydrophone
An underwater sound pressure transducer. A passive electronic device for recording or listening to underwater sound.

intermittent sound
A level of sound that abruptly drops to the background noise level several times during the observation period.

impulsive sound
Sound that is typically brief and intermittent with rapid (within a few seconds) rise time and decay back to ambient levels (NOAA 2013, ANSI S12.7-1986 R2006). For example, seismic airguns and impact pile driving.

masking
Obscuring of sounds of interest by sounds at similar frequencies.

mean-square sound pressure spectral density
Distribution as a function of frequency of the mean-square sound pressure per unit bandwidth (usually 1 Hz) of a sound having a continuous spectrum (ANSI S1.1-1994 R2004). Unit: $\mu Pa^2/Hz$.

median
The 50th percentile of a statistical distribution.

non-impulsive sound
Sound that is broadband, narrowband or tonal, brief or prolonged, continuous or intermittent, and typically does not have a high peak pressure with rapid rise time (typically only small fluctuations in decibel level) that impulsive signals have (ANSI/ASA S3.20-1995 R2008). For example, marine vessels, aircraft, machinery, construction, and vibratory pile driving (NIOSH 1998, NOAA 2015).

octave
The interval between a sound and another sound with double or half the frequency. For example, one octave above 200 Hz is 400 Hz, and one octave below 200 Hz is 100 Hz.

parabolic equation method
A computationally efficient solution to the acoustic wave equation that is used to model transmission loss. The parabolic equation approximation omits effects of back-scattered sound, simplifying the computation of transmission loss. The effect of back-scattered sound is negligible for most ocean-acoustic propagation problems.

percentile level, exceedance
The sound level exceeded *n* % of the time during a measurement.

point source
A source that radiates sound as if from a single point (ANSI S1.1-1994 R2004).

power spectrum density
Generic term, formally defined as power in W/Hz, but sometimes loosely used to refer to the spectral density of other parameters such as square pressure or time-integrated square pressure.

pressure, acoustic
The deviation from the ambient hydrostatic pressure caused by a sound wave. Also called overpressure. Unit: pascal (Pa). Symbol: *p*.

pressure, hydrostatic
The pressure at any given depth in a static liquid that is the result of the weight of the liquid acting on a unit area at that depth, plus any pressure acting on the surface of the liquid. Unit: pascal (Pa).

received level (RL)
The sound level measured (or that would be measured) at a defined location.

rms
root-mean-square.

shear wave
A mechanical vibration wave in which the direction of particle motion is perpendicular to the direction of propagation. Also called secondary wave or S-wave. Shear waves propagate only in solid media, such as sediments or rock. Shear waves in the seabed can be converted to compressional waves in water at the water-seabed interface.

sound
A time-varying pressure disturbance generated by mechanical vibration waves travelling through a fluid medium such as air or water.

sound pressure level (SPL)
The decibel ratio of the time-mean-square sound pressure, in a stated frequency band, to the square of the reference sound pressure (ANSI S1.1-1994 R2004).

For sound in water, the reference sound pressure is one micropascal (p_0 = 1 µPa) and the unit for SPL is dB re 1 µPa^2:

$$L_p = 10\log_{10}(p^2/p_0^2) = 20\log_{10}(p/p_0)$$

Unless otherwise stated, SPL refers to the root-mean-square (rms) pressure level. See also 90% sound pressure level and fast-average sound pressure level. Non-rectangular time window functions may be applied during calculation of the rms value, in which case the SPL unit should identify the window type.

sound speed profile
The speed of sound in the water column as a function of depth below the water surface.

source level (SL)
The sound level measured in the far-field and scaled back to a standard reference distance of 1 metre from the acoustic centre of the source. Unit: dB re 1 µPa·m (pressure level) or dB re 1 µPa^2·s·m (exposure level).

spectral density level
The decibel level (10·log$_{10}$) of the spectral density of a given parameter such as sound pressure level (SPL) or sound exposure level (SEL), for which the units are dB re 1 µPa^2/Hz and dB re 1 µPa^2·s/Hz, respectively.

spectrogram
A visual representation of acoustic amplitude compared with time and frequency.

spectrum
An acoustic signal represented in terms of its power, energy, mean-square sound pressure, or sound exposure distribution with frequency.

surface duct
The upper portion of a water column within which the sound speed profile gradient causes sound to refract upward and therefore reflect off the surface resulting in relatively long-range sound propagation with little loss.

transmission loss (TL)
The decibel reduction in sound level between two stated points that results from sound spreading away from an acoustic source subject to the influence of the surrounding environment. Also referred to as propagation loss.

Very high frequency (VHF)
A frequency range of 30 to 300 megahertz commonly used in radios for marine communications.

wavelength
Distance over which a wave completes one cycle of oscillation. Unit: metre (m). Symbol: λ.

Literature Cited

[ISO] International Organization for Standardization. 2006. *ISO 80000-3:2006. Quantities and Units – Part 3: Space and time*. https://www.iso.org/standard/31888.html.

[ISO] International Organization for Standardization. 2017. *ISO 18405:2017. Underwater acoustics – Terminology*. Geneva. https://www.iso.org/standard/62406.html.

[NGDC] National Geophysical Data Center. 2013. High resolution NOAA digital elevation model. *U.S. Coastal Relief Model (CRM)*. National Oceanic and Atmospheric Administration, U.S. Department of Commerce. http://www.ngdc.noaa.gov/dem/squareCellGrid/download/655.

[NIOSH] National Institute for Occupational Safety and Health. 1998. *Criteria for a recommended standard: Occupational noise exposure. Revised Criteria*. Document Number 98-126. U.S. Department of Health and Human Services, NIOSH, Cincinnati, OH, USA. 122 pp. https://www.cdc.gov/niosh/docs/98-126/pdfs/98-126.pdf.

[NOAA] National Oceanic and Atmospheric Administration (U.S.). 2013. *Draft guidance for assessing the effects of anthropogenic sound on marine mammals: Acoustic threshold levels for onset of permanent and temporary threshold shifts*. National Oceanic and Atmospheric Administration, U.S. Department of Commerce, and NMFS Office of Protected Resources, Silver Spring, MD, USA. 76 pp.

[NOAA] National Oceanic and Atmospheric Administration (U.S.). 2015. *Draft guidance for assessing the effects of anthropogenic sound on marine mammal hearing: Underwater acoustic threshold levels for onset of permanent and temporary threshold shifts*. NMFS Office of Protected Resources, Silver Spring, MD, USA. 180 pp.

[NOAA] National Oceanic and Atmospheric Administration (U.S.). 2017. National Data Buoy Center: Station 46088 (LLNR 16337) - New Dungeness - 17 NM NE of Port Angeles, WA. Department of Commerce, National Oceanic and Atmospheric Administration, National Weather Service. http://www.ndbc.noaa.gov/station_history.php?station=46088 (Accessed 14 Jul 2017).

Aerts, L.A.M., M. Blees, S.B. Blackwell, C.R. Greene, Jr., K.H. Kim, D.E. Hannay, and M.E. Austin. 2008. *Marine mammal monitoring and mitigation during BP Liberty OBC seismic survey in Foggy Island Bay, Beaufort Sea, July-August 2008: 90-day report*. Document Number P1011-1. Report by LGL Alaska Research Associates Inc., LGL Ltd., Greeneridge Sciences Inc., and JASCO Applied Sciences for BP Exploration Alaska. 199 pp. ftp://ftp.library.noaa.gov/noaa_documents.lib/NMFS/Auke%20Bay/AukeBayScans/Removable%20Disk/P1011-1.pdf.

ANSI S12.7-1986. R2006. *American National Standard Methods for Measurements of Impulsive Noise*. American National Standards Institute, NY, USA.

ANSI S1.1-1994. R2004. *American National Standard Acoustical Terminology*. American National Standards Institute, NY, USA.

ANSI/ASA S1.13-2005. R2010. *American National Standard Measurement of Sound Pressure Levels in Air*. American National Standards Institute and Acoustical Society of America, NY, USA.

ANSI/ASA S3.20-1995. R2008. *American National Standard Bioacoustical Terminology*. American National Standards Institute and Acoustical Society of America, NY, USA.

Bassett, C., B. Polagye, M. Holt, and J. Thomson. 2012. A vessel noise budget for Admiralty Inlet, Puget Sound, Washington (USA). *Journal of the Acoustical Society of America* 132(6): 3706-3719. https://doi.org/10.1121/1.4763548.

Collins, M.D. 1993. A split-step Padé solution for the parabolic equation method. *Journal of the Acoustical Society of America* 93(4): 1736-1742. https://doi.org/10.1121/1.406739.

Collins, M.D., R.J. Cederberg, D.B. King, and S. Chin-Bing. 1996. Comparison of algorithms for solving parabolic wave equations. *Journal of the Acoustical Society of America* 100(1): 178-182. https://doi.org/10.1121/1.415921.

Dekeling, R.P.A., M.L. Tasker, M.A. Ainslie, M. Andersson, M. André, M. Castellote, J.F. Borsani, J. Dalen, T. Folegot, et al. 2014. *Monitoring Guidance for Underwater Noise in European Seas, Part I: Executive Summary*. Publications Office of the European Union, JRC Scientific and Policy Report EUR 26557 EN, Luxembourg. http://publications.jrc.ec.europa.eu/repository/handle/JRC88733.

Fisher, F.H. and V.P. Simmons. 1977. Sound absorption in sea water. *Journal of the Acoustical Society of America* 62(3): 558-564. https://doi.org/10.1121/1.381574.

Foreman, M.G.G., W.R. Crawford, J.Y. Cherniawsky, R.F. Henry, and M.R. Tarbottom. 2000. A high-resolution assimilating tidal model for the northeast Pacific Ocean. *Journal of Geophysical Research* 105(C12): 28629-28651. https://doi.org/10.1029/1999JC000122.

Funk, D., D.E. Hannay, D.S. Ireland, R. Rodrigues, and W.R. Koski (eds.). 2008. *Marine mammal monitoring and mitigation during open water seismic exploration by Shell Offshore Inc. in the Chukchi and Beaufort Seas, July–November 2007: 90-day report*. LGL Report P969-1. Prepared by LGL Alaska Research Associates Inc., LGL Ltd., and JASCO Research Ltd. for Shell Offshore Inc., National Marine Fisheries Service (U.S.), and U.S. Fish and Wildlife Service. 218 pp.

Hannay, D.E. and R.G. Racca. 2005. *Acoustic Model Validation*. Document Number 0000-S-90-04-T-7006-00-E, Revision 02. Technical report by JASCO Research Ltd. for Sakhalin Energy Investment Company Ltd. 34 pp.

Heise, K., L. Barrett-Lennard, R. Chapman, T. Dakin, C. Erbe, D.E. Hannay, N. Merchant, J. Pilkington, S. Thornton, et al. 2017. *Proposed Metrics for the Management of Underwater Noise for Southern Resident Killer Whales*. Coastal Ocean Report Series. Volume 2017/2. Report for the Coastal Ocean Research Institute. © Ocean Wise 2017, Vancouver, BC, Canada. 31 pp. http://wildwhales.org/wp-content/uploads/2017/09/Read-the-Report.pdf.

Institute of Ocean Sciences. 2015. WebTide Northeast Pacific Data (v0.7). Bedford Institute of Oceanography. http://www.bio.gc.ca/science/research-recherche/ocean/webtide/nepacific-nepacifique-en.php (Accessed 16 Jan 2019).

Ireland, D.S., R. Rodrigues, D. Funk, W.R. Koski, and D.E. Hannay. 2009. *Marine mammal monitoring and mitigation during open water seismic exploration by Shell Offshore Inc. in the Chukchi and Beaufort Seas, July–October 2008: 90-Day Report*. Document Number P1049-1. 277 pp.

Jensen, F.B., W.A. Kuperman, M.B. Porter, and H. Schmidt. 1994. *Computational Ocean Acoustics*. 1st edition. Modern Acoustics and Signal Processing. AIP Press, New York. 612 pp.

Knudsen, V.O., R.S. Alford, and J.W. Emling. 1948. Underwater ambient noise. *Journal of Marine Research* 7: 410-429.

MacGillivray, A.O. and Z. Li. 2018. *Vessel Noise Measurements from the ECHO Slowdown Trial: Final Report*. Document Number 01518, Version 2.0. Technical Report by JASCO Applied Sciences for Vancouver Fraser Port Authority ECHO Program.

MacGillivray, A.O., Z. Li, D.E. Hannay, K.B. Trounce, and O.M. Robinson. 2019. Slowing deep-sea commercial vessels reduces underwater radiated noise. 146(1): 340-351. https://asa.scitation.org/doi/abs/10.1121/1.5116140.

Martin, B., K. Bröker, M.-N.R. Matthews, J.T. MacDonnell, and L. Bailey. 2015. Comparison of measured and modeled air-gun array sound levels in Baffin Bay, West Greenland. *OceanNoise 2015*. 11-15 May 2015, Barcelona, Spain.

Medwin, H., J.A. Nystuen, P.W. Jacobus, L.H. Ostwald, and D.E. Snyder. 1992. The anatomy of underwater rain noise. *Journal of the Acoustical Society of America* 92(3): 1613-1623. https://doi.org/10.1121/1.403902.

Merchant, N.D., T.R. Barton, P.M. Thompson, E. Pirotta, D.T. Dakin, and J. Dorocicz. 2013. Spectral probability density as a tool for ambient noise analysis. *Journal of the Acoustical Society of America* 133(4): EL262-EL267. https://doi.org/10.1121/1.4794934.

O'Neill, C., D. Leary, and A. McCrodan. 2010. Sound Source Verification. (Chapter 3) *In* Blees, M.K., K.G. Hartin, D.S. Ireland, and D.E. Hannay (eds.). *Marine mammal monitoring and mitigation during open water seismic exploration by Statoil USA E&P Inc. in the Chukchi Sea, August-October 2010: 90-day report*. LGL Report P1119. Prepared by LGL Alaska Research Associates Inc., LGL Ltd., and JASCO Applied Sciences Ltd. for Statoil USA E&P Inc., National Marine Fisheries Service (U.S.), and U.S. Fish and Wildlife Service. pp 1-34.

Porter, M.B. and Y.-C. Liu. 1994. Finite-element ray tracing. *In*: Lee, D. and M.H. Schultz (eds.). *International Conference on Theoretical and Computational Acoustics*. Volume 2. World Scientific Publishing Co. pp 947-956.

Racca, R.G., A. Rutenko, K. Bröker, and M.E. Austin. 2012a. A line in the water - design and enactment of a closed loop, model based sound level boundary estimation strategy for mitigation of behavioural impacts from a seismic survey. *11th European Conference on Underwater Acoustics*. Volume 34(3), Edinburgh, UK.

Racca, R.G., A. Rutenko, K. Bröker, and G. Gailey. 2012b. Model based sound level estimation and in-field adjustment for real-time mitigation of behavioural impacts from a seismic survey and post-event evaluation of sound exposure for individual whales. *In*: McMinn, T. (ed.). *Acoustics 2012 Fremantle: Acoustics, Development and the Environment. Proceedings of the Annual Conference of the Australian Acoustical Society*. Fremantle, Australia. http://www.acoustics.asn.au/conference_proceedings/AAS2012/papers/p92.pdf.

Schulkin, M. and R. Shaffer. 1964. Backscattering of Sound from the Sea Surface. *Journal of the Acoustical Society of America* 36(9): 1699-1703. https://doi.org/10.1121/1.1919267.

Vancouver Fraser Port Authority. 2018. ATC Ambient Noise Evaluation Meeting Summary - February 27, 2018.

Warner, G.A., C. Erbe, and D.E. Hannay. 2010. Underwater Sound Measurements. (Chapter 3) *In* Reiser, C.M., D. Funk, R. Rodrigues, and D.E. Hannay (eds.). *Marine Mammal Monitoring and Mitigation during Open Water Shallow Hazards and Site Clearance Surveys by Shell Offshore Inc. in the Alaskan Chukchi Sea, July-October 2009: 90-Day Report*. LGL Report P1112-1. Report by LGL Alaska Research Associates Inc. and JASCO Applied Sciences for Shell Offshore Inc., National Marine Fisheries Service (U.S.), and Fish and Wildlife Service (U.S.). pp 1-54.

Water Properties Group. 2019. Water Properties. Fisheries and Oceans Canada, Institute of Ocean Sciences. https://www.waterproperties.ca/data/ (Accessed 16 Jan 2019).

Wladichuk, J.L., G. Warner, A. McCrodan, and A.O. MacGillivray. 2014. *Appendix 9.8A Construction and Terminal Activity Underwater Noise Modelling Study*. Roberts Bank Terminal 2 Technical Report—Underwater Noise Construction Activities and Terminal Vessel Operations Noise Modelling Study. Technical report by JASCO Applied Sciences for Port Metro Vancouver. 198 pp. http://www.ceaa-acee.gc.ca/050/documents/p80054/101367E.pdf.

Wood, J., D.J. Tollit, R. Joy, F. Robertson, and T. Yack. 2018. *ECHO slowdown trial: Ambient noise and SRKW acoustic detections. Final Report*. Technical report by SMRU Consulting for the ECHO Program of the Vancouver Fraser Port Authority.

Zhang, Z.Y. and C.T. Tindle. 1995. Improved equivalent fluid approximations for a low shear speed ocean bottom. *Journal of the Acoustical Society of America* 98(6): 3391-3396. https://doi.org/10.1121/1.413789.

Appendix A. Sound Propagation Model

A.1. Transmission Loss with MONM

Underwater sound propagation (i.e., transmission loss) was predicted with JASCO's Marine Operations Noise Model (MONM) for frequencies of 30, 300, 3000, and 30000 Hz. At low frequencies (30 and 300 Hz), MONM computes acoustic propagation via a wide-angle parabolic equation solution to the acoustic wave equation (Collins 1993). The low-frequency module of MONM is based on a version of the U.S. Naval Research Laboratory's Range-dependent Acoustic Model (RAM), which has been modified to account for a solid seabed (Zhang and Tindle 1995). The parabolic equation method has been extensively benchmarked and is widely employed in the underwater acoustics community (Collins et al. 1996). MONM accounts for the additional reflection loss at the seabed, which results from partial conversion of incident compressional waves to shear waves at the seabed and sub-bottom interfaces, and it includes wave attenuations in all layers. MONM incorporates the following site-specific environmental properties: a bathymetric grid of the modelled area, underwater sound speed as a function of depth, and a geoacoustic profile based on the overall stratified composition of the seafloor.

At high frequencies (3000 and 30000 Hz), MONM computes sound propagation using the BELLHOP Gaussian beam acoustic ray-trace model (Porter and Liu 1994). The high-frequency module of MONM accounts for sound attenuation due to energy absorption through ion relaxation and viscosity of water in addition to acoustic attenuation due to reflection at the medium boundaries and internal layers (Fisher and Simmons 1977). The former type of sound attenuation is significant for frequencies higher than 5 kHz and cannot be neglected without noticeably affecting the model results.

MONM computes acoustic fields in three dimensions by modelling transmission loss within two-dimensional (2-D) vertical planes aligned along radials covering a 360° swath from the source, an approach commonly referred to as *N*×2-D. These vertical radial planes are separated by an angular step size of $\Delta\theta$, yielding $N = 360°/\Delta\theta$ number of planes (Figure 65).

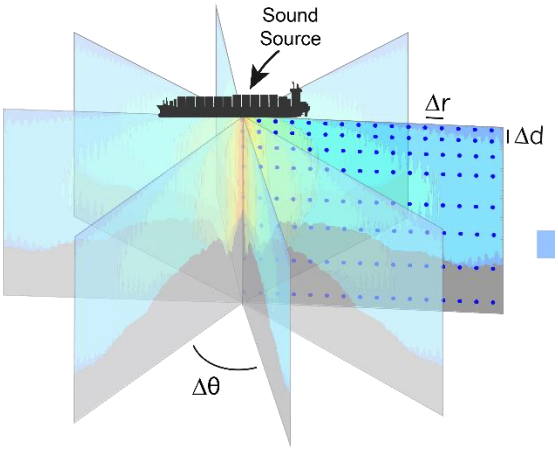

Figure 65. The *N*×2-D modelling approach used by JASCO's Marine Operations Noise Model (MONM).

The transmission loss within each vertical radial plane is calculated at various ranges from the source, generally with a fixed radial step size (Δr in Figure 65). At each sampling range along the surface, the sound field is sampled at various depths (Δd in Figure 65).

For this study, transmission loss was modelled using the principle of reciprocity, which is that transmission loss from a source to a receiver is the same as the transmission loss if the source and receiver switched locations. Transmission loss was modelled with the "source" at the hydrophone location and modelled over a large area for "receivers" at several depths.

MONM's predictions have been validated against experimental data from several underwater acoustic measurement programs conducted by JASCO (Hannay and Racca 2005, Aerts et al. 2008, Funk et al. 2008, Ireland et al. 2009, O'Neill et al. 2010, Warner et al. 2010, Racca et al. 2012a, Racca et al. 2012b, Martin et al. 2015).

A.2. Environmental Properties

MONM uses environmental properties such as bathymetry, geoacoustic properties, and the water sound speed profile to calculate transmission loss (Section 3.3 describes the sound speed profiles). Bathymetry within the study area was compiled from the NOAA digital elevation model (NGDC 2013) and Canadian Hydrographic Service charts. Bathymetry data were gridded onto a 20 m resolution BC Albers grid for transmission loss modelling. Geoacoustic properties were taken from Wladichuk et al. (2014). The Haro Strait geoacoustic properties were used for the Lime Kiln and East Point sites, and the Strait of Georgia properties were used for the ULS. Table 25 lists the geoacoustic properties used for transmission loss modelling in this study.

Table 25. Strait of Georgia: Geoacoustic models for transmission loss modelling. Within each depth range, each parameter varies linearly within the stated range.

Depth below seafloor (m)	Material	Density (g/cm³)	Compressional wave		Shear wave	
			Speed (m/s)	Attenuation (dB/λ)	Speed (m/s)	Attenuation (dB/λ)
0–100	Clayey-silt	1.54	1502–1602	0.61	125	2.2
>100	Bedrock	1.90	2275	0.10		

Table 26. Boundary Pass and Haro Strait: Geoacoustic models for transmission loss modelling. Within each depth range, each parameter varies linearly within the stated range.

Depth below seafloor (m)	Material	Density (g/cm³)	Compressional wave		Shear wave	
			Speed (m/s)	Attenuation (dB/λ)	Speed (m/s)	Attenuation (dB/λ)
0–50	Sand-silt-clay	1.80	1541–1591	0.72	250	1.2
>50	Bedrock	1.90	2275	0.10		

Appendix B. System Noise Figures

This section contains supplementary figures that show effects of system noise on measured sound levels. Also see related figures in Section 3.1.

B.1. East Point

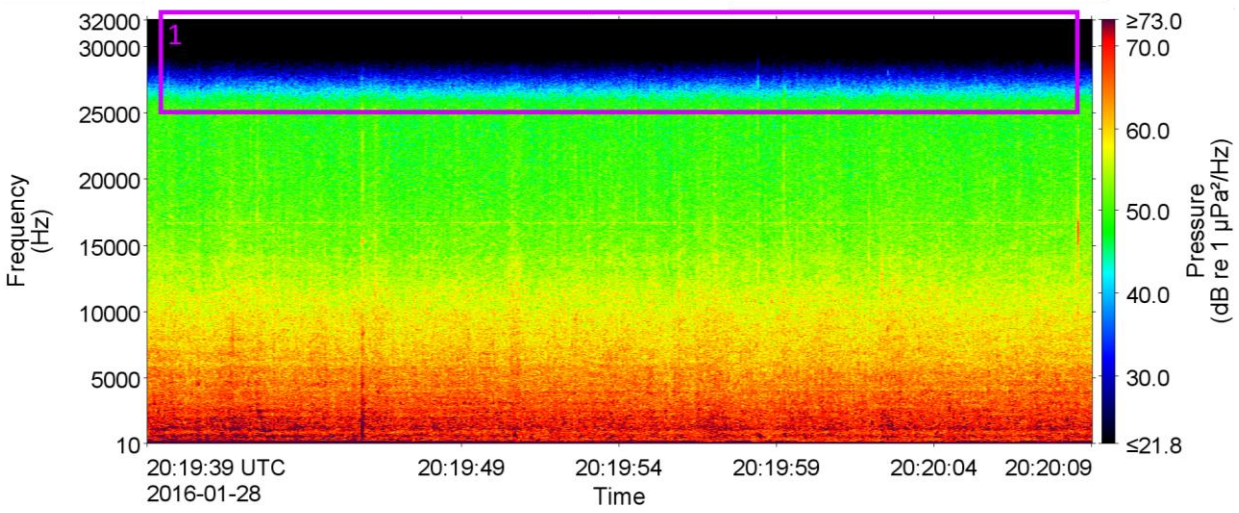

Figure 66. East Point: Spectrogram of recording in January 2016 with a linear frequency scale. Annotation 1 shows the effect of an anti-aliasing filter (see Table 7).

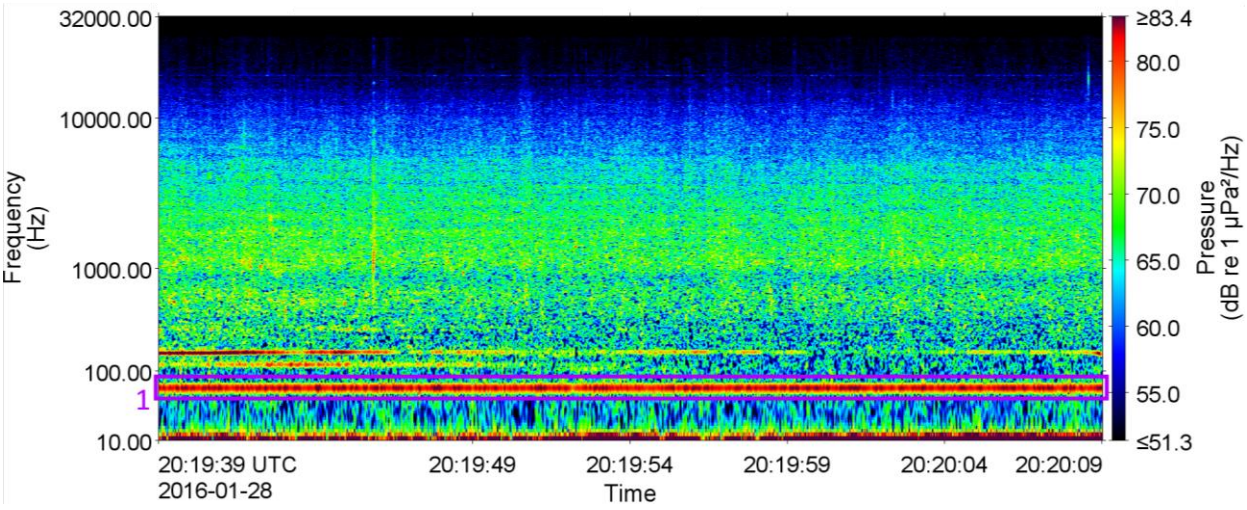

Figure 67. East Point: Spectrogram of recording in January 2016 with a logarithmic frequency scale. Annotation 1 shows the primary (60 Hz) tone from the recorder power supply (see Table 7).

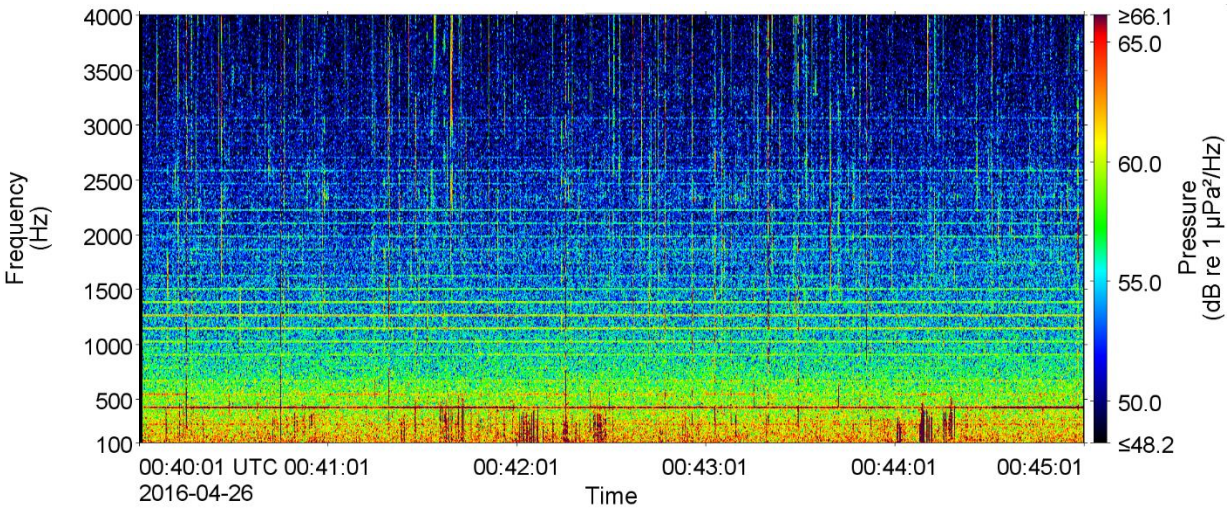

Figure 68. East Point: Spectrogram of recording in April 2016.

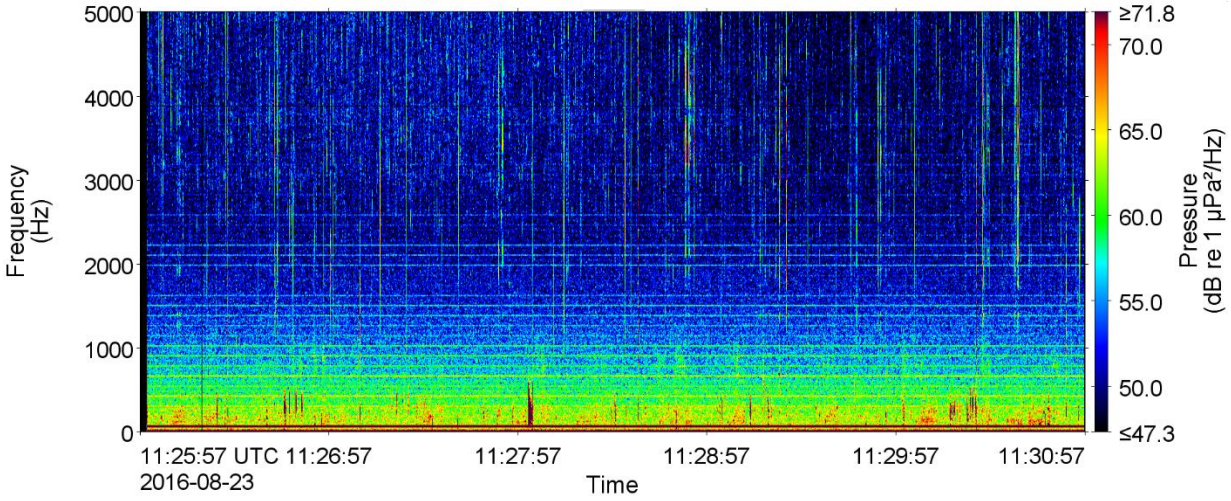

Figure 69. East Point: Spectrogram of recording in August 2016.

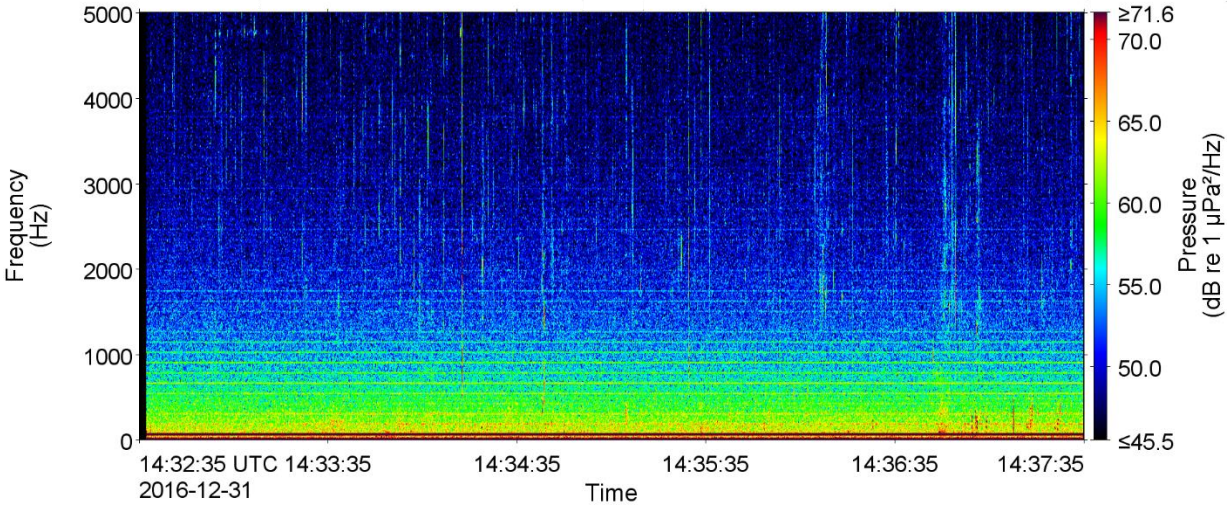

Figure 70. East Point: Spectrogram of recording in December 2016.

B.2. Monarch Head

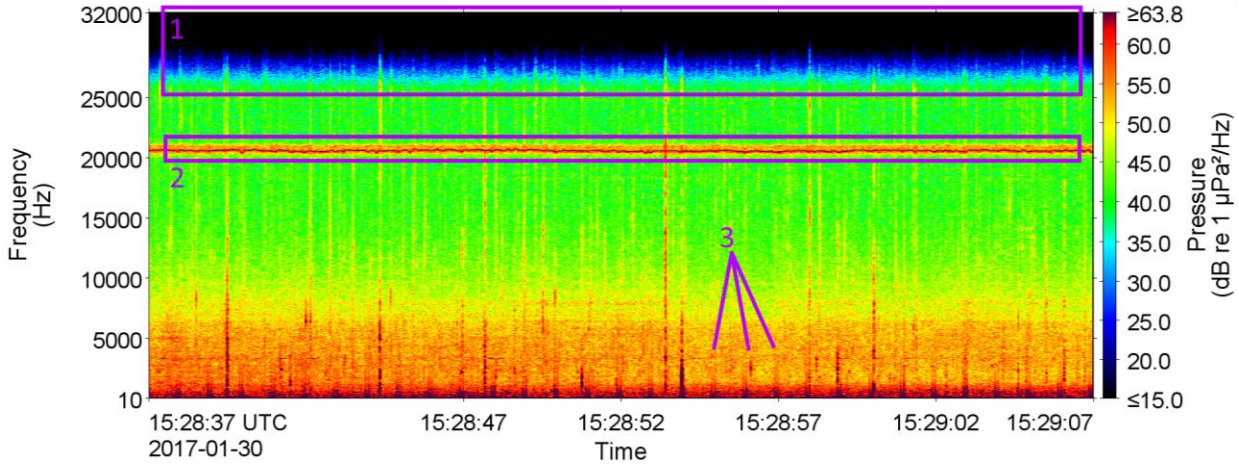

Figure 71. Monarch Head: Spectrogram of recording in January 2017 with a linear frequency scale. See Table 7 for annotation descriptions.

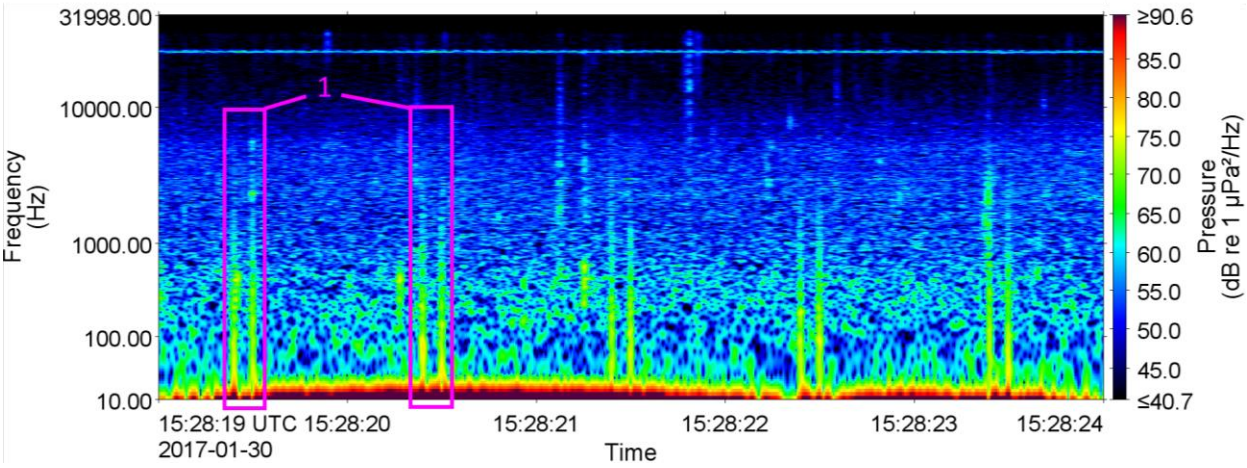

Figure 72. Monarch Head: Spectrogram of recording in January 2017 with a logarithmic frequency scale. See Table 7 for annotation descriptions.

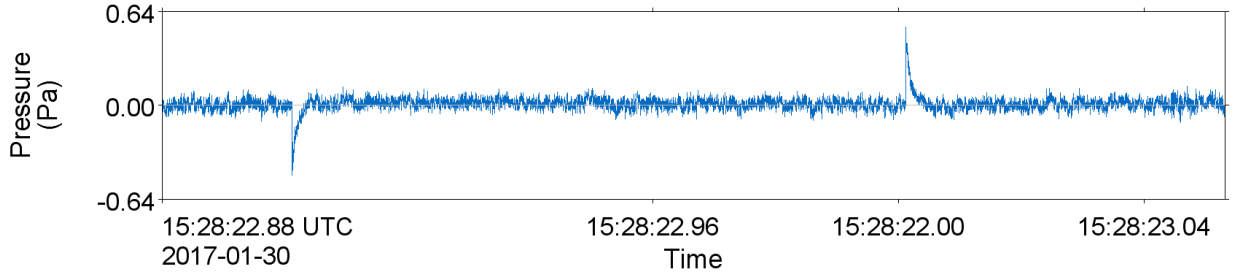

Figure 73. Monarch Head: Waveform of Global Positioning System (GPS) signal on recording in January 2017. The signal was composed of an initial negative pressure signal followed by a positive pressure signal 0.1 s after. The double pulse signal occurred every second.

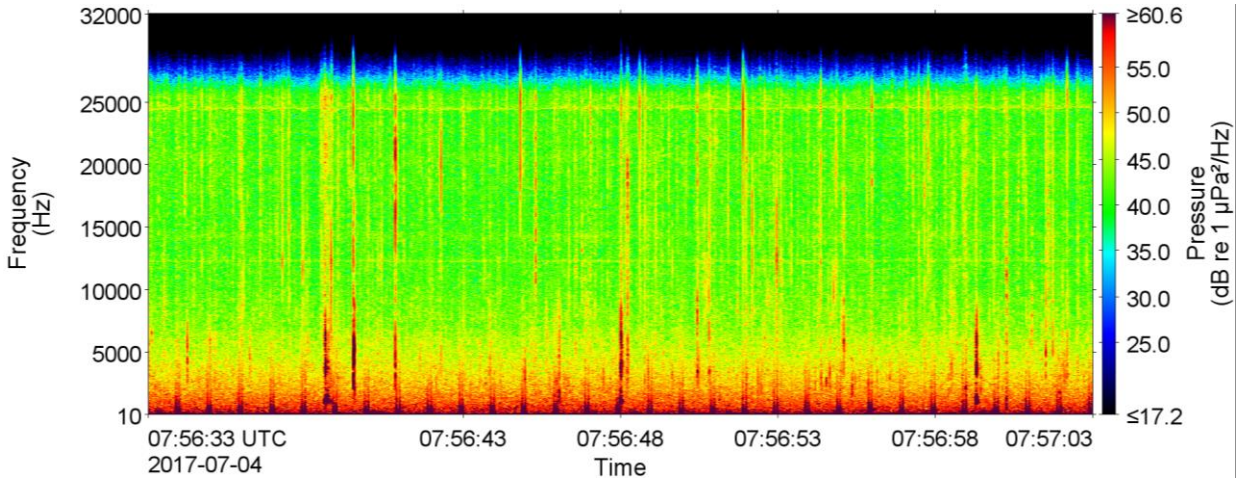

Figure 74. Monarch Head: Spectrogram of recording in July 2017.

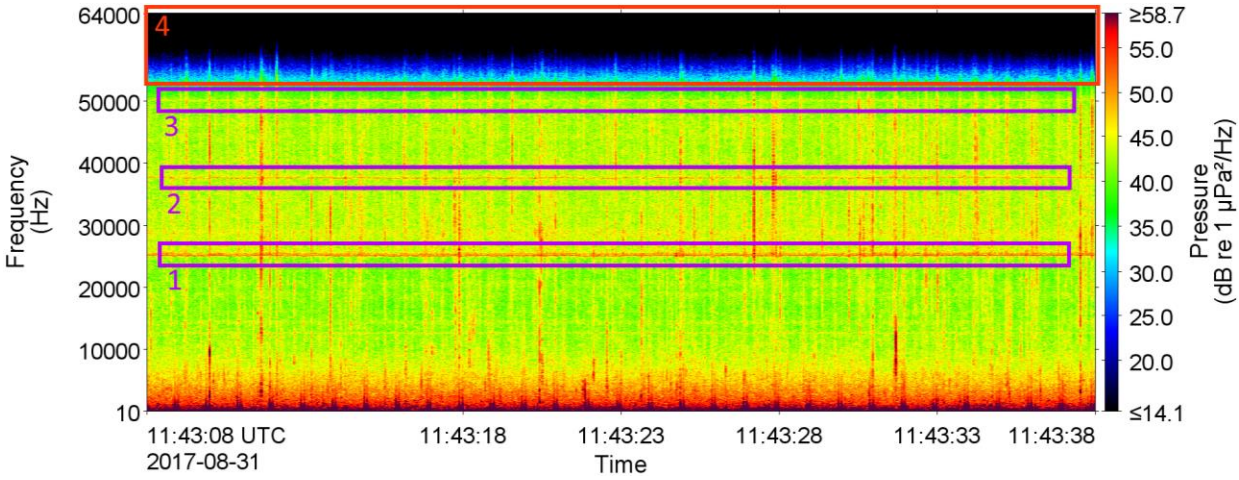

Figure 75. Monarch Head: Spectrogram of recording in August 2017. See Table 7 for annotation descriptions.

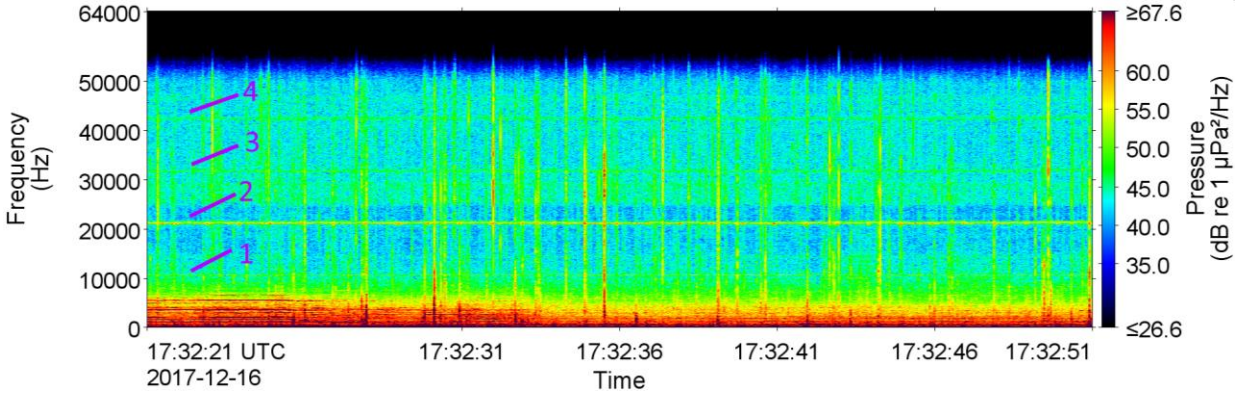

Figure 76. Monarch Head: Spectrogram of recording in December 2017. See Table 7 for annotation descriptions.

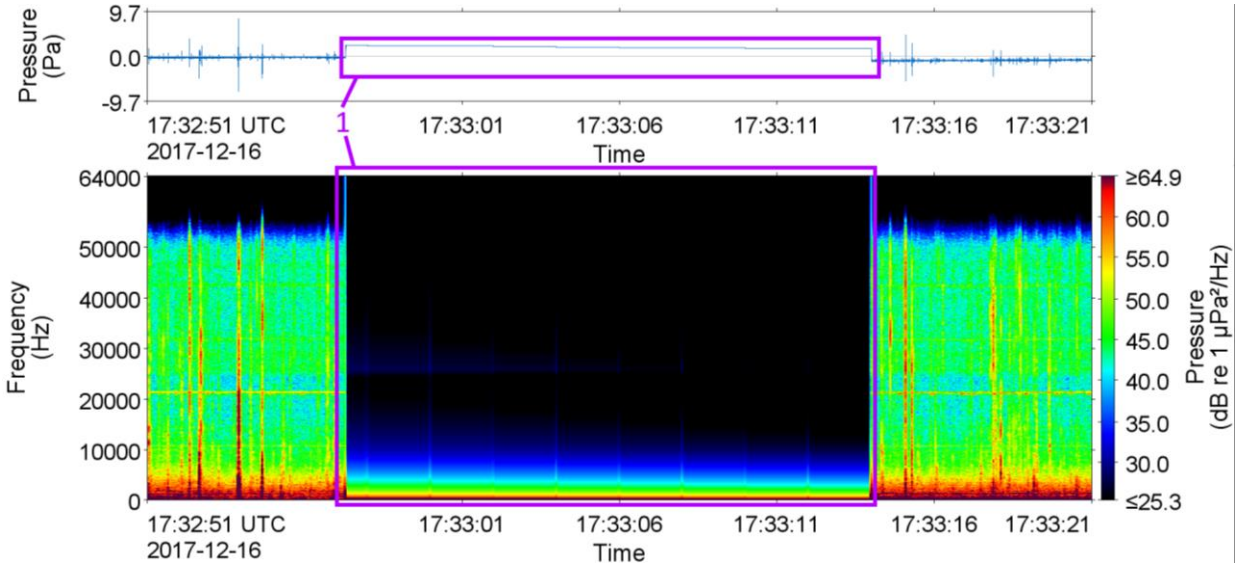

Figure 77. Monarch Head: Spectrogram of recording with major malfunction in December 2017. Annotation 1 shows a time period with a major system malfunction (see Table 7).

B.3. ULS

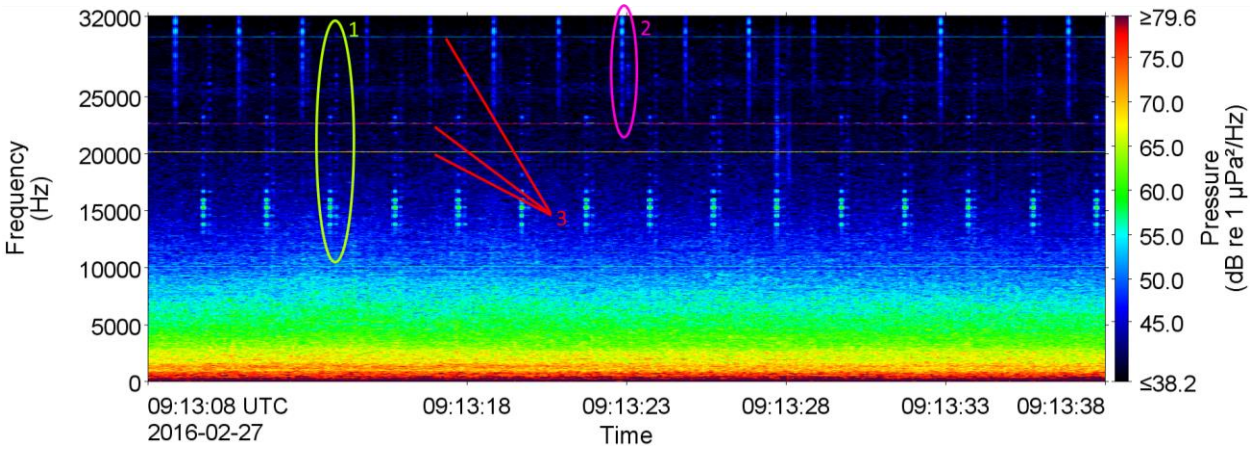

Figure 78. Underwater Listening Station (ULS): Spectrogram of recording in February 2016. Annotations are described in Table 11.

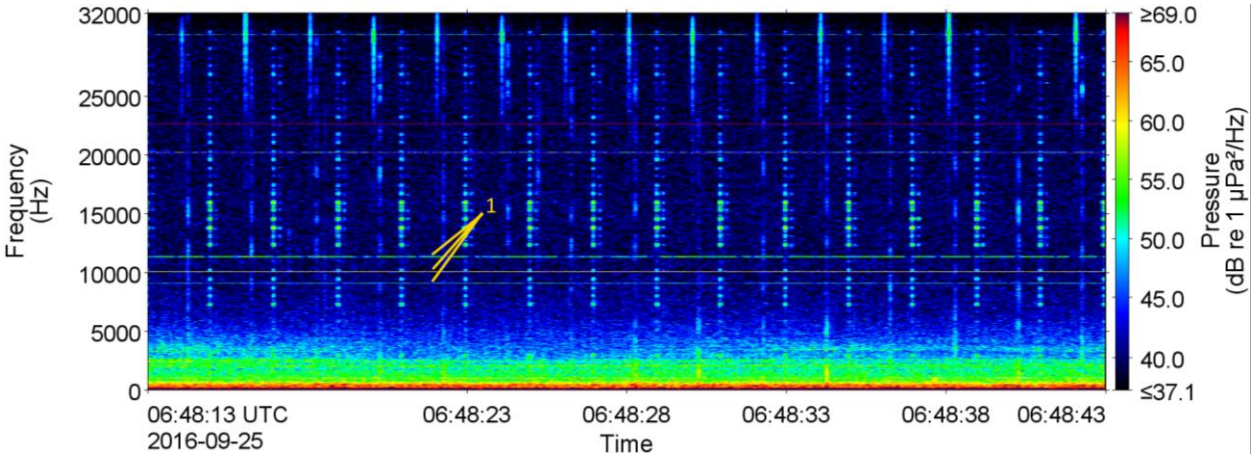

Figure 79. Underwater Listening Station (ULS): Spectrogram of recording in September 2016. Annotation is described in Table 11.

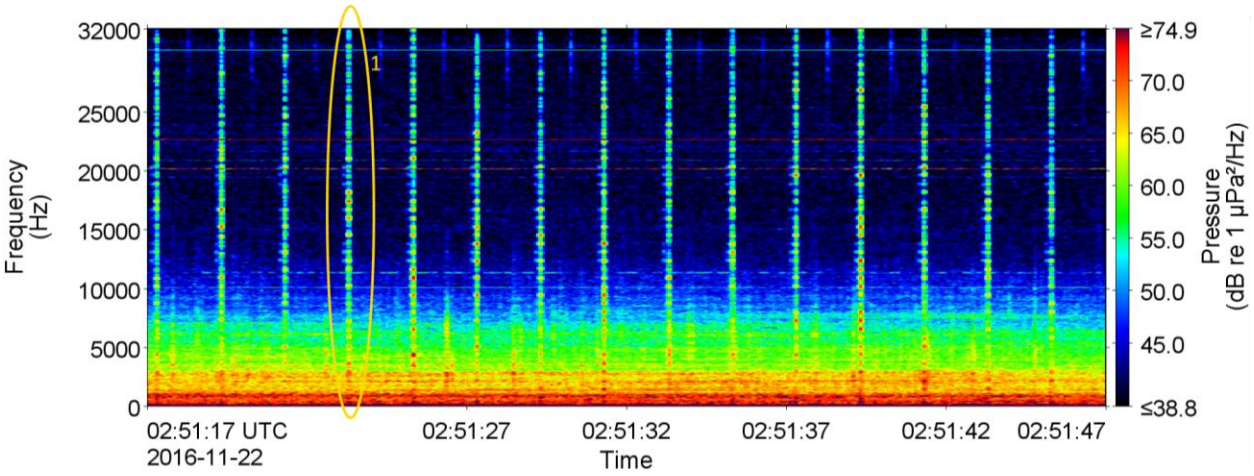

Figure 80. Underwater Listening Station (ULS): Spectrogram of recording in November 2016. Annotation is described in Table 11.

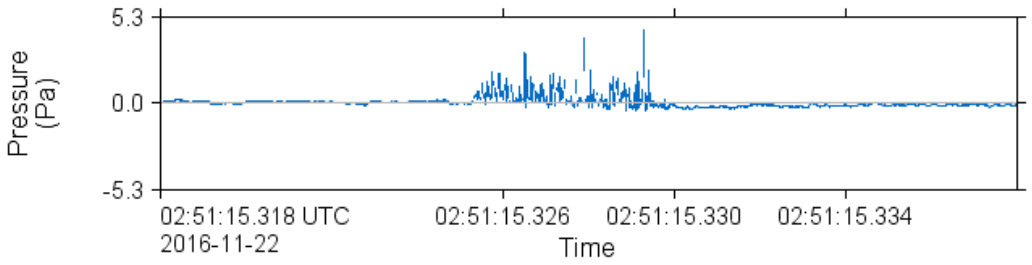

Figure 81. Underwater Listening Station (ULS): Waveform of one instance of broadband electronic noise in November 2016.

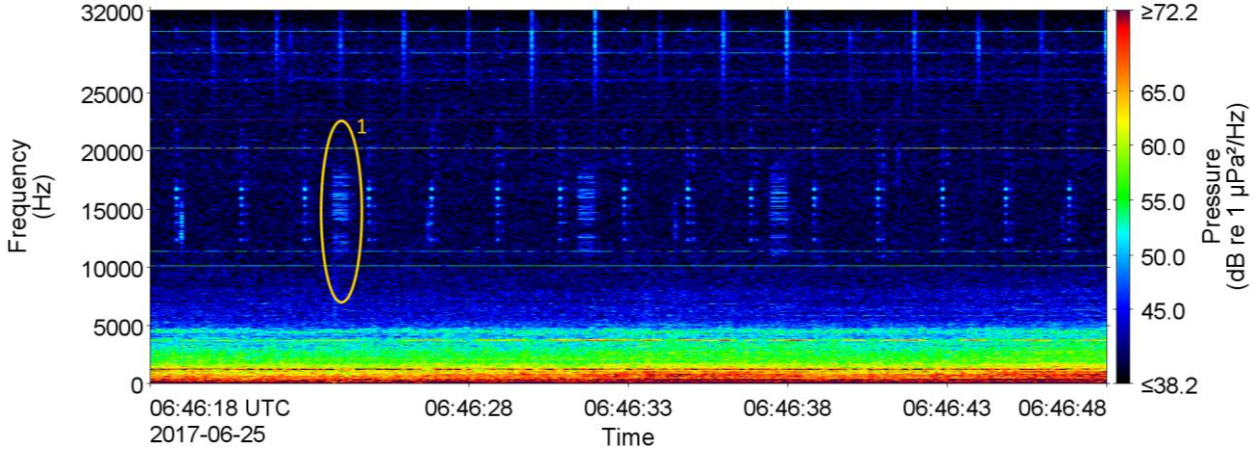

Figure 82. Underwater Listening Station (ULS): Spectrogram of recording in June 2017. Annotation is described in Table 11.

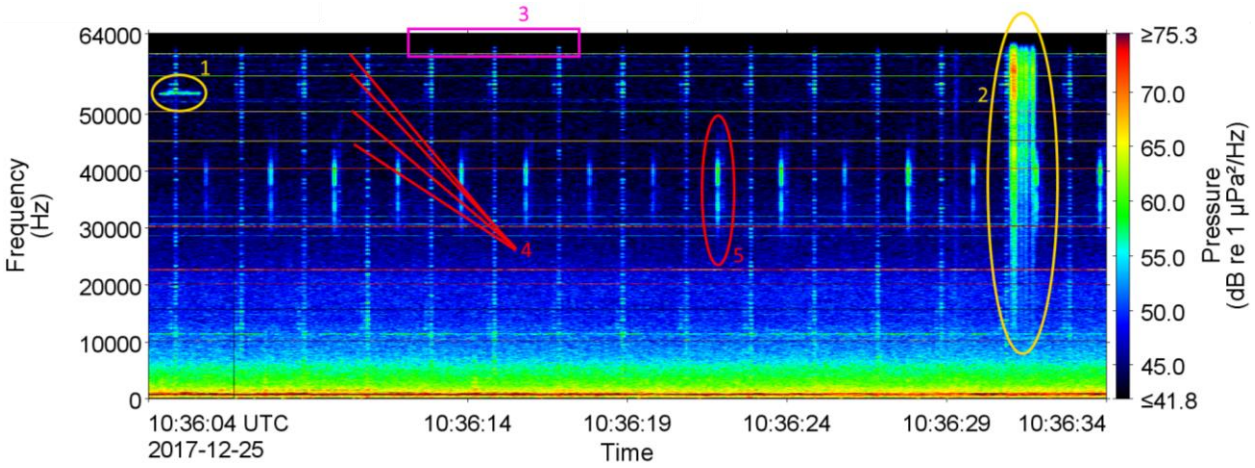

Figure 83. Underwater Listening Station (ULS): Spectrogram of recording in December 2017. Annotations are described in Table 11.

Appendix C. Effect of Sound Speed Profile Variability on Acoustic Propagation

This Appendix contains supplementary figures of transmission loss to show the effect of different sound speed profiles. Methods are described in Section 2.3, and results are summarized in Section 3.3.1. Some figures show small isolated and distant high-TL contours that were caused by sound reflecting off steep bathymetry features towards the surface.

C.1. Maps of Transmission Loss for 30 Hz

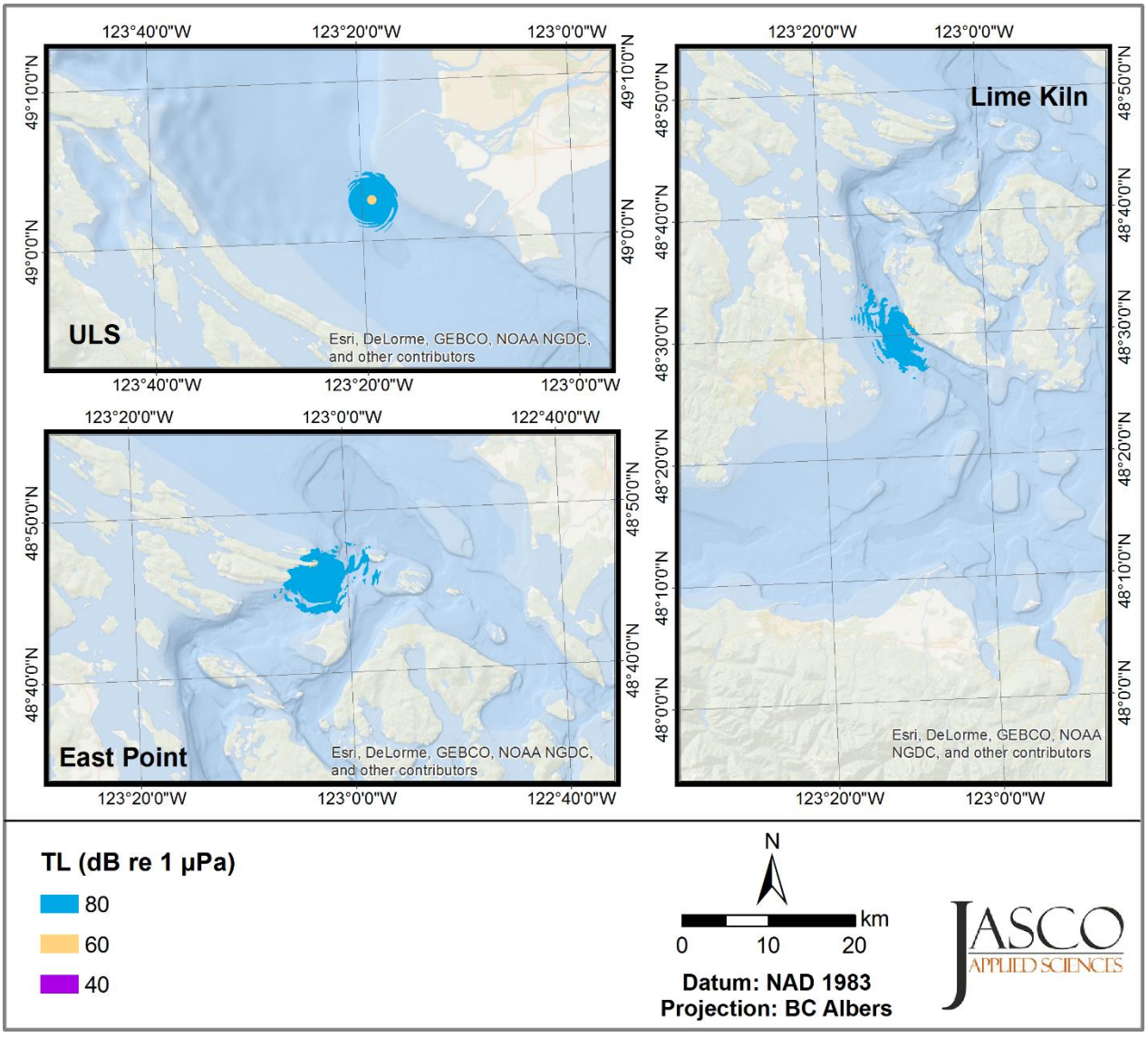

Figure 84. Map of transmission loss (TL) for 30 Hz with sound speed profile (SSP) 1.

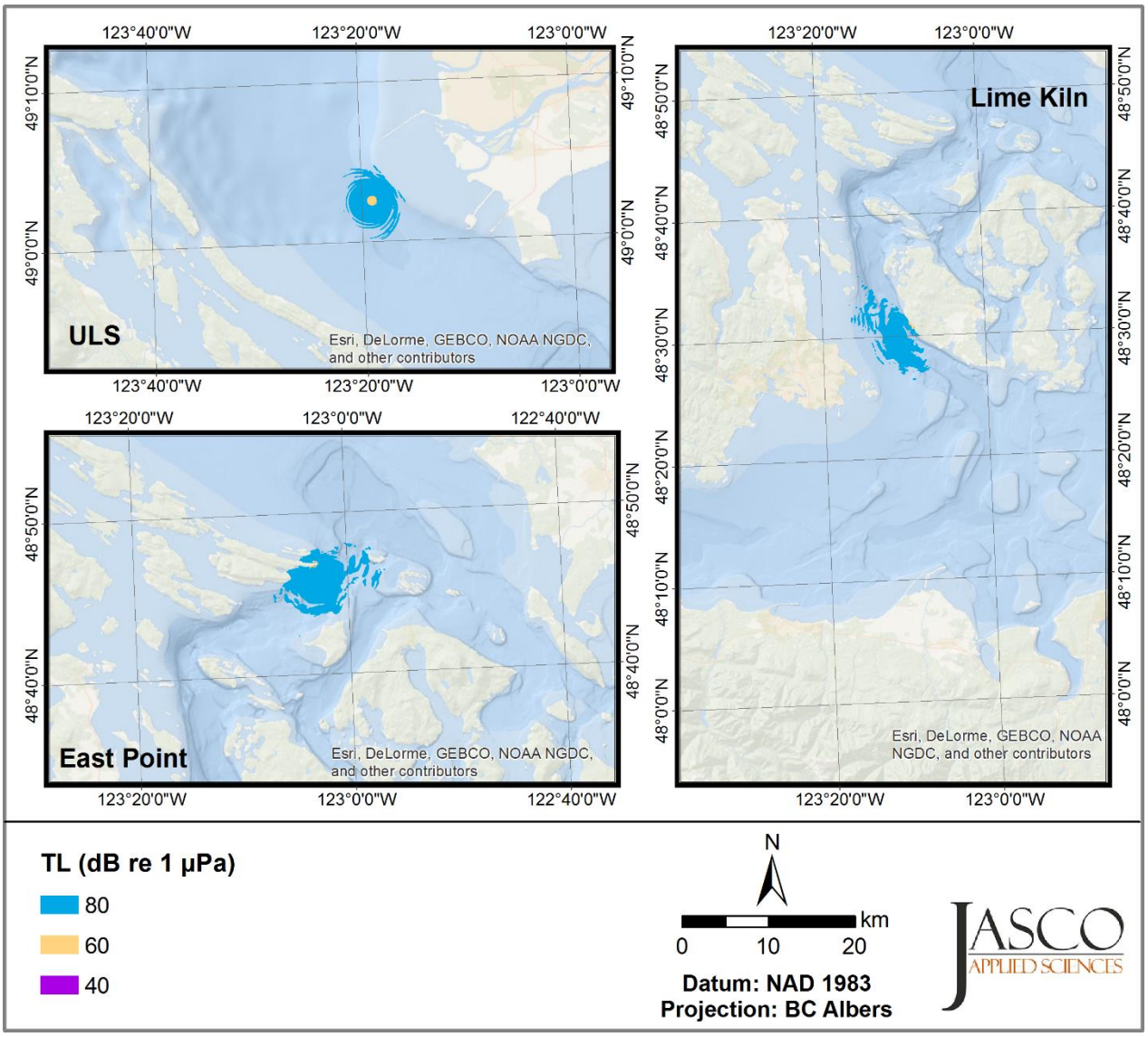

Figure 85. Map of transmission loss (TL) for 30 Hz with sound speed profile (SSP) 2.

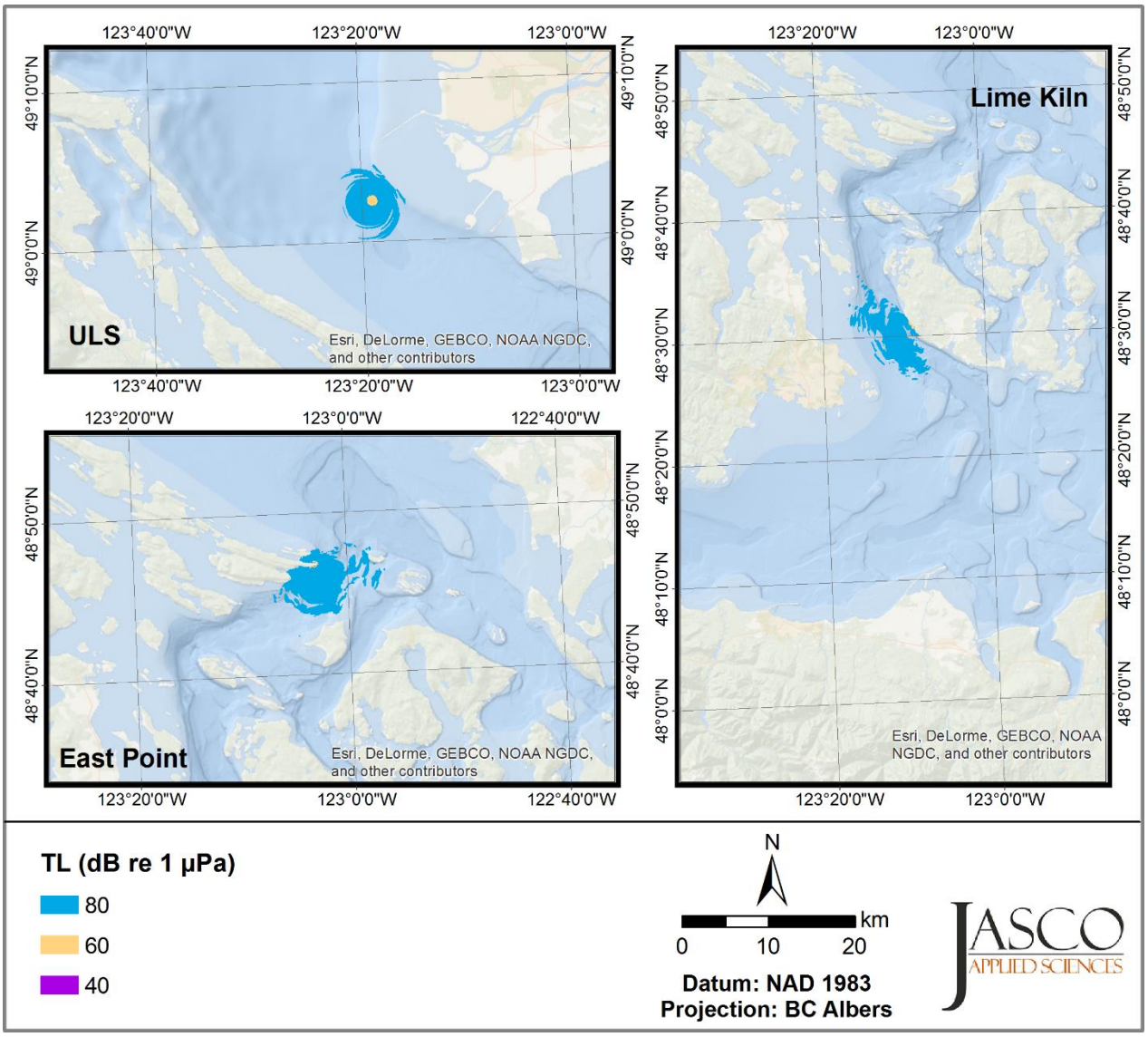

Figure 86. Map of transmission loss (TL) for 30 Hz with sound speed profile (SSP) 3.

C.2. Maps of Transmission Loss for 300 Hz

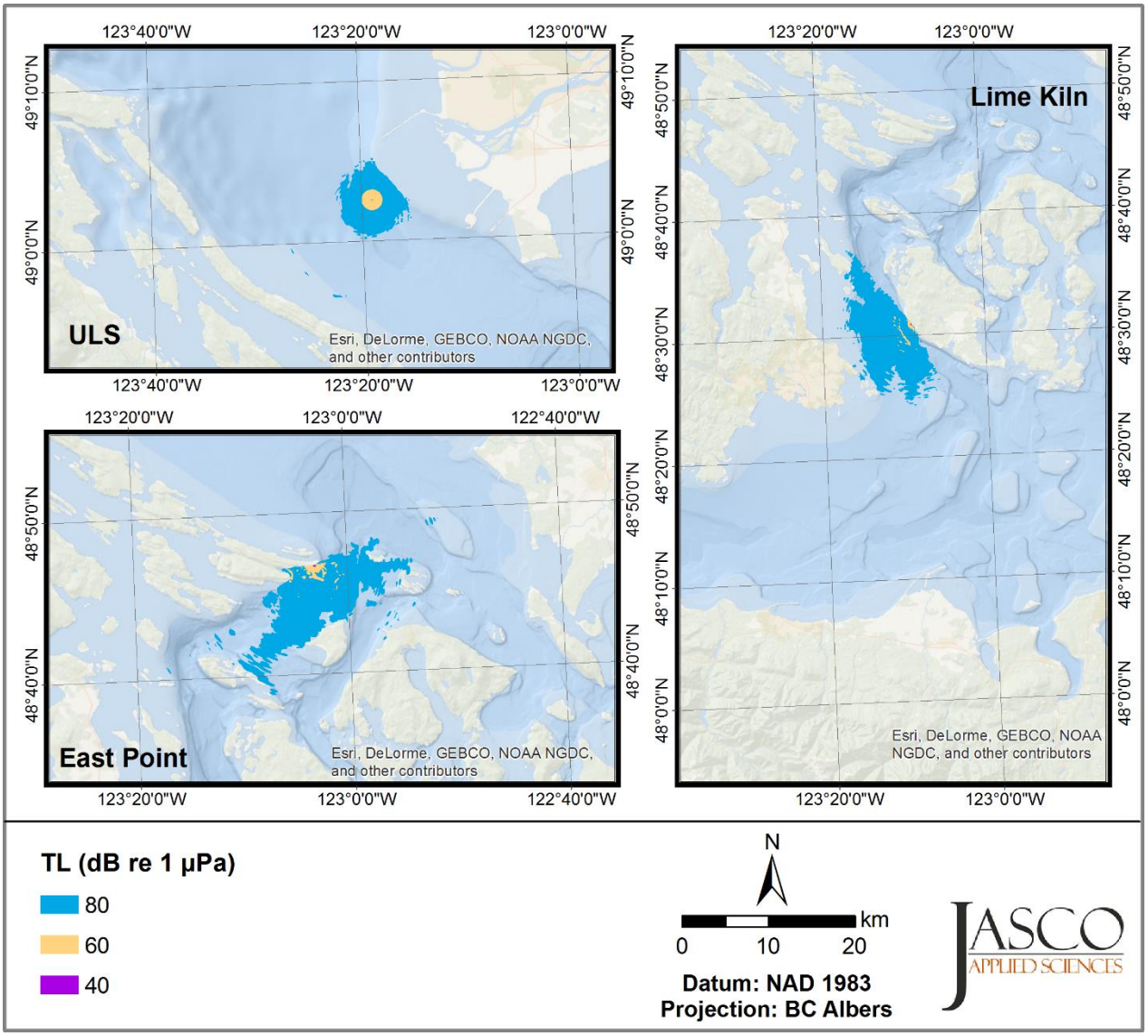

Figure 87. Map of transmission loss (TL) for 300 Hz with sound speed profile (SSP) 1.

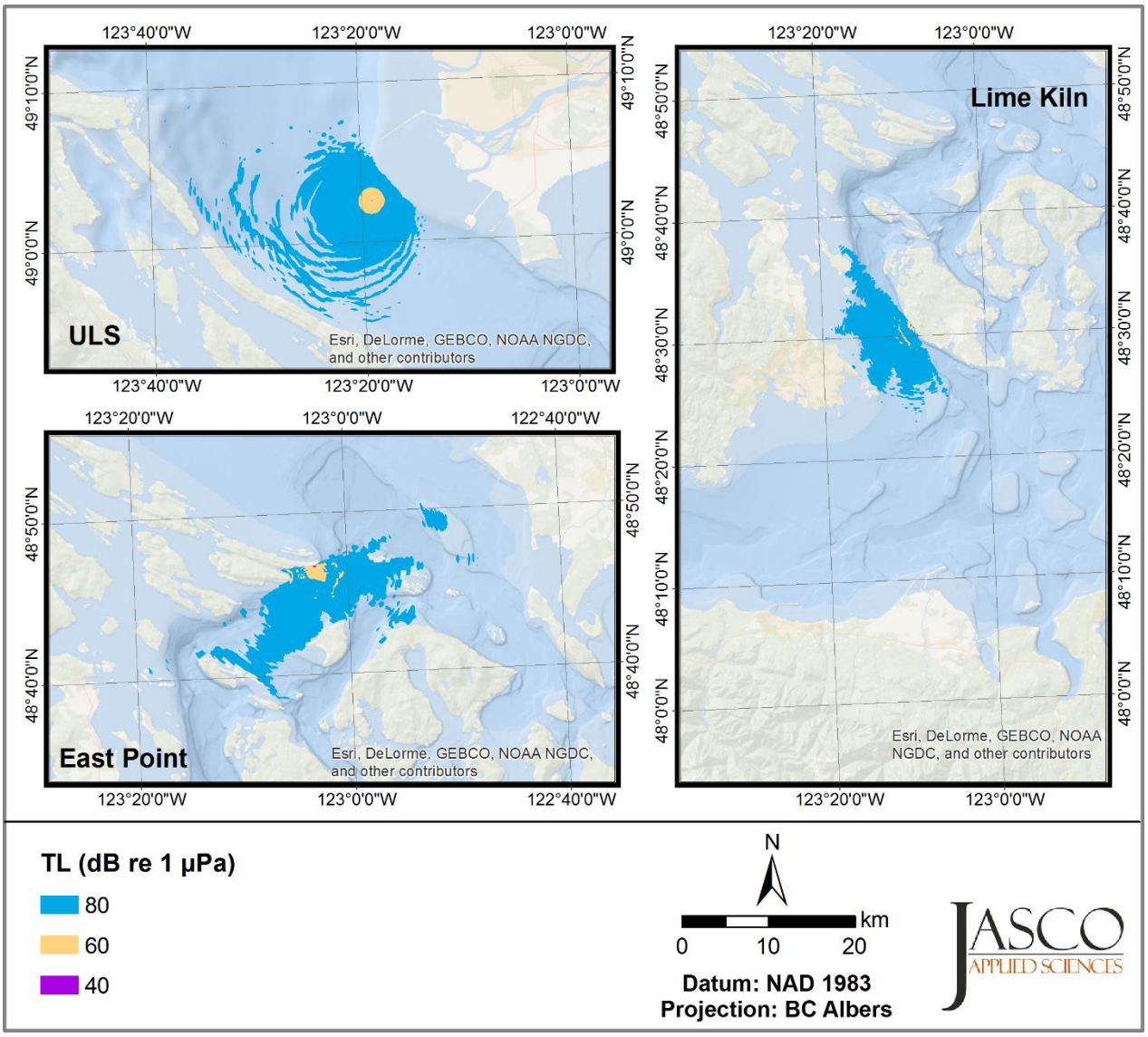

Figure 88. Map of transmission loss (TL) for 300 Hz with sound speed profile (SSP) 2.

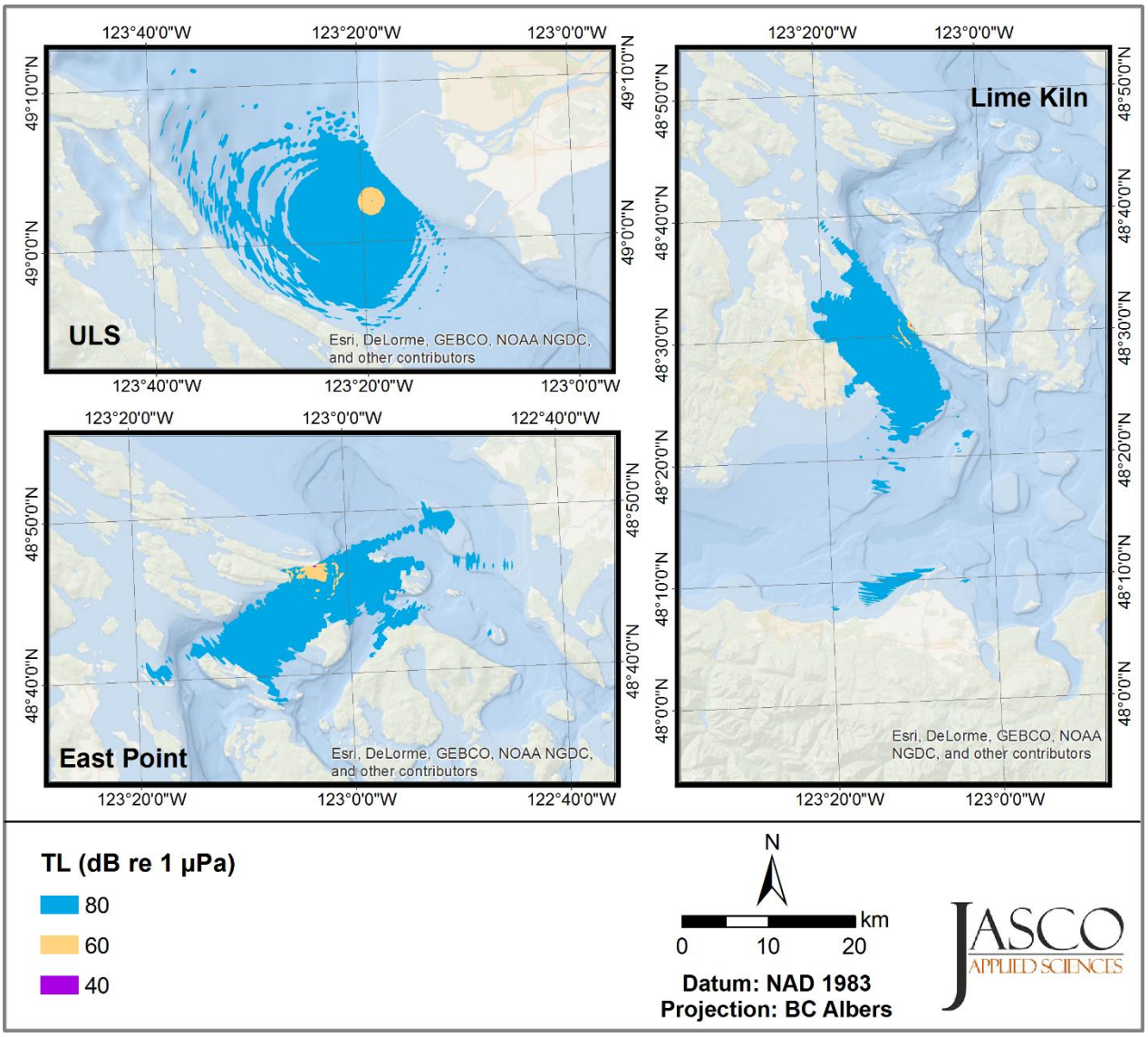

Figure 89. Map of transmission loss (TL) for 300 Hz with sound speed profile (SSP) 3.

C.3. Maps of Transmission Loss for 3 kHz

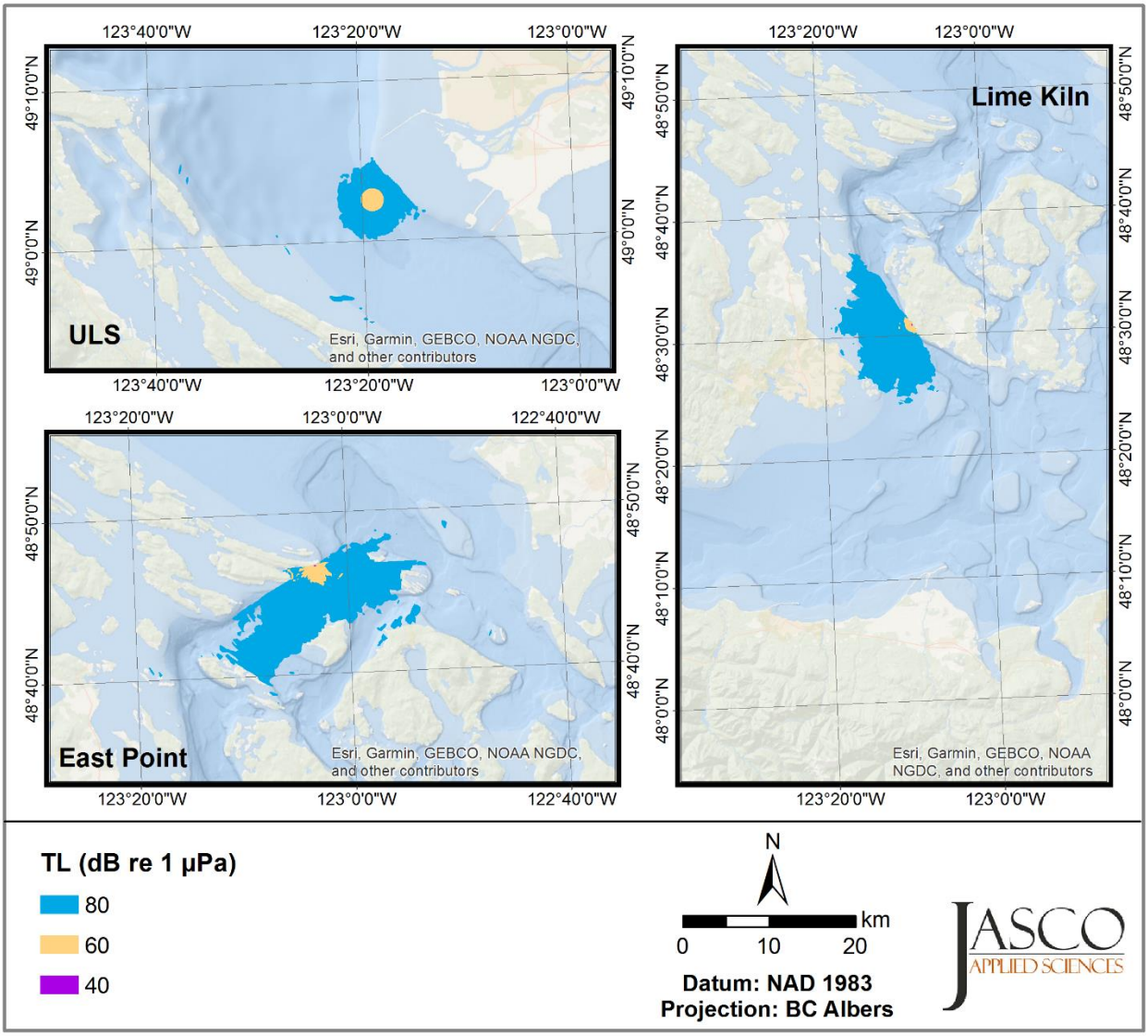

Figure 90. Map of transmission loss (TL) for 3 kHz with sound speed profile (SSP) 1 and wind speed 1 kn.

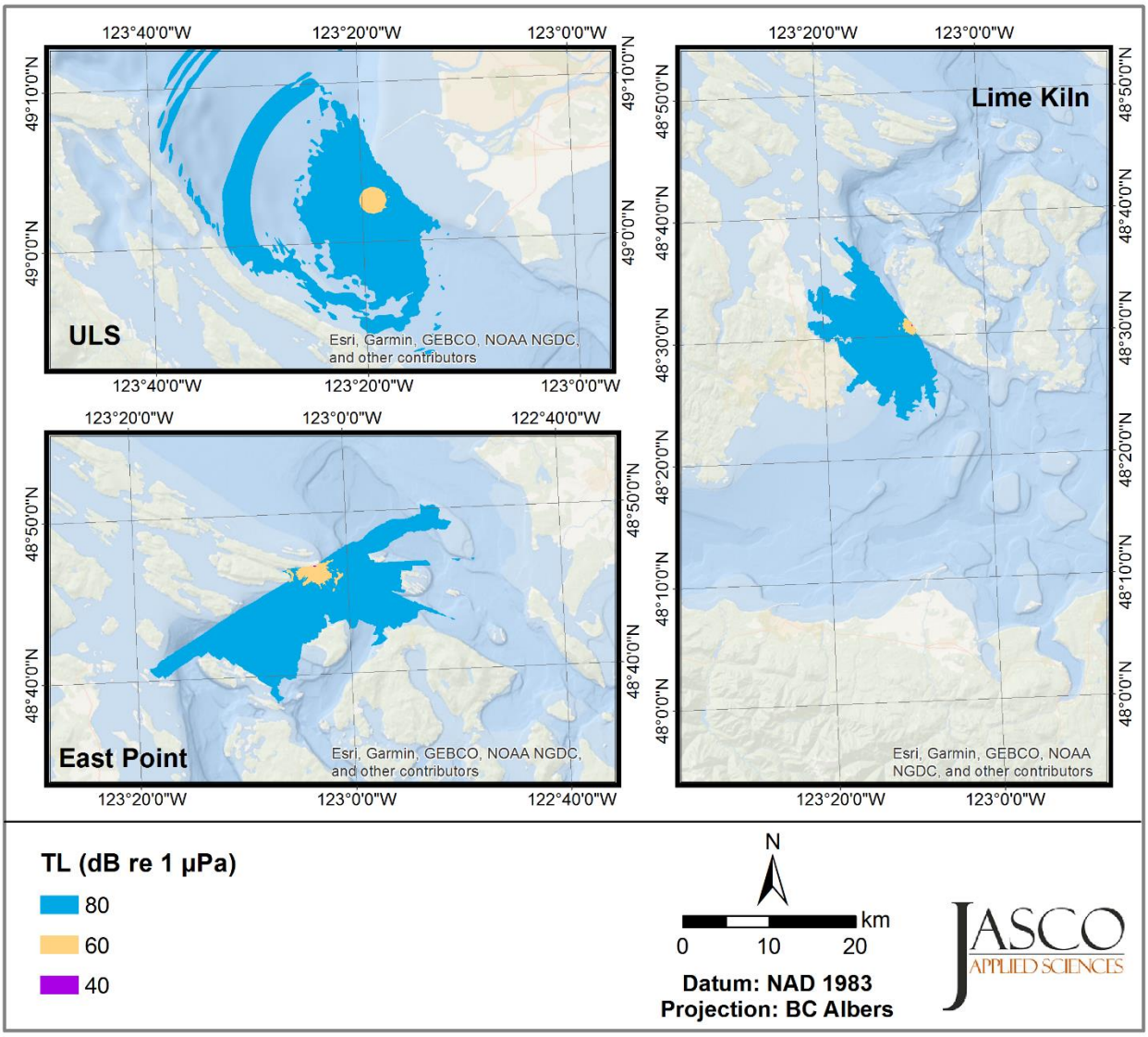

Figure 91. Map of transmission loss (TL) for 3 kHz with sound speed profile (SSP) 2 and wind speed 1 kn.

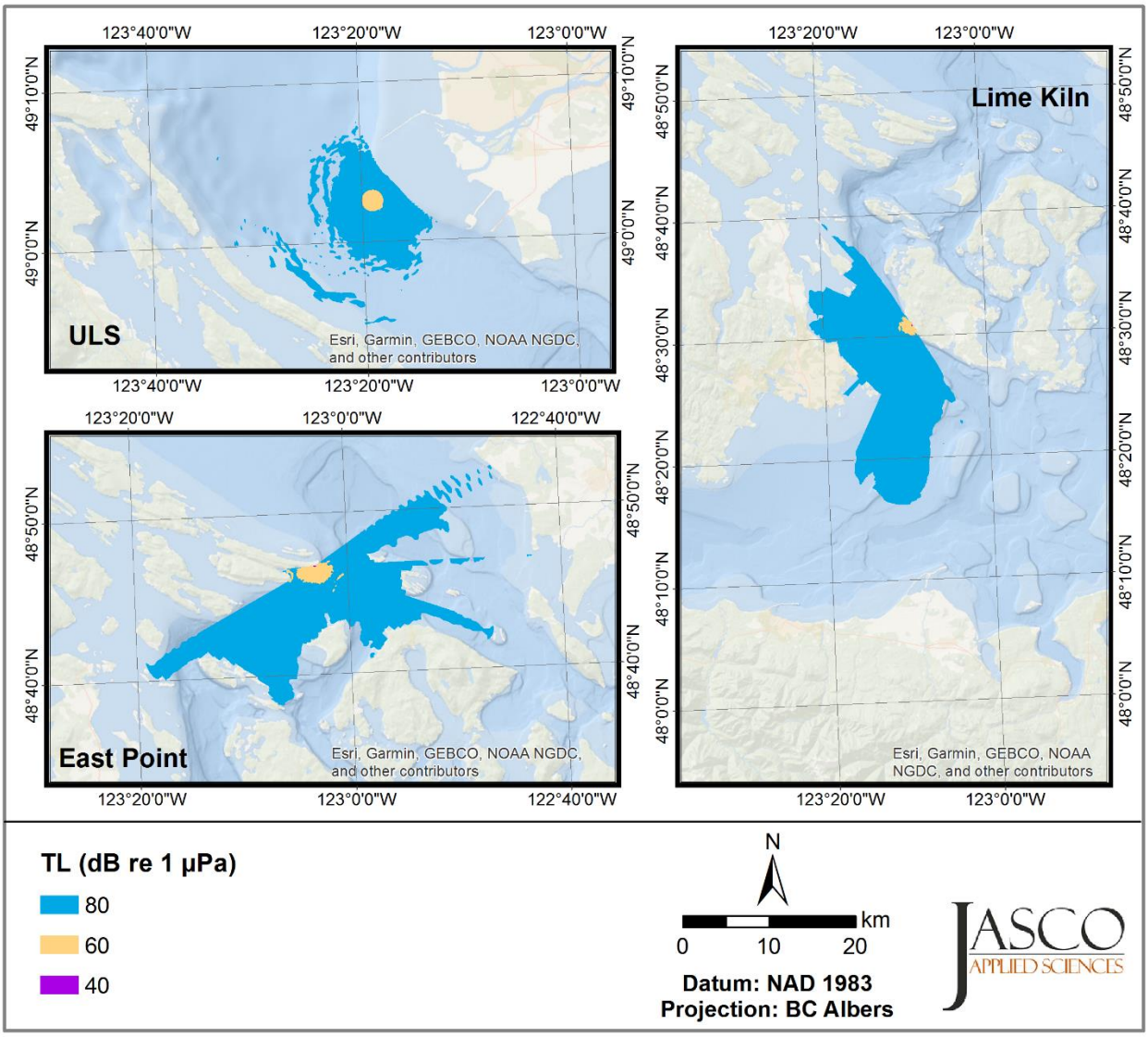

Figure 92. Map of transmission loss (TL) for 3 kHz with sound speed profile (SSP) 3 and wind speed 1 kn.

C.4. Maps of Transmission Loss for 30 kHz

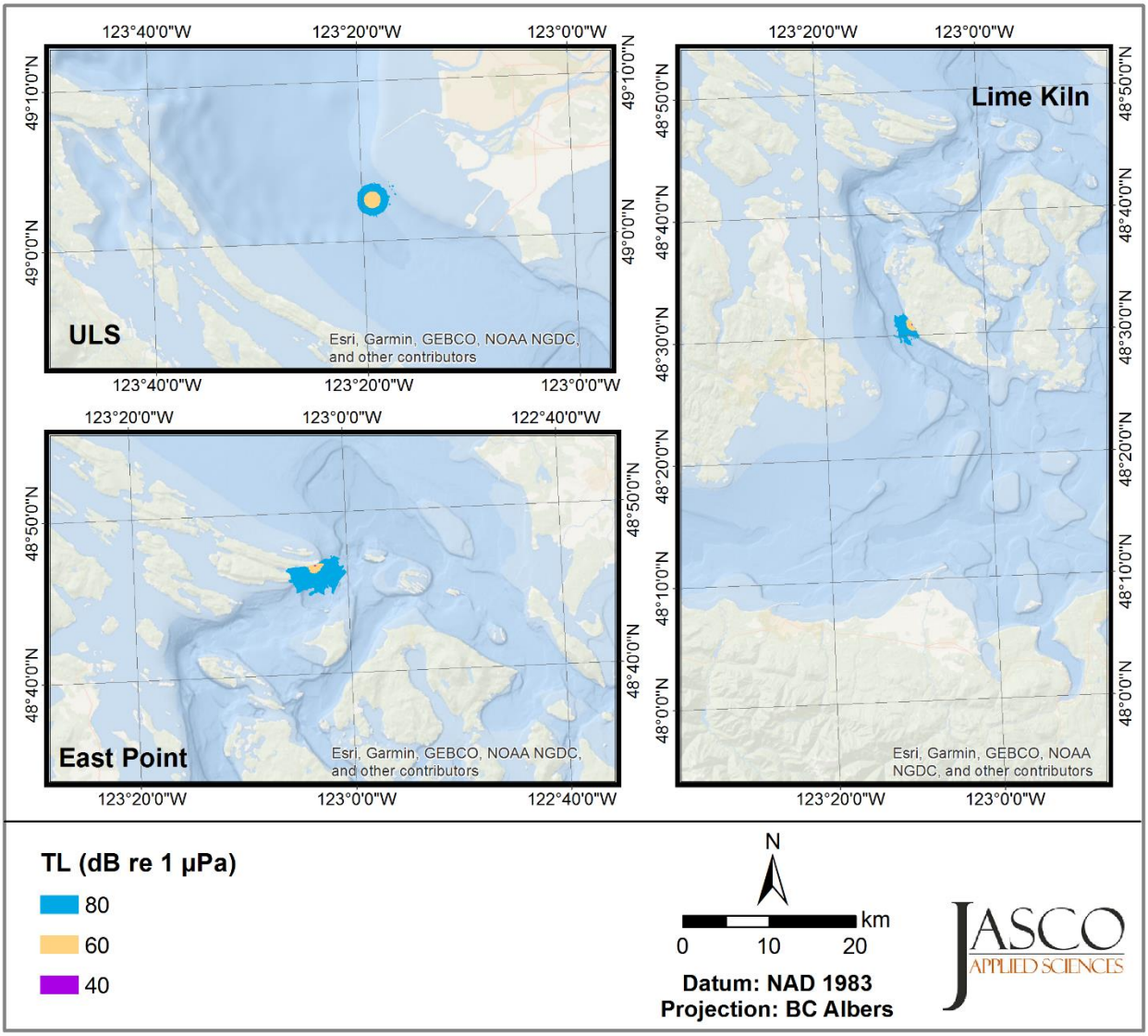

Figure 93. Map of transmission loss (TL) for 30 kHz with sound speed profile (SSP) 1 and wind speed 1 kn.

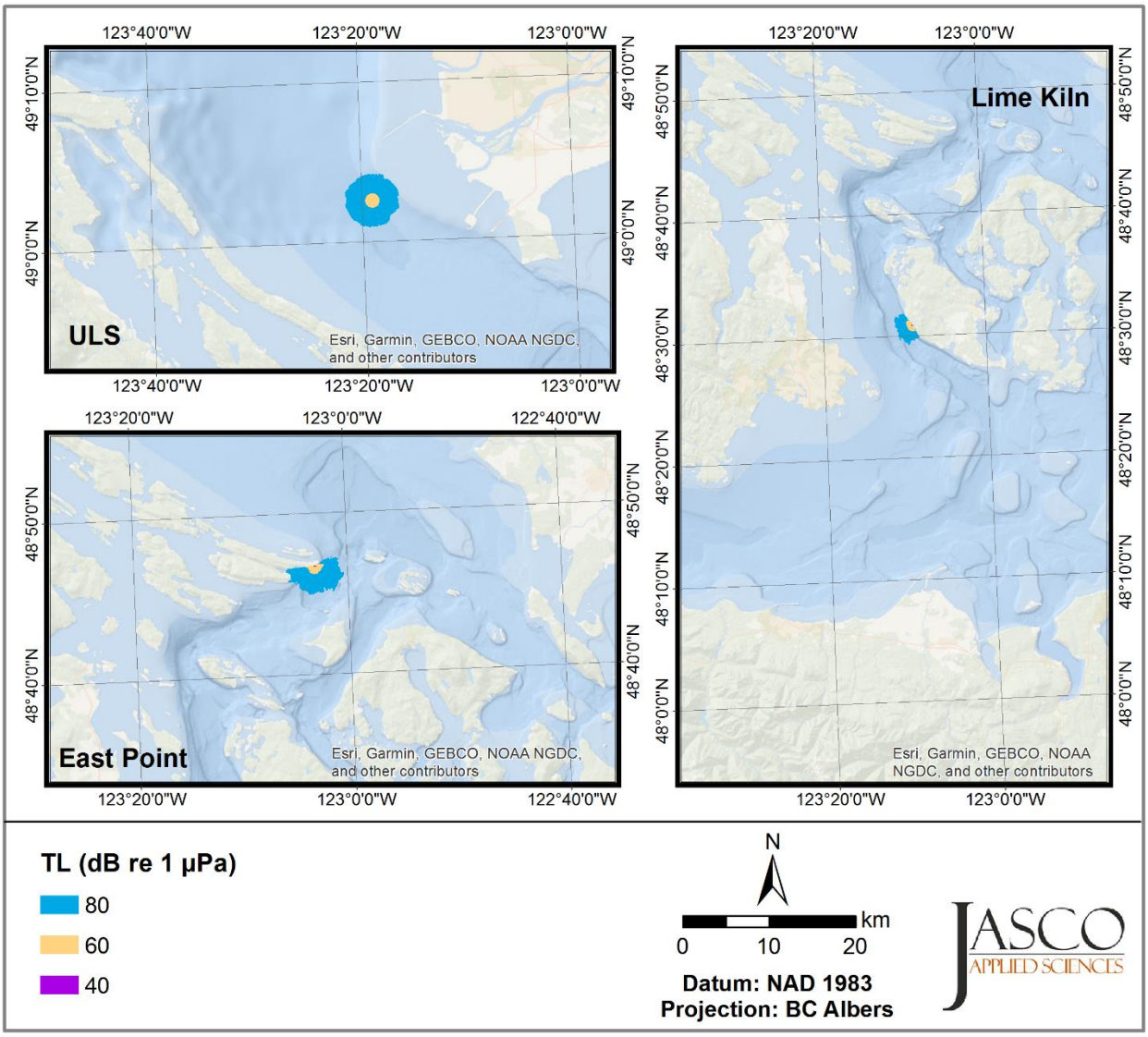

Figure 94. Map of transmission loss (TL) for 30 kHz with sound speed profile (SSP) 2 and wind speed 1 kn.

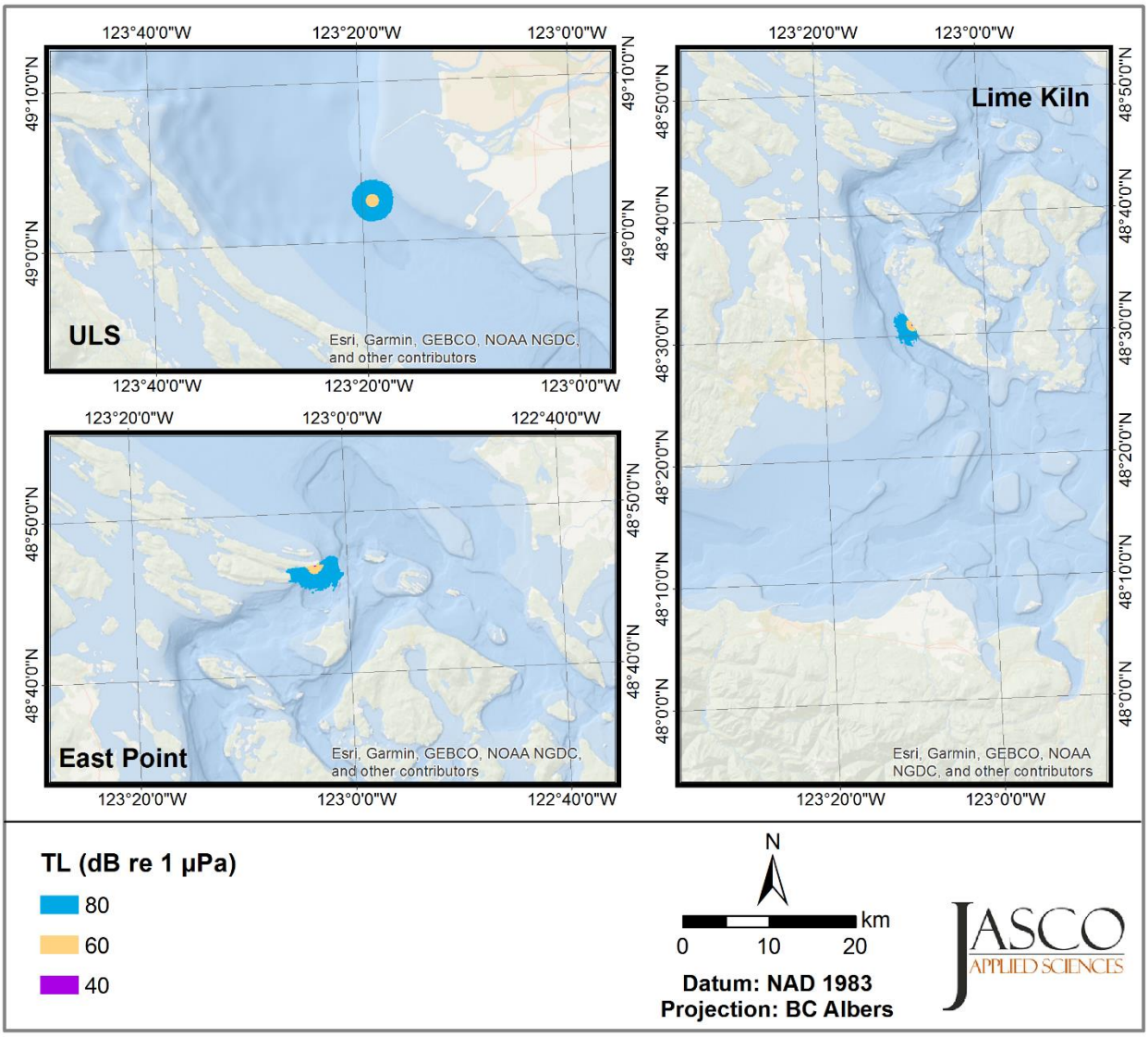

Figure 95. Map of transmission loss (TL) for 30 kHz with sound speed profile (SSP) 3 and wind speed 1 kn.

C.5. Plots of Transmission Loss versus Range

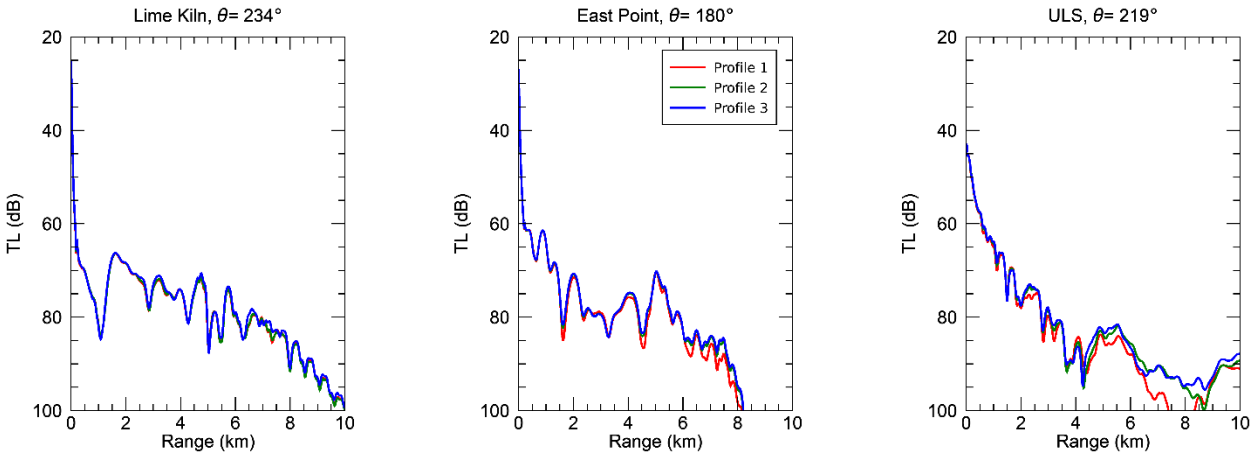

Figure 96. 30 Hz: Transmission loss (TL) versus range at each site with each modelled sound speed profile along a radial toward the international shipping lanes. Site-specific radial headings are specified above each panel in degrees.

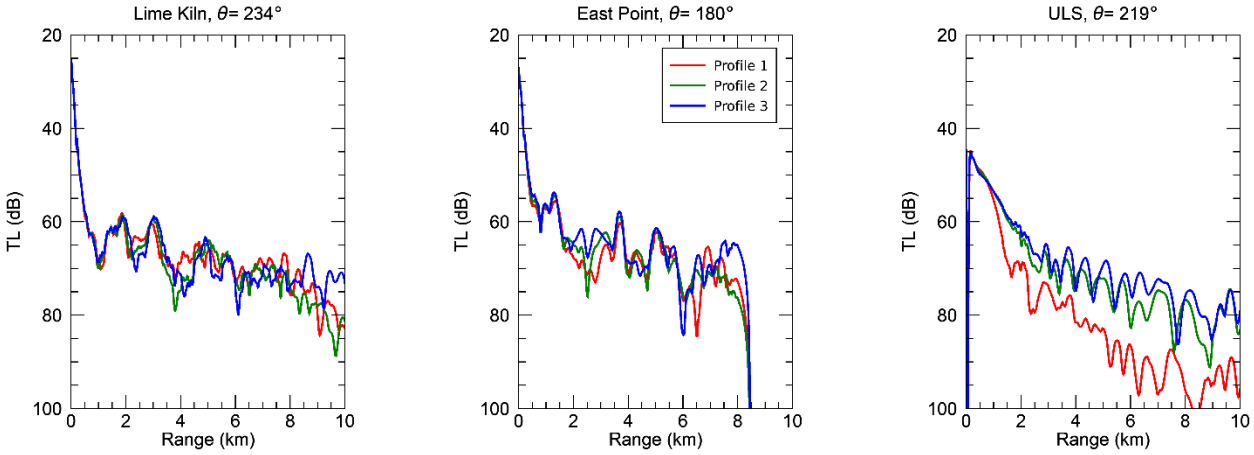

Figure 97. 300 Hz: Transmission loss (TL) versus range at each site with each modelled sound speed profile along a radial toward the international shipping lanes. Site-specific radial headings are specified above each panel in degrees.

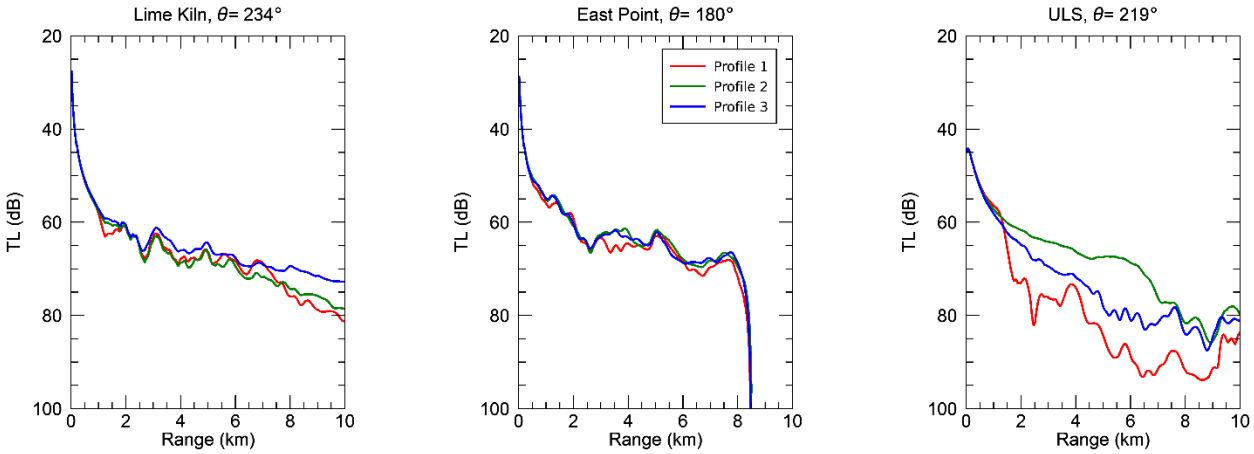

Figure 98. 3000 Hz: Transmission loss (TL) versus range at each site with each modelled sound speed profile along a radial toward the international shipping lanes (1 kn wind speed). Site-specific radial headings are specified above each panel in degrees.

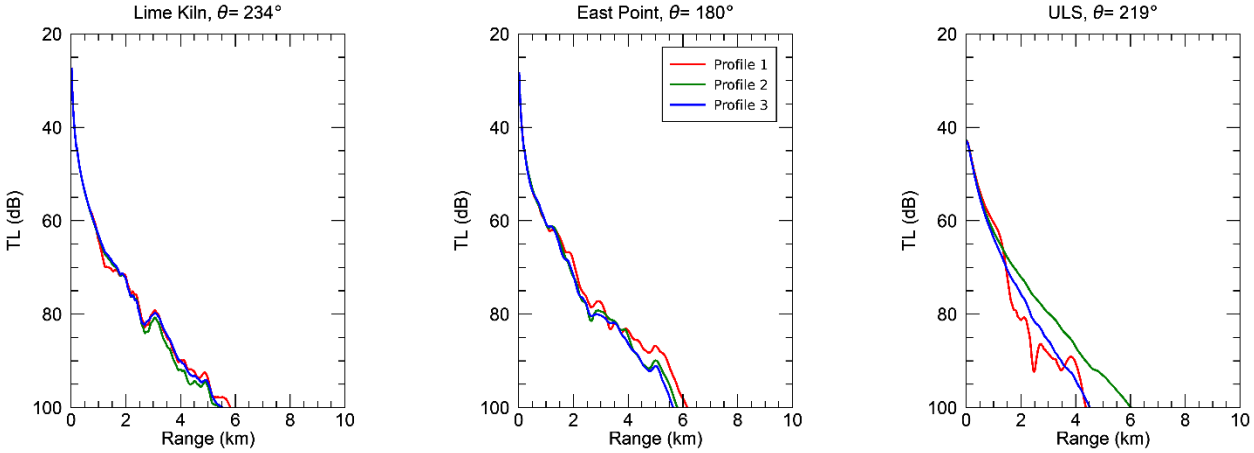

Figure 99. 30000 Hz: Transmission loss (TL) versus range at each site with each modelled sound speed profile along a radial toward the international shipping lanes (1 kn wind speed). Site-specific radial headings are specified above each panel in degrees.

Appendix D. Effect of Wind Speed on Acoustic Propagation

This Appendix contains supplementary figures of transmission loss to show the effect of different wind speeds. Methods are described in Section 2.3, and results are summarized in Section 3.3.2. Some figures show small isolated and distant high-TL contours that were caused by sound reflecting off steep bathymetry features towards the surface.

D.1. Maps of Transmission Loss for 3 kHz

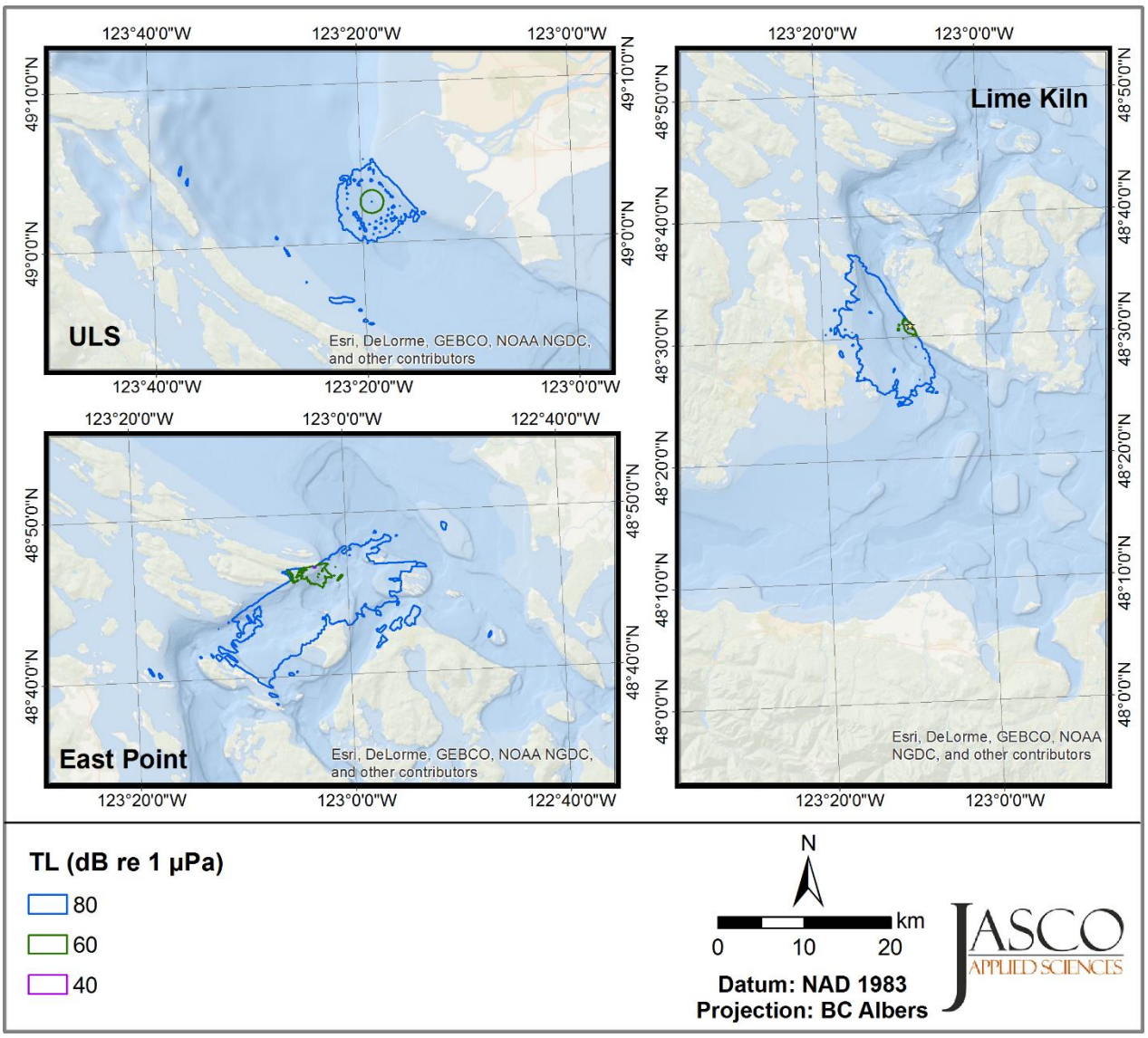

Figure 100. Map of transmission loss (TL) for 3 kHz with sound speed profile (SSP) 1 and wind speed 1 kn.

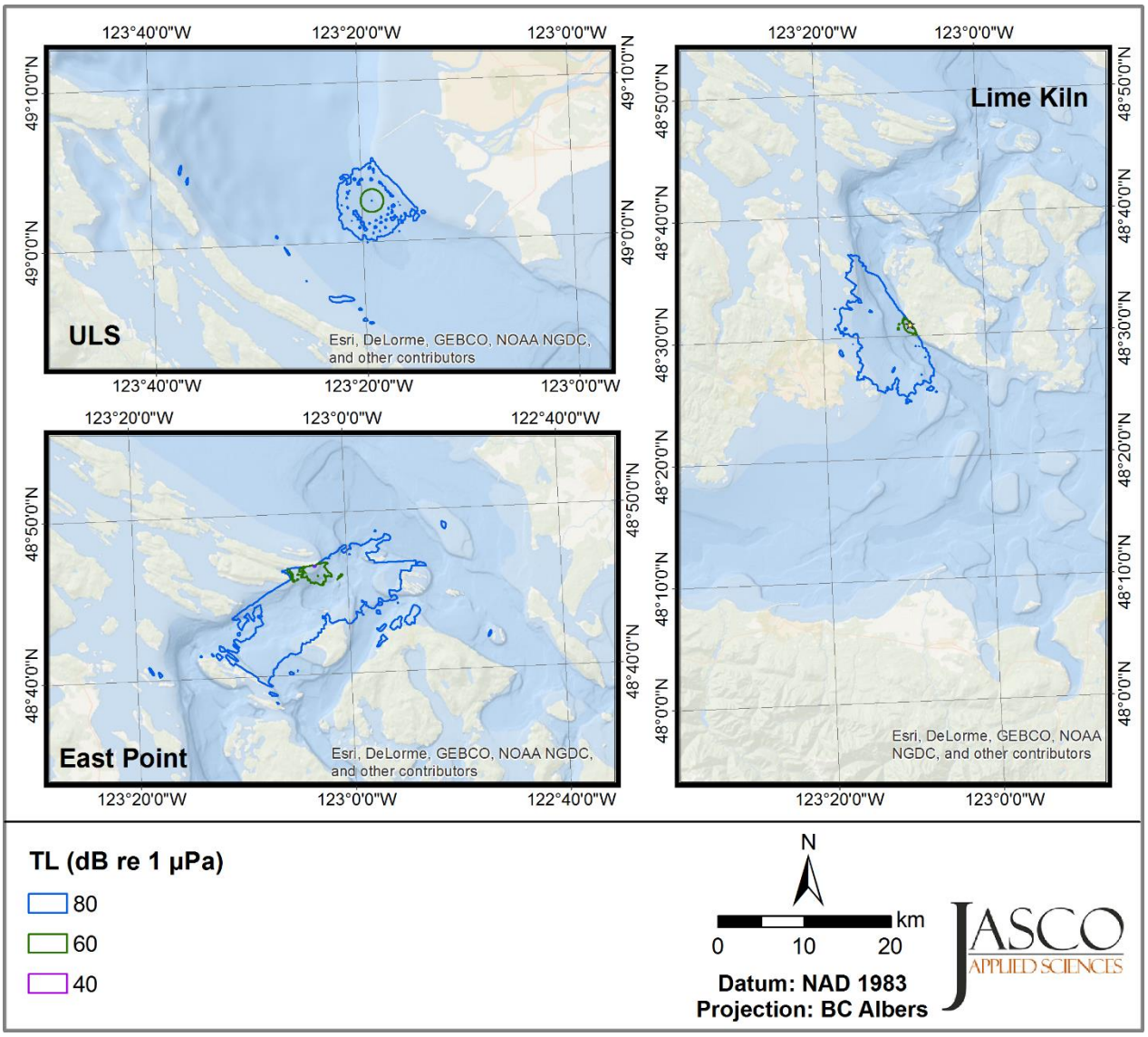

Figure 101. Map of transmission loss (TL) for 3 kHz with sound speed profile (SSP) 1 and wind speed 9 kn.

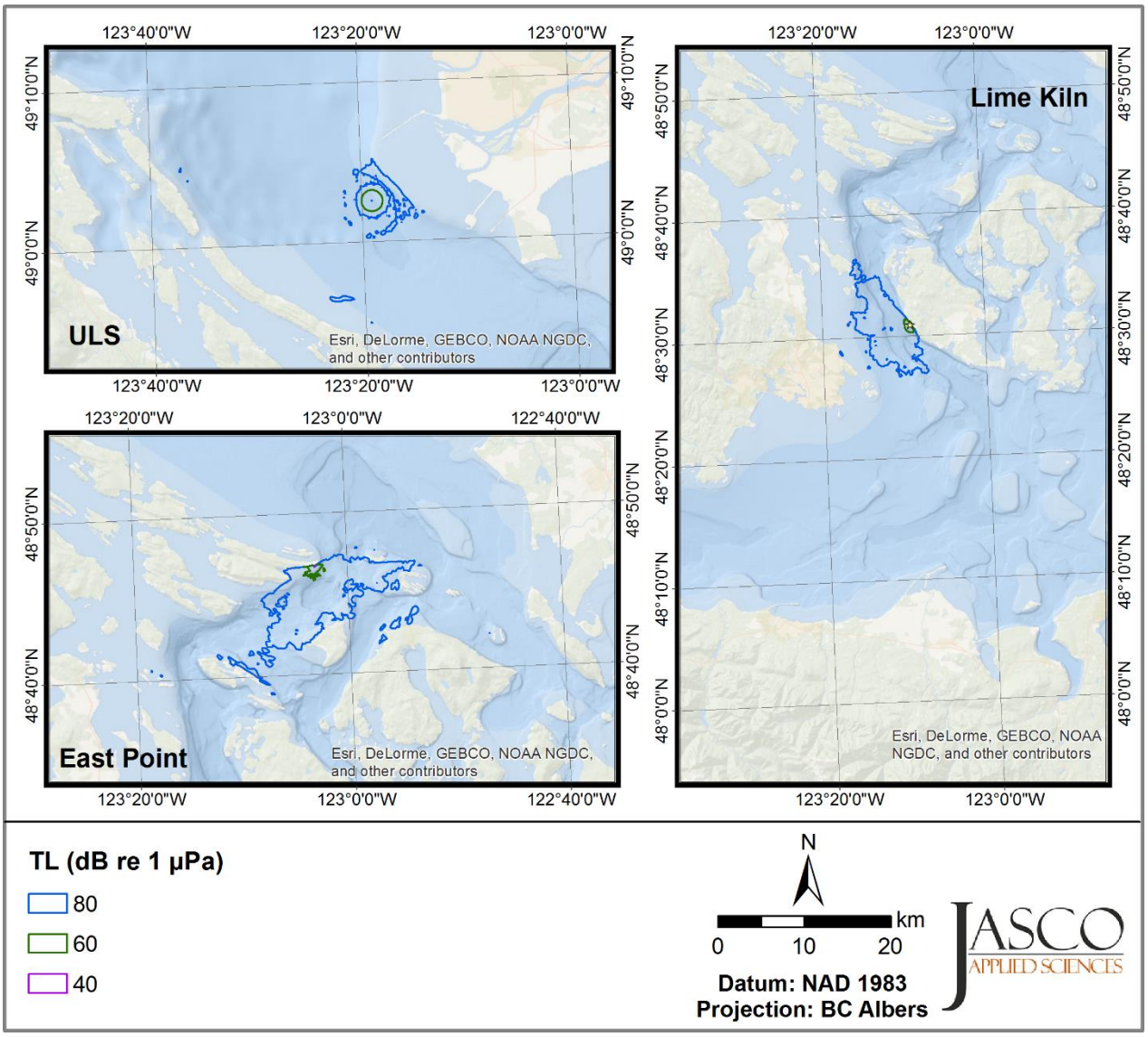

Figure 102. Map of transmission loss (TL) for 3 kHz with sound speed profile (SSP) 1 and wind speed 20 kn.

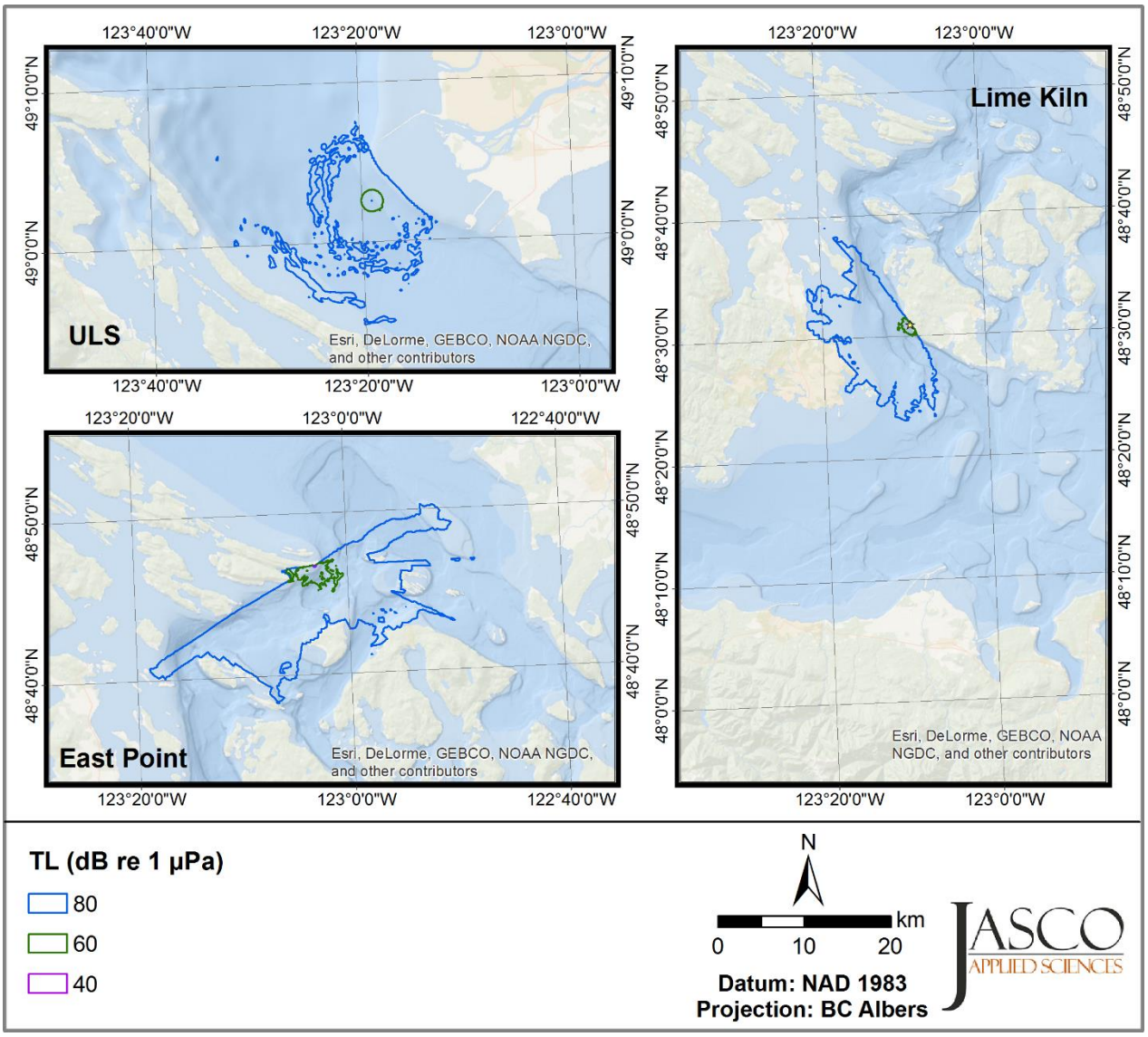

Figure 103. Map of transmission loss (TL) for 3 kHz with sound speed profile (SSP) 2 and wind speed 1 kn.

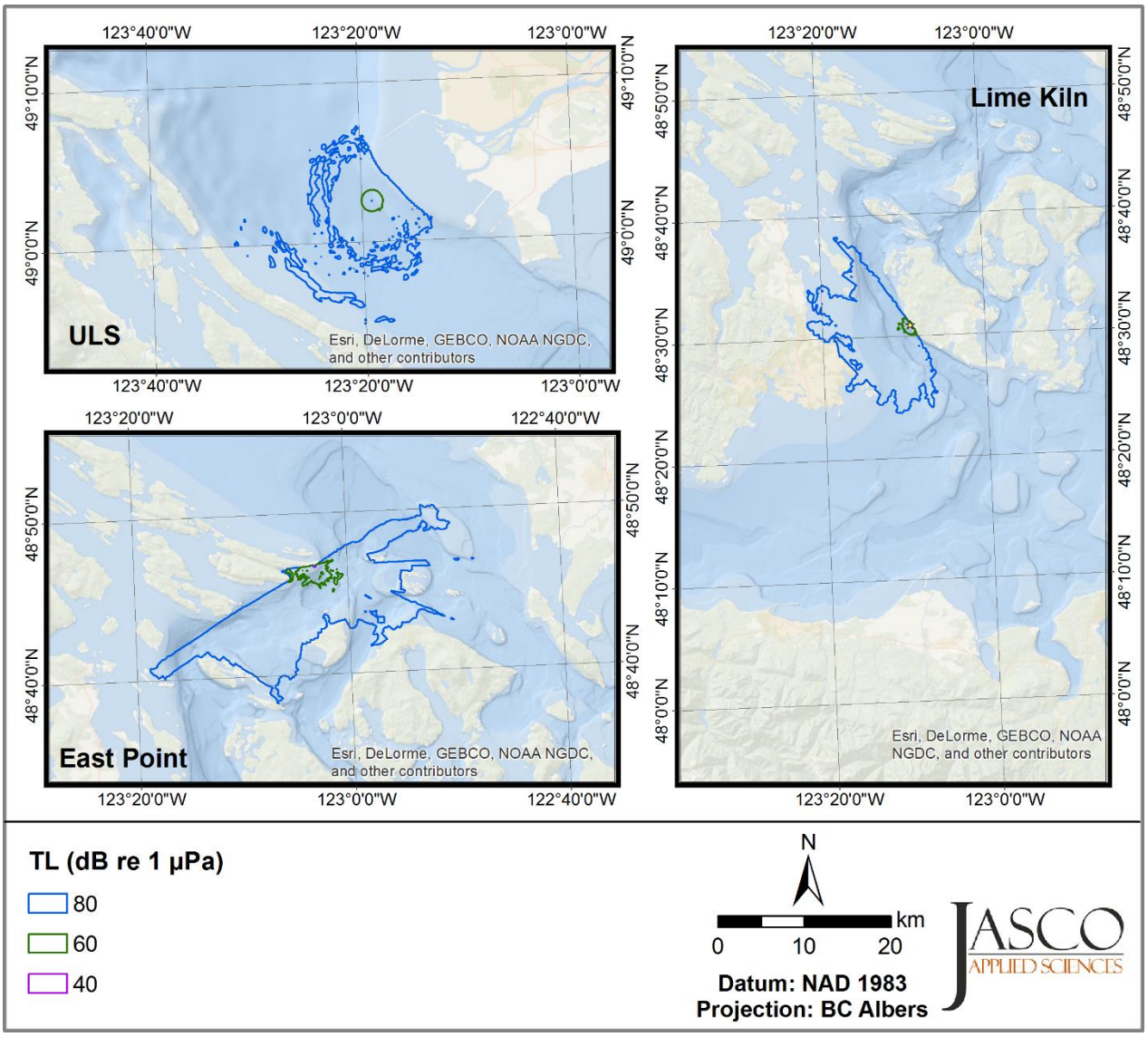

Figure 104. Map of transmission loss (TL) for 3 kHz with sound speed profile (SSP) 2 and wind speed 9 kn.

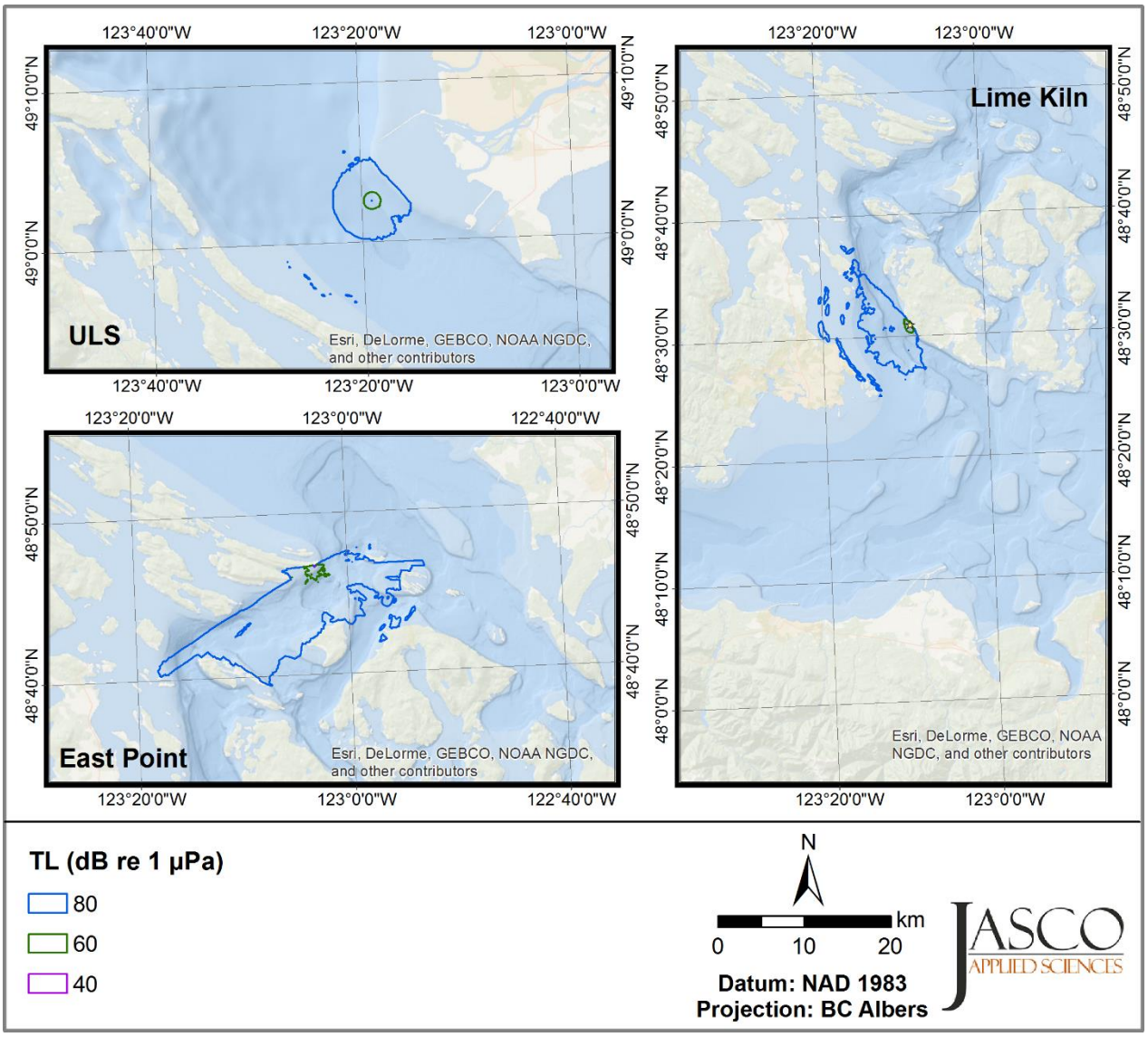

Figure 105. Map of transmission loss (TL) for 3 kHz with sound speed profile (SSP) 2 and wind speed 20 kn.

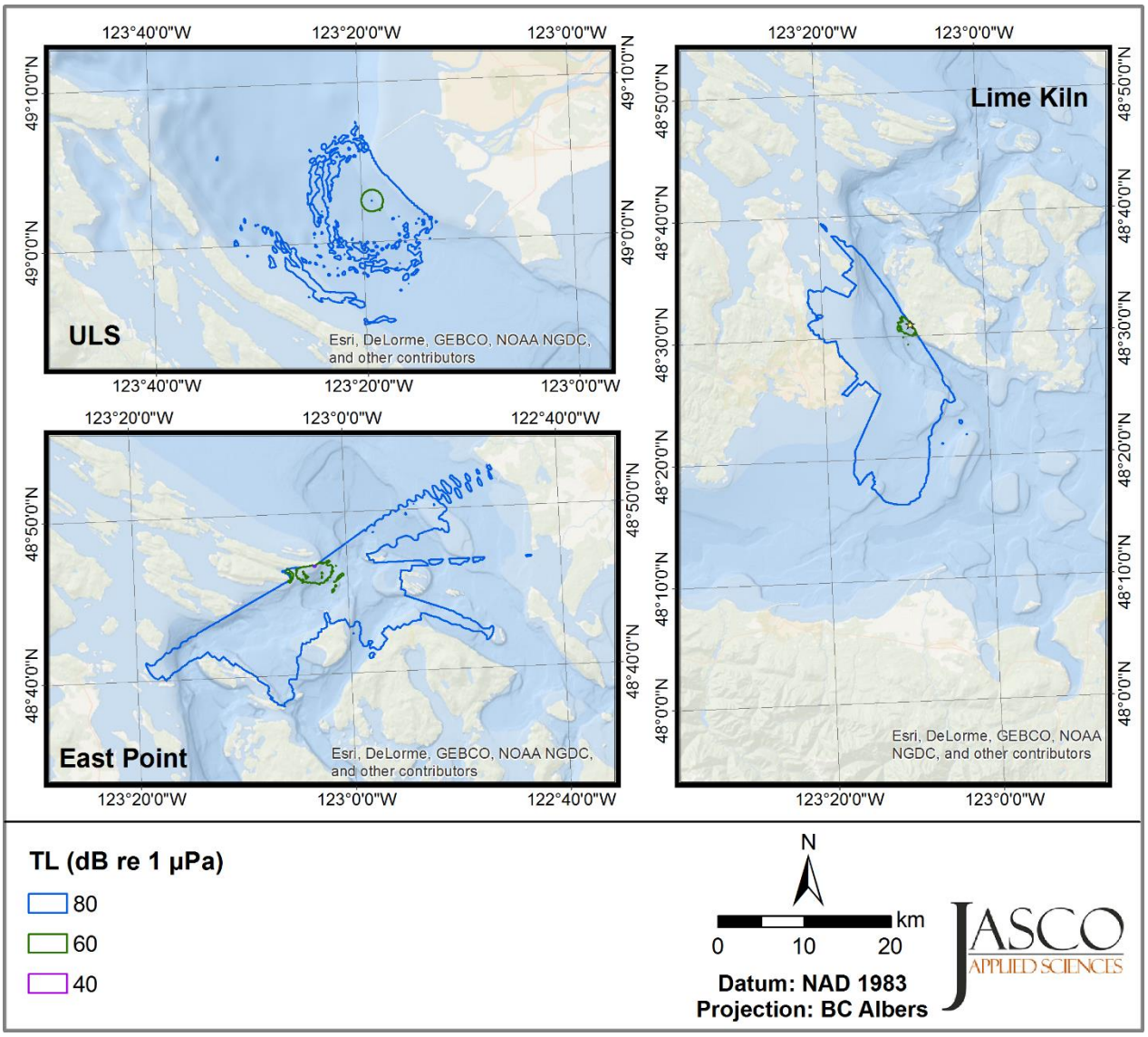

Figure 106. Map of transmission loss (TL) for 3 kHz with sound speed profile (SSP) 3 and wind speed 1 kn.

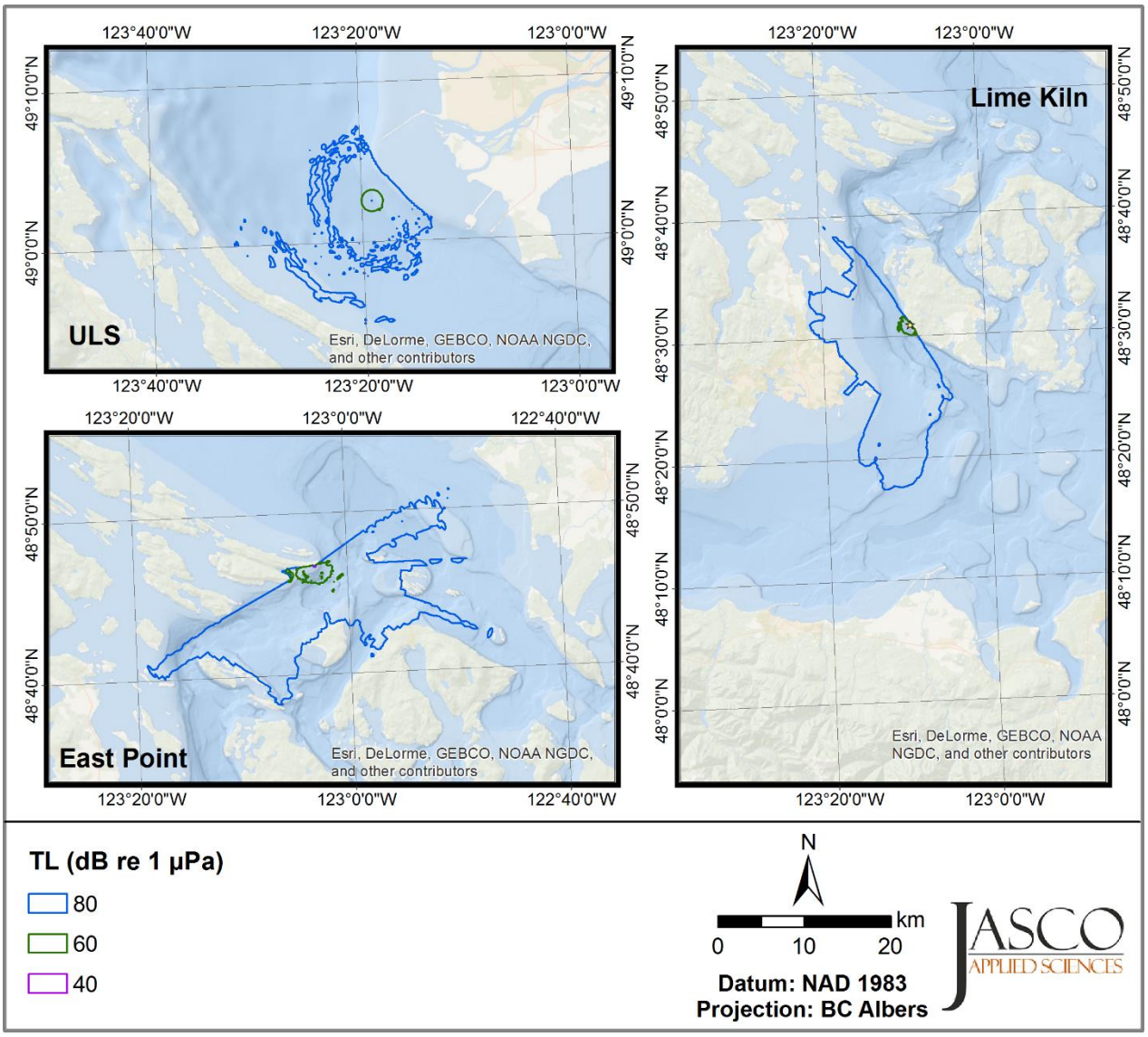

Figure 107. Map of transmission loss (TL) for 3 kHz with sound speed profile (SSP) 3 and wind speed 9 kn.

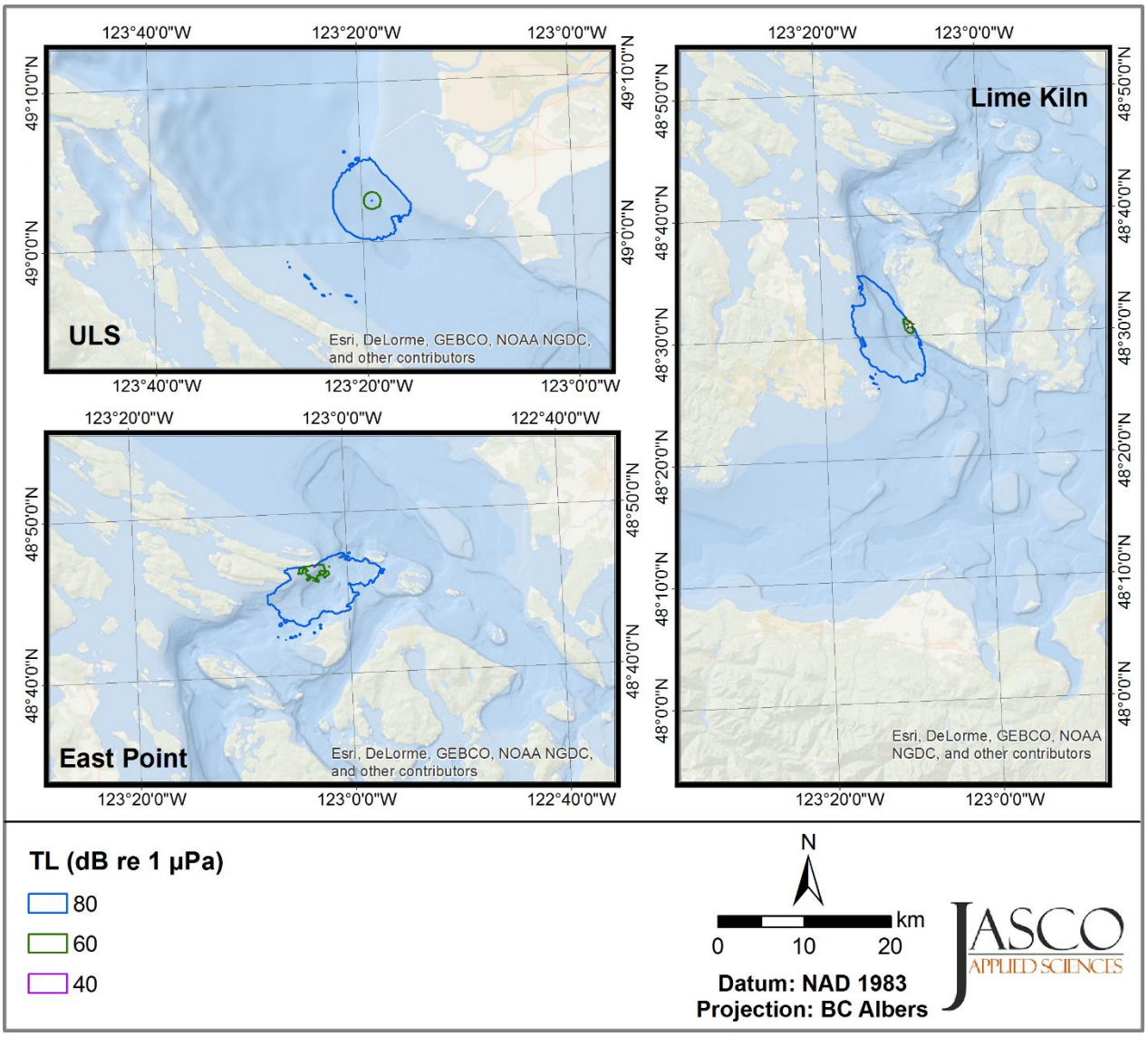

Figure 108. Map of transmission loss (TL) for 3 kHz with sound speed profile (SSP) 3 and wind speed 20 kn.

D.2. Maps of Transmission Loss for 30 kHz

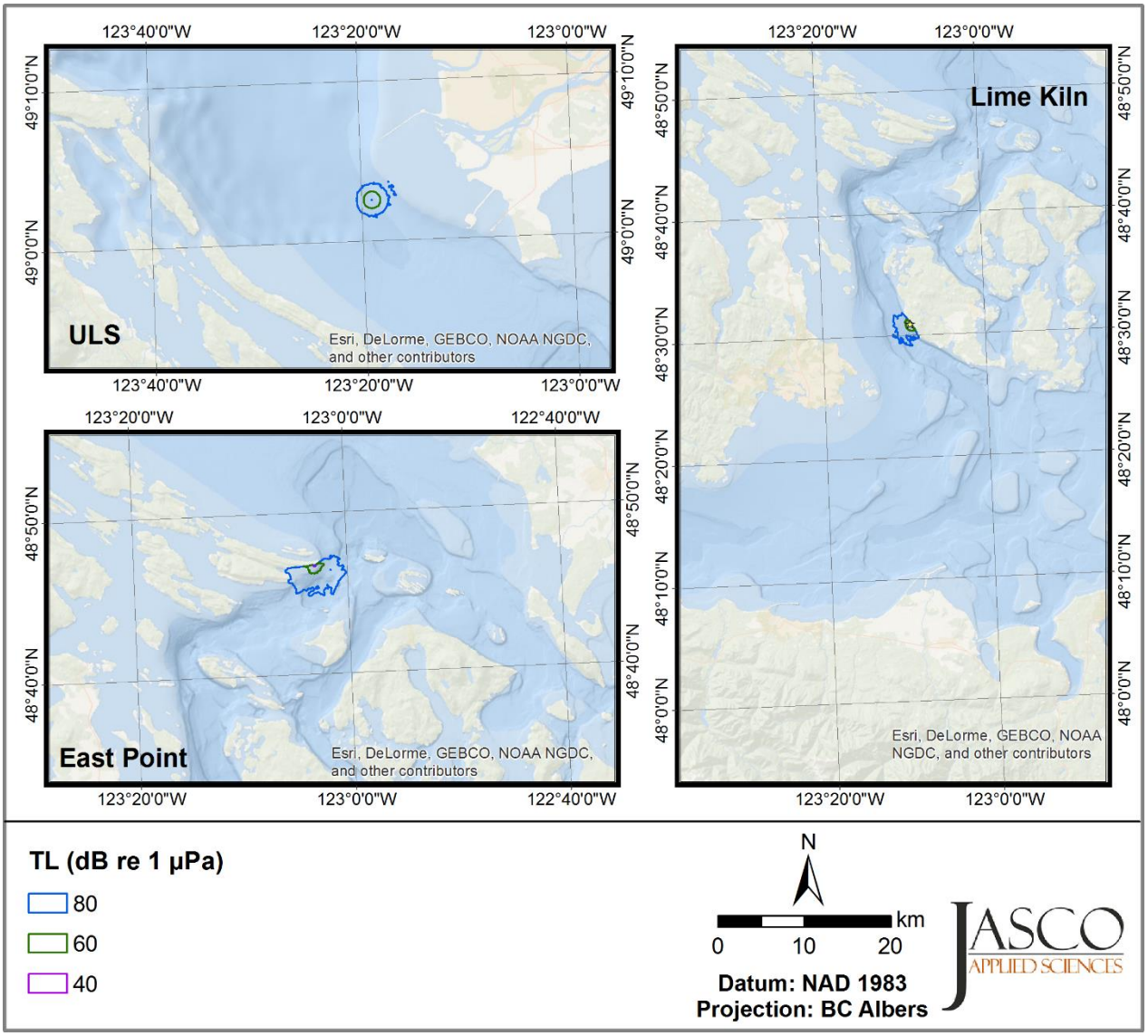

Figure 109. Map of transmission loss (TL) for 30 kHz with sound speed profile (SSP) 1 and wind speed 1 kn.

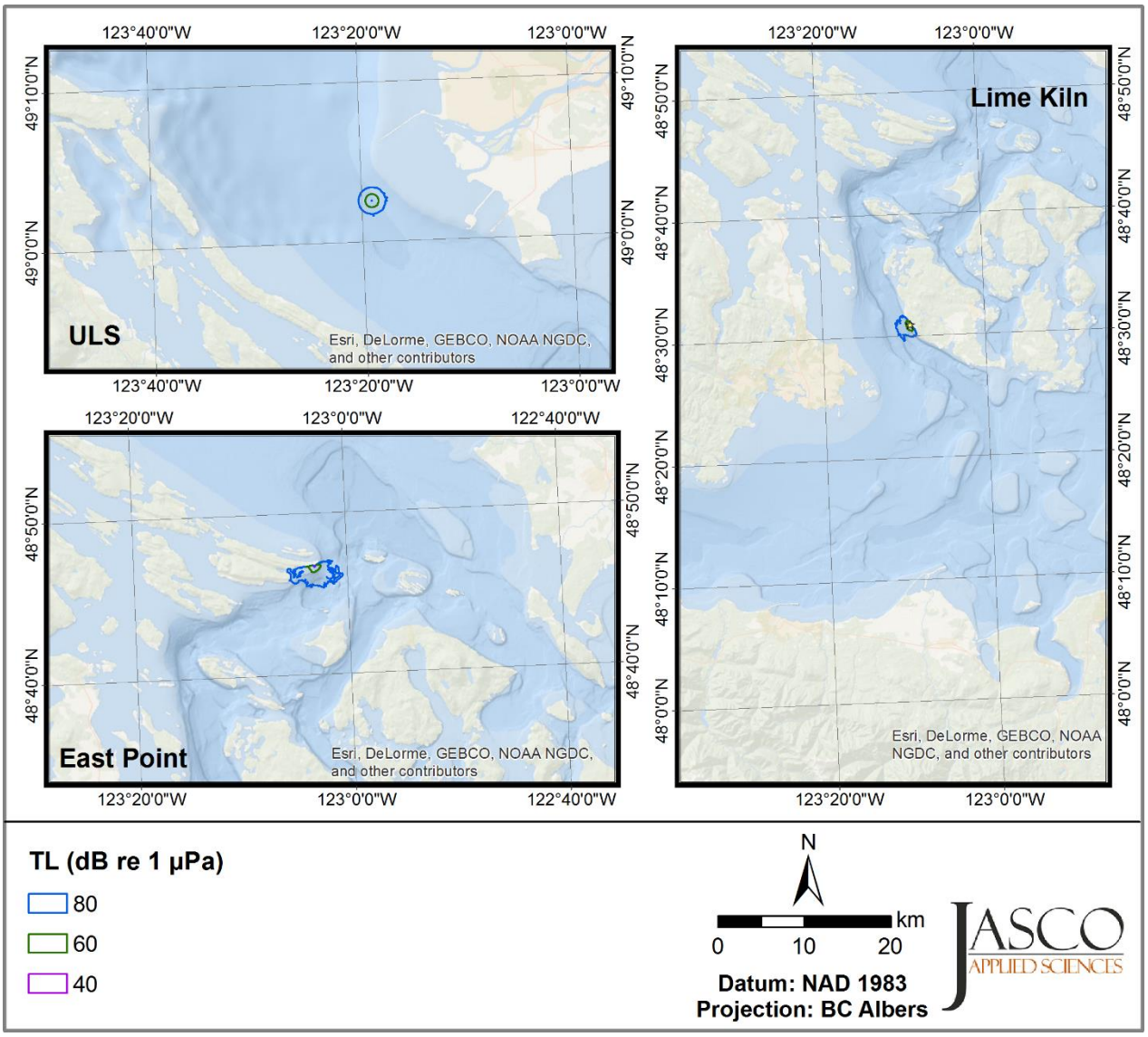

Figure 110. Map of transmission loss (TL) for 30 kHz with sound speed profile (SSP) 1 and wind speed 9 kn.

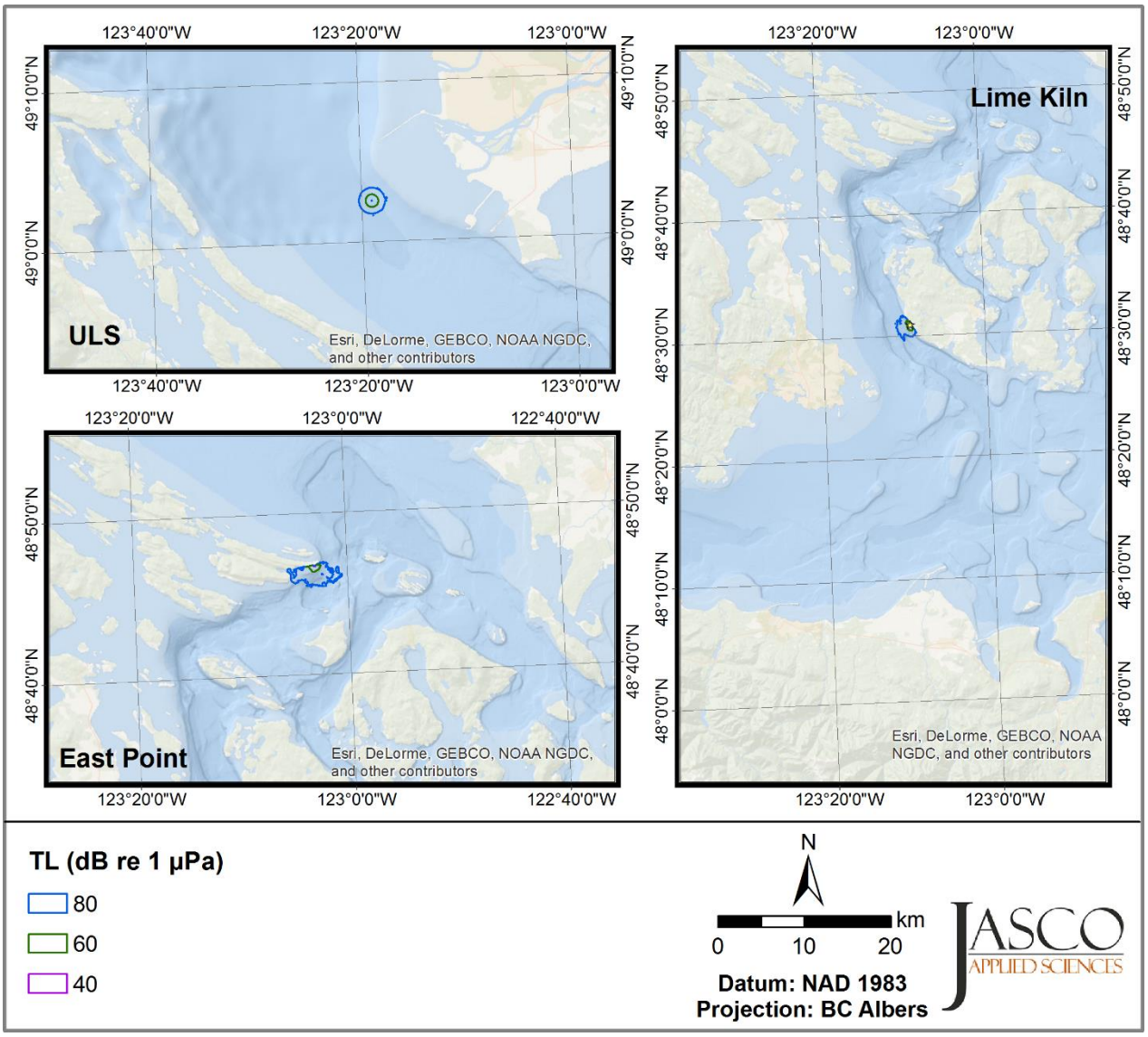

Figure 111. Map of transmission loss (TL) for 30 kHz with sound speed profile (SSP) 1 and wind speed 20 kn.

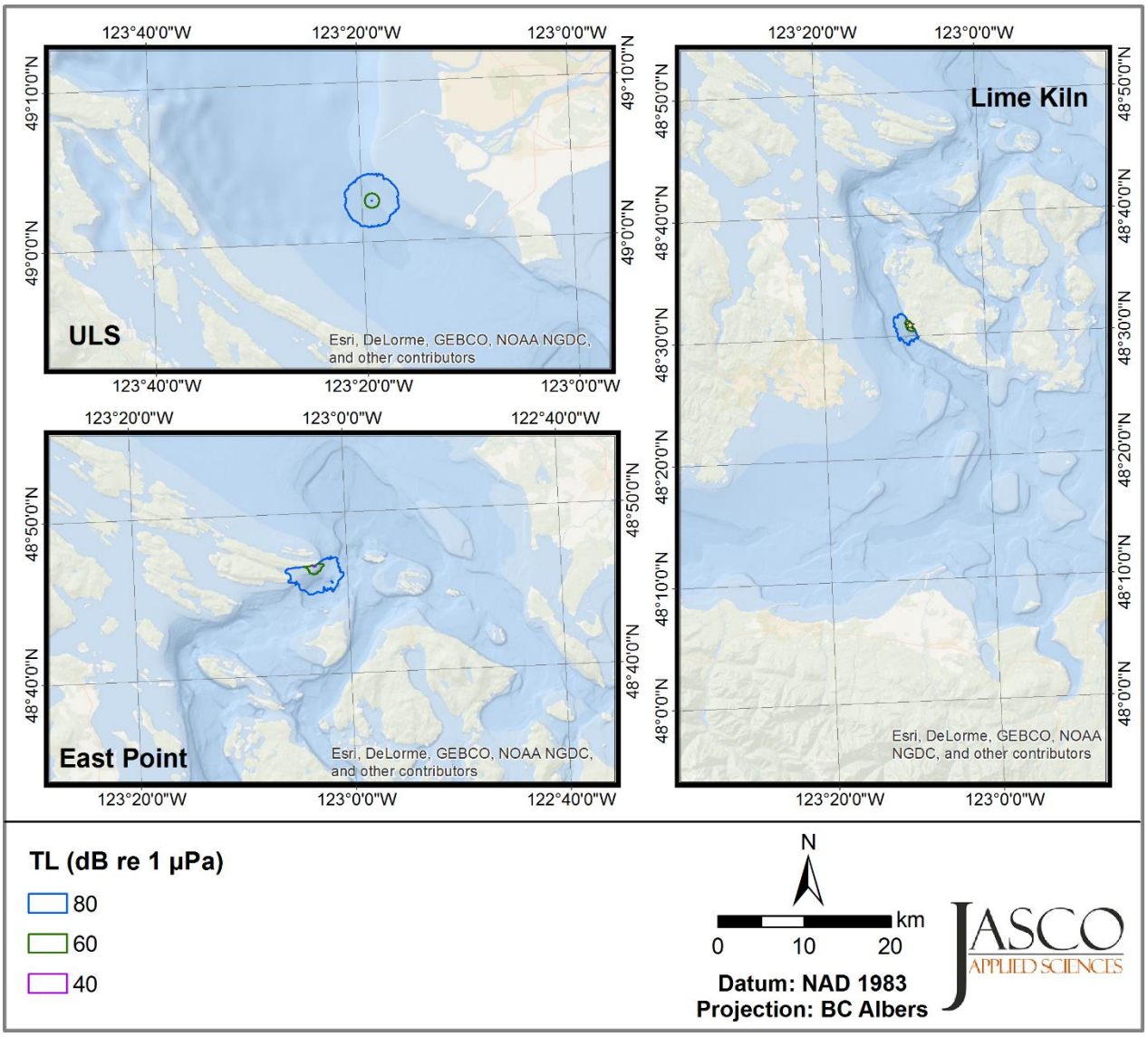

Figure 112. Map of transmission loss (TL) for 30 kHz with sound speed profile (SSP) 2 and wind speed 1 kn.

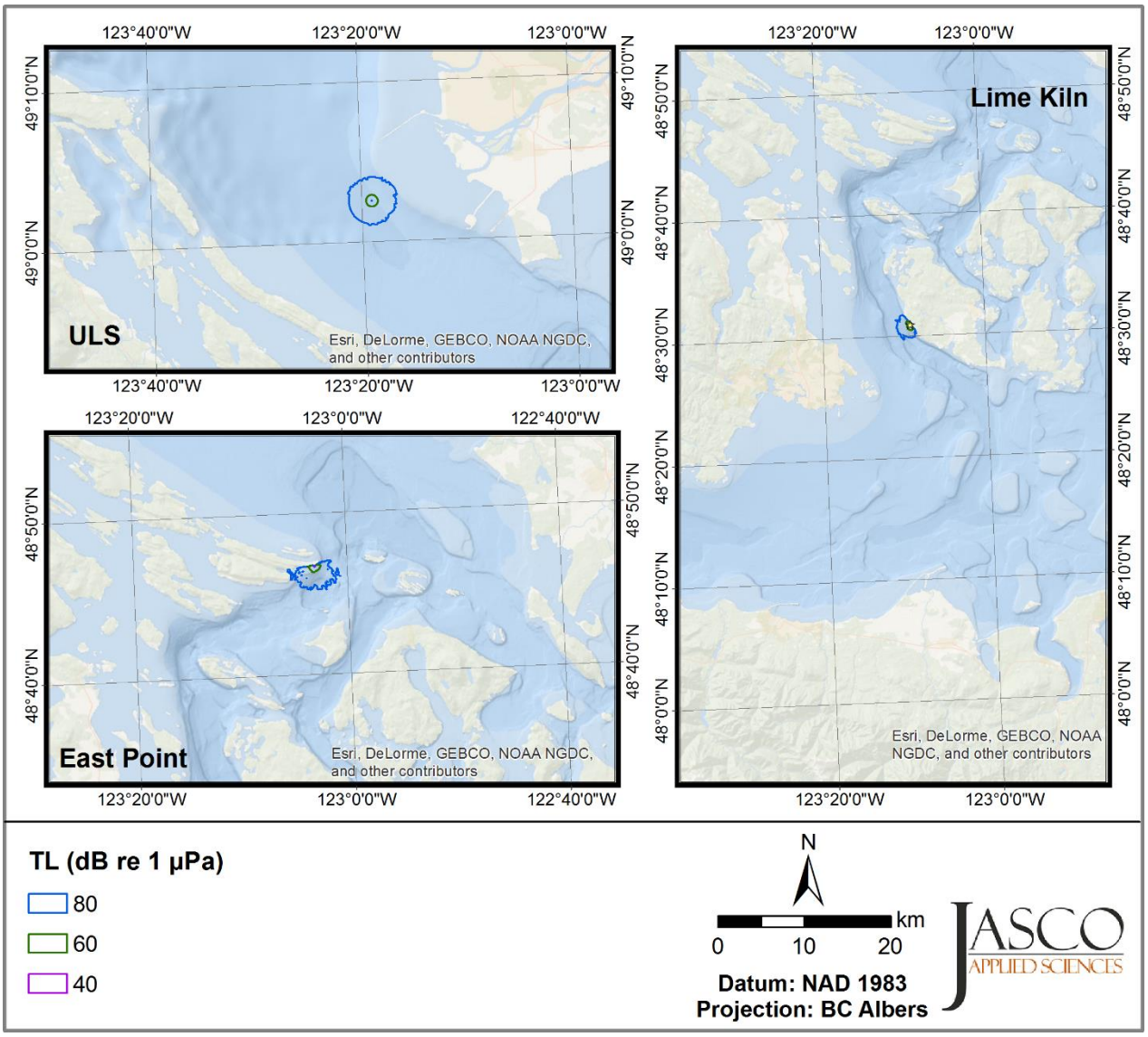

Figure 113. Map of transmission loss (TL) for 30 kHz with sound speed profile (SSP) 2 and wind speed 9 kn.

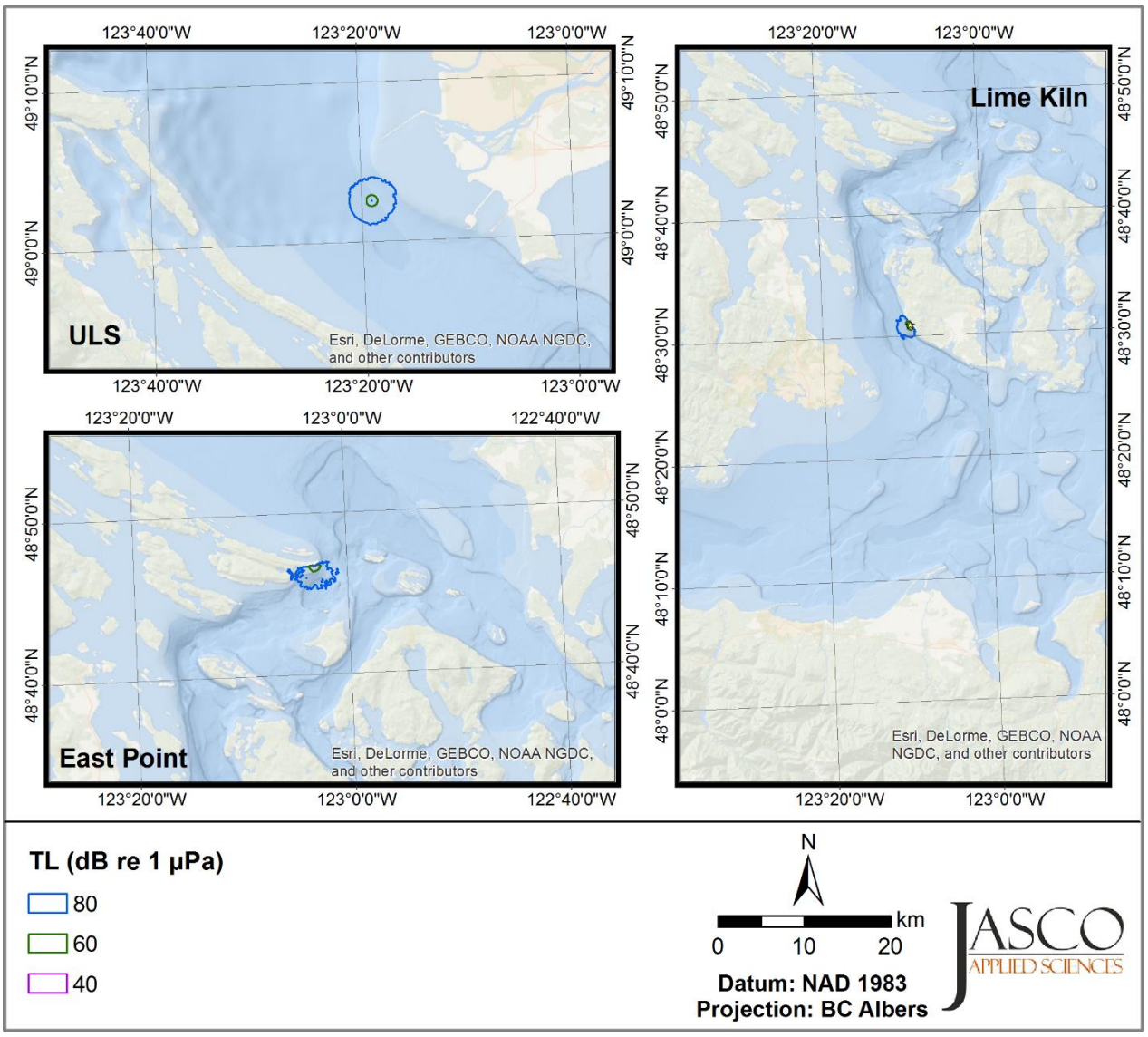

Figure 114. Map of transmission loss (TL) for 30 kHz with sound speed profile (SSP) 2 and wind speed 20 kn.

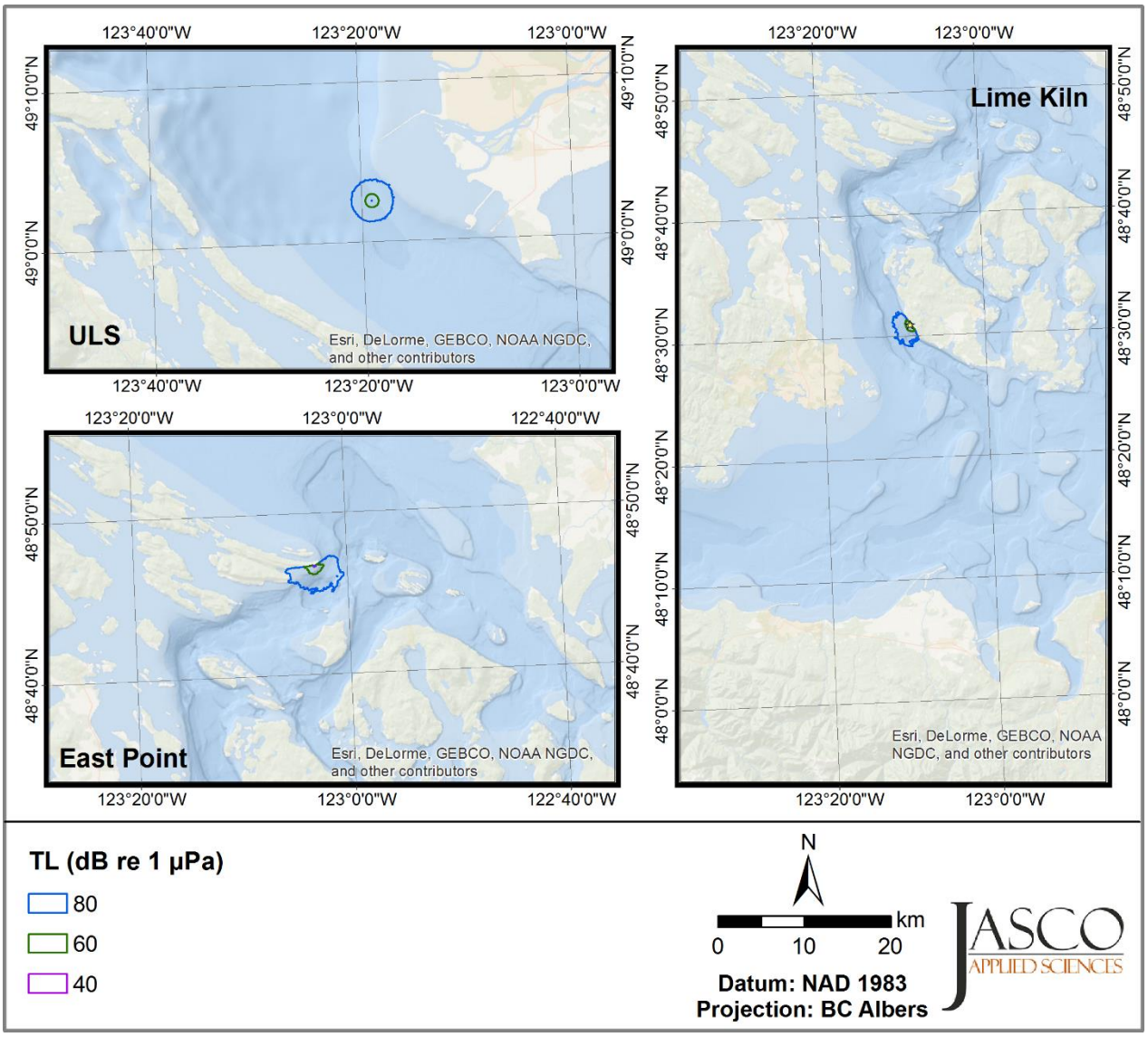

Figure 115. Map of transmission loss (TL) for 30 kHz with sound speed profile (SSP) 3 and wind speed 1 kn.

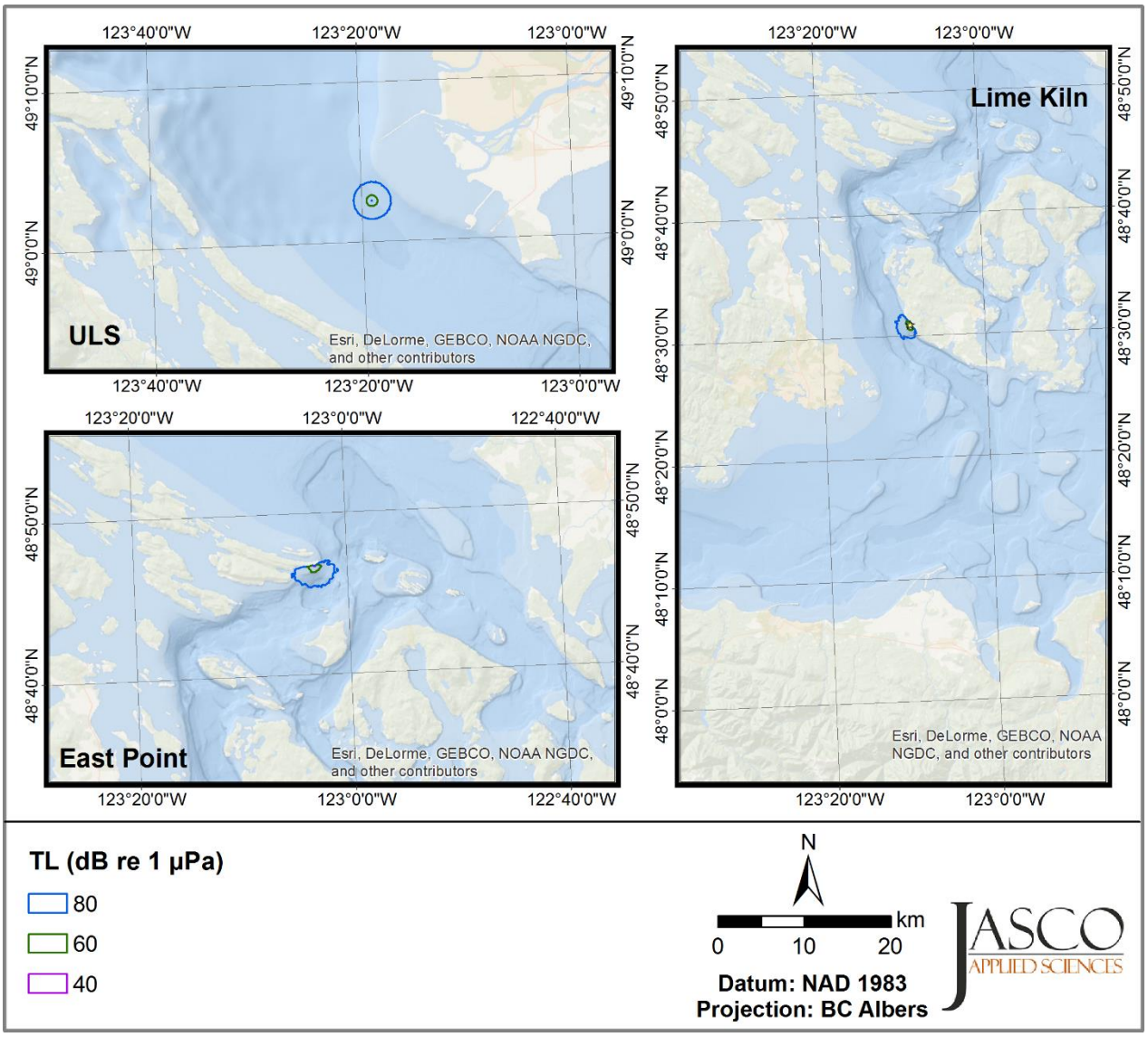

Figure 116. Map of sound speed profile (SSP) for 30 kHz with sound speed profile (SSP) 3 and wind speed 9 kn.

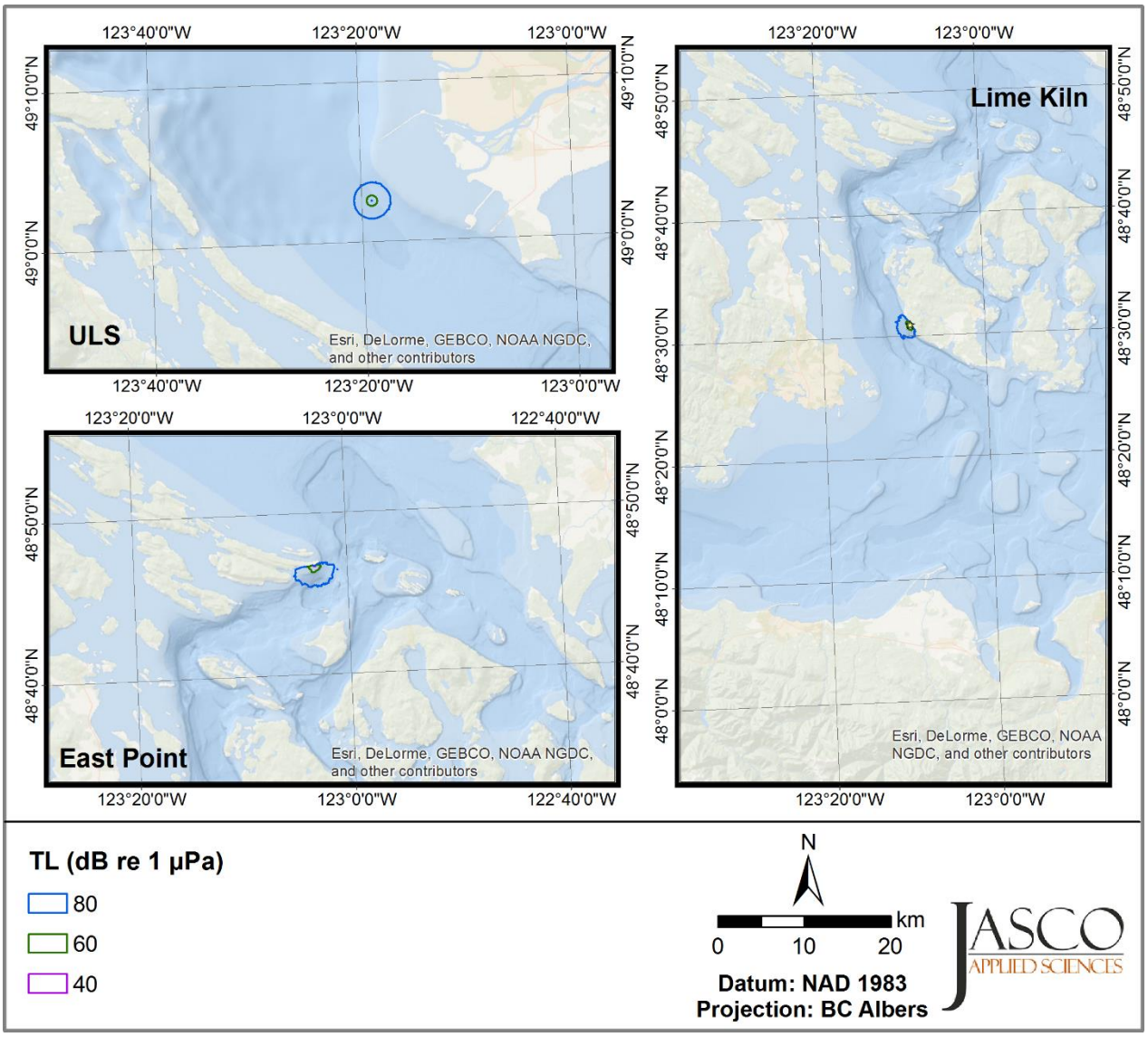

Figure 117. Map of transmission loss (TL) for 30 kHz with sound speed profile (SSP) 3 and wind speed 20 kn.

D.3. Plots of Transmission Loss Range versus Range

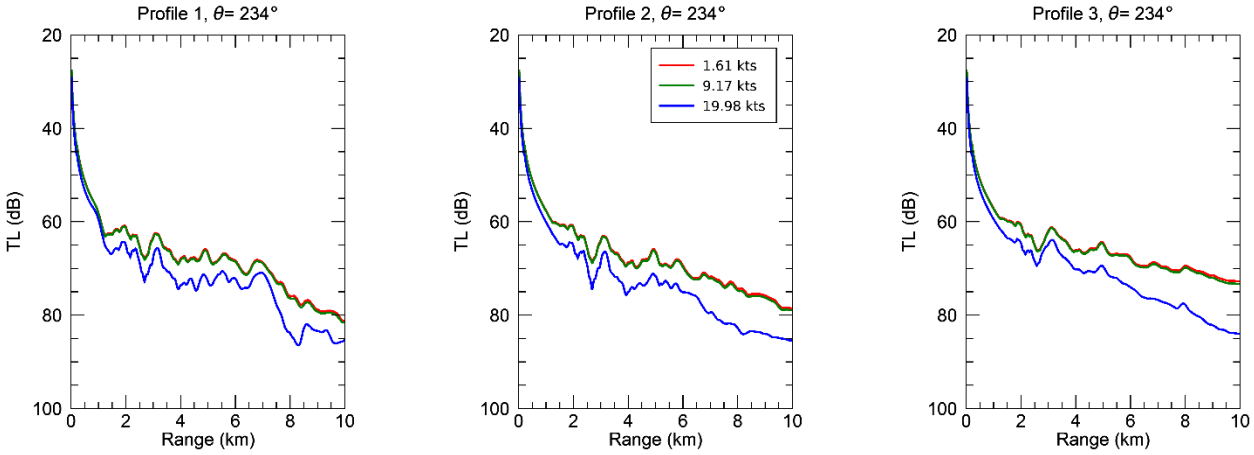

Figure 118. 3 kHz: Transmission loss (TL) versus range at Lime Kiln for each modelled sound speed profile and wind speed along a radial toward the international shipping lanes.

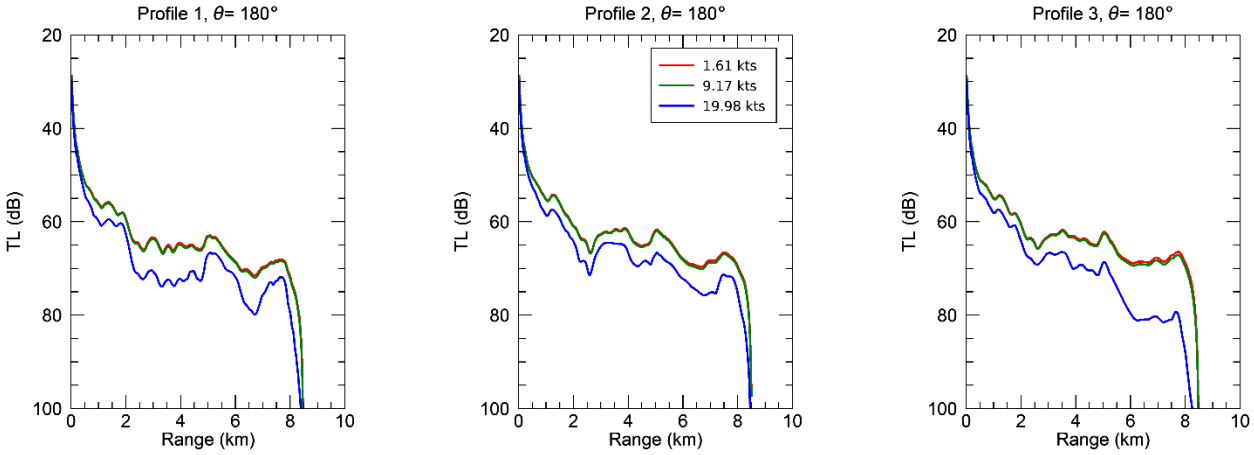

Figure 119. 3 kHz: Transmission loss (TL) versus range at East Point for each modelled sound speed profile and wind speed along a radial toward the international shipping lanes.

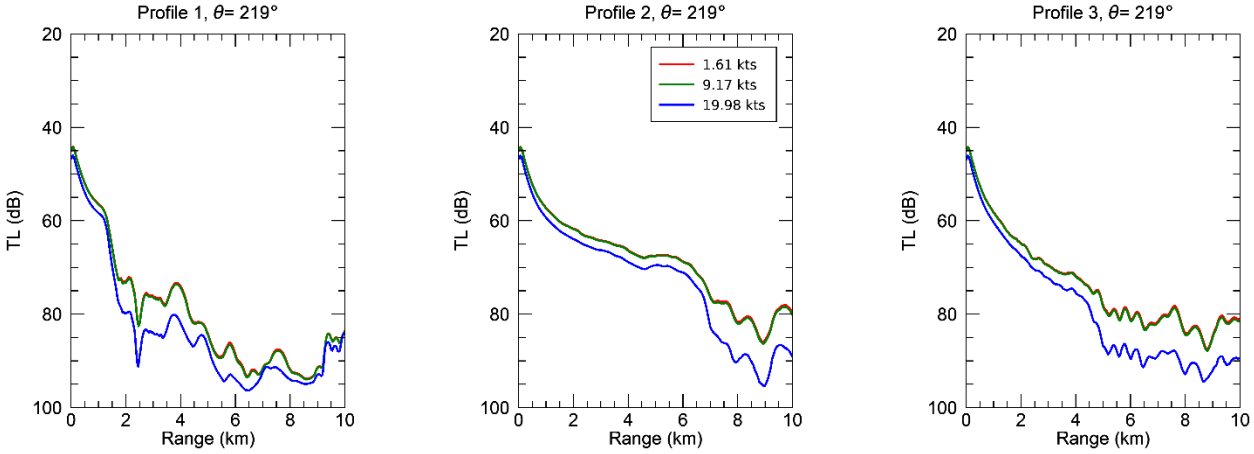

Figure 120. 3 kHz: Transmission loss (TL) versus range at the Underwater Listening Station (ULS) for each modelled sound speed profile and wind speed along a radial toward the international shipping lanes.

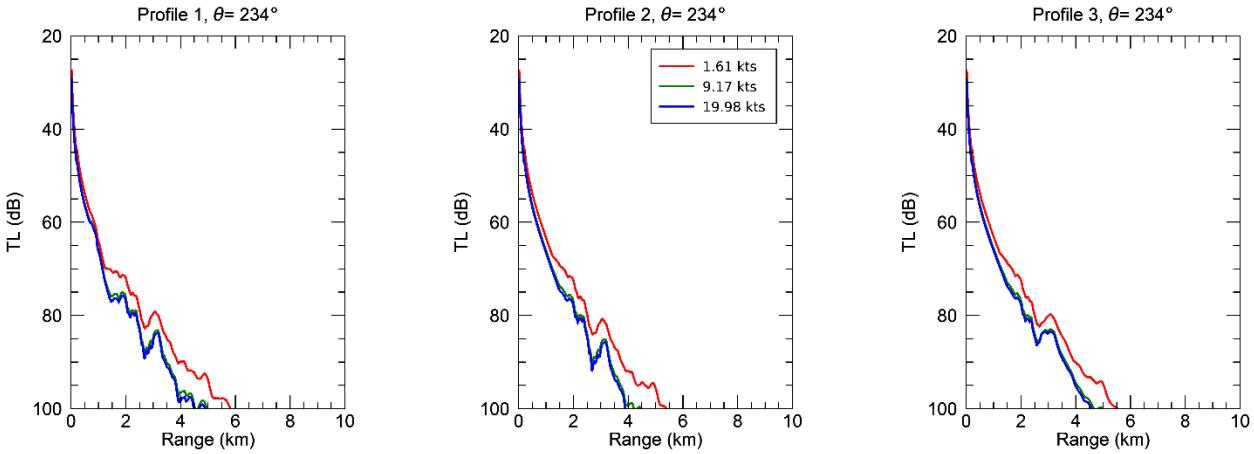

Figure 121. 30 kHz: Transmission loss (TL) versus range at Lime Kiln for each modelled sound speed profile and wind speed along a radial toward the international shipping lanes.

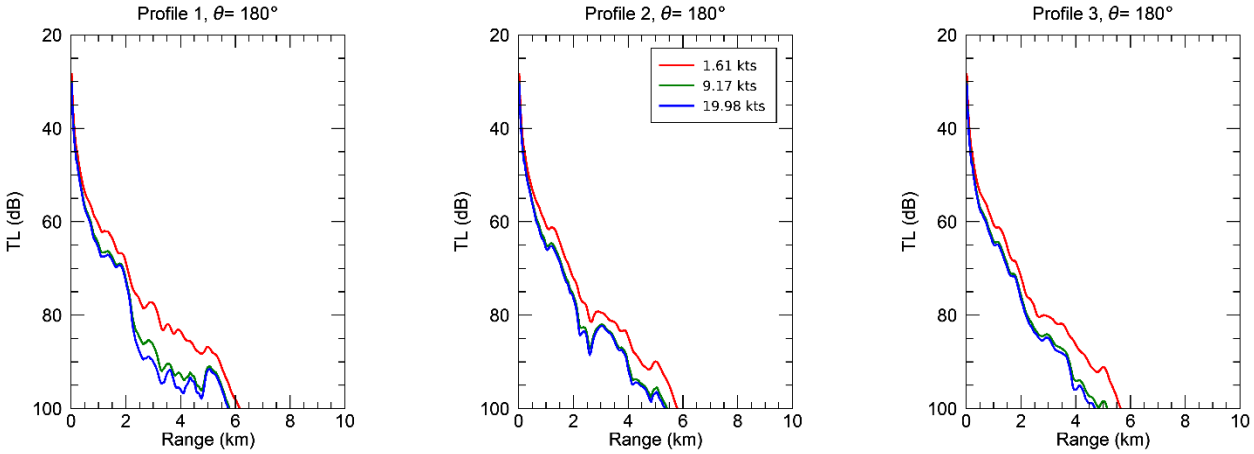

Figure 122. 30 kHz: Transmission loss (TL) versus range at East Point for each modelled sound speed profile and wind speed along a radial toward the international shipping lanes.

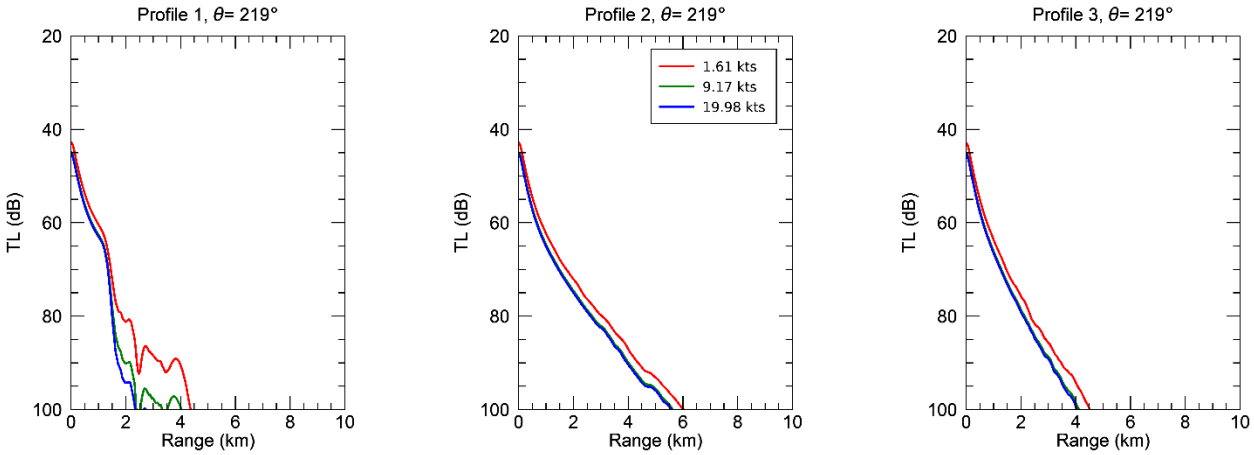

Figure 123. 30 kHz: Transmission loss (TL) versus range at the Underwater Listening Station (ULS) for each modelled sound speed profile and wind speed along a radial toward the international shipping lanes.

Appendix E. AIS and Non-AIS Vessel Traffic Analyses in Boundary Pass

Table 27. List and descriptions of Automated Identification System (AIS)-broadcasting ("AIS") vessel categories.

ECHO vessel category	AIS type name	Detailed summary
Cargo	Cargo	General Cargo Bulk Carrier Heavy Load Carrier Vehicle Carrier
Container Ship	Cargo	Container Ship
Tanker	Tanker	Crude Oil Tanker Oil/Chemical Tanker
Tug	Tug	Tug
Naval Vessel	Special Craft	Military Ops Naval/Naval Auxiliary Vessel
Pleasure Craft	Pleasure Craft	Yacht
Sailboat	Sailing Vessel	Sailing Vessels
Ferry	Passenger	BC Ferry
Cruise	Passenger	Cruise Ship
Fishing	Fishing Vessel	Fishing Vessel Trawler
Ecotourism	Passenger	Whale Watching/Ecotourism
Research/Coastguard	Search and Rescue	Canadian/U.S. Coast Guard Vessels Research Vessels Enforcement
Passenger	Passenger	Passenger Ship Other Ferries

Table 28. List and description of non-broadcasting ("Non-AIS") vessel categories.

Category name	Detailed summary
Motorboat	Motor-powered vessel, or any small (5–10 m) vessel with no discernable sails or mast
Sailboat	Sailing vessel (on motor or sail)
Fishing	Vessel with visible fishing gear
Miscellaneous	Kayak, coast guard, tug, other

Table 29. Selected dates from the winter (February) and summer (August) 2017 sample periods for vessel traffic analysis based on camera imagery data of Boundary Pass. Within each month, a 21 day sampling period was selected during which the camera was fully operational.

Month	Selected dates with complete camera data (Total days)
February	1, 2, 4, 6, 10–16, 18–26, 28 (21)
August	1–17, 19, 20, 22, 23 (21)

Table 30. Number of days with available East Point acoustic and camera imagery data across the 2016–2017 winter sampling period. For each sampling day, the data were truncated to daytime hours corresponding to the approximate civil twilight period (±30 minutes) for the first day of each month. The truncated period for March was updated following daylight savings time (DST).

Month	Dates with acoustic data (Total days)	Dates with camera data (Total days)	Total number of days with acoustic and camera data	Truncated period (GMT)	Civil twilight period at the first day of each month (GMT)
December	1–30 (30)	1–4, 11, 13, 14, 16–18, 21, 22, 34, 25, 27–31 (20)	20	15:00–01:00	15:08–00:56
January	26–31 (6)	1, 3, 5–17, 19–22, 24, 25, 27–31 (26)	5	15:00–01:00	15:28–01:06
February	1–28 (28)	1, 2, 4, 6, 10–16, 18–26, 28 (21)	21	15:00–02:00	15:08–01:46
March	1–31 (31)	1–4, 6, 7, 10–12, 14–17, 28 (14)	14	14:00–02:00 (pre-DST) 15:00–03:00 (DST)	14:22–02:29 (pre-DST) 15:22–03:29 (DST)

Table 31. Number of days with available Monarch Head acoustic data and East Point camera imagery data across the 2017 summer sampling period between 28 Jun to 4 Jul. For each sampling day, the data were truncated to daytime hours corresponding to the approximate civil twilight period (±30 minutes) for the first day of July.

Month	Dates with acoustic data (Total days)	Dates with camera data (Total days)	Total number of days with acoustic and camera data	Truncated period (GMT)	Civil twilight period for 1 Jul 2017 (GMT)
June	28–30 (3)	28–30 (3)	3	12:00–05:00	11:34–4:59
July	1–4 (4)	1–4 (4)	4		

Table 32. Median ambient noise levels (dB re 1 µPa) detected when no vessels, AIS only, non-AIS only, or both Automated Identification System (AIS) and non-AIS vessels were detected on camera. Winter acoustic data were collected via the onsite East Point hydrophone, while summer acoustic data were collected via the Monarch Head hydrophone 3 km southeast of the camera.

Season	Median ambient noise level (dB re 1 µPa)			
	No vessels	AIS	Non-AIS	Both
Winter (East Point)				
10 to 100 Hz	99.2	110.4	99.1	110.7
100 to 1000 Hz	90.0	114.8	90.9	117.7
1000 to 10000 Hz	93.9	111.4	95.1	112.7
10 to 25 kHz	85.5	96.1	86.0	97.6
Summer (Monarch Head)				
10 to 100 Hz	85.2	90.2	85.2	85.6
100 to 1000 Hz	87.7	96.9	88.8	91.4
1000 to 10000 Hz	88.3	96.3	90.4	94.1
10 to 25 kHz	81.3	85.3	81.3	82.7

Table 33. Median ambient noise levels (dB re 1 µPa) recorded across different distance zones for Automated Identification System (AIS) and non-AIS vessels detected on camera. Winter acoustic data were collected via the onsite East Point hydrophone, while summer acoustic data were collected via the Monarch Head hydrophone 3 km southeast of the camera. Vessel detections in the “Near” zone were binned with “Mid” zone vessels for summer.

Season	Median ambient noise level (dB re 1 µPa)						
	No vessels	AIS near	AIS mid	AIS far	Non-AIS near	Non-AIS mid	Non-AIS far
Winter (East Point)							
10 to 100 Hz	99.2	110.7	110.4	108.3	99.3	99.6	99.0
100 to 1000 Hz	90.0	117.0	114.7	112.6	98.2	97.8	90.4
1000 to 10000 Hz	93.9	115.2	111.2	110.9	103.3	101.8	93.3
10 to 25 kHz	85.5	98.7	95.9	96.3	94.5	91.4	85.3
Summer (Monarch Head)							
10 to 100 Hz	85.2	NA	94.6	85.7	NA	85.1	85.2
100 to 1000 Hz	87.7	NA	98.9	90.3	NA	89.4	88.5
1000 to 10000 Hz	88.3	NA	96.9	94.1	NA	91.5	89.6
10 to 25 kHz	81.3	NA	85.8	82.9	NA	82.0	80.8

Appendix F. Influence of Large- and Small-Vessel Traffic at Lime Kiln

This Appendix provides additional noise metrics, in decade bands, during periods with large-, small- and no-vessel detections, as well as AIS signals <6km of Lime Kiln to match the broadband results reported in Section 3.4.5.

Table 34. One-minute 10–100 Hz decade band sound pressure level (SPL; dB re 1 µPa) statistics during time periods with different acoustic detections and times when there were Automated Identification System (AIS) transmissions <6 km from Lime Kiln during January and July 2017. L_n is the sound level exceeded n% of the time. L_{eq} is the power-average sound level (i.e., the decibel level of the average 1-minute mean-square pressure).

Detector	Large vessel	Small vessel	No vessel	AIS <6 km
January				
L_{95}	99.6	97.8	81.7	97.2
L_{50}	115.8	121.2	98.6	115.9
L_5	128.5	138.3	119.0	127.9
L_{eq}	115.6	121.2	99.4	115.3
July				
L_{95}	97.9	95.6	83.4	92.8
L_{50}	115.2	112.3	97.6	114
L_5	127.3	128.7	117.4	126.3
L_{eq}	114.6	112.7	99	112.7

Table 35. One-minute 100–1000 Hz decade band sound pressure level (SPL; dB re 1 µPa) statistics during time periods with different acoustic detections and times when there were Automated Identification System (AIS) transmissions <6 km from Lime Kiln during January and July 2017. L_n is the sound level exceeded n% of the time. L_{eq} is the power-average sound level (i.e., the decibel level of the average 1-minute mean-square pressure).

Detector	Large vessel	Small vessel	No vessel	AIS <6 km
January				
L_{95}	105.3	106.1	85.9	99.1
L_{50}	113.1	120.9	95.2	113.6
L_5	122.4	128.8	102.8	122.8
L_{eq}	113.7	120.0	95.4	113.2
July				
L_{95}	105.1	105.5	84.2	96.3
L_{50}	112	113.8	94.7	112.1
L_5	122.2	127	103.4	122.8
L_{eq}	113.1	115.2	94.8	111.7

Table 36. One-minute 1–10 kHz decade band sound pressure level (SPL; dB re 1 µPa) statistics during time periods with different acoustic detections and times when there were Automated Identification System (AIS) transmissions <6 km from Lime Kiln during January and July 2017. L_n is the sound level exceeded n% of the time. L_{eq} is the power-average sound level (i.e., the decibel level of the average 1-minute mean-square pressure).

Detector	Large vessel	Small vessel	No vessel	AIS <6 km
January				
L_{95}	100.1	107.7	89.6	97.6
L_{50}	108.1	116.6	97.6	108.1
L_5	115.7	124.2	104.5	116.2
L_{eq}	108.5	116.5	98.0	108.1
July				
L_{95}	95.7	105.1	84.6	93
L_{50}	105	115.4	93.4	104.8
L_5	114	126.4	104.2	115.9
L_{eq}	105.4	116	94.1	105.1

Table 37. One-minute 10–100 kHz decade band sound pressure level (SPL; dB re 1 µPa) statistics during time periods with different acoustic detections and times when there were Automated Identification System (AIS) transmissions <6 km from Lime Kiln during January and July 2017. L_n is the sound level exceeded n% of the time. L_{eq} is the power-average sound level (i.e., the decibel level of the average 1-minute mean-square pressure).

Detector	Large vessel	Small vessel	No vessel	AIS <6 km
January				
L_{95}	85.4	104.2	83.2	85.0
L_{50}	92.1	106.9	86.7	92.3
L_5	101.3	114.7	96.5	103.0
L_{eq}	93.0	108.3	88.5	93.3
July				
L_{95}	87.2	104.8	86.1	86.9
L_{50}	91.7	109.4	88.1	91.1
L_5	101.9	121.3	99.4	105.1
L_{eq}	93.1	111.3	90	93.2